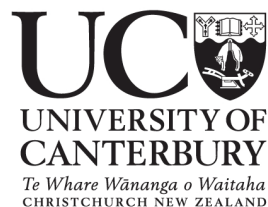

Influence of Oxygen Supply on Metabolism and Energetics in Fish Muscles

**Leonard George Forgan, BSc (Zoology),
MSc Hons (1st class) (Animal Physiology) (Canterbury)**

**A thesis submitted in fulfilment of the requirements of the degree of
Doctor of Philosophy in Animal Physiology at the
University of Canterbury,
Christchurch, New Zealand
2009**



Plant & Food RESEARCH
RANGAHAU AHUMĀRA KAI



Table of Contents

Acknowledgements.....	VI
Thesis abstract.....	VII
1 General introduction.....	1
1.1 Background information on the New Zealand seafood industry.....	2
1.2 Rationale for the thesis.....	4
1.2.1 Applied aspects.....	4
1.2.2 Contribution to knowledge: physiology.....	5
1.3 Oxygen and its role in metabolism.....	6
1.3.1 Harnessing oxygen for energy.....	6
1.3.2 The critical role of the cardiovascular system in metabolism....	7
1.4 Energy metabolism.....	8
1.4.1 Energetic pathways in muscle.....	8
1.4.2 Aerobic metabolic pathways.....	9
1.4.3 Anaerobic metabolic pathways.....	12
1.5 Muscle.....	14
1.5.1 Vertebrate Muscle.....	14
1.5.2 Striated muscle.....	16
1.5.3 Skeletal muscle.....	16
1.5.4 Skeletal muscle of fishes.....	18
1.5.5 Cardiac muscle.....	21
1.5.6 Smooth muscle.....	21
1.6 Aims and outline of the thesis.....	22
2 Oxygen consumption and blood flow distribution in perfused skeletal muscle of Chinook salmon (<i>Oncorhynchus tshawytscha</i>).....	24
2.1 Abstract.....	25
2.2 Keywords.....	25
2.3 Introduction.....	26
2.4 Materials and Methods.....	27
2.4.1 <i>Animals</i>	27
2.4.2 <i>Tail preparation</i>	28

2.4.3	<i>Perfusion solution</i>	30
2.4.4	<i>Chemicals</i>	30
2.4.5	<i>RBCs</i>	30
2.4.6	<i>DAP</i>	31
2.4.7	<i>VO₂ measurements</i>	32
2.4.8	<i>Electrical stimulation</i>	33
2.4.9	<i>Cut surface pH</i>	33
2.4.10	<i>BFD</i>	33
2.4.11	<i>Mitochondrial activity</i>	34
2.4.12	<i>Statistical analysis</i>	35
2.5	Results	36
2.5.1	<i>VO₂</i>	36
2.5.2	<i>DAP, cut surface pH, resistance and oedema</i>	36
2.5.3	<i>BFD</i>	40
2.5.4	<i>Mitochondrial activity</i>	40
2.6	Discussion	42
2.6.1	<i>DAP, vascular resistance and oedema</i>	42
2.6.2	<i>VO₂</i>	43
2.6.3	<i>Muscle pH changes</i>	45
2.6.4	<i>BFD and mitochondrial activity</i>	46
2.6.5	<i>Summary</i>	47

3 Oxygen-dependence of metabolic rate in the striated muscles of vertebrates.....48

3.1	Abstract	49
3.2	Keywords	50
3.3	Introduction	51
3.4	Materials and Methods	52
3.4.1	<i>Animals</i>	52
3.4.2	<i>Tissue biopsy</i>	54
3.4.3	<i>Fish</i>	54
3.4.4	<i>Hagfish</i>	55
3.4.5	<i>Rat</i>	55
3.4.6	<i>Tissue slice and vessel preparation</i>	56
3.4.7	<i>Mitochondrial activity</i>	56
3.4.8	<i>Respirometry</i>	57
3.4.9	<i>Haem protein assay</i>	59
3.4.10	<i>Muscle energetics experiment</i>	60
3.4.11	<i>Cut surface tissue pH</i>	61
3.4.12	<i>Tissue extraction for energetics experiment</i>	61
3.4.12.1	<i>Creatine compounds, purine nucleotides and nucleosides and related bases</i>	61
3.4.12.2	<i>Glucose, glycogen and lactate</i>	62
3.4.13	<i>Assays</i>	62

3.4.13.1	<i>Glucose and glycogen assay</i>	62
3.4.13.2	<i>Lactate assay</i>	63
3.4.13.3	<i>Creatine compounds, purine nucleotides and nucleosides and related bases</i>	63
3.4.14	<i>Nucleotide ratios and total pool and potential energy</i>	64
3.4.15	<i>Chemicals</i>	64
3.4.16	<i>Statistical analysis</i>	64
3.5	Results	65
3.5.1	<i>Muscle VO₂ and mitochondrial activity</i>	65
3.5.2	<i>Haem protein concentration</i>	73
3.5.3	<i>Energetics experiment</i>	75
3.5.3.1	<i>Glycogen, glucose, lactate and pH</i>	75
3.5.3.2	<i>Creatine phosphate, creatine, creatinine and potential energy</i>	76
3.5.3.3	<i>ATP, ADP, AMP and NAD⁺</i>	77
3.5.3.4	<i>IMP, Inosine, hypoxanthine and uric acid</i>	78
3.5.3.5	<i>Ratios and total nucleotide pool</i>	79
3.6	Discussion	80

4 Oxygen consumption, ventilation frequency and cytochrome c oxidase activity in blue cod (*Parapercis colias*) exposed to hydrogen sulphide or isoeugenol...92

4.1	Abstract	93
4.2	Keywords	93
4.3	Introduction	94
4.4	Materials and Methods	97
4.4.1	<i>Animals</i>	97
4.4.2	<i>Respirometry</i>	97
4.4.3	<i>Introduction of chemicals</i>	98
4.4.4	<i>Ventilation frequency and activity</i>	100
4.4.5	<i>Cytochrome c oxidase activity</i>	100
4.4.6	<i>Chemicals</i>	101
4.4.7	<i>Calculations and statistical analysis</i>	101
4.5	Results	102
4.5.1	<i>Isoeugenol respirometry</i>	102
4.5.2	<i>H₂S respirometry</i>	104
4.5.3	<i>Cytochrome c oxidase activity</i>	107
4.6	Discussion	109
4.6.1	<i>Physiological consequences of H₂S and isoeugenol exposure</i>	109
4.6.2	<i>Hypoxia and hypometabolism</i>	112
4.6.3	<i>Narcotic properties of H₂S</i>	116
4.6.4	<i>Summary</i>	117

5 Post-mortem calorimetric and biochemical profiles of Chinook salmon (*Oncorhynchus tshawytscha*) white muscle following rested and exhausted harvesting....118

5.1 Abstract.....	119
5.2 Keywords.....	119
5.3 Introduction.....	120
5.4 Materials and Methods.....	122
5.4.1 <i>Animals</i>	122
5.4.2 <i>Exhausted harvest</i>	122
5.4.3 <i>Rested harvest</i>	123
5.4.4 <i>Muscle biopsy</i>	123
5.4.5 <i>Calorimetry</i>	123
5.4.6 <i>Biochemical profile experiment</i>	124
5.4.7 <i>Cut surface pH</i>	125
5.4.8 <i>Tissue extraction</i>	125
5.4.8.1 <i>Creatine compounds, purine nucleotides and nucleosides and related bases</i>	125
5.4.8.2 <i>Glucose, glycogen and lactate</i>	126
5.4.9 <i>Assays</i>	126
5.4.9.1 <i>Glucose and glycogen assay</i>	126
5.4.9.2 <i>Lactate assay</i>	127
5.4.9.3 <i>Creatine compounds, purine nucleotides and nucleosides and related bases</i>	127
5.4.10 <i>Nucleotide ratios and total pool, K-values and potential energy</i> ..	128
5.4.11 <i>Chemicals</i>	129
5.4.12 <i>Statistical analysis</i>	129
5.5 Results.....	129
5.5.1 <i>Harvest regimen associated activity</i>	129
5.5.2 <i>Calorimetry</i>	130
5.5.3 <i>Biochemical profiles</i>	132
5.5.3.1 <i>Glycogen, glucose, lactate and pH</i>	132
5.5.3.2 <i>Creatine phosphate, creatine, creatinine and potential energy</i> ...	133
5.5.3.3 <i>ATP, ADP, AMP and NAD⁺</i>	135
5.5.3.4 <i>IMP, inosine, hypoxanthine and uric acid</i>	137
5.5.4 <i>Nucleotide ratios and total pool, K-values and correlations</i>	139
5.6 Discussion.....	142

6 Oxygen dependency of hydrogen sulfide-mediated vasoconstriction in cyclostome aortas.....152

6.1 Abstract.....	153
6.2 Keywords.....	153
6.3 Introduction.....	154

6.4 Materials and Methods	157
6.4.1 <i>Animals</i>	157
6.4.2 <i>Myography</i>	158
6.4.3 <i>Protocols</i>	158
6.4.3.1 <i>Carbachol dose response</i>	158
6.4.3.2 <i>Effect of H₂S on buffer pH</i>	159
6.4.3.3 <i>H₂S dose-dependent responses</i>	159
6.4.3.4 <i>Effect of PO₂ on H₂S responses</i>	159
6.4.3.5 <i>Involvement of H₂S mechanisms in hagfish hypoxic vasoconstriction</i>	160
6.4.4 <i>Oxygen consumption</i>	161
6.4.4.1 <i>Oxygen consumption by hagfish dorsal aortas</i>	161
6.4.4.2 <i>Oxygen consumption by salmon vessels</i>	162
6.4.5 <i>Chemicals</i>	162
6.4.6 <i>Calculations and statistical analysis</i>	163
6.5 Results	164
6.5.1 <i>Carbachol dose response of hagfish efferent branchial arteries</i>	164
6.5.2 <i>Effects of H₂S on pH</i>	164
6.5.3 <i>Vascular effects of H₂S</i>	165
6.5.4 <i>Effect of PO₂ on H₂S responses of hagfish and lamprey dorsal aortas</i>	166
6.5.5 <i>Involvement of H₂S mechanisms in hagfish hypoxic vasoconstriction</i>	167
6.5.6 <i>Vessel MO₂</i>	170
6.6 Discussion	174
6.6.1 <i>H₂S as a vasoconstrictor</i>	174
6.6.2 <i>H₂S metabolism in O₂ sensing</i>	175
6.6.3 <i>Similarity of vascular responses to H₂S and hypoxia</i>	176
6.6.4 <i>Metabolic coupling of HVC to H₂S production</i>	177
6.6.5 <i>Effect of PO₂ on MO₂</i>	179
6.6.6 <i>Relationship between MO₂ and H₂S production</i>	180
7 Final discussion	182
7.1 Important findings and implications of this thesis	183
7.1.1 Summary of thesis	183
7.1.2 Metabolic rates in perfused and isolated tissues	183
7.1.3 The effects of anaesthesia, narcosis and harvest technique on animals and tissues	189
7.1.4 H₂S: an emerging O₂ sensor	194
7.2 Future work	195
7.2.1 O₂-sensing and diffusion limitation	195
7.2.2 Anaesthesia, rested harvesting and hypometabolism	199
References	202

Appendix 1	Conference presentations and abstracts.....	228
Appendix 2	Forgan and Forster (2008).....	232
Appendix 3	Olson, Forgan, Dombkowski and Forster (2008).....	243

Acknowledgements

Many thanks to my primary supervisor Malcolm Forster for his guidance, support and friendship throughout my PhD. Thanks to Alistair Jerrett and Suzanne Black for valuable input into the research. Thanks to Ken Olson for assistance and our enjoyable collaboration. I acknowledge Steven Giese, Nickolas Tuckey and Denham Cook for valuable advice on analytical procedures. I greatly value the technical assistance received from Gavin Robinson, Nick Ethridge and John Scott. I greatly appreciate the PhD scholarships from the New Zealand Institute for Plant and Food Research and the University of Canterbury and the conference funding from the Society for Experimental Biology and the Royal Society of New Zealand (Canterbury Branch). Thanks to Isaac Salmon Farm for salmon and facilities, Plant and Food Research for the snapper and Dr. Drusilla Mason for the rats. I greatly appreciate the collection of the blue cod and hagfish by Rennie Bishop and lamprey by B. Swink. Finally, many thanks to my partner Bryony McNeill and my family for supporting me and encouraging me in my studies.

Thesis abstract

The five discrete, but related studies presented in this thesis investigate several aspects of the physiology and biochemistry of whole animals, perfused and isolated tissues from fishes and other vertebrates. Important fundamental questions about tissue metabolism and energy supply and utilisation in relation to oxygen supply, in addition to applied questions relating to commercial harvesting and post-mortem muscle physiology were addressed. Oxyconformance of oxygen consumption (VO_2) at low oxygen delivery rates was shown using an isolated, perfused salmon tail preparation, composed primarily of skeletal muscle. Addition of pig red blood cells to the perfusing solution at a haematocrit of 5 or 10%, increasing the capacitance, resulted in oxyregulation of VO_2 by the tail tissues. Below c.60 ml $\text{O}_2 \cdot \text{kg}^{-1} \cdot \text{h}^{-1}$ of oxygen delivery, VO_2 was delivery dependent. Above this value additional oxygen delivery did not increase VO_2 of resting muscle above c.35 ml $\text{O}_2 \cdot \text{kg}^{-1} \cdot \text{h}^{-1}$. The preparation was validated by measuring mitochondrial activity using MTT and blood flow distribution to the red and white muscle using fluorescent microspheres.

Evidence of both O_2 -independence of VO_2 in the vasculature and strict O_2 -dependence of VO_2 in striated muscles of fishes and a mammal is presented using isolated vascular tissue and an *in vitro* tissue slice model. VO_2 by vessels from rat, salmon and hagfish showed varying degrees of independence between PO_2 s of 15-95 mmHg *in vitro* (1 mmHg = 0.133 kPa). Above and below these values, VO_2 was highly PO_2 -dependent. VO_2 by cardiac and skeletal muscles from rat, salmon, snapper and hagfish were shown to relate linearly to PO_2 between zero and 125 mmHg. VO_2 in these tissues was highly dependent on tissue type (cardiac, red and white muscle) which correlated with haem protein concentration. The increase in VO_2 in muscle slice mitochondria uncoupled with FCCP and DNP ruled out diffusion-limitation as a constraint on VO_2 .

Mitochondrial activity was constant over time and reoxygenation of the Ringer bathing the tissues after the initial run down in PO_2 resulted in VO_2 rates that were unchanged from the starting values, demonstrating that the tissues remained viable over time. ATP turnover in red muscle was significantly increased at 100 mmHg relative to 30 mmHg, and increased in both treatments from values at the start. Our data suggest that ATP supply and ATP demand were reduced in conjunction with falling PO_2 .

The effects of hydrogen sulphide (H_2S) (derived from Na_2S) and isoeugenol exposure on activity, VO_2 and ventilation frequency (V_f) in a teleost fish are reported. In the H_2S treatment group (200 μM Na_2S) both resting VO_2 and V_f decreased after 30 minutes of exposure, concurrent with narcosis and a loss of equilibrium. These events corresponded with a significant fall in VO_2 (33%) and V_f (20%) by 15 minutes, both declining further to a nadir of 40% of resting values at 30 minutes. After flushing, VO_2 increased to resting levels, with V_f remaining significantly depressed until 30 minutes of recovery. Recovery was accompanied by regained mobility and equilibrium and significantly increased VO_2 and V_f . Isoeugenol anaesthetised fish (0.011 $g.L^{-1}$) reached stage 4-5 of anaesthesia accompanied by significant decreases in VO_2 (45%) and V_f (25%) at 25 minutes, both parameters declining further to around 64% and 38% respectively by 35 minutes. Similar to H_2S exposed fish, VO_2 increased to resting values after flushing, followed by a significant rise in VO_2 . Likewise, V_f had risen to resting values post-flushing, subsequently increasing significantly during recovery. Overall, VO_2 in relation to resting rate was reduced in the isoeugenol treated animals, while in H_2S treated fish, exposure there was increased oxygen usage, possibly associated with a toxic effect. H_2S significantly reduced cytochrome c oxidase activity in muscle and gill tissue *in vitro* between 69-79% at 20 μM and 77-97% at 200 μM Na_2S , while isoeugenol had no effect on activity in any tissue.

Calorimetric and biochemical profiles of anoxic, post-mortem white muscle from Chinook salmon subjected to rested and exhausted harvesting regimens at their acclimation temperature (10°C) are reported. Prior to harvest rested animals were anaesthetised with 0.012 g.L⁻¹ isoeugenol without disturbance. The muscle of these animals had a high metabolic rate at the time of death, at around 400 $\mu\text{W.g}^{-1}$, which declined rapidly over the first 12 hours to 15 $\mu\text{W.g}^{-1}$. Exhausted animals were forced to swim and were crowded before capture, resulting in an initial heat output of <10 $\mu\text{W.g}^{-1}$. Heat output was significantly greater in the rested group at the time of death and for 7 hours post-mortem. In both groups there was an exothermic event, occurring between 4 and 6 hours post-mortem amounting to a rise of around 35 $\mu\text{W.g}^{-1}$. A one-phase exponential decay model appropriately described the net heat output of the rested profile minus the exhausted data. Rested animals had significantly higher initial cut surface pH (7.5 vs 6.7), tissue glycogen (16 vs 2 $\mu\text{mol.g}^{-1}$), creatine phosphate (18 vs 0.1 $\mu\text{mol.g}^{-1}$), ATP (6 vs 3.5 $\mu\text{mol.g}^{-1}$) and potential energy (30 vs 7 $\mu\text{mol.g}^{-1}$) than the exhausted group, which had significantly elevated tissue concentrations of lactate (43 vs 18 $\mu\text{mol.g}^{-1}$) and glucose (5 vs 2 $\mu\text{mol.g}^{-1}$). Potential energy in the form of ATP, glycogen and creatine phosphate remained elevated for an extended period post-mortem in rested animals while catabolites further down the chain such as inosine, hypoxanthine and uric acid accumulated at similar rates in both groups.

We examined the relationship between exogenous and endogenous H₂S and oxygen partial pressure in isolated hagfish and lamprey vessels that exhibit profound hypoxic vasoconstriction (HVC). In myography studies, H₂S (Na₂S) dose-dependently constricted dorsal aortas (DA) and efferent branchial arteries but did not affect ventral aortas or afferent branchial arteries, which was similar to the effects produced by hypoxia. Sensitivity of H₂S-mediated contraction in hagfish and lamprey DA was enhanced by hypoxia. HVC in hagfish DA was enhanced by the H₂S precursor cysteine and inhibited by amino-oxyacetate (AOA), an inhibitor of the H₂S-synthesising enzyme, cystathionine β -synthase, and unaffected by propargyl glycine, an inhibitor of cystathionine λ -lyase.

Oxygen consumption (MO_2) of hagfish DA was constant between a PO_2 of 15 and 115 mmHg, decreased when $\text{PO}_2 < 15$ mmHg, and increased if PO_2 exceeded 115 mmHg. $10 \mu\text{mol.l}^{-1}$ H_2S increased and concentrations above $100 \mu\text{mol.l}^{-1}$ H_2S decreased MO_2 . Consistent with the effects on HVC, cysteine increased and AOA and hydroxylamine, an inhibitor of pyridoxyl 5'-phosphate-dependent enzymes, decreased MO_2 . These data show that H_2S is a monophasic vasoconstrictor of specific cyclostome vessels and because hagfish lack vascular NO, and vascular sensitivity to H_2S was enhanced at low PO_2 , it is unlikely that H_2S contractions are mediated by either an H_2S -NO interaction or an oxidation product of H_2S . These experiments provide additional support for the hypothesis that the metabolism of H_2S is involved in oxygen sensing/signal transduction in vertebrate vascular smooth muscle.

Together the findings of this thesis contribute to the understanding of oxygen utilisation and energetics in relation to oxygen supply in a number of tissues. These data further our understanding of respiratory physiology and may have practical applications in the seafood industry.

Chapter 1

General introduction

1.1 Background information on the New Zealand seafood industry

Fisheries currently provide 20% of the animal protein consumed by humans worldwide and generate jobs for more than 200 million people, mostly in small-scale fisheries (Zabel *et al.* 2003). Boasting the fourth largest exclusive economic zone (EEZ) in the world, New Zealand has the potential for large earnings from seafood. Exports contribute significantly to the economy, amounting to around NZ\$ 1.36 billion in 2008 with a resource assessment asset value of 3.97 billion dollars in the same year (SeaFIC 2009). Animals sold are sourced primarily from wild populations and are sold to Australasia, Asia, Europe and the Americas. The largest buyers are China, Japan, Australia and the USA. Typically international demand for New Zealand products exceeds supply and proportionately, very little is sold on the local market. Cultured animals also contribute significantly to the New Zealand economy, at about NZ\$ 300 million in 2008. Cultured New Zealand green-lipped mussels and Chinook salmon contributed around NZ\$ 204 million and NZ\$ 44 million dollars to the economy respectively in 2008 (SeaFIC 2009). The USA is the largest buyer of aquaculture products at approximately 30% of all production.

Given that seafood is such a major contributor to the New Zealand economy, it follows that expansion of this industry might be of benefit to all New Zealanders. This is easier said than done, as many of New Zealand's major fisheries are either already being harvested maximally or have been over-exploited. The relatively recent targeting of deep-water species exemplifies this. The deep-water fishery for orange roughy (*Hoplostethus atlanticus*) has been severely overexploited in New Zealand and southern Australia. During a major rush to target the rich spawning aggregations around deep seamounts in the 1980s large numbers of animals were taken (Roberts 2002). In just over ten years the population collapsed to less than 20% of the pre-exploitation abundance, the major cause attributed to the sequential depletion of aggregations (Koslow 1997; Clark 1999; Roberts 2002). This kind of reduction is a common feature of exploited fish populations (Russ 1991).

In addition, significant ecological damage has been documented as a result of the bottom trawl catch method employed by this fishery (Koslow 2000).

The example given is just one of the many that have received widespread criticism from experts and the general public for a lack of sustainability and the serious ecological damage caused by them both in New Zealand and elsewhere. While many fisheries are moving toward improvements in sustainability and harvest methods that reduce by-catch, partly driven by consumer demand, the progress is slow. It is clear that increased financial gains are not possible simply by increasing landings.

Seafood export growth from aquaculture expansion has been restricted in New Zealand due to a moratorium on aquaculture development in the early part of this decade and the numerous resource consents required for new operations. However, the recent removal of the moratorium and the passing of the Aquaculture Legislation Amendment Bill in 2008 should greatly facilitate future development (Mallard 2008). Fewer barriers to development in recent years has resulted in significant capital investment into the aquaculture of various new species. Examples include facilities developed by crown research institutes (e.g. National Institute of Water and Atmospheric Research), private companies (New Zealand King Salmon Company) and Iwi trust groups (Te Atiawa Manuwhenua Ki Te Tau Ihu Trust, Wakatu group). These kinds of initiatives are now being supported by a contestable fund made available by the government to facilitate aquaculture development. In total, NZ\$ 6.5 billion dollars has been allocated for “sustainable, high quality and value-added products” until the end of 2011 (Mallard 2008). The outcome of these investments should mature over the coming years, with the total value of the industry expected to reach NZ\$ 1 billion annually by 2025 (Mallard 2008).

1.2 Rationale for the thesis

1.2.1 Applied aspects

Given the limiting growth potential in the fishing industry outlined, increasing the value of existing products, by improving quality of caught items, is the most sustainable and cost effective way to increase capital gain. Furthermore, it is important to ensure a good price is attained for farmed products produced by the growing aquaculture industry. Fisheries and aquaculture businesses stand to benefit greatly from research into improved tissue integrity in number of ways: (1) by increasing the value of existing products catch per unit effort can be maximised. (2) These higher value products could create new markets (e.g. sashimi) from species previously considered unfit for purpose due to poor condition. Furthermore, (3) better harvesting protocols can reduce wastage and extend the shelf-life of products. (4) These benefits have the additive effect of reduced catch/production requirements to maintain industry profitability, and could therefore relieve fishing pressure on wild populations.

Understanding the physiology of both wild-caught and cultured species is fundamental to optimal harvesting procedures, peri-mortem treatment and post-harvest storage. A knowledge of the energetics associated with normal behaviours and those induced by fishing practices assists in establishing harvest processes that do not unnecessarily stress, exhaust or harm animals. However, data are still lacking both on the energetics of muscle from living animals and also how this may impact tissue degradation post-mortem (Iversen *et al.* 2003; Bosworth *et al.* 2007). This is particularly so for New Zealand animals. These data are crucial in understanding the onset of rigor mortis and cellular autolysis that occurs once both aerobic and anaerobic metabolism have irreversibly deteriorated. Furthermore, the relative contribution of the muscle type favoured for consumption in fish - white muscle for the most part, red and pink muscle to a lesser extent - to total live (and post-mortem) metabolic demand is relatively uncharacterised.

Knowledge of the differences in the metabolic requirements of these muscles is vital since these factors greatly affect the metabolic state in which these tissues reach the processors, or the marketplace in the case of live specimens (Iversen *et al.* 2003; Bosworth *et al.* 2007). Consequently this is one of the central themes of the current thesis.

1.2.2 Contribution to knowledge: physiology

Further to the applied aspects outlined, the role of oxygen supply in metabolism and energetics in muscle and other tissues is also a central theme. This fundamentally important line of investigation in physiology is relevant to almost all life forms, since most organisms utilise oxygen to generate energy (Hochachka and Guppy 1987; Olson 2008). The arrangement of the skeletal myotome in fishes (outlined below), represents an excellent model for the study of vertebrate muscle as the fibre types differ spatially, metabolically and functionally (Goolish 1991). Applications from research in this area are vast. For example, research into the role of oxygen supply in metabolism is important in medicine, exercise physiology, comparative physiology, ecology and behaviour, to name but a few. Thus, oxygen and its relationship to metabolism and energetics in vertebrate muscles, with special reference to fishes, are investigated in all five studies presented in the thesis. Important factors influencing oxygen delivery and its role in energy metabolism are introduced below.

1.3 Oxygen and its role in metabolism

1.3.1 Harnessing oxygen for energy

Oxygen concentration in the atmosphere (currently 21%) has varied throughout the evolution of life on the planet (Schopf 1978; Kasting 1993), increasing in concentration from about 2 billion years ago in the previously anoxic atmosphere (Schopf 1978; Kasting 1993). This change is thought to have been a significant evolutionary driving force (Schopf 1978).

It is generally accepted that approximately 1-2 billion years ago, the ancestors of most eukaryotes came together in a symbiotic relationship (Schopf 1978; Ballantyne and Chamberlin 1988). Based on similarities in ribosomal protein sequences, tRNA characteristics and histone-like proteins, it has been suggested that the cytoplasmic cell belonged to the archaebacteria (Ballantyne and Chamberlin 1988). The endosymbiont, which is now known as the mitochondrion, is thought to have come from another kingdom. Based on 16S ribosomal RNA sequences, these have been identified as belonging to the α subdivision of the purple bacterial phylum - the present day forms are bacteria with an electron transport chain using oxygen as a terminal electron receptor (Ballantyne and Chamberlin 1988). The newly included endosymbiont was exploited by the cytoplasmic cell for its ability to harness energy, which provided a constant source of adenosine triphosphate (ATP), and provided a mechanism to neutralise the ever increasing atmospheric concentration of a very toxic gas (oxygen) (Schopf 1978).

In almost all extant eukaryotic organisms, the utilisation of oxygen by mitochondria to generate ATP is conserved (Schopf 1978). This process is known as aerobic metabolism, which supplies the majority of the ATP for cellular activities and is crucial for muscle contraction. The converse of this, anaerobic metabolism, which is also present in almost all known eukaryotes, usually requires oxygen for recovery of metabolite pools (e.g. Lee *et al.* 2003a; Lee *et al.* 2003b). This is known as oxygen debt.

1.3.2 The critical role of the cardiovascular system in metabolism

In most metazoans some form of cardiovascular system is present (Withers 1992b). In vertebrates, the cardiovascular system plays an integral role in the transport of metabolites, most importantly oxygen, and humoral factors to tissues. The system is also crucial for the elimination of by-products of catabolism and waste products. The central element, the heart, is a muscular pump under both neural and humoral control which ejects blood from a thick-walled ventricle (in many species) propelling it through the body, ultimately reaching the peripheral circulation (Opie 1998). Haemoglobin contained within erythrocytes is responsible for the transport of oxygen to tissues. Loading of haemoglobin with oxygen occurs in the pulmonary, gill or cutaneous circulations, depending on species. From capillaries, oxygen moves down the partial pressure gradient into cells where it is used by mitochondria for oxidative phosphorylation (Opie 1998). Carbon dioxide from tissues enters the blood, is converted to HCO_3^- in the red blood cells and is transported into the pulmonary circulation where it is eliminated at the lungs (Opie 1998).

The fish heart is divided into four functional units: the sinus venosus, which stores and collects venous blood, the thin-walled atrium which has a high storage capacity and weak propulsive force; the ventricle which serves as the primary propulsive force and the conus or bulbus arteriosus which absorbs and stores the kinetic energy produced by ventricular blood ejection (Olson and Farrell 2006). The vasculature (arteries and veins) dynamically controls blood flow by contracting or relaxing constituent smooth muscle. Another significant component of the vasculature is the endothelium, which has a vast surface area and combined mass - greater than that of the liver in mammals - with many metabolic and endocrine activities (Olson and Farrell 2006). Different vessel types are recognised; elastance, conductance, resistance, exchange and capacitance vessels (Olson and Farrell 2006). In fishes the gills metabolise or remove many hormones affecting the heart (Olson and Farrell 2006).

1.4 Energy metabolism

1.4.1 Energetic pathways in muscle

Muscle cells have a basic energy cost of survival, including maintenance of intracellular ion-gradients and protein synthesis (Guppy and Withers 1999). In addition, muscle (particularly striated muscle) has a considerable scope to increase ATP utilisation (Champe *et al.* 2008), to accommodate the energetically expensive process of muscle contraction.

The need for a constant supply of ATP, coupled with the varied requirements of the different muscle types has meant metabolic pathway and substrate preferences have evolved. These can be classified into aerobic (involving the electron transport chain and oxidative phosphorylation) and anaerobic (involving substrate level phosphorylation) metabolic pathways. The two processes are summarised in figure 1.1.

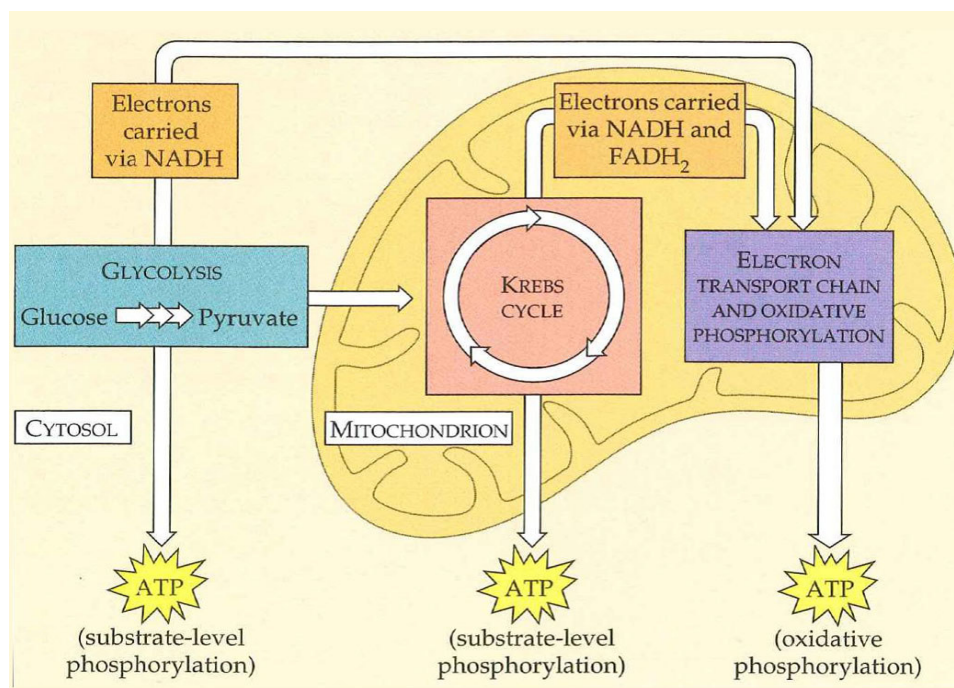


Figure 1.1. Schematic representation of anaerobic and aerobic ATP generating processes using glucose as a substrate. Modified from Campbell *et al.* (1999b).

1.4.2 Aerobic metabolic pathways

Aerobic metabolism, also referred to as oxidative phosphorylation, involves the production of ATP by ATP-synthase, a mitochondrial membrane bound enzyme, which is powered by the electron transport chain, with oxygen used as the final electron acceptor (Champe *et al.* 2008). This occurs through the generation of metabolic intermediates (adenine dinucleotide (NADH) and flavin adenine dinucleotide (FADH₂)) from acetyl-CoA. These intermediates can donate electrons to the enzyme complexes of the mitochondrial electron transport chain, which is energetically favoured because NADH and FADH₂ are strong electron donors while oxygen is a potent electron acceptor (Champe *et al.* 2008). This process drives proton translocation across the mitochondrial inner membrane which in turn drives conformational changes in ATP synthase which phosphorylates ADP to create ATP (Champe *et al.* 2008). These processes are summarised in figures 1.2A and 1.2B. The key to oxidative phosphorylation is an adequate supply of acetyl-CoA or other intermediates (in the case of amino acids) to fuel the tricarboxylic acid cycle and oxygen to act as the terminal electron acceptor of the mitochondrial electron transport chain (Champe *et al.* 2008). Acetyl-CoA can be derived from three sources: (1) various carbohydrates (e.g. glucose), (2) β -oxidised fatty acids or from (3) various modified amino acids (Champe *et al.* 2008) (figure 1.3). The net yield from one molecule of glucose is approximately 29 molecules of ATP (Brand 2003).

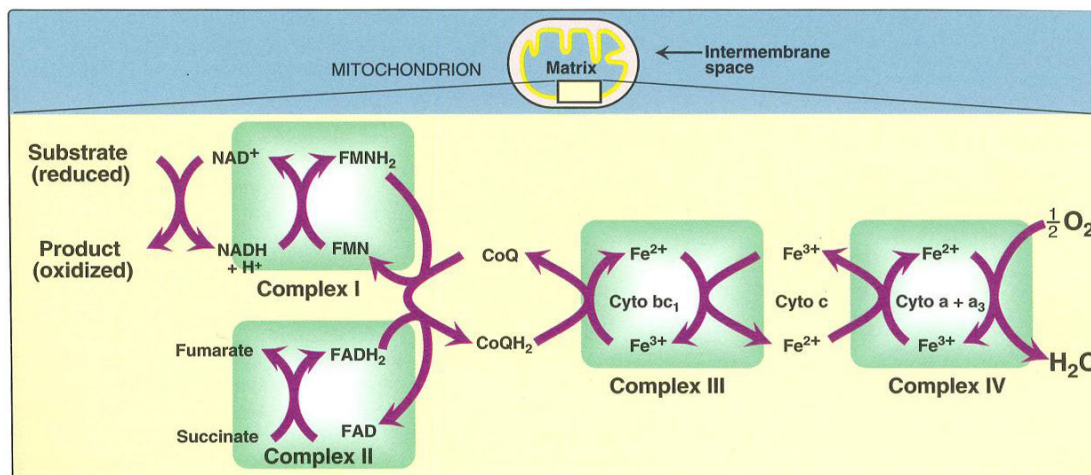
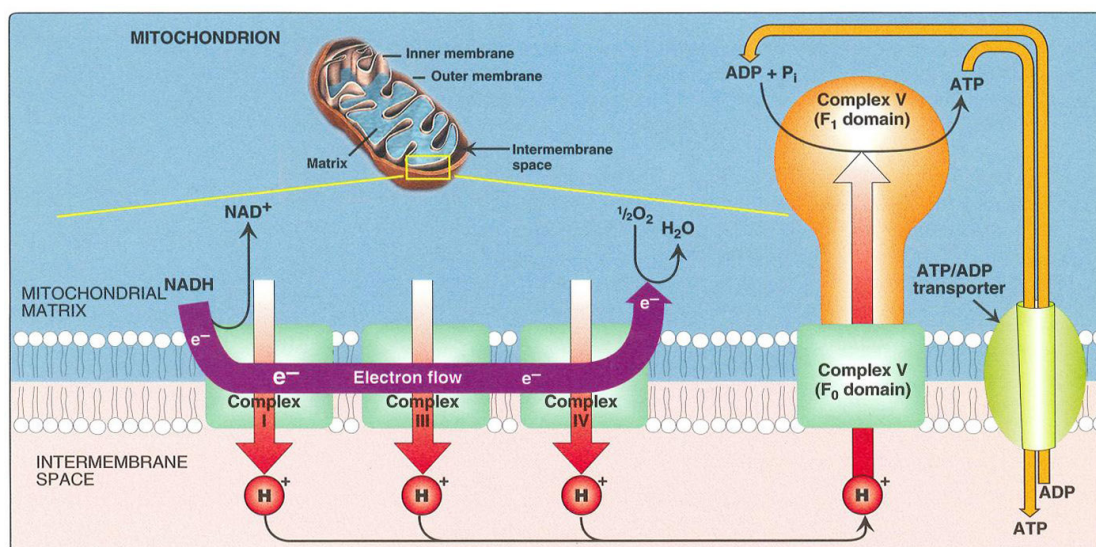
A**B**

Figure 1.2. Schematic representation of the electron transport chain located in the inner mitochondrial membrane. **A.** Important oxidation – reduction steps involved in transfer of electrons along the electron transport chain associated with enzyme complexes I-IV. Note complex V is not shown. NADH is a strong electron donor and oxygen is a strong electron acceptor. **B.** Mitochondrial electron transport chain coupled to the enzyme complex, ATP synthase (complex V/F₁/F₀ ATPase). Electron transport drives a proton gradient created by complexes I, III and IV which drives conformational changes in the F₁ domain of ATP synthase which catalyses the synthesis of ATP from ADP and P_i. ATP and ADP are translocated by an ATP/ADP transporter into the intermembrane space. Note complex II is not shown. Modified from Champe *et al.* (2008).

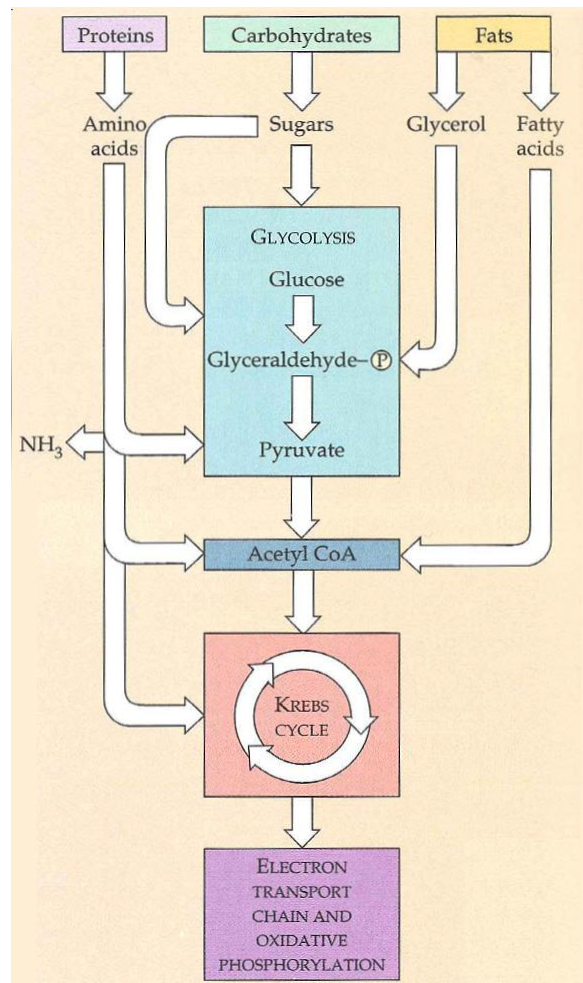


Figure 1.3. Sources of substrates for the tricarboxylic acid cycle (Krebs cycle). Modified from Campbell *et al.* (1999b).

In fish red muscle oxidative phosphorylation is thought to meet the majority of the energy requirements necessary for homeostasis and for sustained swimming, which can be almost continuous in some species (Wang *et al.* 1994; Richards *et al.* 2002a). The predominant pathway for tricarboxylic acid cycle substrates may vary under different conditions. If the animal receives adequate energy through its diet, metabolism of stored carbohydrate (figure 1.4B) and lipid predominates as the primary source of acetyl-CoA from pyruvate (Richards *et al.* 2002a), but if starved, the animal may revert to protein catabolism for pyruvate (Yang and Somero 1993). Fish white muscle is able to meet its basal metabolic requirements by oxidative phosphorylation (Milligan 1996).

However, when recruited for “burst-type” activity, the aerobic capacity of the tissue is exceeded and there is a reliance on anaerobic pathways to meet energy requirements (Johnston 1975; Milligan and Wood 1987; Milligan and McDonald 1988; Pagnotta and Milligan 1991; Milligan 1996; Schulte *et al.* 1992; Wang *et al.* 1994; Thomas *et al.* 1999).

1.4.3 Anaerobic metabolic pathways

When aerobic potential is exceeded or oxygen supply is limiting or absent, creatine phosphate, via the creatine kinase pathway (creatine phosphate + ADP + H⁺ ↔ creatine + ATP) and anaerobic glycolysis can contribute to energy supply (figure 1.4C) (Hochachka and M^cClelland 1997). Glycolytic energy production in the absence of oxygen is by the direct conversion of glucose to two molecules of pyruvate by NADH conversion to NAD⁺ (figure 1.5). This results in a net yield of 2 molecules of ATP per molecule of glucose. As a consequence of this process, lactate (coupled to NAD⁺ oxidation to NADH) and H⁺ accumulate in cells, since they are generated faster than they can be metabolised. The H⁺ generated readily diffuses into the blood. In mammalian myocytes, lactate diffuses out of the cell, down its concentration gradient, and is actively transported via monocarboxylate transporters into the bloodstream where it is translocated to the liver and converted to pyruvate by lactate dehydrogenase and eventually back to glucose which is used for glycogenesis at sites where the substrate is required (the Cori-cycle, Campbell *et al.* 1999b).

As mentioned, anaerobic glycolysis prevails as the primary process for generating ATP in fish white muscle during “burst-type” exercise. In this tissue the end products of this process (lactate and H⁺) are known to remain primarily *in situ*, as fish are thought to lack a Cori-cycle (Kam and Milligan 2006). As a consequence of the high intracellular lactate concentration, a small proportion is lost into the blood (Milligan 1996) via diffusion post-exercise (Sharpe and Milligan 2003).

This diffusion is minimal, since the sarcolemma is relatively impermeable to lactate, despite a large concentration gradient favouring diffusion (Laberee and Milligan 1999).

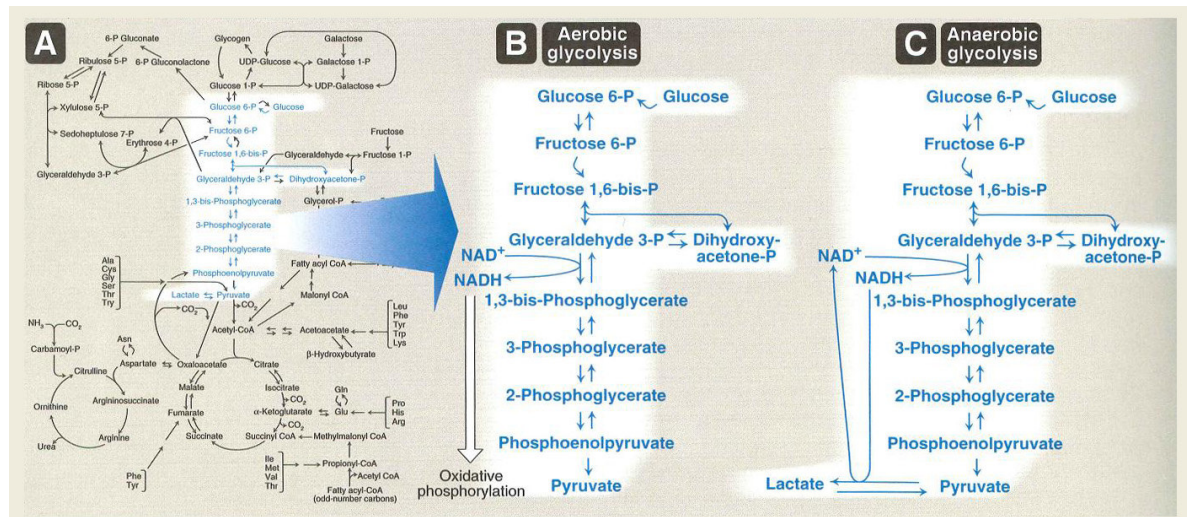


Figure 1.4. The fate of glucose with and without oxygen. **A.** Important steps in energy metabolism showing glucose, derived from glycogen as one of the essential pathways of energy metabolism. **B.** Aerobic glycolysis. **C.** Anaerobic glycolysis. Modified from Champe *et al.* (2008).

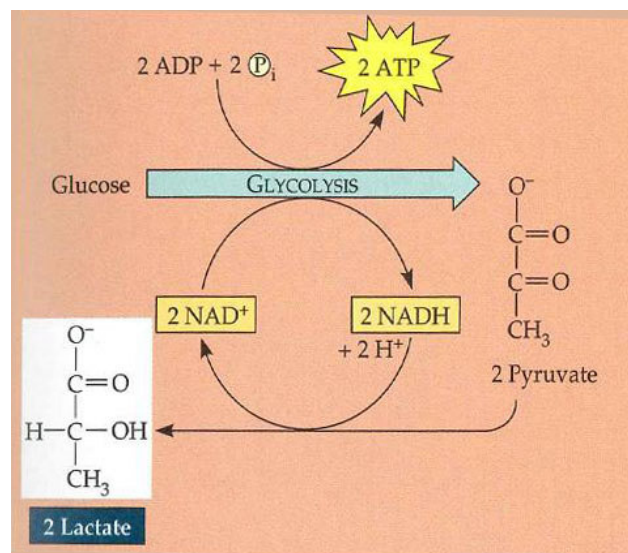


Figure 1.5. Substrate level phosphorylation resulting in the formation of pyruvate. Lactate formation from pyruvate follows and is coupled to $NADH$. The process results in the formation of 2 molecules of ATP from every glucose molecule, and results in lactate and H^+ accumulation. Modified from Campbell *et al.* (1999b).

In fish, lactate is taken back up from the bloodstream into myocytes via a low-affinity, high-capacity monocarboxylate transporter ($K_m=55.6 \text{ mmol.l}^{-1}$ and $V_{\max}= 44.5 \text{ nmol.mg}^{-1} \text{ protein.min}^{-1}$), and subsequently converted to pyruvate, via lactate dehydrogenase and used as a substrate for oxidative ATP generation (Laberee and Milligan 1999). This lactate meets the cell's basal metabolic requirements, while intracellular lactate is “spared” for *in situ* glyconeogenesis (Kam and Milligan 2006). Thus in fish white muscle, energy is conserved by avoiding the export of lactate to the liver via the bloodstream.

Lactate-fuelled glyconeogenesis is known to occur only once muscle H^+ load begins to clear, which is linked to lactate metabolism (Hochachka 1985), and can begin only once a significant amount of the oxygen debt associated with “burst-type” activity is repaid (Kam and Milligan 2006). The process is also greatly accelerated by low tissue glycogen concentration and high exogenous hormone concentrations (i.e. glucocorticoids and adrenaline) (Frolow and Milligan 2004). In contrast to mammalian muscle cells, blood glucose plays virtually no role in the restoration of white muscle glycogen stores in teleost fishes, contributing only 0.36% to the re-synthesised glycogen pool 6-8 hours post-exercise in rainbow trout (*Oncorhynchus mykiss*) (Pagnotta and Milligan 1991). Other substrates such as fatty acids and amino derivatives play a lesser role in recovery from “burst-type” exercise (Kam and Milligan 2006).

1.5 Muscle

Important features of vertebrate muscles, with special reference to fishes are introduced below.

1.5.1 Vertebrate Muscle

Muscle is a specialised tissue found in both invertebrates and vertebrates and is under neural and humoral control (Withers 1992a; Campbell *et al.* 1999a). It is designed to contract (shorten) and relax (lengthen) in a coordinated fashion.

Muscle can be generally grouped into striated and smooth muscle. Striated muscle can be further divided into cardiac and skeletal muscle. This division is based on the degree of organisation of the contractile apparatus (Withers 1992a). Smooth muscle lacks the visibly ordered structure typical of striated muscle and distinct differences exist between the various types of striated muscle. Despite these differences, all muscle cells share a common contractile mechanism.

Empirical evidence has validated the sliding filament model of muscle contraction (Luther *et al.* 1995; Campbell *et al.* 1999a). According to this model, contraction is due to the interaction between two specialised muscle proteins; actin and myosin. These proteins bind to one another, causing them to slide past each other. This process relies on ATP-mediated conformational changes which result in thick myosin filaments forming reversible cross-links to the parallel thin actin filaments via globular head regions. The two proteins sliding past each other effectively shorten the functional muscle unit. This process is known to be calcium and magnesium dependent. Activation of muscle contraction occurs via excitation-contraction coupling; neural input depolarises the sarcolemma via an action potential, resulting in calcium release. Calcium ions binds to a specialised protein complex, the troponin complex, causing the regulatory protein tropomyosin to change conformation, freeing myosin binding sites on the actin filament. In most vertebrate striated muscles, the source of calcium is the sarcoplasmic reticulum that forms the T-tubule system, which greatly facilitates the delivery of calcium ions. In contrast, many fish hearts have a poorly developed sarcoplasmic reticulum and generally have small muscle fibres, which facilitates the entry of calcium ions across the sarcolemma (Farrell 1996; Shiels and Farrell 1997). Magnesium is utilised in conjunction with ATP, forming the ATP-Mg²⁺ substrate for the enzyme myosin ATPase.

1.5.2 Striated muscle

The two types of vertebrate striated muscle, skeletal and cardiac muscle, differ more in their innervation pattern and mechanical and electrical properties than in ultrastructure (Luther *et al.* 1995; Withers 1992a). Both are composed of a series of parallel units arranged in a hierarchical fashion. The basic unit of muscle tissue is the muscle fibre. This is a multinucleated cell formed by the fusion of multiple cells during embryonic development (Withers 1992a). The fibre consists of longitudinally arranged myofibrils, composed of myofilaments. The functional contractile unit of striated muscle cell is the sarcomere. It is this unit that gives striated muscle its most obvious feature, pronounced banding, which appears as alternately dark and light under polarised light. Only myosin filaments are found in the dark banded regions which are referred to as A bands. The lighter regions where only actin filaments are found are referred to as I bands. Myosin and actin filaments are anchored along the M and Z lines respectively.

1.5.3 Skeletal muscle

Skeletal muscle is usually under voluntary control, mediated by motor neuron synaptic connections to individual muscle cells. The different skeletal muscle fibre types can be classified on the pattern of activation, structure and function (Johnston and Ward 1975; Withers 1992a; Luther *et al.* 1995; Campbell *et al.* 1999a).

There are two main activation patterns in muscle: fast and slow activation, which relates to the speed at which muscle fibres contract (Johnston 1991). Slow fibres are generally slow contracting and slow to fatigue (Johnston 1991). These muscle cells rely primarily on oxidative (aerobic) metabolism for a consistent supply of ATP for continued muscle work. Myocytes with high aerobic potential typically contain many mitochondria, rich in cristae, and contain high cytosolic concentrations of the haem-protein, myoglobin.

This protein is thought to facilitate oxygen transfer from the circulatory system to the mitochondria and to act as a buffer to perturbations in oxygen availability (Wittenberg *et al.* 1975; Wittenberg and Wittenberg 1987; Wittenberg and Wittenberg 2003; Wittenberg and Wittenberg 2007). Slow twitch fibres are also referred to as red muscle due to the red appearance of the myoglobin. Fast twitch muscle fibres contract and fatigue much more rapidly than their counterparts. These fibres are employed for rapid movement and rely primarily on anaerobic metabolism, meaning they can become quickly depleted (Johnston 1975; Johnston 1991). Fast twitch muscle fibres are also referred to as white muscle as they have little or no myoglobin and have fewer mitochondria which typically contain less cristae than slow twitch muscle fibres.

While most fibres can generally be classified as either fast or slow twitch, there is a great variation in specific activation speed and the biochemical pathways to fuel the locomotory response elicited by contraction (Johnston and Ward 1975; Rome 1994). Bat cricothroid muscle is an example of a fast red muscle (Johnston and Ward 1975). Many mammalian muscles are termed mosaic muscle (Withers 1992a). This means that there are a mix of slow (red) and fast (white) muscle fibres in various proportions in different muscle groups specialised for specific functions. Certain muscles, for example the soleus muscle in mammals, are dominated primarily by red fibres (Withers 1992a). The situation in other animals is somewhat different. Fish for example have separate populations of red and white muscle fibres (Johnston 1991; Lauder 2006). Intermediate (pink) muscle, found in variable quantities in most species, represents a unique fibre type sharing properties of both red and white muscle.

1.5.4 Skeletal muscle of fishes

The skeletal muscle of present day vertebrates reflects evolution around a rigid internal skeleton and a central backbone. The points of attachment that the skeleton provides allow for powerful muscle contractions which were critical to the evolutionary radiation of vertebrates (Griffith 1994). The typical vertebrate skeletal muscle cell evolved early; analysis of the musculature of the primitive protochordate, the ascidian *Ciona intestinalis*, revealed that typical vertebrate skeletal muscle characteristics, as determined by the presence of troponin 1 genes, had evolved before the ascidian/chordate divergence, possibly in an earlier deuterostome (Cleto *et al.* 2003). Surviving members of other primitive groups such as the cephalochordata, e.g. *Amphioxus* spp., show a series of V-shaped myotomes running at right angles to the axial notochord (Griffith 1994), which is similar to fossil remains of “Pikaia”, an extinct middle Cambrian cephalochordate (535 million years old) (Gardiner 1999). It is worth noting that the aforementioned *C. intestinalis* also shows an analogous series of “flanking rows of sarcomeric muscle cells” (Cleto *et al.* 2003). Similarly, within Craniata, the living cyclostomes (lampreys and hagfishes) show an equivalent series of myotomal blocks running the length of the notochord, which allow shortening of similar length in fibres across the width of the body (Flood 1965). In fact, this basic arrangement has remained relatively unmodified in all extant fishes; both chondrichthyans (Bone 1988) and osteichthyans (actinopterygii and sarcopterygii) (Millot and Anthony 1958; Takashima and Hibiya 1995; Dunn *et al.* 1981) show this basic pattern. Thus the general design has been retained despite extensive species radiation. This simple but highly effective arrangement, where multiple opposing segmental muscle blocks are anchored to a stiff but flexible central element that can be bent into sinuous waves, represents a highly effective system for locomotion in water, which is readily coordinated by motor neurons (Johnston and Ward 1975; Rome 1994; Lauder 2006).

The specialisation of the skeletal muscle cells into specific roles, based on functional requirements, resulted in the development of three distinct muscle fibre aggregations in fishes; red, pink and white muscle blocks. There is a great diversity in the number and spatial arranging of these muscle groups in extant fishes (Dunn *et al.* 1981). Even cephalochordates show a cryptic compartmentalisation of muscle sub-types. Hardisty (1979) describes sections within the “uniform myotome” (white muscle) of the cephalochordates that show myofibrils that have higher mitochondrial densities (red muscle), which are possibly incipient to differentiation in higher chordates. The most primitive chordate, the hagfish, also shows compartmentalisation of the three aforementioned muscle fibre types, which occur in the following proportions in a typical mid-body segment of skeletal muscle: 36% red fibres, 49% white fibres and 15% pink fibres (Flood 1965). Interestingly, the compartmentalisation of these fibres represents a unique arrangement which may be highly derived; myotomal blocks show a distinct stratification into bands, which run in a parallel arrangement to the notochord, comprised of a larger proportion of white muscle with a thinner band of red muscle on the dorsal surface of each myotomal block (Flood 1979). On the axial side of the myotome, a distinct population of intermediate fibres can be distinguished (Flood 1979).

In the majority of teleosts, with the exception of tunas and other highly active fish, most of the transverse cross sectional area of the myotome is made up of white muscle fibres, with red and intermediate fibres occupying only a thin band, concentrated along the lateral line into a wedge of muscle (Luther *et al.* 1995) (figure 1.6). Consequently, white muscle makes up the majority of the skeletal muscle mass in most species, which is generally between 50-60% of the total body mass (Greer-Walker and Pull 1975). This general arrangement is also present in extant chondrichthyans, sarcopterygii and other actinopterygii (Dunn *et al.* 1981; Bone 1988).

The white muscle of fishes generally has a less well developed vascular system (Luther *et al.* 1995; Egginton *et al.* 1988) and a smaller aerobic capacity (Moyes *et al.* 1989; Moyes and West 1995), due in most part to the differences in mitochondrial density, as opposed to efficiency (Leary *et al.* 2003).

The mitochondrial volume-density of white muscle is similar to mammalian (mosaic) skeletal muscles, but the mitochondrial volume-density of red muscle can be up to 10-fold greater (Leary *et al.* 2003). Typically, fish exhibit an approximately 5-fold difference in mitochondrial volume-density between red and white muscle; the density of the red muscles sometimes exceeding that of the heart (Moyes and Hood 2003).

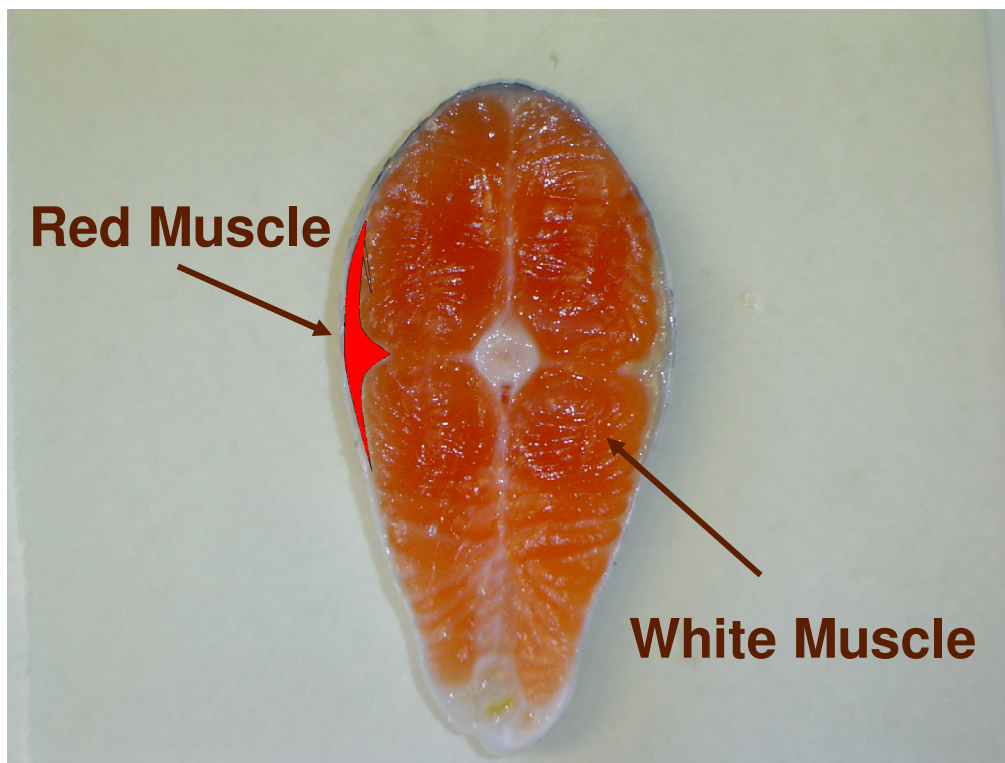


Figure 1.6. Cross-section of Chinook salmon myotome showing the locations of the red and white muscle. Red muscle (placed laterally, coloured red on the left) is predominantly aerobic. It is a slow twitch muscle, used for continuous swimming. White muscle (occupying the majority of the cross sectional area) is fast twitch muscle, that relies primarily on anaerobic metabolism for the “burst-type” swimming that is typical of escape and predatory behaviours and has large glycogen stores. Pink fibres are found between these two groups of muscle and contribute to both continuous and “burst-type” swimming. Photo: L.G. Forgan.

1.5.5 Cardiac muscle

Cardiac muscle is found only in the heart, which is under involuntary neural and humoral control (Withers 1992a; Campbell *et al.* 1999a; Olson and Farrell 2006). Composed of striated muscle cells, this tissue is designed to contract with great force. Cardiac myocytes are similar to skeletal muscle in that they contain many mitochondria and the haem protein myoglobin, but they do differ morphologically; in avian and mammalian hearts they are small bifurcating cells that are usually uni- or binucleate (Opie 1998; Withers 1992a) and joined by specialised regions known as intercalated discs - where gap junctions couple excitation from one cell to the next - making for a functional syncytium (Opie 1998). This is also true of other vertebrate groups, although the cells do not bifurcate. The spread of cellular depolarisation must occur in a coordinated fashion, so as to efficiently eject blood from the various chambers of the heart. Thus, specialised pacemaker regions in the heart, which depolarise faster than all other regions initiate a coordinated membrane depolarisation that results in a contraction that spreads along the heart in a given direction (Withers 1992a; Opie 1998). Since the heart must be continuously active, cardiac muscle fibres rely critically on aerobic metabolism - interruption of the supply of oxygen to the heart can be extremely detrimental (Nelson *et al.* 2005). Brief periods of ischemia are associated with tissue necrosis (infarction) and oxidative stress on reperfusion which can both cause severe damage to the heart (Nelson *et al.* 2005). Consequently, the contribution of anaerobic glycolysis to energy supply during hypoxia is important (Farrell 2007).

1.5.6 Smooth muscle

Smooth muscle does not have the obvious striations of striated muscle and consists of small, spindle shaped cells with a single nucleus (Withers 1992a). Furthermore, smooth muscle cells typically lack myoglobin, although there are examples of smooth muscle cells that do contain small quantities of the protein

(Qui *et al.* 1998). As outlined, the basic contractile mechanism is the same as that of the striated muscles, although in smooth muscle the source of calcium ions is cytosolic (Campbell *et al.* 1999a). Smooth muscle is found in many locations, with most occurring in the viscera and in the vasculature as fenestrated sheets of cells (Withers 1992a). Typically smooth muscle lining a luminal surface such as the stomach and the vasculature occurs in two distinct layers, an outer longitudinal and inner circular layer. These layers act in a coordinated fashion, as action potentials propagate down the length of the muscle sheets via synapses (Withers 1992a). This often results in entire muscular beds contracting or results in rhythmic activity, as is often the case in visceral smooth muscle cell populations. Smooth muscle may also contract or relax upon exposure to certain humoral factors in both vascular (e.g. adrenaline, Hjelm Dahl *et al.* 1979) and gastric smooth muscle (e.g. cholecystokinin, Forgan and Forster 2007). Similarly, changes in smooth muscle tone can mitigate physiological stressors such as hypoxia (Olson *et al.* 2001) or changes in pH (Smith *et al.* 2006). Smooth muscle cells rely on both aerobic and anaerobic metabolic pathways for energy production (Lindqvist *et al.* 2002).

1.6 Aims and outline of the thesis

The overall aim of the current PhD project was: to gain a fundamental understanding of metabolism and energetics in living and post-mortem muscles - primarily in relation to the supply of oxygen - from commercially important species of fish (Chinook salmon, blue cod, and New Zealand snapper) and other relevant vertebrates. This aim was addressed in number of discrete but related studies employing a number of techniques in intact animals, perfused and isolated preparations. These studies form the basis of the current doctoral thesis and 5 scientific papers. Thus, the work contributes to the scientific literature. Consequently, chapters 2, 3, 4, 5 and 6 are presented in the format in which they will appear in the published literature.

At the time of going to press, articles written from the data presented in chapters 2 and 6 have been published (see appendices 2 and 3) and articles from data presented in chapters 3-5 are under review or in preparation. Conference presentations, titles and abstracts from material presented in this thesis are included in appendix 1.

In brief, experimental work completed in this thesis includes the investigation of the metabolic rate in muscle and its relationship to the oxygen delivery and partial pressure (PO_2), in perfused (chapter 2) and isolated muscle tissue (chapter 3) respectively. With respect to the latter, the results are compared with the responses of the muscles of other vertebrate taxa (the Pacific hagfish (*Eptatretus cirrhatus*) and the rat (*Rattus rattus*)). Biochemical pathways associated with these responses were also elucidated. Investigation of the effects of isoeugenol, a commonly used anaesthetic, and hydrogen sulphide (H_2S), a molecule touted as capable of reducing metabolic rate in mammals (Blackstone *et al.* 2005), on metabolic rate, ventilation frequency and physical activity also forms a major component of this thesis (chapter 4). Furthermore, anaerobic metabolic rate and associated energetics in white muscle from fish harvested under different conditions - representative of those typical during commercial handling and slaughter - were also investigated (chapter 5). Finally, a study on the vasoactive effects of H_2S in two ancestral vertebrates, the hagfish and lamprey (*Petromyzon marinus*), contribute to the emerging biological role of H_2S as a key mediator of oxygen-sensing in the vasculature of vertebrates (chapter 6). In chapter 7, the implications of the findings of the thesis are discussed and possible future work outlined.

Chapter 2

Oxygen consumption and blood flow distribution in perfused skeletal muscle of Chinook salmon (*Oncorhynchus tshawytscha*)

2.1 Abstract

An isolated, perfused salmon tail preparation showed oxyconformance of VO_2 at low oxygen delivery rates. Addition of pig red blood cells to the perfusing solution at a haematocrit of 5 or 10%, increasing the capacitance, resulted in oxyregulation of VO_2 by the tail tissues. Below $60 \text{ ml O}_2 \cdot \text{kg}^{-1} \cdot \text{h}^{-1}$ of oxygen delivery (DO_2), VO_2 was delivery dependent. Above this value additional oxygen delivery did not increase VO_2 of resting muscle above $35 \text{ ml O}_2 \cdot \text{kg}^{-1} \cdot \text{h}^{-1}$. Following electrical stimulation, VO_2 increased to $65 \text{ ml O}_2 \cdot \text{kg}^{-1} \cdot \text{h}^{-1}$, with a critical DO_2 of $150 \text{ ml O}_2 \cdot \text{kg}^{-1} \cdot \text{h}^{-1}$. Dorsal aortic pressure fell to 69% of the prestimulation value after 5 minutes of stimulation and to 54% after 10 minutes. Microspheres were used to determine blood flow distribution (BFD) to red (RM) and white muscle (WM) within the perfused myotome. Mass specific BFD ratio at rest was found to be 4.03 ± 0.49 (RM:WM). After 5 minutes of electrical stimulation the ratio did not change. Perfusion with Ringer containing the tetrazolium salt, 3-(4,5-dimethylthiazol-2-yl)-2,5-diphenyl tetrazolium bromide (MTT) revealed significantly more mitochondrial activity in RM. Formazan production from MTT by succinate dehydrogenase was directly proportional to time of perfusion in both red and white muscle. The mitochondrial activity ratio (RM:WM) did not change over 90 minutes of perfusion.

2.2 Keywords

Oxygen consumption, skeletal muscle, salmon, blood flow, perfusion

2.3 Introduction

Oxygen consumption (VO_2) by skeletal muscle preparations in a number of vertebrate animals has been shown to conform to two distinct trends; oxyconformance at levels of oxygen delivery (DO_2) below the critical oxygen tension and regulation of VO_2 at higher levels of delivery (Kolář and Janský, 1984; Hogan *et al.* 1992; Boutilier 2001b; Shenkman *et al.* 2003). Furthermore, the rate of VO_2 in perfused skeletal muscle preparations has been shown to be dependent on the level of physical activity (Ruderman *et al.* 1980; Hogan *et al.* 1992; Berlin *et al.* 2002; Schenkman *et al.* 2003). These observations suggest that once oxygen delivery satisfies the metabolic requirement of skeletal muscle, VO_2 is delivery independent. During increased aerobic muscle work and while recovering from anaerobic activity the oxygen requirement of muscle increases. Furthermore, basal metabolic rate and aerobic scope of muscle is related to the fibres that constitute it. For example, mitochondrial density (Egginton and Sidell 1989) and aerobic metabolic activity (Ruderman *et al.* 1980) are greater in red muscle (RM) than white muscle (WM).

I have developed a preparation to study the metabolic rate of a section of fish myotome, which is primarily WM. I rapidly cannulate the dorsal aorta (DA) and caudal vein (CV) of a transaxially sectioned salmon. Perfusion at physiological pressure with an osmotically balanced physiological saline with a low hematocrit (Hct) supplies adequate oxygen to the preparation. The use of red blood cells (RBCs) in perfusion solutions has been shown to contribute significantly to myocardial myoglobin saturation (Schenkman *et al.* 2003) and performance (Berlin *et al.* 2002). RBCs are also used in isolated rat hindquarter experiments (e.g. Ruderman *et al.* 1980). Diluted or undiluted natural whole blood is also sometimes used in this type of preparation (Sutherland and Hearse 2000). Extracorporeal haemoglobin (Hb), while useful in delivering oxygen, has been shown to be responsible for numerous deleterious side effects in isolated preparations and human patients (Jones 1995).

In addition to achieving adequate oxygen supply, the perfusion pressure was maintained close to the dorsal aortic pressure (DAP) reported for Chinook salmon *in vivo*. Rothwell *et al.* (2005) report a resting value of 41.2 ± 3.4 cm H₂O and Hill and Forster (2004) report a slightly higher value of 46.0 ± 1.9 cm H₂O.

While much data on VO₂ in perfused skeletal muscle preparations have been reported using mammalian models, no study to date has measured VO₂ in perfused skeletal muscle of a fish. Therefore, the aim of the present study was to (1) develop a viable perfusion preparation for the study of metabolism in teleost skeletal muscle, (2) indirectly measure the basal metabolic rate in the preparation, (3) determine the effect of simulated exercise and (4) elucidate the relationship between DO₂ and VO₂. The latter was achieved by manipulating perfusate flow (Q) and Hct. In addition, (5) the effects of simulated exercise on DAP and the (6) blood flow distribution (BFD) between WM and RM are reported. (7) Mitochondrial activity in the preparation over time in both WM and RM compliment these data.

2.4 Materials and Methods

2.4.1 Animals

Female Chinook salmon (*Oncorhynchus tshawytscha*, Walbaum) (mass 1.470 ± 0.085 kg; fork length 46.98 ± 0.96 cm; condition factor 1.40 ± 0.04 ; n = 28) were obtained from a local freshwater salmon farm (Isaac Salmon Farm, Canterbury, New Zealand). The animals were transferred from commercial raceways, where they had been fed up until the time of transfer on Reliance stock feeds salmon pellets (CRT, Dunedin, New Zealand), into an 1800 L capacity holding tank which had a continuous flow of high quality bore-water (11 °C). The animals were not fed after transfer to the holding tanks. Fish were left undisturbed for a minimum of 48 hours before being used in an experiment, and used within 2 weeks of transfer.

Prior to an experiment, the fish were anaesthetised to stage 4-5 (not reactive to stimuli, but still showing limited ventilation: Summerfelt and Smith 1990) with AQUI-S™ (AQUI-S NZ, Lower Hutt, New Zealand) at a concentration of 22 ppm (0.011 g.L^{-1}). The anaesthetic was introduced gradually into the holding tank, without alerting the animals, and mixed with a Maxi-Jet MJ1000 water pump (Aquarium Systems, Loreggia, Italy). The animals were subsequently netted and placed into 20 L of holding tank water (22 ppm AQUI-S™) in an insulated transport container. The water was gassed with 100% oxygen for 10 minutes before transfer and the air-space in the container filled with oxygen. The animals were then transported to the University. Immediately on arrival (<25 min), the immobile fish was placed in a sling and killed by inserting the tip of an “iki jime” fish harvesting tool directly into the brain. This method of killing results in minimal stress and muscular activity. All manipulations described in this manuscript were approved by the University of Canterbury Animal Ethics Committee.

2.4.2 Tail preparation

Isolated salmon tails ($300 \pm 17 \text{ g}$) were prepared immediately after death. Approximately 1 ml of a 0.9% NaCl solution containing heparin sulphate ($2500 \text{ IU.ml}^{-1}.\text{kg}^{-1}$) was administered directly into the DA through the roof of the mouth, and allowed to circulate for several minutes. A transaxial cut was then made around the entire circumference of the animal, immediately caudal to the dorsal fin, leaving only the spine and haemal arch intact. This cut was repeated a second time c.2.5 cm caudal to the first. All the tissue between the two cut surfaces was then dissected away. The vertebral column was then cut, leaving a 2.5 cm section which could be ligatured to secure the cannula in the DA and CV. The tail was quickly weighed before the DA was cannulated with an appropriately sized polythene cannula with oxygenated perfusion solution (10°C), flowing through it at an initial flow rate of $1.0 \text{ ml.min}^{-1}.\text{100g}^{-1}$. Flow was generated by a Gilson Minipuls 3 perfusion pump (Villers, Le Bel, France), calibrated before each experiment and validated at the end. The DA was cannulated within 1 minute of the final cut being made.

An outflow cannula was fitted to the CV, and the height of its outflow was set to the height of the CV. Profuse bleeding from the DA and CV prevented air entering either vessel. Once the cannulae were in place, the vertebral column and surrounding tissue was ligatured to further secure them. Flow through the preparation was adjusted to manipulate oxygen delivery ($\text{c.}3.25 \text{ ml} \cdot \text{min}^{-1} \cdot 100\text{g}^{-1}$) while maintaining physiological pressures. There was a 10 minute equilibration period before VO_2 measurements were made. The whole preparation was housed in an insulated box held at 10°C , with a Tropicool XC3000A (Christchurch, New Zealand) temperature control unit. Major components of the perfusion preparation are shown in figure 2.1.

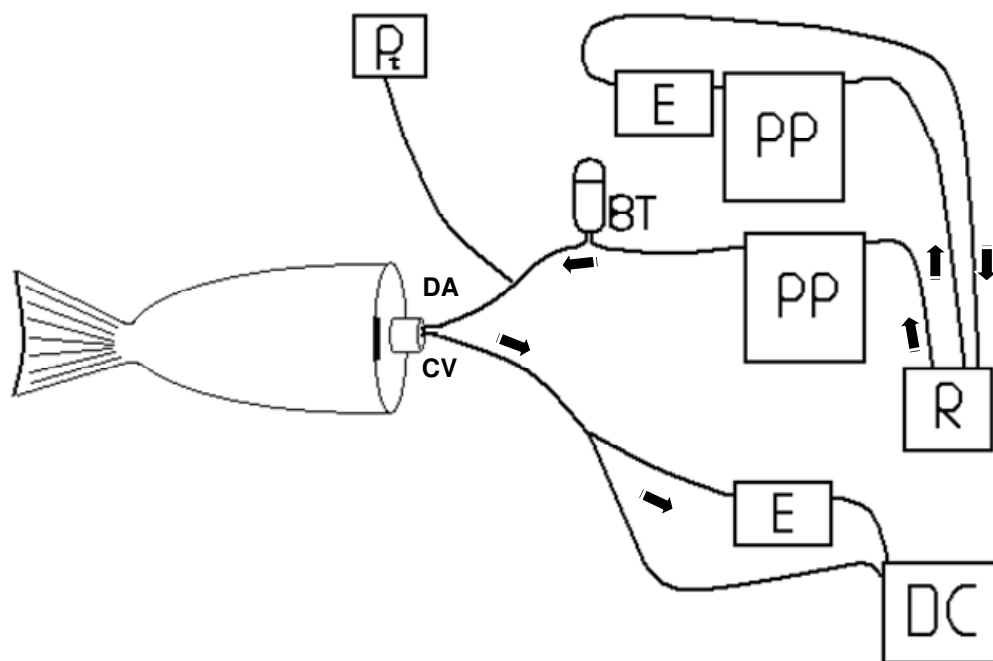


Figure 2.1. Schematic representation of the isolated fish tail perfusion model, developed to study VO_2 . R-Ringer, PP-peristaltic pump, E-electrode, BT-bubble trap, Pt-pressure transducer, DC-drop counter, DA-dorsal aorta and CV-caudal vein. Arrows indicate the direction of flow.

2.4.3 Perfusion solution

The tail preparation was perfused with a physiological saline modified from Clements and Rees (1998). The composition of the freshwater teleost saline (FTS) was (in mM): NaCl 136.9; KCl 2.1; MgCl₂ 1; CaCl₂ 1.3; glucose 10; HEPES (N-[2-Hydroxyethyl] piperazine-N=[2-ethane-sulfonic acid]) acid form 3; HEPES sodium salt 7.0; Na⁺-glutamate 0.3; L-glutamate 0.4; Na⁺-aspartate 0.02; DL-carnitine 0.05; polyvinylpyrrolidone (PVP) (mw 40,000) 30 g.L⁻¹; bovine serum albumen (BSA) 20 g.L⁻¹ (Invitrogen Corporation, Auckland, New Zealand); Insulin 1 mg.L⁻¹; TPP-co-carboxylase 1 mg.L⁻¹). The FTS had an osmolality of 299 ± 5 mOsmol.l⁻¹ and pH of 7.6. The FTS was filtered through #1 Whatman cellulose filter paper (Maidstone, Kent, UK) and stored for no more than a week at 4°C. In mitochondrial activity experiments, the tetrazolium salt, 3-(4,5-dimethylthiazol-2-yl)-2,5-diphenyl tetrazolium bromide (MTT) was added to FTS at a concentration of 1 mg.ml⁻¹.

2.4.4 Chemicals

All chemicals listed in this manuscript were sourced from Sigma-Aldrich chemical company (St. Louis, MO, USA) unless otherwise stated.

2.4.5 RBCs

Fresh pig blood was collected into a 2 L flask containing c.10 ml of an isotonic (0.9%) NaCl solution containing 30,000 IU.l⁻¹ of heparin sulphate. The blood was kept at 4°C for 4 hours, thus allowing the blood to cool and the RBCs to settle. The visible plasma and white blood cells were then aspirated off. The cells were washed in an equal volume of Krebs-Hanseleit Ringer (KHR) (in mM: NaCl 136.9, KCl 4.7, CaCl₂ 1.8, MgSO₄ 1.1, KH₂PO₄ 1.2, NaHCO₃ 25, glucose 5 and pyruvate 2, pH 7.4) and centrifuged at 500 g for 10 minutes and the supernatant aspirated off. This step was repeated twice. The washed RBCs were stored in an equal volume of KHR overnight and used within 24 hours.

When preparing the blood cell enriched FTS, the RBCs stored in KHR were centrifuged at 500 *g* for 10 minutes, and the supernatant aspirated off. The RBCs were then added to FTS to make up a final hematocrit of 5 or 10% (v/v) as appropriate. This was verified using hematocrit tubes in the standard way. In order to keep the RBCs in suspension, the storage reservoir for the perfusion experiments was a mechanically rotated 2 L tonometer, submerged in a water bath held at 10°C. The RBC enriched FTS did not contain PVP.

2.4.6 DAP

DAP was determined using a Gould model P23 ID pressure transducer (Statham, USA) connected to the DA cannula immediately anterior to the DA cannulation site. The transducer signal was fed via a 4 channel bioamplifier into an ADInstruments Powerlab 4SP (Waverley, Australia) archiving on a PC laptop running Chart 5 software (ADInstruments). Total pressure in the closed system, without the tail, was determined prior to and at the end of each experiment to determine the resistance of the circuit and to check for anomalies. The system pressure was then subtracted from the absolute pressure to determine the contribution of the tail. Outflow perfusate was collected and the volume determined gravimetrically using a Grass Instruments FTO3C (West Warwick, RI, USA) force-displacement transducer, logged in the same way as the DAP transducer. This was done to validate flow through the preparation. Vascular resistance of the tail preparation was calculated from DAP and Q according to equation 1:

$$R = \text{DAP} / Q \quad \text{eq 1.}$$

Where R is resistance (cm H₂O.100 g.min.ml⁻¹), DAP (cm H₂O) is dorsal aortic pressure and Q (ml.kg⁻¹.h⁻¹) is flow through the preparation.

2.4.7 VO_2 measurements

VO_2 was determined in RBC-free FTS perfused preparations by determining the difference in oxygen partial pressure (PO_2) across the perfused tissues in simultaneously withdrawn perfusate samples, measuring inflow and outflow PO_2 with a Strathkelvin Instruments (Strathkelvin, Glasgow, Scotland) water-jacketed (10°C) oxygen electrode (model IL1302) and meter (model 781), with the signal fed into the Powerlab 4SP archiving on the laptop. VO_2 was calculated from equation 2:

$$VO_2 = \Delta PO_2 \times \alpha O_2 \times Q \quad \text{eq 2.}$$

Where VO_2 ($\text{ml O}_2 \cdot \text{kg}^{-1} \cdot \text{h}^{-1}$) is the rate of oxygen consumption, ΔPO_2 (mmHg , $1 \text{ mmHg} = 0.133 \text{ kPa}$) is the change in the partial pressure of oxygen, αO_2 is the oxygen capacitance ($\text{FTS } 46.8 \mu\text{l} \cdot \text{l}^{-1} \cdot \text{mmHg}^{-1}$) and Q is the flow ($\text{ml} \cdot \text{kg}^{-1} \cdot \text{h}^{-1}$) through the preparation. Using RBCs to deliver oxygen required a different method to estimate VO_2 since the PO_2 of an RBC containing solution does not relate in a linear fashion to the amount of O_2 bound to intracellular Hb. Therefore, the method of Tucker (1967) was used to determine oxygen content of perfusate samples. Briefly, samples were injected with a gastight $50 \mu\text{l}$ Hamilton syringe (Reno, Nevada, USA) into a water-jacketed (32°C) Tucker cell, filled with a solution containing $6 \text{ g} \cdot \text{L}^{-1}$ potassium ferricyanide and $3 \text{ g} \cdot \text{L}^{-1}$ saponin. The change in PO_2 , measured with a Strathkelvin oxygen electrode and meter, was used to calculate oxygen content of the sample from the equation derived by Tucker (1967). The oxygen consumption by the preparation was determined by multiplying the oxygen content difference in the two samples by the rate of perfusate flow ($\text{ml} \cdot \text{kg}^{-1} \cdot \text{h}^{-1}$).

2.4.8 Electrical stimulation

Exhaustive exercise was simulated in the tail preparation by stimulating the tail with an AQUI-S™ twitch tester, incorporating a 9 v battery, stimulating at 1.65 Hz for either one or two 5-minute periods during the course of an experiment.

The first electrode was placed on the skin, immediately in front of the caudal fin on the lateral line, while the second was placed on the WM, immediately proximal to the exposed section of haemal arch on the lateral line. This side of the tail was then stimulated for 2.5 minutes, followed by stimulation of the opposite side for a further 2.5 minutes.

2.4.9 Cut surface pH

Immediately after the tail was isolated and cannulated, a transaxial cut was made through the body from the unused, posterior facing myotome. Using a Sensorex model 450C surface pH electrode (Garden Grove, CA, USA) with Radiometer model PHM84 pH meter (Copenhagen, Denmark) I measured the initial cut surface pH (pH_i) of the WM by averaging 6 measurements (a dorsal, medial and ventral measurement from each side of the vertebral column) from the freshly cut surface. Immediately after an experiment was terminated, a final cut surface pH (pH_f) measurement was taken from a freshly cut cross-section of the tail, in the same way as described for the first, this time from the cephalad surface. This was used as an indicator of anaerobic glycolysis, since H^+ is produced as a by-product of this process (Hochachka and Mommsen 1983).

2.4.10 BFD

The BFD of perfused tissues was determined before and after a 5-minute stimulation period by injecting 15 μm fluorescently dyed polystyrene microspheres (Molecular probes, CA, USA) with different excitation and emission wavelengths into the inflow line via a modified catheter.

It was assumed that the microspheres lodged in the vasculature homogeneously and gave a direct measure of blood flow to perfused tissues at a given point in time. The microspheres were injected into the inflow line mixed 1:10 (v/v) with FTS at a concentration of 1000 microspheres per gram of tissue. Six parallel RM and WM samples, aligned with the lateral line, were collected from both fillets of the perfused tail about 5, 10 and 15 cm from cannulation site after an experiment was terminated. The microspheres were released from the samples by dissolving the tissue (1:10 (w/v) in 2 M KOH in 95 % ethanol, 4.5% distilled water and 0.5% Tween 80 (w/v) for 48 hours at 37°C in the dark with periodic vortexing. The dissolved samples were then centrifuged for 10 minutes at 10,000 *g*. The supernatant was removed and the pellet suspended in 10 ml of 0.25% (w/v) Tween 80 in distilled water. The samples were then centrifuged for 10 minutes at 10,000 *g*, the supernatant removed and the pellet resuspended in distilled water. This was again centrifuged for 10 minutes at 10,000 *g* and the supernatant removed. The fluorescent dye was released from the microspheres by suspending the pellet in 3 ml of 100% di(ethylene glycol) ethyl ether acetate and incubated in the dark for 3 hours at 37°C with periodic vortexing. The sample was then centrifuged for 10 minutes at 10,000 *g*. Fluorescence in the supernatant was determined in duplicate at 495 nm (excitation) and 505 nm (emission) for yellow green and 612 nm (excitation) and 638nm (emission) for crimson dyes on a Cary Eclipse fluorescence spectrophotometer (Palo Alto, CA, USA). The number of microspheres per gram tissue was determined by comparison with a standard curve. The relative mass specific perfusion of RM and WM was calculated, based on an average from within muscle type. This is expressed as the BFD ratio (RM:WM). A value of 1 represents an equal mass specific perfusion of the two muscle types.

2.4.11 Mitochondrial activity

Mitochondrial membrane bound succinate dehydrogenase cleaves MTT to formazan. This process has been widely exploited as a measure of mitochondrial activity (Mosmann 1983; Hamid *et al.* 2004).

Mitochondrial activity was thus inferred from mass-specific formazan absorbance in tails perfused at $3.25 \text{ ml} \cdot \text{min}^{-1} \cdot 100 \text{ g}^{-1}$. Six parallel RM and WM samples were collected in the same way as BFD samples after 15, 30, 45, 75 and 90 minutes of perfusion. A subsample (c.100 mg) of fresh tissue was added to 10 volumes of absolute ethanol in a 1.8 ml Nunc cryotube vial (Roskilde, Denmark). This immediately killed the cells and acted as an appropriate solvent for the extraction of formazan. The muscle was coarsely minced using scissors and homogenised for 1 minute using a Heidolf Instruments DIAX 900 (Schwanbach, Germany) homogeniser on setting 6. The homogenate was centrifuged at $10,000 \text{ g}$ for 5 minutes and the supernatant used for absorbance readings on a Shimadzu UV-1700 PharmaSpec spectrophotometer (Shimadzu Scientific Instruments, Columbia, USA) at 560 nm. Samples measured in duplicate. The supernatant was diluted in absolute ethanol when necessary to prevent readings exceeding 0.8 absorbance units. The final values are expressed as absorbance units per gram of tissue. Mass specific mitochondrial activity ratios (MAR) (RM:WM) were calculated from the mass specific absorbance of the two muscle types.

2.4.12 Statistical analysis

Data on VO_2 as a function of DO_2 were fitted with single-phase exponential association curves. Differences between the datasets were tested using an F-test, comparing whether the same curve fitted both datasets. A one-way ANOVA with a Tukey's post-hoc test was used to determine differences in DAP before and after stimulation, differences in the vascular resistance at the three Hcts (0, 5 and 10%) and differences between MARs at each time point. Paired Student's t-tests were used to determine differences in cut surface pH before and after perfusion and BFD before and after a 5-minute period of stimulation. Differences in VO_2 as a function of resistance were determined using a one-way ANOVA, with a Bonferroni selected comparisons post-test. Linear regression was used to describe the relationship between weight change, DAP and mass corrected formazan absorbance over time.

An F-test was used to determine if the slope of the lines differed significantly from zero and whether the slopes and intercepts of the RM and WM lines were significantly different. The level of significance used was $P < 0.05$ but actual P -values or higher significance levels are reported where appropriate. All analyses were performed in Prism 4.00 (Graphpad software, San Diego, CA, USA). All data are expressed as mean \pm SEM, except the best fit model of the VO_2 values which are mean \pm 95% CI.

2.5 Results

2.5.1 VO_2

VO_2 in the tail preparation was found to be dependent on the DO_2 below c.60 ml $\text{O}_2 \cdot \text{kg}^{-1} \cdot \text{h}^{-1}$ in resting and c.150 ml $\text{O}_2 \cdot \text{kg}^{-1} \cdot \text{h}^{-1}$ in post-stimulation tails: above these values the VO_2 was independent of DO_2 (figure 2.2). Thus increasing the oxygen capacitance of the perfusing solution with RBCs was vital. The additional oxygen delivered by increasing the Hct of the perfusate from 5 to 10%, did not facilitate an increased VO_2 . The steady-state VO_2 was c.35 ml $\text{O}_2 \cdot \text{kg}^{-1} \cdot \text{h}^{-1}$ at rest and c.65 ml $\text{O}_2 \cdot \text{kg}^{-1} \cdot \text{h}^{-1}$ after stimulation. Single-phase exponential association curves fitted the data well (rest $R^2 = 0.59$, stimulated $R^2 = 0.91$). The curves were significantly different ($P < 0.001$).

2.5.2 DAP, cut surface pH, resistance and oedema

DAP was maintained between c.20-50 cm H_2O in resting preparations with an average of 40.7 ± 6.3 cm H_2O . Upon stimulation the DAP fell significantly ($P < 0.001$) to 69% (28.1 ± 4.7 cm H_2O) of the initial value (figure 2.3). A second 5-minute period of stimulation, produced a further fall ($P < 0.001$) to 54% (22.1 ± 2.6 cm H_2O) of the initial value. The DAPs after a 5- and 10-minute period of stimulation were also significantly different from each other ($P < 0.01$).

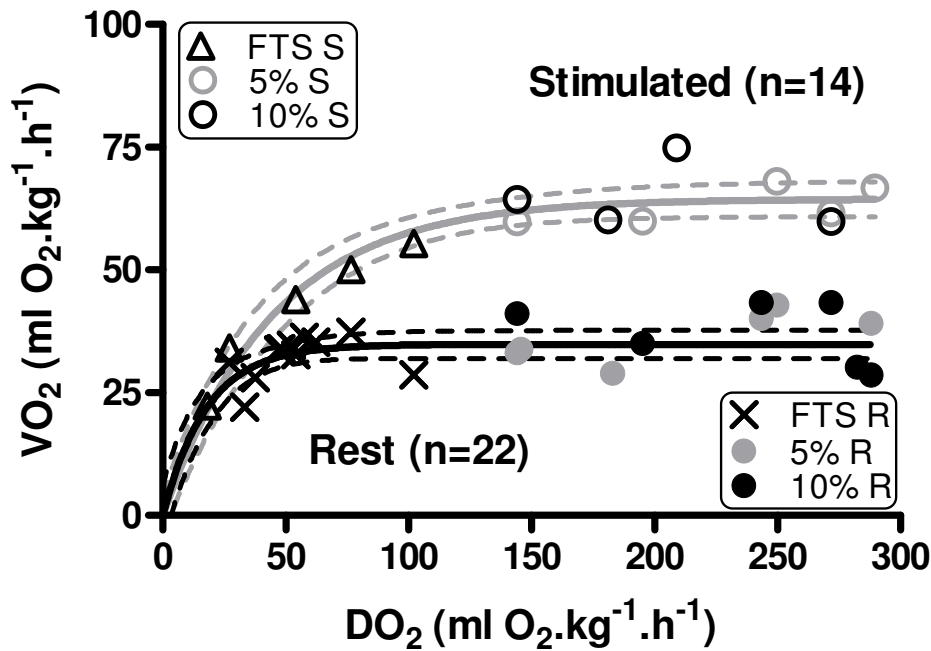


Figure 2.2. Oxygen consumption (VO_2) by isolated salmon tail preparation as a function of oxygen delivery (DO_2). FTS is freshwater teleost saline, the percentages relate to the hematocrit, R is rested and S is stimulated for 5 minutes with an AQUI-S™ twitch-tester. Single-phase exponential association curves are fitted to the data (rest $R^2=0.59$, stimulated $R^2=0.91$). The dashed lines are 95% confidence intervals of the fitted models. The equations are: rested $y=34.72*(1-\exp(-0.05558*x))$ and stimulated $y=64.46*(1-\exp(-0.02237*x))$. The curves were significantly different ($P<0.0001$) when compared using an F-test.

The cut surface pH_i of the WM was 7.47 ± 0.02 which fell to a pH_f in unstimulated preparations of 7.42 ± 0.02 and 6.94 ± 0.03 post-stimulation (pH_{fs}). Paired t-tests revealed that the pH_f was significantly less than the pH_i ($P=0.03$) and higher than pH_{fs} ($P<0.001$).

Vascular resistance was increased above that of FTS by c.1.6-fold and 2.25-fold by the addition RBCs at 5 and 10% Hct respectively (figure 2.4), with only the latter being significantly different from FTS ($P<0.001$). To maintain pressures in the physiological range, Q had to be reduced, offsetting oxygen delivery gains of the higher oxygen capacitance of the RBC enriched perfusate.

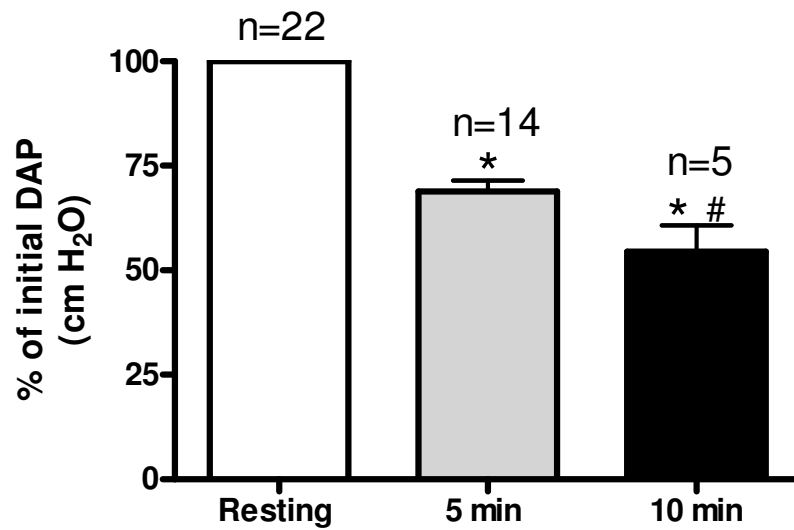


Figure 2.3. Change in dorsal aortic pressure (DAP) after 5 and 10 minutes of stimulation with an AQUI-S™ twitch-tester. DAP is expressed as a percentage of the initial. * indicates significantly different from initial ($P < 0.001$). # indicates significantly different from pre-treatment group ($P < 0.01$). Data are mean \pm SEM.

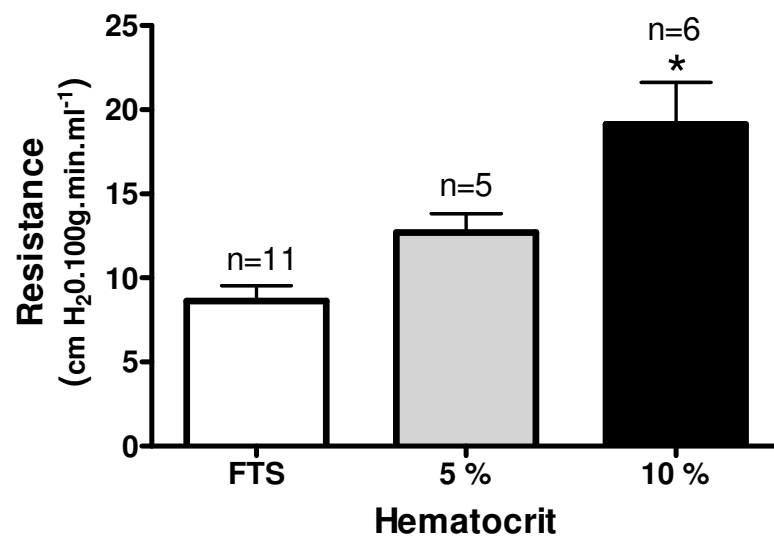


Figure 2.4. Vascular resistance of perfused salmon tail preparation perfused with FTS containing 0, 5 or 10% RBCs (v/v). * indicates significantly different from FTS ($P < 0.05$). Data are mean \pm SEM.

Figure 2.5 shows the relationship between VO_2 and resistance before and after stimulation at the different Hcts used. Stimulated preparations showed a significant increase ($P < 0.05$) in VO_2 with a simultaneous decrease in resistance except for preparations perfused with RBC-free FTS.

Weight change over time in the perfused tail preparation was related to DAP. Figure 2.6 clearly shows a weight change of $c. \pm 5\%$ in the preparation over the DAP range. The correlation coefficient (r^2) was 0.50 and the slope deviated significantly from zero ($P < 0.05$).

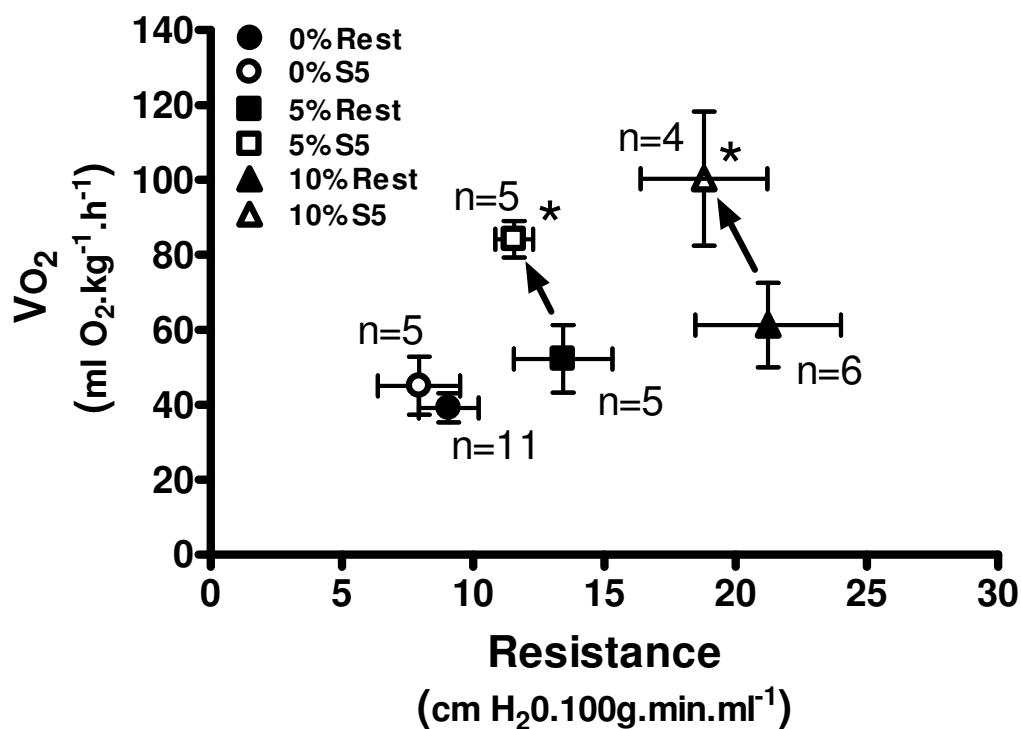


Figure 2.5. Oxygen consumption (VO_2) as a function of vascular resistance in the perfused salmon tail preparation at 0, 5 or 10% Hct before and after stimulation. * indicates significantly different from pre-stimulation group ($P < 0.05$). Data are mean \pm SEM.

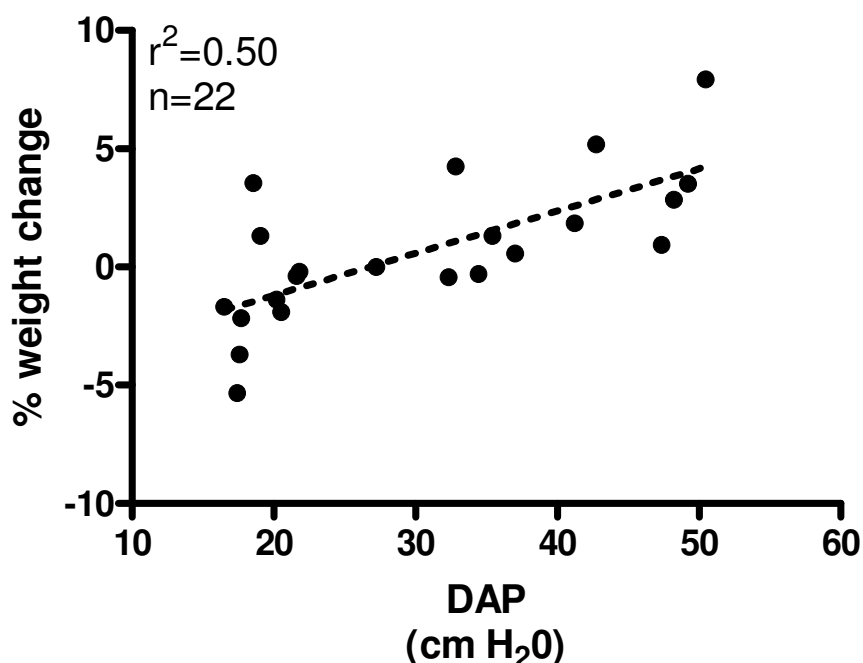


Figure 2.6. Weight change in the perfused salmon tail preparation as a function of DAP. The dashed line is a linear regression best-fit model which has been fitted to the data ($r^2=0.50$). The equation is $y=0.1782x - 4.762$. The slope is significantly non-zero ($P<0.05$).

2.5.3 BFD

Similar readings were obtained from the two sides of the tail, indicating that the microspheres were distributed equally to both sides of the myotome. This is consistent with other work in our laboratory (Janssen 2003). BFD at rest was 4.03 ± 0.49 (RM:WM). After a 5 minute period of electrical stimulation the ratio was found not to be significantly different at 3.98 ± 0.32 .

2.5.4 Mitochondrial activity

Perfusion with FTS containing MTT caused the bulk of the myotome to become dyed intensely purple. The skin, bones and the small portion of the myotome proximal to the cannulation site were also dyed but to a lesser extent.

Formazan production from MTT was found to be directly proportional to time of perfusion in both RM and WM (linear regression: WM $r^2=0.99$ and RM $r^2=0.98$) (figure 2.7). The mass specific mitochondrial activity ratios (RM:WM) over time were calculated to be 24.3 ± 4.1 , 19.5 ± 3.3 , 20.2 ± 4.6 , 24.6 ± 5.0 and 26.97 ± 5.4 after 15, 30, 45, 75 and 90 minutes of perfusion respectively. No significant difference was detected between mitochondrial activity ratios at any time.

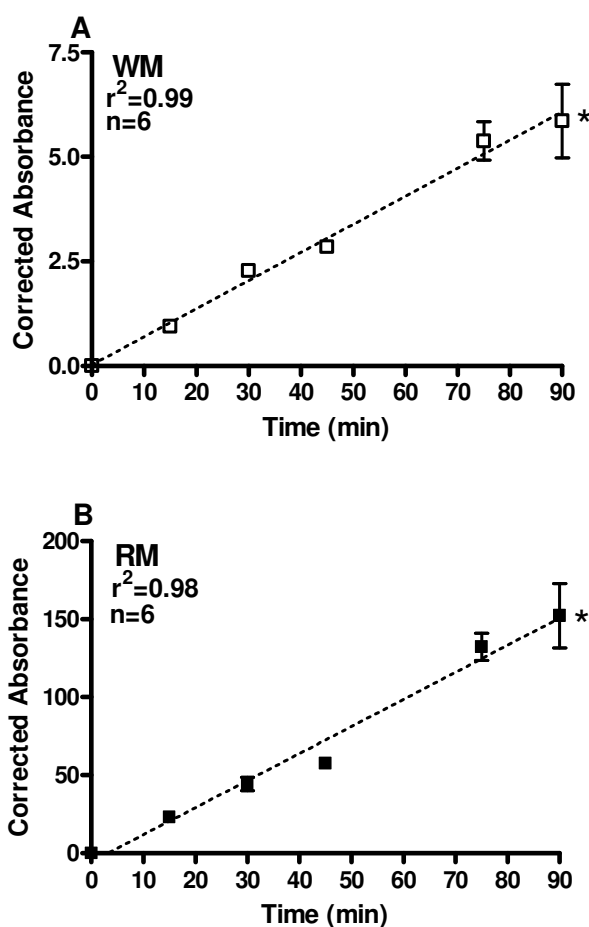


Figure 2.7. Mass corrected formazan absorbance by white (**A**) (white squares) and red (**B**) (black squares) muscle perfused with FTS containing 1 mg.ml^{-1} MTT as a function of time. The dashed lines are linear regression best fit models (WM $r^2=0.99$, RM $r^2=0.98$). The equations are: $y=0.06x - 0.003$ (WM) and $y=1.74x - 5.54$ (RM). Both lines were found to be significantly non-zero (both $P<0.0001$). * Indicates significantly different ($P<0.001$) from each other. Data are mean \pm SEM. Data markers obscure some small SEM bars.

2.6 Discussion

2.6.1 DAP, vascular resistance and oedema

At a constant flow rate, changes in DAP were used as a measure of the vasoactivity of the preparation. With the addition of amino acids to the perfusion solution (Clements and Reese 1998) and careful matching of osmotic pressure I were able to maintain physiological pressures for a period exceeding 2 hours. Perfused preparations are often subject to ramping vascular resistance over time (Wood and Shelton 1974; Perry *et al.* 1984; Perry and Farrell 1989), presumably as filtration rate exceeds resorption at the level of the capillaries and tissue oedema develops. The influence of raised vascular pressures is illustrated in figure 2.6. Over the c.2 hour time course of the experiment there was minimal haemolysis of the pig RBCs (data not shown) and in the unlikely event of an immune response against foreign antigens in the pig blood, this was without significant effect on vascular resistance. Lowered vascular resistance has been demonstrated following exposure to the anaesthetic AQUI-S™, though recovery was rapid (Rothwell and Forster 2005). Thus the effects of AQUI-S™ in the current study were likely abolished once the equilibration period was over.

The addition of RBCs in the current study greatly increased the capacitance of our preparation and satisfied the tissues' oxygen requirements. However, the addition of 10% RBCs also resulted in a 2.25-fold increase in the vascular resistance of the preparation, despite the omission of PVP. This is likely the result of an increase in the viscosity of the FTS. The higher pressure preparations gained significant weight, the likely result of oedema. Thus Q and Hct should be optimised for a given perfusion preparation (Wells and Weber 1991).

That a mammalian haemoglobin was used with a lower intracorporeal oxygen affinity might favour oxygen unloading at the tissues, as demonstrated previously (Berlin *et al.* 2002).

The presence of haemoglobin in the perfusing solution might also facilitate interactions between oxygen and the vasodilator, nitric oxide (Sonveaux *et al.* 2007).

2.6.2 VO_2

Resting metabolic rates in *Oncorhynchus* species are temperature dependent, and values for VO_2 range from c. 35 to 90 ml $O_2 \cdot kg^{-1} \cdot h^{-1}$ (Brett and Glass 1973; Bushnell *et al.* 1984; Kiceniuk and Jones 1977; Lee *et al.* 2003). Our tail preparation excluded metabolically active tissues such as heart, liver and opercular muscles, so it is not surprising that our VO_2 values for the isolated tail fall below most of those listed above. It is also possible that some regions of the tail were not as well perfused as others, particularly those proximal to the point at which the cannula entered the dorsal aorta. The less intensely dyed region of the myotome proximal to the cannulation site in MTT perfused tails is evidence of this. I manipulated both Q and Hct to elucidate the relationship between DO_2 and VO_2 in the skeletal muscle preparation, identifying the critical DO_2 under resting and stimulated conditions. Above a DO_2 of c.60 ml $O_2 \cdot kg^{-1} \cdot h^{-1}$, VO_2 at rest was independent of DO_2 , and a 5-fold increase in capacitance by the addition of RBCs did not increase VO_2 . Figure 2.2 demonstrates just how efficient the uptake of oxygen was around the critical DO_2 , with the resting preparation extracting c.60%, and the stimulated preparation c.40% of the oxygen supplied. It is likely that the supraphysiological PO_2 of FTS would have elevated the extraction efficiency of our preparation. It is also highly likely that the extraction efficiency of RM would have been greater than that of WM, due to its higher mitochondrial density, the presence of myoglobin and aerobic scope (McKenzie *et al.* 2004).

Similar to our findings, mammalian studies have demonstrated oxygen dependent VO_2 at low delivery rates. Kolář and Janský (1984) reported a perfused rat hindlimb skeletal muscle preparation resting steady-state VO_2 value of $595.5 \text{ ml O}_2 \cdot \text{kg}^{-1} \cdot \text{h}^{-1}$ and at the critical DO_2 of $c.1050 \text{ ml O}_2 \cdot \text{kg}^{-1} \cdot \text{h}^{-1}$, had a similar extraction efficiency to the salmon tail (60%). However, Hogan *et al.* (1992) using an isolated dog gastrocnemius muscle preparation reported a steady-state VO_2 value of $480 \text{ ml O}_2 \cdot \text{kg}^{-1} \cdot \text{h}^{-1}$ at a DO_2 of $4260 \text{ ml O}_2 \cdot \text{kg}^{-1} \cdot \text{h}^{-1}$, indicating an extraction efficiency of only $c.10\%$. VO_2 by the vascularly-isolated slow twitch fibre-dominated soleus in cats was $162 \text{ ml O}_2 \cdot \text{kg}^{-1} \cdot \text{h}^{-1}$ at a DO_2 of $3780 \text{ ml O}_2 \cdot \text{kg}^{-1} \cdot \text{h}^{-1}$, an extraction efficiency more than 12-fold less than our preparation (Bockman 1983). Interestingly, the resting VO_2 of the cat soleus did not differ significantly from similarly isolated fast-twitch gracilis muscle, however maximum VO_2 of soleus was twice that of gracilis despite similar blood flow (Bockman 1983). This is consistent with the idea that red muscles can extract and utilise more oxygen when required.

The proportion of WM in the fish tail is high (55 - 65% of the animals mass is WM which forms 90-95% of the muscle mass, Satchell 1991; Janssen 2003), while mammalian muscles are comprised of a mixture of fibre types, but are typically dominated by red fibres. Therefore, given the greater proportion of red muscle fibres comprising mammalian muscles, the high temperatures used in those studies and the much greater metabolic rates of endotherms (Hemmingsen 1960), it is not surprising that our VO_2 values fall well below reported mammalian values in equivalent preparations.

In vivo, the supply of oxygen by the cardiovascular system to respiring tissues must match demand. When the demands of locomotion and recovery from exercise are included the metabolic requirements of working muscle are significantly increased (Turner *et al.* 2006). In muscles with large aerobic potential (i.e. red muscles) oxygen supply and demand are reported as being stoichiometric.

Thus, it has been argued that oxygen may play a regulatory role in aerobic metabolism, particularly in skeletal muscle, since numerous studies have found essentially a 1:1 relationship between DO_2 and muscle work (Hochachka 2003). Work on dog gastrocnemius muscle (RM and WM) found such a relationship over an 18-fold change in the rate of ATP turnover (Hogan *et al.* 1992). A supply and demand matched relationship seems highly plausible, since supplying oxygen in excess of requirements could result in the formation of free radicals (Gnaiger 2003). Our supraphysiological PO_2 might have facilitated free radical damage in the tissues en route to the mitochondria (Gnaiger 2003; Tuckey 2008; Tuckey *et al.* 2009b).

2.6.3 Muscle pH changes

Scope to increase muscle activity for locomotion is crucial for survival in most vertebrates. The capacity to increase VO_2 for locomotion and the increase associated with exercise and recovery in fish is well described in the literature. White muscle of the salmonid myotome engages in “burst-type” activity (Johnston and Ward 1975) typical of escape and predatory behaviour. In the current study, “burst-type” exercise was simulated by an electrical stimulus. The excess post-exercise oxygen consumption (EPOC) (Lee *at al.* 2003a; Lee *et al.* 2003b) roughly doubled the critical oxygen delivery and resting VO_2 in the current study. The more than doubling of the hydrogen ion concentration of the WM post-stimulation (a drop of cut surface pH of 0.53 units) almost certainly reflected anaerobic glycolysis and the build-up of lactic acid. The drop in pH in unstimulated preparations was only 0.05 pH units (representing a 15% rise in proton concentration over the c.2 hour perfusion period), indicating that appreciable anaerobic glycolysis did not occur.

With a constant perfusion rate, the drop in DAP post-stimulation in the current study must have resulted from a decrease in smooth muscle tone in the vasculature of the perfused tail. Vasodilation can be caused by a fall in pH (McKenzie *et al.* 1991; Smith *et al.* 2006), though the FTS was well buffered, and it can be induced by metabolites released from active tissues (Olson 2002).

2.6.4 BFD and mitochondrial activity

The mass specific BFD ratio between RM and WM was c.4 at rest; this was unchanged post-exercise, despite the dilation of the vasculature. Similarly, Barron *et al.* (1987) reported an averaged *in vivo* value over 3 temperatures for the BFD in rainbow trout (*Oncorhynchus mykiss*) of 3.8 (RM:WM). The higher degree of vascularisation (Egginton *et al.* 1988) of the red muscle no doubt facilitated blood flow and consequently oxygen transfer. The latter was also probably facilitated by the high myoglobin content of red muscle (Wittenberg and Wittenberg 2003). The vasodilation and increased VO_2 post-stimulation suggest capillary recruitment. *In vivo* the reduced vascular resistance of the tail might cause a redistribution of the cardiac output. Increased tissue perfusion post-exercise in resting and electrically stimulated rainbow trout has also been reported *in vivo* (Neumann *et al.* 1983). These authors report a c.2.25 BFD ratio (RM:WM) at rest with blood flow increased 2.5- and 5-fold in WM and RM respectively, thus causing the BFD to increase to 4.5 on stimulation. Increased blood flow to the RM (1-11%) but not the WM, which showed a decrease (15-44%), has been reported *in vivo* in rested large-scale sucker (*Catostomus macrocheilus*) injected with dyed microspheres *in vivo* (Kolok *et al.* 1993). Wilson and Egginton (1994) found a large increase in BFD from 8.4 to 160 when rainbow trout were forced to swim at their aerobic maximum, without the recruitment of fast glycolytic fibres, which they described as a “steal effect”. I did not observe this in our preparation, in which all fibre types would have been stimulated.

The constancy of our BFD ratio compared to changes reported by both groups discussed above may reflect the fact that their fish were alive, with fully functioning nervous and endocrine systems, and were thus capable of manipulating blood flow as required.

Despite the 4-fold difference in perfusion of the two muscle types, the mitochondrial activity of RM was c.20 times that of the WM. This almost certainly reflects the greater mitochondrial volume-density in RM fibres (Egginton and Siddel 1989; Luther *et al.* 1995) and higher degree of vascularisation (Egginton *et al.* 1988). Thus, in our preparation WM seems to be over-perfused relative to RM, in terms of aerobic potential.

2.6.5 Summary

I have developed a simple perfusion preparation for the study of respiratory parameters in fish muscle. This preparation has significant other potential uses. The linear production rate of formazan in both muscle types over the 2 hour period reflects the viability of this preparation. Furthermore, the small drop in pH associated with the unstimulated preparations suggests that the preparation was not significantly hypoxic for any length of time and the brief period of ischemia (<1 min) in preparation of the tail had no lasting effect.

Chapter 3

Oxygen-dependence of metabolic rate in the striated muscles of craniates

3.1 Abstract

O₂-dependence and independence of cellular respiration has been observed in a number of experimental models and whole animals under a range of conditions. I present evidence of both; relative O₂-independence in the vasculature and strict O₂-dependence in striated muscles of fishes and mammals. Vessel VO₂ from rat, salmon and hagfish showed varying degrees of independence between PO₂s of 15-95 mmHg *in vitro*. Above and below these values, VO₂ was highly PO₂-dependent. Using an *in vitro* tissue slice system, VO₂ by cardiac and skeletal muscles from rat, salmon, snapper and hagfish were shown to relate linearly to PO₂ between zero and 125 mmHg. VO₂ in these tissues was dependent on tissue type (cardiac, red and white muscle) which correlated with haem protein concentration. Application of carbamylcholine chloride to the vessels resulted in changes in VO₂ of rat and salmon vessels, likely reflecting altered mechanical activity. Uncoupling of mitochondria in the salmon vessels resulted in a large increase in VO₂ well above that induced by contraction. The increase in VO₂ in muscle slices uncoupled with *p*-trifluoromethoxylphenyl-hydrazone (FCCP) and 2,4-dinitrophenol (DNP) ruled out diffusion-limitation as a constraint on VO₂. Mitochondrial succinate dehydrogenase activity was constant over time and reoxygenation of the Ringer bathing the tissues after the initial run down in PO₂ resulted in VO₂ rates that were unchanged from the starting values, demonstrating that the tissues remained viable over time. VO₂ by salmon liver slices also showed O₂-dependence but the relationship ceased to be linear below 35 mmHg. O₂-dependence in salmon red muscle was further investigated by biochemical analysis of tissue maintained at either low (30 mmHg) or high (100 mmHg) PO₂ for 1 hour. Potential energy, a proxy of ATP turnover, was significantly increased at 100 mmHg relative to 30 mmHg, and rose in both treatments from values at the start. Furthermore, there was no evidence of lactate accumulation in red muscle.

Our data indicate that ATP supply and demand were reduced in conjunction with falling PO₂, and that the observed oxyconformance of VO₂ and ATP turnover in muscle is likely the result of some kind of O₂ sensing mechanism.

3.2 Keywords

Skeletal muscle, O₂, hypoxia, PO₂, vertebrate, ATP

3.3 Introduction

The tissues of most animals experience hypoxia through environmental, metabolic and/or circulatory inadequacies to some degree in their life. When O₂ is limited or absent, ATP supply is restricted and maintenance of cellular homeostasis becomes a challenge. In these situations energy supply must be maintained to avoid chronic membrane damage and other processes, eventually leading to necrosis (Boutilier 2001a). Compromised energy supply during hypoxia is mitigated by one or a combination of two generalised strategies. Firstly, ATP is rapidly regenerated from ADP by creatine phosphate, via the creatine kinase pathway, and by anaerobic glycolysis (Hochachka and Guppy 1987; Fields 1988; Hochachka and McClelland 1997). Secondly, concomitant with decreased ATP supply, ATP demand pathways may be downregulated, which often inhibits glycolysis (Hochachka 1985; Dunn and Hochachka 1986; Hochachka and Guppy 1987; Buck and Hochachka 1993; Buck *et al.* 1993; Hochachka *et al.* 1996). This process of “metabolic arrest” has been reported in animals from numerous taxa, mostly those that must survive prolonged hypoxia/anoxia and/or undergo a period of hibernation (Hochachka 1980; Boutilier and St-Pierre 2002). The outward manifestation of this phenomenon in hypoxic tissues is often a decrease in VO₂, which may be in part due to increased phosphorylation efficiency and also a reduced mitochondrial proton leak, which accounts for about 20% of resting VO₂ (Gnaiger *et al.* 2000; St-Pierre *et al.* 2000; Boutilier and St-Pierre 2002).

An immediate drop in VO₂ during hypoperfusion (i.e. hypoxia) has been demonstrated in cat (Whalen *et al.* 1973), dog (Hogan *et al.* 1992), rat (Kolář and Janský, 1984), frog (Boutilier 2001b), turtle (Platzack and Hicks 2001) and fish (Forgan and Forster 2008) skeletal muscle. It has also been observed in isolated tissues and cultured cells that VO₂, ATP and NAD⁺ generation (Schumacker *et al.* 1993), cytochrome c oxidase activity and ATP:ADP ratio (Wilson *et al.* 1979), contractility and protein synthesis (Stary and Hogan 1999; Gnaiger 2003) are compromised over a wide PO₂ range (anoxia-air saturation).

These reports are consistent with changes in numerous other metabolites at PO₂s well above the K_m of mitochondria for O₂ (Hochachka and Guppy 1987). The phenomenon of O₂ conformance of VO₂ has been explained as either the result of O₂ sensing mechanisms and/or O₂ diffusion-limitation, since critical O₂ tensions required for mitochondrial respiration are about 2 mmHg, above which oxyregulation of VO₂ over a wide PO₂ range occurs (Boutilier and St-Pierre 2002; Gnaiger 2003). Interestingly, isolated cells and cell cultures can also be O₂-independent (Wilson *et al.* 1979; Rumsey *et al.* 1990) over a wide PO₂ range. The apparently paradoxical difference between intact tissues (both *in vivo* and *in vitro*) and isolated cells and mitochondria makes for difficult interpretation of these data. Consequently, the relationship between oxygen supply and utilisation in tissues and the requirements of the delivery systems (i.e. the heart and vasculature) remains unclear.

Therefore, the aim of the current study was to investigate whether VO₂ conformed to PO₂ in the vasculature and striated muscles of vertebrates. These relationships are explored in a mammal, and representatives of two other vertebrate taxa (a cyclostome and two teleosts) that to our knowledge have not been investigated previously. Furthermore, I tested whether a reduced PO₂ induced changes in muscle metabolite pools and ATP turnover in skeletal muscle.

3.4 Materials and Methods

3.4.1 Animals

Animals were legally obtained, with Ministry of Fisheries special permits where appropriate. All manipulations described in this manuscript were approved by the University of Canterbury Animal Ethics Committee.

Female Chinook salmon (*Oncorhynchus tshawytscha*, Walbaum) (mass 1.530 ± 0.115 kg; fork length 47 ± 2 cm; condition factor 1.38 ± 0.04 ; $n = 50$) were obtained from a local freshwater salmon farm (Isaac Salmon Farm, Canterbury, New Zealand), where they were fed twice daily with commercial salmon pellets (Reliance stock feeds, Dunedin, New Zealand), before transfer into a holding tank which had a continuous flow of high quality bore-water (a constant 11 °C). These fish were left undisturbed for a minimum of 48 hours and were used within 1 week of transfer into the holding tanks.

Mixed sex hatchery-raised snapper (*Pagrus auratus*, Bloch and Schneider) (mass 125 ± 4 g; fork length 18.1 ± 0.2 cm; condition factor 2.09 ± 0.04 ; $n = 13$) were obtained from Plant and Food Research (Nelson, New Zealand). The animals were held in tanks with flow-through seawater at approximately 12 °C, where they were fed daily with an equal mix of alginate, squid, fish and salmon pellets, except in the 48 hours preceding an experiment. The animals were anaesthetised in the same way as for salmon. The laboratory in Nelson was adjacent to the tank room so the anaesthetised animals were transferred to a small volume of water using a net and immediately moved into the laboratory.

Mixed sex Pacific hagfish (*Eptatretus cirrhatus*, Forster) (mass 1.014 ± 0.065 kg; $n = 13$) were caught over several trips in baited cages set from the departmental research boat in Lyttleton and Akaroa harbours (Canterbury, New Zealand). Once captured, the fish were held in aerated seawater filled tanks while being transported back to the University's seawater aquaria (16 °C). They were fed a mixed diet of squid and mussels twice weekly, but not within the 48 hours preceding an experiment. The animals were killed by placing them in a bucket containing 200 ppm AQUI-STM, 400 ppm MS-222 and 400 ppm benzocaine in 20 L of seawater for 1 hour.

Female rats (*Rattus rattus*, Linnaeus) (mass 148 ± 9 g; $n=9$) were obtained from Agresearch (Hamilton, New Zealand) and fed with commercial rat pellets (Reliance stock feeds, Dunedin, New Zealand). Animals were killed by cervical dislocation.

3.4.2 Tissue biopsy

The preparation time of all biopsies did not exceed 10 minutes. All equipment was made sterile before preparation.

3.4.3 Fish

The fish were anaesthetised to stage 4 (not reactive to stimuli, but still showing limited ventilation: Summerfelt and Smith 1990) with AQUI-S™ (AQUI-S NZ, Lower Hutt, New Zealand) at a concentration of 22 ppm (0.012 g.L⁻¹ isoeugenol). Without alerting the animals, a concentrated stock solution of anaesthetic was gradually introduced into the holding tank gravimetrically and mixed with a Maxi-Jet MJ1000 water pump (Aquarium Systems, Loreggia, Italy). The animals were transported to the University. Immediately on arrival (<25 minutes), animals were restrained in a custom sling and killed by inserting the tip of an “iki jime” fish harvesting tool directly into the brain. Immediately after death, c.1 ml a 0.9% NaCl solution containing heparin sulphate (2500 IU.ml⁻¹.kg⁻¹) was injected into the dorsal aorta through the roof of the mouth, and allowed to circulate briefly before the animal was exsanguinated by cutting the dorsal aorta and caudal vein close to the caudal fin, allowing it to bleed into the water. Immediately after exsanguination the heart and liver were dissected out, cut in half and thoroughly rinsed in the appropriate Ringer, blotted and stored in Petri-dishes on ice in the appropriate aerated freshwater (salmon) or saltwater (snapper) teleost Ringer (in mM: 136.89 NaCl freshwater, 159.6 NaCl saltwater; 2.11 KCl; 0.99 MgCl₂; 1.30 CaCl₂; 10 glucose; 3 HEPES {N-[2-hydroxyethyl]piperazine-N=[2-ethane-sulfonic acid]} acid form; 6.99 HEPES sodium salt; 0.30 Na⁺-glutamate; 0.40 L-glutamate; 0.02 Na⁺-aspartate; 0.05 DL-carnitine; 1 mg.L⁻¹Insulin; 1 mg.L⁻¹ TPP-co-carboxylase, 200 mg.L⁻¹ gentamycin sulphate, pH 7.6). Gentamycin sulphate was included to reduce the potential for micro-organisms to contribute to VO₂ (Rudin *et al.* 1970). Both fillets were then removed from the carcass and skinned.

A razor blade was used to cut several c.1 cm³ square blocks of white muscle from the D-block of the anterior part of the fillet. Red muscle was removed by slicing several c.1 cm³ square blocks of muscle from along the lateral line. The biopsies were stored in Petri-dishes on ice. The ventral aorta and afferent branchial arteries were dissected out via an incision made above the vessels on the ventral surface of the head and placed into a Petri-dish containing aerated teleost Ringer and stored on ice.

3.4.4 Hagfish

A cut was made along the ventral surface of the animal. Then c.1 ml a hagfish Ringer (in mM: 497.95 NaCl, 8.05 KCl, 5.10 CaCl₂, 9.00 MgCl₂, 3.04 MgSO₄, 3 HEPES, 6.99 HEPES sodium salt, 5.55 glucose, 200 mg.L⁻¹ gentamycin sulphate, pH 7.8) containing 2500 IU.ml⁻¹.kg⁻¹ heparin sulphate, was injected into the dorsal aorta, before it was cut open and allowed to drain. An approximately 10 cm section of dorsal aorta rostral to the heart was then dissected out and placed in hagfish Ringer. The heart was removed and stored in the same way as described for the fish hearts. Following this, several c.1 cm³ mosaic skeletal muscle blocks were cut with a razor blade from adjacent to the notochord, and from the white muscle rich “tongue” and stored in the same way as fish biopsies.

3.4.5 Rat

Immediately after death a ventral incision was made in the skin between the rib-cage and the anus. The body wall was then opened via a second incision. The abdominal aorta was injected with about 0.5 ml of 0.9 NaCl, containing 2500 IU.ml⁻¹.kg⁻¹ heparin sulphate, which was briefly allowed to circulate.

Following this, the abdominal aorta was cut and allowed to drain, and a 5 cm section removed and placed into modified Krebs Ringer (in mM: 136.9 NaCl, 4.7 KCl, 1.8 CaCl₂, 1.1 MgSO₄, 3 HEPES, 6.99 NaHEPES, 10 glucose, 200 mg.L⁻¹ gentamycin sulphate, pH 7.4). The heart was removed and stored in the same way as described for the fish hearts. Soleus (predominantly red) muscle and the visually white fibres of the gastrocnemius (predominantly white) muscle were then dissected from both hindlegs and stored in the same way as fish biopsies.

3.4.6 Tissue slice and vessel preparation

Biopsies were divided into approximately 125 mm³ blocks and tissue slices cut from them with a Stadie-Riggs microtome (Thomas Scientific, Swedesboro, NJ). The thin, uniform c.25 mm³ (approximately: 1 mm thick, sides 5 mm, c.50 mg) sections of fresh tissue were cut from white muscle, red muscle and cardiac muscle (ventricular spongy myocardium). The white muscle and red muscle were sectioned along the longitudinal plane of the muscle fibres while cardiac muscle and liver was sectioned along any plane. Vessels were cut open along their long axis and then into c.0.25 cm² sheets. Care was taken to minimise damage to the endothelium. After preparation, the slices and vessels were immediately transferred to Petri-dishes containing fresh aerated Ringer. All tissues were used within 5 minutes of preparation.

3.4.7 Mitochondrial activity

Mitochondrial membrane bound succinate dehydrogenase cleaves 3-(4,5-dimethylthiazol)-2,5-diphenyl-2*H*-tetrazolium bromide (MTT) to formazan. This process has been widely exploited as a measure of mitochondrial activity (Mosmann 1983; Hamid *et al.* 2004). Mitochondrial activity was thus inferred from the mass-specific formazan absorbance in salmon red and white muscle slices, prepared as above and incubated in 5 ml of air-saturated freshwater teleost Ringer, containing 1 mg.ml⁻¹ MTT over a 2 hour period.

About 5 slices representing time zero were immediately blotted and freeze-clamped between two aluminium blocks and stored at -80°C. A further 5 slices were frozen in the same way after 30, 60, 90 and 120 minutes of incubation. On thawing, a subsample (c.100mg) was coarsely minced using scissors and placed in a 1.8 ml Nunc cryotube vial (Roskilde, Denmark) and 10 volumes of absolute ethanol added. This immediately stopped cellular activity and acted as an appropriate solvent for the extraction of formazan. The tissue was homogenised for 1 minute using a Heidolf Instruments DIAX 900 (Schwanbach, Germany) homogeniser on setting 6. The homogenate was centrifuged at 10,000 *g* for 5 minutes and the supernatant used for absorbance readings on a Shimadzu Corporation UV-1700 PharmaSpec spectrophotometer (Shimadzu Scientific Instruments, Columbia, USA) at 560 nm. The supernatant was diluted in absolute ethanol when necessary to prevent readings exceeding 0.8 absorbance units. Samples were measured in duplicate. The final values are expressed as absorbance units per gram of tissue.

3.4.8 Respirometry

O₂ consumption (VO₂) was determined by measuring the change in the partial pressure of O₂ (PO₂) in the Ringers solution bathing the tissues. About 10 pieces of vessel (mounted onto a 280 µm diameter stainless steel wire frame) or 5 tissue slices were placed into 1 ml of stirred air-saturated Ringer in temperature controlled (10°C fish and hagfish and 37°C rats) Strathkelvin Instruments model RC 300 respirometers (Strathkelvin, Glasgow, Scotland) fitted with model IL1302 O₂ electrodes and model 781 meters, with the signal fed via a Powerlab 4SP into a notebook computer running Chart 5 software (both ADInstruments, Castle Hill, Waverley, NSW, Australia) recording at 1 Hz. Since the slices were constantly moving, it was assumed that there was no unstirred boundary layer. The experiment was terminated when the PO₂ fell to below 2 mmHg. At that point the tissues were blotted down and weighed.

VO₂ was calculated using equation 1.

$$VO_2 = \frac{\Delta PO_2 \times \alpha O_2 \times V}{t \times M} \times 22.39 \quad \text{eq.1}$$

Where VO₂ is the rate of O₂ consumption (ml O₂.kg⁻¹.h⁻¹), ΔPO₂ is the change in PO₂ (mmHg, 1 mmHg = 0.133 kPa) during the treatment period, αO₂ is the O₂ solubility of the Ringer (ml O₂.l⁻¹.mmHg⁻¹) based on the temperature and osmolality (in μmol.l⁻¹.mmHg⁻¹ freshwater teleost ringer 2.11; saltwater teleost Ringer 2.09; hagfish Ringer 1.83; modified Krebs Ringer 1.32), V is the volume of the respirometer (l), t is the time (hours) between PO₂ measurements, M is the wet mass (kg) of the vessels in the respirometer and 22.39 is a constant used to convert moles to litres. The PO₂ in the respirometers was allowed to deplete from air saturation (PO₂ c.150 mmHg) down to zero. Typically, the rundown in PO₂ took between 0.5 - 2 hours with striated muscles and liver but took longer in vessels (up to 12 hours for hagfish vessels).

In vessels treated with the acetylcholine agonist carbamylcholine chloride (CBC), Ringer's solution containing 10⁻⁴ M CBC was used. Uncoupling in salmon muscle mitochondria (increasing mitochondrial proton leak via ionophores) was achieved using freshwater teleost Ringer containing either 10⁻⁴ M 2,4-dinitrophenol (DNP) or 10⁻⁶ M *p*-trifluoromethoxyphenyl-hydrazine (FCCP), concentrations shown to maximally stimulate VO₂ in preliminary experiments. Stock solutions were made up using a small volume of dimethylsulfoxide (DMSO), which was made up to volume and then serially diluted. The final concentration of DMSO in the stock solution was <0.0001%.

In experiments where the PO₂ was increased in the respirometer after it had fully depleted, the electrode holder was removed and the Ringer's solution aerated for 5 minutes via a length of PE50 polythene tubing (Portex Ltd., Hythe, Kent, England) before the electrode holder was replaced. This was sufficient to aerate the 1 ml of Ringers solution to near air saturation.

3.4.9 Haem protein assay

Haem protein (myoglobin and haemoglobin) was determined in extracts from salmon, snapper, hagfish and rat muscles by measuring the peroxidase activity of the haem moiety via an adaptation of the methods reported by O' Brien *et al.* (1992). The haem moiety of the globins reacts with tertiary-butyl hydroperoxide and orthotolidine to generate a blue colour that is quantifiable using spectrophotometry. O' Brien *et al.* (1992) removed haemoglobin from extracts by precipitation using ammonium sulphate followed by ultrafiltration. Using standards (ovine skeletal muscle myoglobin and human haemoglobin), I found that unacceptable quantities of myoglobin were precipitated with the haemoglobin using this method. Similarly, Lee-de Groot *et al.* (1998) report that precipitation using ammonium sulphate resulted in reduced accuracy and sensitivity in myoglobin assays. Kranen *et al.* (1999) also note that significant concentrations of myoglobin precipitated when removing haemoglobin using ammonium sulphate. Furthermore, as I did not have native myoglobins and haemoglobins available to properly ascertain differential precipitation characteristics of the various globins, it was decided not to precipitate haemoglobin from muscle extracts. Since animals were thoroughly ensanguined and the tissue biopsies rinsed in Ringer and blotted, it was assumed very little haemoglobin was present in the biopsies.

Muscle samples were removed and cleaned as described in the tissue biopsy section, frozen in liquid nitrogen and stored at -80°C for a maximum of 6 months before assay. The frozen muscle biopsies were ground in a porcelain pestle and mortar under liquid nitrogen. Approximately 80 mg of frozen powder was placed into a 1.8 ml Nunc cryotube vial with a pre-cooled spatula. The tissue was diluted 20-fold with ice cold extraction buffer (in mM: 80 KCl, 50 Tris-HCl, 1 EDTA, pH 8) and homogenised for c.1 min using a Heidolf Instruments DIAx 900 homogeniser on setting 6. The samples were centrifuged at 10,000 *g* for 5 minutes and the supernatant transferred to 1.7 ml microtubes (Axygen, Union City, CA, USA).

Cytochromes were assumed to sediment with mitochondria and other cell organelles (Kranen *et al.* 1999). The extracts were frozen at -80°C and assayed within a week.

On thawing, red and cardiac muscle extracts were further diluted with extraction buffer to 40- and 160-fold respectively. One hundred microlitres of muscle extract was mixed with 1 ml of reaction medium (2 mM orthotolidine, 200 mM tertiary-butyl hydroperoxide) in a microtube and incubated at 30°C for 30 minutes in a shaking water-bath. The samples were then placed in ice for 5 minutes before being transferred to cuvettes and the absorbance measured in duplicate at 364 nm on a Shimadzu Corporation UV-1700 PharmaSpec spectrophotometer at 20°C. Absorbance was related to ovine skeletal muscle myoglobin standards of known concentration. The corresponding concentration was multiplied by the appropriate dilution factor and expressed per gram wet mass of tissue. Stock solutions of orthotolidine (50 mM in DMSO) and tertiary butyl-hydroperoxide (1 M) were made fresh each day.

3.4.10 Muscle energetics experiment

Salmon red muscle was chosen as a representative tissue. The effect of PO₂ on energetics was assessed by incubating muscle slices in freshwater teleost ringer at low (30 mmHg) and high (100 mmHg) PO₂ at 10°C and measuring changes in key metabolites. Red muscle slices were prepared as described above.

Approximately 10 slices were immediately frozen as described above and another 10 slices each were placed in the RC 300 respirometers with 5 ml of continuously stirred and gassed (via a length of PE50 polythene tubing) freshwater teleost ringer, equilibrated to either 30 or 100 mmHg using a Wöstoff type 1M 300/a-F gas mixing pump (Wöstoff, Bochum, Germany) that mixed air and N₂. The tissues were incubated for 1 hour with the PO₂ continuously monitored using the Strathkelvin electrodes before being frozen as described above.

3.4.11 Cut surface tissue pH

Immediately after the muscle biopsies were removed, a transaxial cut was made through the two unused parts of the fillets. Using a Sensorex model 450C surface pH electrode (Garden Grove, CA, USA) with Radiometer model PHM84 pH meter (Copenhagen, Denmark) the initial cut surface pH of the white muscle was measured; mean of 6 measurements (a dorsal, medial and ventral measurement from each side of the fillet) from the freshly cut surfaces. After incubation for 1 hour and prior to freezing, the tissue slices were blotted on paper towelling and additional surface pH measurements made, this time recording an average value of all the slices.

3.4.12 Tissue extraction for energetics experiment

3.4.12.1 Creatine compounds, purine nucleotides and nucleosides and related bases

The frozen muscle biopsies were ground in a porcelain pestle and mortar with liquid nitrogen. Approximately 100 mg of frozen powder was placed into a 1.8 ml Nunc cryotube vial with a pre-cooled spatula, 1.5 ml of ice cold 0.4 N perchloric acid added and the powder homogenised for c.1 minute using a Heidolf Instruments DIAX 900 homogeniser on setting 6. The homogeniser blade was rinsed with 100 µl of perchloric acid and the mass made up to 1.80 g on a balance using perchloric acid. The extract was centrifuged at 6,000 *g* for 5 minutes and the supernatant transferred into a 1.7 ml microtube and neutralised (pH 7) with 2 M K₂CO₃. The extract was frozen at -80°C until assayed (within 2 weeks).

3.4.12.2 Glucose, glycogen and lactate

Muscle samples were prepared in the same way as before except that the extraction medium was 500 µl of ice-cold 0.6 N perchloric acid mixed in a ratio of 7:3 with absolute methanol and the mass made up to 0.80 g. This homogenate was frozen at -80 °C until assayed (within 2 weeks). On thawing the extracts for analysis, a subsample was removed for the glycogen assay. This sample was neutralised with 2 M K₂CO₃. The remaining unneutralised homogenate was centrifuged at 10,000 *g* for 5 minutes. The supernatant was neutralised in a new microtube using 2 M K₂CO₃ and further diluted with distilled water (1-fold). Glucose and lactate concentrations were determined in this extract.

3.4 13 Assays

3.4.13.1 Glucose and glycogen assay

Glucosyl units were determined in the glucose and glycogen extracts using a modified version of the method of Keppler and Decker (1974). Briefly, glycogen extracts were diluted with five volumes of 200 mM acetate buffer (120 mM sodium acetate and 80 mM glacial acetic acid, pH 4.8) containing 2 g.ml⁻¹ amyloglucosidase and incubated for 2.5 hours in a shaking water-bath heated to 37 °C then placed on ice until assayed. Glucosyl units were measured in both extracts using the hexokinase method, employing a Roche Gluco-quant Glucose/HK assay kit (Mannheim, Germany) adapted for use in cuvettes. In this method the production of NADPH is stoichiometric with glucose conversion. The NADPH was quantified using a Shimadzu Corporation UV-1700 PharmaSpec spectrophotometer at 340 nm. Net glycogen-derived glucosyl units were determined by subtracting the tissue glucose concentration from the glycogen values. Samples were measured in duplicate.

3.4.13.2 Lactate assay

L-lactate in the neutralised and diluted muscle extracts was determined using the L-lactate dehydrogenase method, utilising a Megazyme L-lactic acid assay kit (Wicklow, Ireland). Here NADH production is stoichiometric with the L-lactate dehydrogenation, and NADH was measured as above. Samples were measured in duplicate.

3.4.13.3 Creatine compounds, purine nucleotides and nucleosides and related bases

Creatine compounds, purine nucleosides and nucleotides and related bases were separated by ion-pair reversed phase high performance liquid chromatography (HPLC) and quantified using UV-Vis detection on a Shimadzu Scientific Instruments SIL-10A with a reversed phase 5 µm ODS (C18) 250 x 4.6 mm column protected with a C18 SecurityGuard guard column (both Phenomenex Inc., Torrance, CA, USA) based on the methods of Fürst and Hallstrom (1992) and Tuckey *et al.* (2009a). The neutralised muscle extracts were centrifuged at 10,000 *g* and a 20 µl subsample injected onto the column. The column oven was held constant at 32 °C and sample cooler at 2 °C. A solvent gradient was run between two mobile phases over a 50 minute period; mobile phase A (MPA) (0.05 M phosphate buffer (NaH₂PO₄) containing 2 g.L⁻¹ of HPLC grade tetrabutylammonium bisulfate (ion-pair reagent) (Fluka, ex Sigma Aldrich Chemical Co.) (pH 5.5) and mobile phase B (MPB) (75% MPA and 25% acetonitrile, pH 5.5). System flow was maintained at 1 ml.min⁻¹ throughout the gradient cycle, which began with 100% MPA for 5 minutes followed by a 20 minute gradient to 70% MPB. This was held for 3 minutes followed by a 2 minute gradient back to 100% MPA. The column was then equilibrated with 100% MPA for a further 20 minutes, totalling 50 minutes. Dual wavelength UV-Vis detection was used to accurately quantify the absorbance of both the creatine compounds (214 nm) and the other compounds (254 nm).

Peak areas were calculated and adjusted with Shimadzu post-run software and compared to standards of known concentration. All values were corrected for dilution factor. Samples were measured in duplicate.

3.4.14 Nucleotide ratios and total pool and potential energy

ATP:ADP, ATP:AMP and ATP:IMP ratios were calculated from the chromatography nucleotide data. The total nucleotide pool was calculated in nmol.g⁻¹ as the sum of ATP, ADP, AMP, IMP, NAD⁺, inosine, hypoxanthine and uric acid.

Potential energy was calculated using equation 2 (Connett 1988; Arthur *et al.* 1992).

$$Pe \text{ (nmol.g}^{-1}\text{)} = \text{creatine phosphate} + 2[\text{ATP}] + \text{ADP} \quad \text{eq. 2}$$

Where Pe is the cell potential energy, phosphate bond state or energetic state, since ATP has 2 and ADP and creatine phosphate have 1 available phosphate for phosphorylation (Connett 1988; Arthur *et al.* 1992).

3.4.15 Chemicals

All chemicals listed in this manuscript were sourced from Sigma-Aldrich chemical company (St. Louis, MO, USA) unless otherwise stated.

3.4.16 Statistical analysis

All data were subjected to normality and equal variance testing prior to analysis. The vessel VO₂ data were fitted with third-order polynomial regression models. Differences between treatments were determined by testing differences between the fitted models, using an F-test. All the muscle and liver VO₂ and mitochondrial activity data were analysed using linear regression.

From the regression analysis, linearity was tested using a runs test, and deviation of the slope from a zero slope was tested using an F-test, to determine whether the slopes and intercepts differed significantly. Differences between treatments in the regression analysis were also determined using an F-test. Differences between control and uncoupled tissues were determined by two-way ANOVA followed by a Bonferroni post-test. Differences in haem protein, both within species and tissues type, and metabolite concentrations were determined using one-way ANOVA followed by a Tukey's post-test. Differences in metabolite concentrations were determined using repeated measures one-way ANOVA with a Bonferroni post-test. Differences in adenylate ratios were determined using repeated measures one-way ANOVA with a Bonferroni post-test on the log₁₀ of the data. All analyses were performed in Prism 4.00 (Graphpad software, San Diego, CA, USA). The significance level used was $P < 0.05$ but actual P-values or greater significance are shown where appropriate. All data appear as mean \pm SEM.

3.5 Results

3.5.1 Muscle VO₂ and mitochondrial activity

VO₂ by vessels from rat, salmon and hagfish showed varying degrees of PO₂-independence between 15-95 mmHg; below and above these values, VO₂ was highly PO₂-dependent (figure 3.1A). The absolute rates of VO₂ in quiescent and CBC treated vessels were well described by third-order polynomial regression models. All fitted models significantly differed between species ($P < 0.0001$). Best-fit equations and R² values are summarised in table 3.1. Rat abdominal aorta showed limited regulation over the range of PO₂s used; regulating the rate to between 95 and 160 ml O₂.kg⁻¹.h⁻¹ between 15-95 mmHg. When exposed to CBC, the VO₂ significantly decreased ($P < 0.0001$). In contrast, salmon ventral aorta and afferent branchial arteries regulated VO₂ better to between 17-20 ml O₂.kg⁻¹.h⁻¹ in quiescent tissue between 15-95 mmHg.

CBC significantly stimulated VO₂ ($P < 0.0001$) to between 27-37 ml O₂.kg⁻¹.h⁻¹ between 15-95 mmHg. VO₂ in the hagfish dorsal aorta was well below that of salmon and rat tissues at only 3 ml O₂.kg⁻¹.h⁻¹ which did not vary between 15-115 mmHg, which was not significantly different to CBC treated vessels.

In contrast to the vessels, VO₂ by cardiac (figure 3.1B) and skeletal (figure 3.1C) muscles in rat, salmon, snapper and hagfish was linearly related to PO₂ over the range examined (0-125 mmHg), and the slope of all treatments was significantly non-zero ($P < 0.0001$). Best-fit equations, r^2 values and non-zero slope tests are summarised in table 3.2 and lines of best-fit presented in figures 3.1B and 3.1C respectively. Rat striated muscles had the highest mass-specific VO₂ of all tissues ranging between 0-1000 ml O₂.kg⁻¹.h⁻¹ in cardiac and soleus muscle and 500 ml O₂.kg⁻¹.h⁻¹ in gastrocnemius muscle over the PO₂ range. Salmon and snapper cardiac muscle VO₂ was not significantly different from each other and ranged between zero and about 350 ml O₂.kg⁻¹.h⁻¹. Salmon and snapper white muscle had similar rates of VO₂, which ranged between 0-115 ml O₂.kg⁻¹.h⁻¹. In contrast, salmon and snapper red muscle VO₂s ranged between 0-220 and 300 ml O₂.kg⁻¹.h⁻¹ respectively, and differed significantly ($P < 0.0001$). Hagfish muscles had the lowest rates of all species, ranging between 0-30 ml O₂.kg⁻¹.h⁻¹ for skeletal muscle and 100 ml O₂.kg⁻¹.h⁻¹ for cardiac muscle at 125 mmHg. As with the striated muscles, VO₂ in salmon liver was linearly related to PO₂ except that below 25 mmHg, the relationship was no longer linear (figure 3.1D). Consequently, a regression line was fitted between 25-125 mmHg. The best-fit equation, r^2 value and non-zero slope test are shown in table 3.2.

Table 3.1. Summary of polynomial regression statistics of O₂ consumption (VO₂) as a function of O₂ partial pressure (PO₂) in quiescent and carbachol (CBC) treated rat, salmon, snapper and hagfish vascular tissues.

Animal	Treatment	Equation	R ²
Rat	Control	$y=5.64x-0.070x^2+3.35e-4x^3$	0.81
	CBC	$y=5.24x-0.071x^2+3.32e-4x^3$	0.84
Salmon	Control	$y=1.01x-0.016x^2+7.61e-5x^3$	0.46
	CBC	$y=1.57x-0.022x^2+1.03e-4x^3$	0.68
Hagfish	Control	$y=0.18x-0.003x^2+1.35e-5x^3$	0.52
	CBC	$y=0.20x-0.003x^2+1.69e-5x^3$	0.51

Table 3.2. Summary of linear regression statistics of O₂ consumption (VO₂) as a function of O₂ partial pressure (PO₂) in quiescent rat, salmon, snapper and hagfish tissues.

Animal	Tissue	Equation	r ²	Non-zero?
Rat	CM	$y=7.904x-49.11$	0.94	P<0.0001
	WM	$y=3.894x-29.58$	0.78	P<0.0001
	RM	$y=7.606x-53.34$	0.77	P<0.0001
Salmon	CM	$y=2.424x+21.40$	0.69	P<0.0001
	WM	$y=0.090x-2.17$	0.87	P<0.0001
	RM	$y=1.678x-3.91$	0.90	P<0.0001
	Liver	$y=2.135x-29.31$	0.48	P<0.0001
Snapper	CM	$y=2.671x+13.69$	0.68	P<0.0001
	WM	$y=1.007x-5.88$	0.91	P<0.0001
	RM	$y=2.345x+6.33$	0.91	P<0.0001
Hagfish	CM	$y=0.737x+10.99$	0.62	P<0.0001
	SM	$y=0.260x+2.89$	0.38	P<0.0001

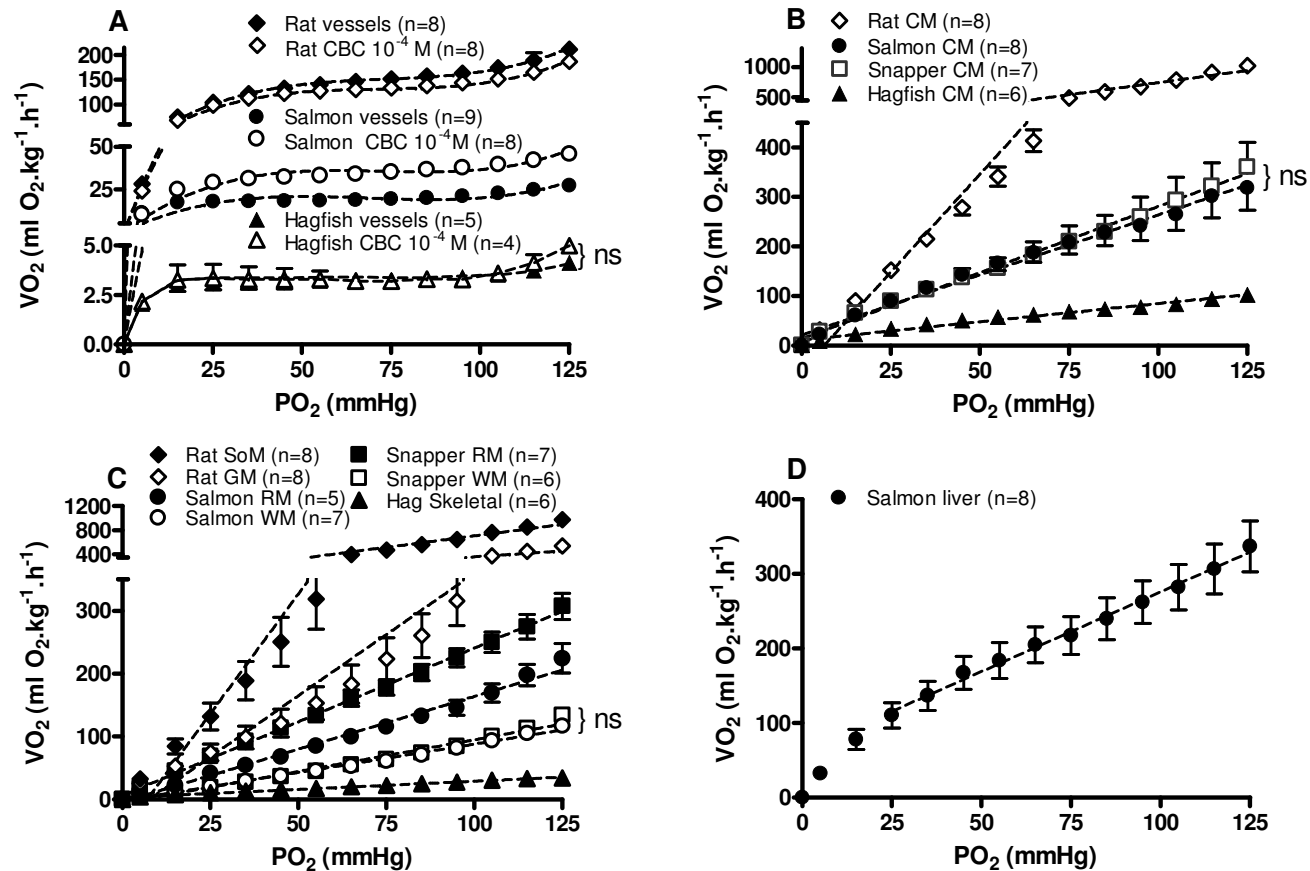


Figure 3.1. O₂ consumption (VO₂) as a function of O₂ partial pressure (PO₂) in rat, salmon, snapper and hagfish tissue slices. **A.** Vessels. Dashed lines are third-order polynomial regression best-fit values. **B.** Cardiac muscle (CM). Dashed lines are linear regression best-fit values. **C.** Skeletal muscles: skeletal muscle (SM), white muscle (WM), red muscle (RM), soleus muscle (SoM), gastrocnemius muscle (GM). Dashed lines are linear regression best-fit models. **D.** Salmon liver. Dashed line is linear regression best-fit model. All regression lines within tissue type are significantly different ($P < 0.0001$) from each other except those indicated by ns (not significant). Regression equations and correlation coefficients are summarised in tables 3.1 and 3.2. Data are mean \pm SEM

VO₂ significantly increased in response to uncoupling in all salmon tissues (figure 3.2). The increase was the most pronounced in the vessels, which no longer oxyregulated, and showed a non-linear O₂ dependency (figure 3.2A). DNP caused a significant increase in VO₂ ($P < 0.01$) above control between 25-125 mmHg, peaking at a 5.2-fold greater rate at 125 mmHg. Similarly, FCCP caused a significant increase ($P < 0.01$) in VO₂ above control between 35-125 mmHg, peaking at a 4.6-fold increase at 125 mmHg. The VO₂ of striated muscles was also significantly increased by treatment with uncouplers. In all striated muscles FCCP stimulated VO₂ the most. FCCP increased cardiac muscle VO₂ above resting between 45-125 mmHg, amounting to a maximal increase of 1.5-fold at 125 mmHg (figure 3.2B). In uncoupled skeletal muscle the trend for increased VO₂ at PO₂s above 15 mmHg was not significant for DNP. However, FCCP significantly raised VO₂ above control values at PO₂s between 65-125 mmHg for red muscle (figures 3.2C) and 95-125 mmHg in white muscle (figures 3.2D).

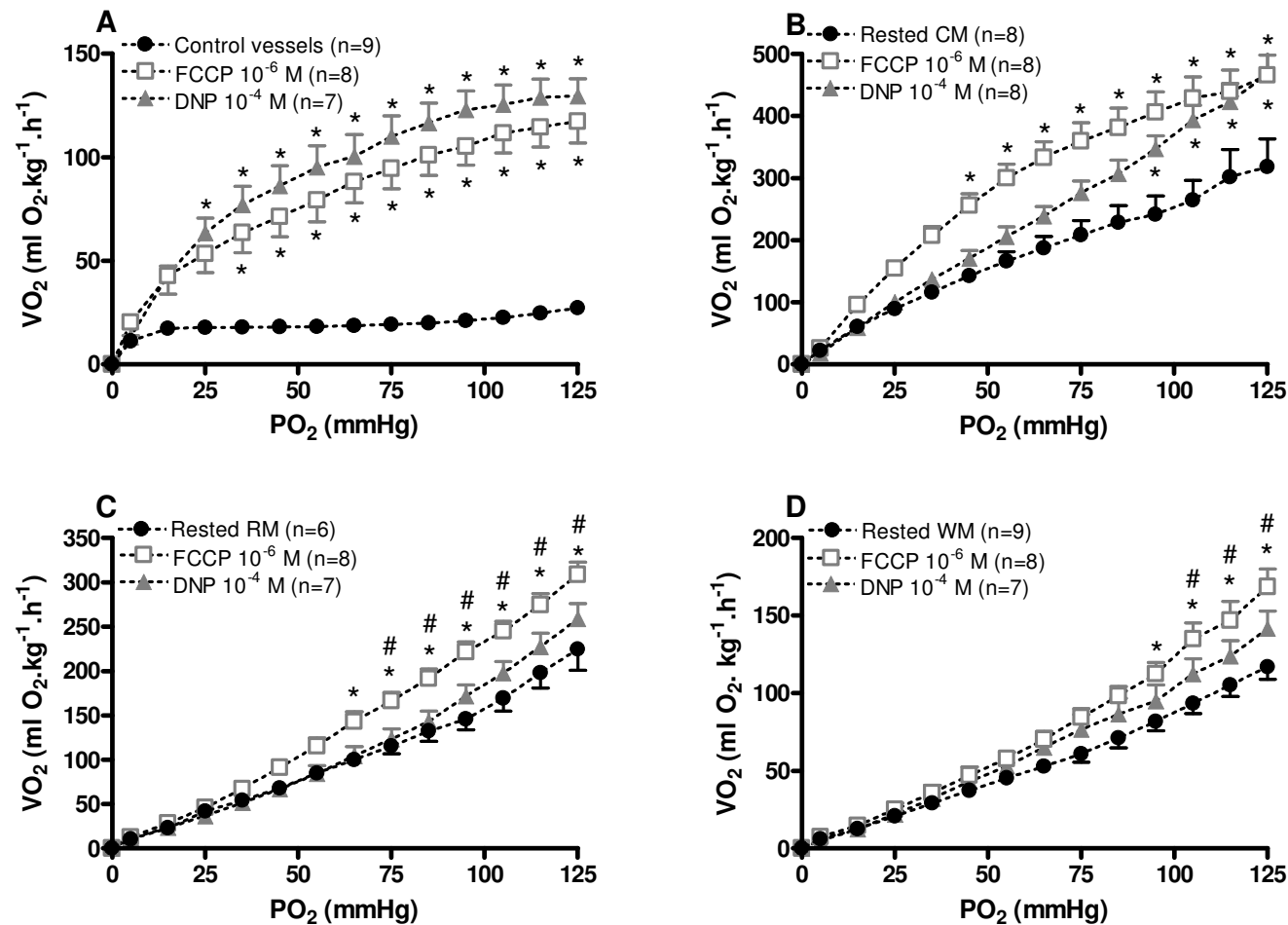


Figure 3.2. O₂ consumption (VO₂) as a function of O₂ partial pressure (PO₂) in quiescent and uncoupled (using DNP and FCCP) salmon tissue. **A.** Vessels. **B.** Cardiac muscle (CM). **C.** Red muscle (RM). **D.** White muscle (WM). * indicates significantly different to control values at corresponding PO₂ and # indicates significantly different between uncoupled treatments (both $P < 0.05$) (two-way ANOVA with Bonferroni post-test). Data are mean \pm SEM.

When subjected to a second PO₂ depletion treatment, the slope of salmon cardiac muscle VO₂ as a function of PO₂ was not significantly different from the initial determination, ranging from zero to around 350 ml O₂.kg⁻¹.h⁻¹ (1st run; $r^2=0.77$ equation: $y=2.716x-8.181$, 2nd run; $r^2=0.76$ equation: $y=2.439x-9.484$, both slopes significantly non-zero $P<0.0001$) (figure 3.3A). The increase in formazan concentration in red and white muscle slices was linearly related to time (red muscle $r^2=0.83$; equation: $y=0.450x-4.426$, white muscle $r^2=0.88$; equation: $y=0.173x-14.140$, both slopes significantly non-zero and different between groups $P<0.0001$) (figure 3.3B). Red muscle formazan production was approximately twice that of white muscle at each time point.

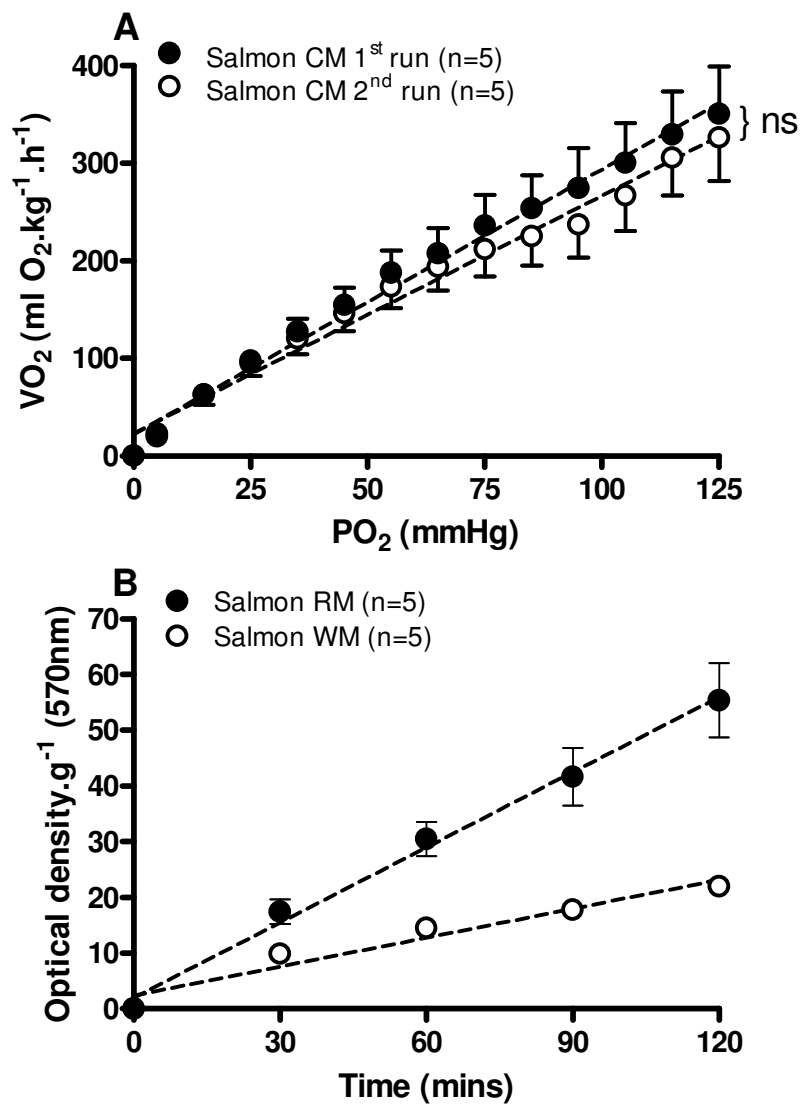


Figure 3.3. Validation of tissue slice viability in salmon tissues. **A.** O₂ consumption (VO₂) as a function of O₂ partial pressure (PO₂) in cardiac muscle subjected to successive O₂ depletion experiments. Dashed lines are linear regression best-fit values (1st run; $r^2=0.77$ equation: $y=2.716x-8.181$, 2nd run; $r^2=0.76$ equation: $y=2.439x-9.484$). Both lines have significantly non-zero slopes ($P<0.0001$). ns indicates that the best-fit regression lines from the two treatments are not significantly different from each other. **B.** Mitochondrial activity in red and white muscle over two hours as indicated by the cleavage of MTT to formazan by succinate dehydrogenase. Dashed lines are linear regression best-fit values (red muscle $r^2=0.83$; equation: $y=0.450x-4.426$, white muscle $r^2=0.88$; equation: $y=0.173x-14.140$). Both lines have significantly non-zero slopes and are significantly different from each other (both $P<0.0001$). Data are mean \pm SEM.

3.5.2 Haem protein concentration

Haem protein concentration in cardiac muscles was significantly greater than in the skeletal muscles in all species ($P < 0.01$) (figure 3.4). Similarly, red muscles had significantly higher concentrations than white muscles within species ($P < 0.05$). Cardiac muscle haem protein concentration varied widely: $3.9 \pm 0.23 \text{ mg.g}^{-1}$ in hagfish, $7.66 \pm 0.63 \text{ mg.g}^{-1}$ in salmon, $11.66 \pm 0.38 \text{ mg.g}^{-1}$ in snapper and $14.16 \pm 1.44 \text{ mg.g}^{-1}$ in rats, consequently all cardiac muscle values were significantly different ($P < 0.05$) from each other, apart from snapper and rat cardiac muscles. Red muscle values varied less: $1.09 \pm 0.08 \text{ mg.g}^{-1}$ in hagfish, $2.49 \pm 0.24 \text{ mg.g}^{-1}$ in salmon, $2.62 \pm 0.12 \text{ mg.g}^{-1}$ in snapper and $3.91 \pm 0.35 \text{ mg.g}^{-1}$ in rats. All values were significantly different from each other ($P < 0.01$), except for salmon and snapper red muscle. Haem protein concentration in the white muscles was very low: $0.28 \pm 0.03 \text{ mg.g}^{-1}$ in hagfish, $0.26 \pm 0.03 \text{ mg.g}^{-1}$ in salmon, $0.12 \pm 0.02 \text{ mg.g}^{-1}$ in snapper and $0.76 \pm 0.13 \text{ mg.g}^{-1}$ in rats. The rat white muscle value was significantly greater ($P < 0.001$) than the other three species, which did not differ.

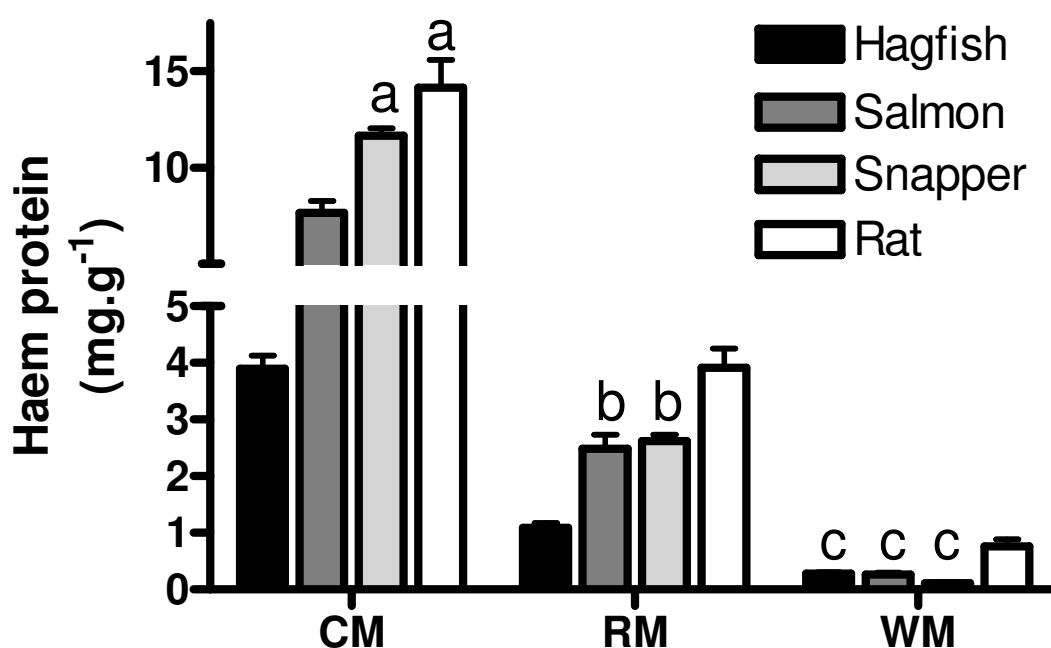


Figure 3.4. Haem protein concentration in rat, salmon, snapper and hagfish striated muscles. Cardiac muscles are from the ventricular spongy myocardium. Rat red muscle is soleus muscle, salmon and snapper red muscle is from the wedge along the lateral line and hagfish red muscle is mosaic skeletal muscle (white and red muscle bands). Rat white muscle is white fibres of the gastrocnemius muscle, salmon and snapper white muscle is from the D-block and hagfish white muscle is “tongue” muscle. All concentrations between tissue types within species are significantly different ($P < 0.05$) (One-way ANOVA with Tukey’s post test). Within tissue type, concentrations that are not significantly different share the same letter ($P < 0.05$) (One-way ANOVA with Tukey’s post test).

3.5.3 Energetics experiment

3.5.3.1 Glycogen, glucose, lactate and pH

Glycogen concentration significantly decreased ($P < 0.05$) after 1 hour of incubation at 30 mmHg and was unchanged at 100 mmHg (figure 3.5A). Glucose concentration was unchanged from initial in either treatment (figure 3.5B). Lactate concentration was significantly reduced over time in both 30 and 100 mmHg incubations ($P < 0.05$, figure 3.5C). Conversely, pH significantly increased ($P < 0.05$) in both incubations and again no difference was determined between incubation treatments (figure 3.5D).

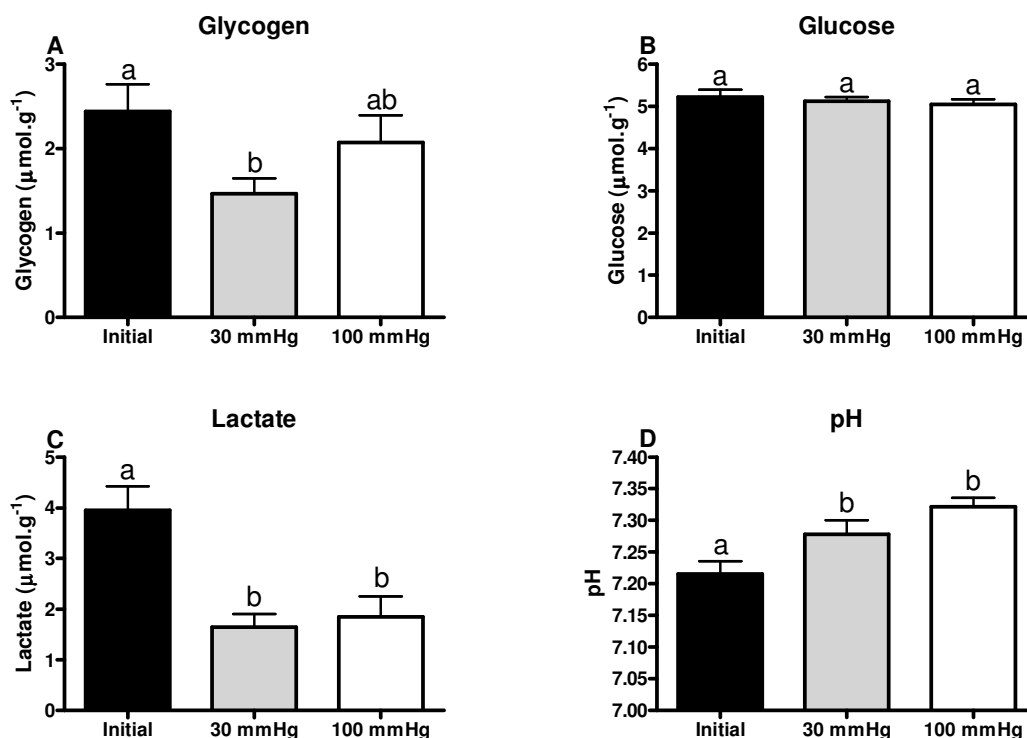


Figure 3.5. Metabolite profiles from salmon red muscle slices immediately after death and after 1 hour of incubation at either 30 or 100 mmHg O₂ in freshwater teleost Ringers solution. **A.** Glycogen. **B.** Glucose. **C.** Lactate. **D.** pH. Treatments which share the same letter are not significantly different from each other ($P > 0.05$) (one-way repeated measures ANOVA with Bonferroni post-test). Data are mean \pm SEM.

3.5.3.2 Creatine phosphate, creatine, creatinine and potential energy

Creatine phosphate was increased ($P < 0.05$) above initial only at 100 mmHg (figure 3.6A). Creatine and creatinine significantly decreased ($P < 0.05$) in both groups (figure 3.6B and 3.6C). Potential energy significantly increased ($P < 0.05$) at 100 mmHg (figure 3.6D).

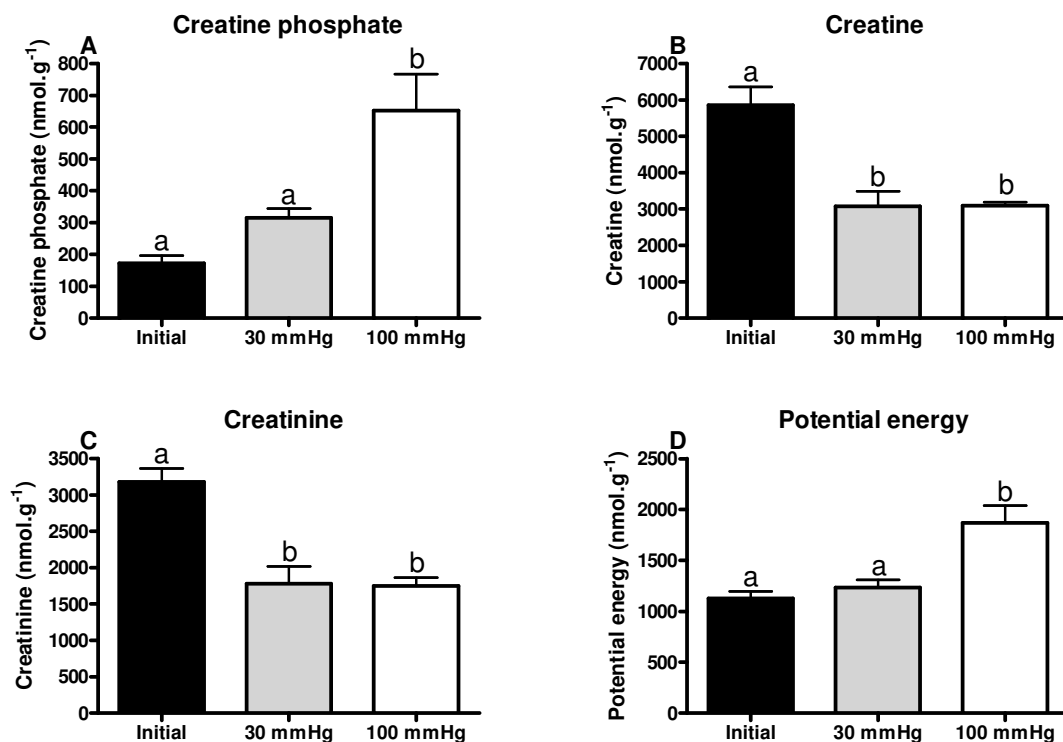


Figure 3.6. Metabolite profiles from salmon red muscle slices immediately after death and after 1 hour of incubation at either 30 or 100 mmHg O₂ in freshwater teleost Ringers solution. **A.** Creatine phosphate. **B.** Creatine. **C.** Creatinine. **D.** Potential energy. Treatments which share the same letter are not significantly different from each other ($P > 0.05$) (one-way repeated measures ANOVA with Bonferroni post-test). Data are mean \pm SEM.

3.5.3.3 ATP, ADP, AMP and NAD⁺

ATP concentration was significantly increased ($P < 0.05$) at 100 mmHg (figure 3.7A) while ADP (figure 3.7B) was unchanged from initial. AMP (figure 3.7C) and NAD⁺ concentrations (figure 3.7D) both significantly decreased ($P < 0.05$) from initial at both PO₂s and there was no difference between incubation treatments.

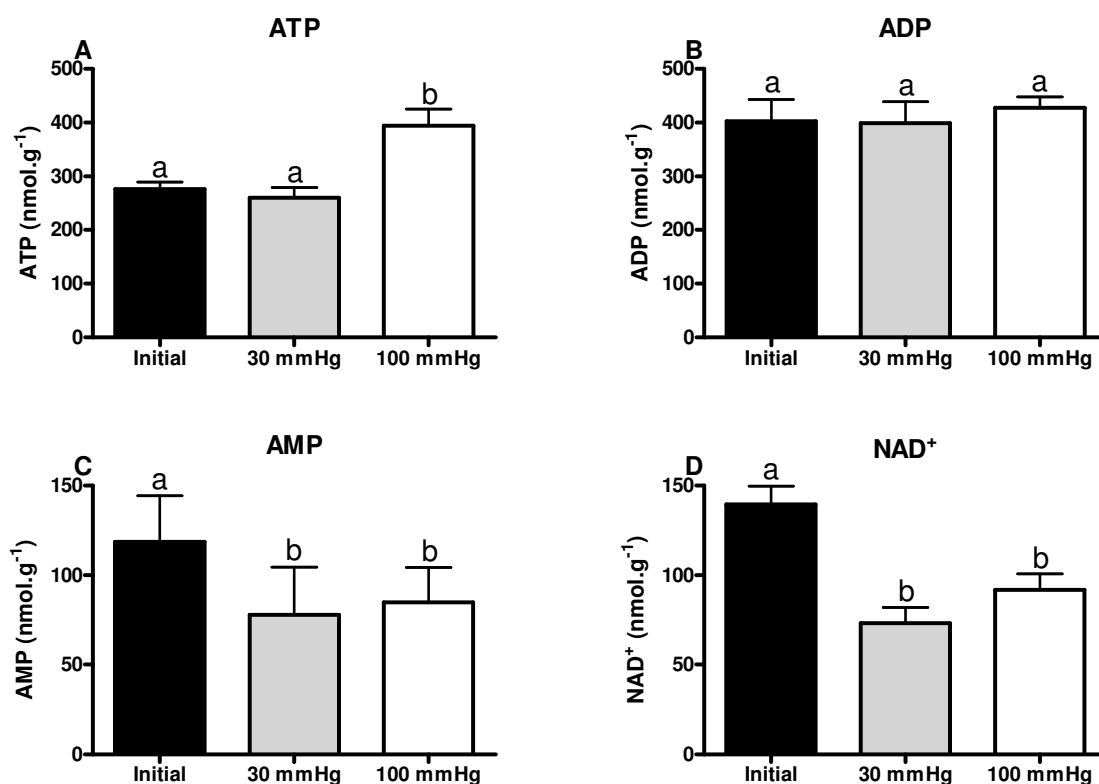


Figure 3.7. Metabolite profiles from salmon red muscle slices immediately after death and after 1 hour of incubation at either 30 or 100 mmHg O₂ in freshwater teleost Ringers solution. **A.** ATP. **B.** ADP. **C.** AMP. **D.** NAD⁺. Treatments which share the same letter are not significantly different from each other ($P > 0.05$) (one-way repeated measures ANOVA with Bonferroni post-test). Data are mean \pm SEM.

3.5.3.4 IMP, Inosine, hypoxanthine and uric acid

IMP (figure 3.8A) and hypoxanthine (figure 3.8C) concentrations were significantly decreased ($P < 0.05$) at both 30 and 100 mmHg. In contrast, inosine (figure 3.8B) and uric acid (figure 3.8D) concentration did not change at either PO₂.

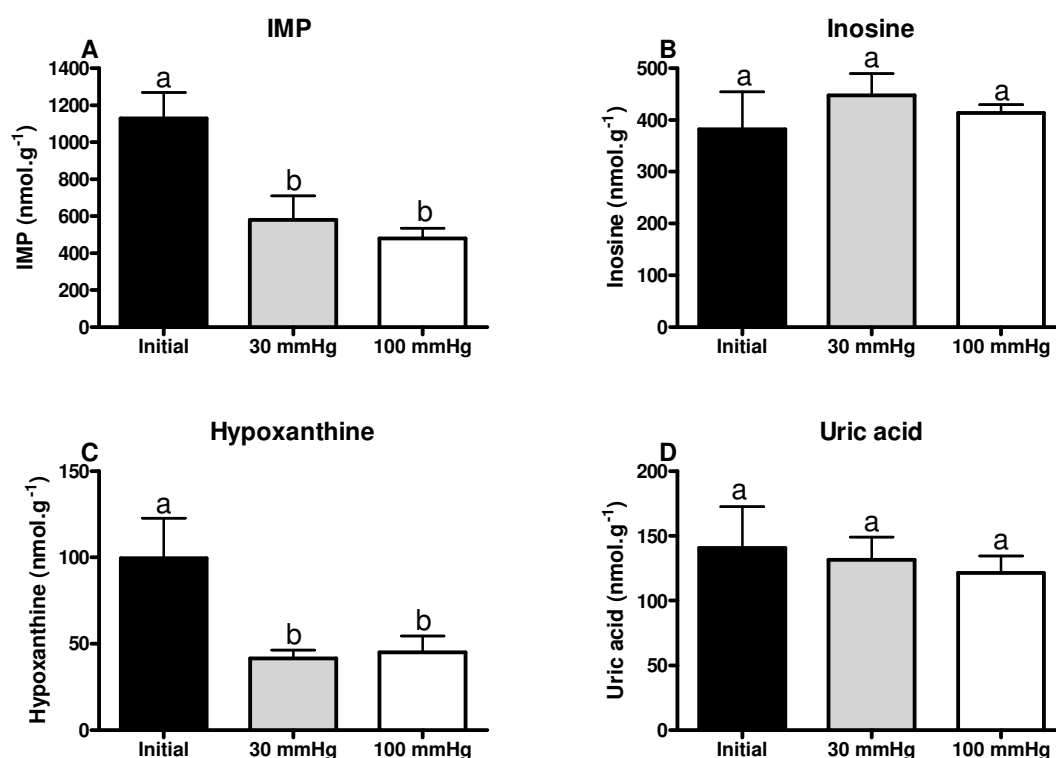


Figure 3.8. Metabolite profiles from salmon red muscle slices immediately after death and after 1 hour of incubation at either 30 or 100 mmHg O₂ in freshwater teleost Ringers solution. **A.** Inosine. **B.** Uric acid. **C.** Hypoxanthine. **D.** IMP. Treatments which share the same letter are not significantly different from each other ($P > 0.05$) (one-way repeated measures ANOVA with Bonferroni post-test). Data are mean \pm SEM.

3.5.3.5 Ratios and total nucleotide pool

ATP:ADP ratio did not change significantly from initial at either PO₂, although there was a positive trend at 100 mmHg (figure 3.9A). Similarly, ATP:AMP ratio increased above initial values in both groups (figure 3.9B). ATP:IMP ratio followed the same pattern except that the two PO₂s differed significantly ($P < 0.05$) from each other (figure 3.9C). Total nucleotide pool significantly decreased ($P < 0.05$) in concentration in both treatments but no difference was detected between the two PO₂ treatments (figure 3.9D).

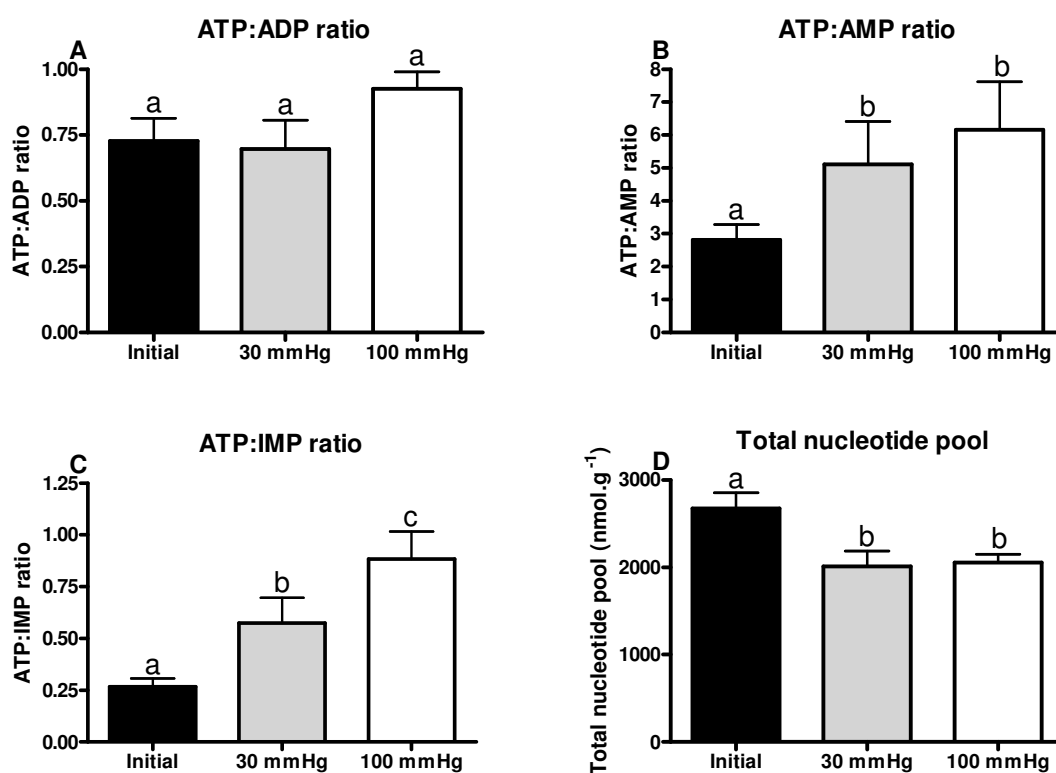


Figure 3.9. Ratios of selected metabolites to ATP and the total nucleotide pool from salmon red muscle slices immediately after death and after 1 hour of incubation at either 30 or 100 mmHg O₂ in freshwater teleost Ringers solution. **A.** ATP:ADP. **B.** ATP:AMP. **C.** ATP:IMP. **D.** Total nucleotide pool. Treatments which share the same letter are not significantly different from each other ($P > 0.05$) (one-way repeated measures ANOVA with Bonferroni post-test). Data are mean \pm SEM.

3.6 Discussion

The vessels from all species regulated VO₂ over a wide range of PO₂s (15-95 mmHg). A steady state metabolism has been reported in other tissues critical for survival; for example, anoxic goldfish (*Carassius auratus*) brain tissue slices showed regulation of heat output at 400 $\mu\text{W}\cdot\text{g}^{-1}$ over an 18 hour period, albeit reduced by a third from oxygenated values (Johansson *et al.* 1995). Application of the acetylcholine agonist CBC to the rat abdominal aorta, which is known to cause vasodilation through acetylcholine-activated endothelium-derived relaxing factor (Furchgott and Zawadzki 1980; Griffith *et al.* 1984; Furchgott *et al.* 1987), caused a significant decrease in VO₂. Conversely, the significant increase in VO₂ in response to CBC in salmon ventral aorta and afferent branchial arteries was most likely due to increased mechanical activity of the smooth muscle.

Acetylcholine-induced vasoconstriction has been reported in numerous vessels from the closely related rainbow trout (*Oncorhynchus mykiss*), which lack acetylcholine-activated endothelium-derived relaxing factor pathways (Small *et al.* 1990; Olson and Villa 1991). Eel (*Anguilla anguilla*) ventral aorta has also been shown to constrict in response to acetylcholine (Guerrero *et al.* 2000). Hagfish vessels, which are known to contract in response to CBC (Olson *et al.* 2008a), showed no increase in VO₂. The reason for this is uncertain. It is possible that some kind of catch mechanism may be able to hold tension in contracted vessels, since hagfish vessels have been reported to maintain tension for extended periods in complete anoxia (Olson *et al.* 2001; Olson *et al.* 2008a), a phenomena possible only if a constant ATP supply from oxidative phosphorylation is not critical to maintaining tension. Interestingly, VO₂ was increased in the hagfish dorsal aorta (n=3 data not shown) when uncoupled with DNP, which indicates that additional scope for oxidative phosphorylation was present in the tissue, despite the lack of VO₂ increase in response to the application of CBC.

Changes in VO₂ due to pharmacologically induced mechanical activity have been reported in other experimental models. For example, Weston (1972) characterised the relationship between smooth muscle tension and VO₂ in the guinea pig taenia coli and rabbit duodenum and abdominal aorta. The taenia coli and duodenum relaxation in response to isoprenaline and phenylephrine resulted in a dose-dependent fall in VO₂. Conversely, phenylephrine contraction in the abdominal aorta resulted in a dose-dependent rise in VO₂. Similar to the current study, VO₂ was O₂-independent in their preparation, which was O₂ rather than air-saturated. Dog femoral arteries in O₂ saturated Ringer were found to oxyregulate over a 2 hour period and VO₂ increased in response to treatment with adrenaline (Kosan and Burton 1966). Our regulated rates for rat abdominal aorta ranged between 95 and 160 ml O₂.kg⁻¹.h⁻¹, which is in accordance with Koenitzer *et al.* (2007) who report a regulated rate above 20 mmHg of about 100 ml O₂.kg⁻¹.h⁻¹ in the same tissue. These values agree well with a range of values (66-270 ml O₂.kg⁻¹.h⁻¹) reported for *in vitro* studies on mammalian vessels (Paul 1980).

Intravascular PO₂ measured in rat vascular tissue of between 52-65 mmHg (Shibata *et al.* 2005; Golub *et al.* 2008) are within the regulated VO₂ range in the current study. The scope to increase in VO₂ approximately 5-fold around these tensions in salmon vessels by uncoupling indicates a significant ability to increase mitochondrial ATP production. Similarly, Steinlechner-Maran *et al.* (1996) reported a 3.5-fold increase in VO₂ in response to both DNP and FCCP in cultured endothelial cells, which oxyregulated above about 4 mmHg. There was a much smaller increase (about 1.75-fold) in VO₂ in response to the high titre of CBC in the current study, which suggests that the cost of contraction is low in relation to total energetic scope. The capacity to increase ATP supply may relate to the significant energy requirements of endothelial cells. For example, energy is required for the formation of molecules associated with nitric oxide, prostaglandins, renin, collagen, endothelin, prostacyclin, interleukin, ROS, Factor VIII, degradation of bradykinin and prostaglandins, expression of antigens and conversion of angiotension I to II (Friesenecker 2007).

In stark contrast to the vessel data, the liver and striated muscles showed strict linear O₂-conformance of VO₂. This phenomenon occurred at PO₂s well above reported *in vivo* values, which range widely from <15 mmHg (Marcinek *et al.* 2003) in resting mouse skeletal muscle to as high as 60 mmHg in resting red muscle in rainbow trout (McKenzie *et al.* 2004). Interestingly, the regression lines fitted to the striated muscle data show in all tissues that c.0 mmHg is the origin, except rat striated muscles where VO₂ was reduced to zero at around 10 mmHg, suggesting a higher critical PO₂ for continued VO₂. This is not surprising considering the greater VO₂ by these tissues and decreased solubility of O₂ at higher temperature. Conversely, liver VO₂ was partially maintained; below a critical PO₂ of around 25 mmHg the VO₂ was below that predicted by the trajectory of the regression line fitted to the data between 25-100 mmHg.

Given that metabolic rates are an order of magnitude higher in endotherms (Hemmingsen 1960), it is not surprising that the ectothermic fish and hagfish tissues produced much lower VO₂ values than the rat tissues. Interestingly, most of the difference between the endo- and ectothermic tissues can be accounted for by temperature effects in the current study. Based on a conservative Q₁₀ of 2, a 27 °C difference in temperature equates to a 5.4-fold difference in VO₂. This correction brings the rat VO₂ values down into the same range as salmon and snapper tissues. Rat vessels had a VO₂ of about 120 ml O₂.kg⁻¹.h⁻¹ at a PO₂ of 55 mmHg. When corrected for temperature, the value becomes 22 ml O₂.kg⁻¹.h⁻¹, very similar to the salmon value of around 20 ml O₂.kg⁻¹.h⁻¹ at the same PO₂. Maximum rates at 125 mmHg of around 1000 ml O₂.kg⁻¹.h⁻¹ in rat cardiac and soleus muscle and 500 ml O₂.kg⁻¹.h⁻¹ in gastrocnemius would decrease to around 180 and 90 ml O₂.kg⁻¹.h⁻¹ respectively. Interestingly, the adjusted rat cardiac muscle value falls well below the fish rates. The adjusted rat red muscle rates are lower than that of the fishes, while the adjusted rat white muscle rates are approximately equal to the rates in fish white muscles. Nonetheless, all the red muscle rates are much greater than the white muscles. The differences between tissue types are likely due to differences in mitochondrial volume-density.

The mitochondrial volume-density of white muscle is similar to mammalian (mosaic) skeletal muscles, but the mitochondrial volume-density of red muscle can be up to 10-fold greater (Leary *et al.* 2003).

The O₂-dependence of VO₂ and ATP turnover on PO₂ is a well documented phenomenon in whole organisms and isolated tissue preparations, including skeletal muscles and liver (Hochachka and Guppy 1987; Hochachka *et al.* 1996; Hogan *et al.* 1992; Boutilier *et al.* 1997; Kuznetsov *et al.* 1998; West and Boutilier 1998; Boutilier 2001a; Boutilier 2001b; Singer *et al.* 2002; Hochachka 2003; Singer 2004). For example, in permeabilised skeletal muscle fibre bundles, a PO₂-dependent VO₂ is reported within and above the physiological range (Kuznetsov *et al.* 1998). Furthermore, Wilson *et al.* (1979) demonstrate that cytochrome c oxidase activity and ATP:ADP ratio are PO₂-dependent below about 75 mmHg in cultured tumour, neuroblastoma and *Tetrahymena pyriformis* cells. An O₂ supply-utilisation relationship is also evident during muscle work. For example, dog skeletal muscle O₂ delivery and consumption was stoichiometric over an 18-fold increase in the rate of ATP turnover induced by progressively increased work, with no measurable change in the concentrations of creatine phosphate, ATP and other metabolites (Arthur *et al.* 1992; Hogan *et al.* 1992). The only parameter in this study that varied directly with ATP turnover was O₂. Consistent with these data are the findings of Stary and Hogan (1999) who report that muscle fatigue is induced more rapidly at 30 mmHg than 159 mmHg in continuously contracted single skeletal muscle fibres. Together with our findings, all these data suggest that O₂ plays a key role in the up- or down-regulation of VO₂ (and by proxy, ATP supply) in a number of endo- and ectothermic vertebrate tissues at PO₂s below, at or above normoxic tissue concentrations. In contrast, some studies suggest that O₂ may simply act as a substrate for respiration under physiological conditions (Marcinek *et al.* 2003), although most authors favour some kind of regulatory role for O₂.

It has been suggested by various authors (e.g. Schumacher *et al.* 1993; Kuznetsov *et al.* 1998; Stary and Hogan 1999; Boutilier 2001b; Boutilier and St-Pierre 2002; Gnaiger 2003) that diffusion-limitation or some kind of O₂ sensing mechanism is induced in tissues well above PO₂s which limit oxidative phosphorylation in mitochondria. Proposed O₂ sensing mechanisms in a number of O₂-sensitive tissues include: metabolite concentrations (e.g. creatine phosphate, ADP, ATP) (Connett 1988), AMP-activated protein kinase (Jibb and Richards 2008), ATP-sensitive potassium channels (Weir and Archer 1995), haem based sensors (Gilles-Gonzalez 2003), activated O₂ species, such as superoxide and hydrogen peroxide, from the mitochondria, nitric oxide (Beurk and Lahiri 2003), NADPH oxidases (Pozeg *et al.* 2003) and cytochrome c oxidase (Wilson *et al.* 2000), amongst many others (for summary see Lahiri *et al.* 2000). However, despite all the work in this area, understanding of the O₂ sensing mechanisms and signal-transduction cascades remain incomplete (Aaronson *et al.* 2006; Olson 2008). Recently H₂S has been suggested as being universally involved in the O₂ sensing/signal-transduction cascade involved in vasodilation and vasoconstriction in smooth muscle in a number of vertebrates (Dombkowski *et al.* 2004; Dombkowski *et al.* 2005; Dombkowski *et al.* 2006; Olson *et al.* 2006; Russell *et al.* 2007; Olson *et al.* 2008a; Olson 2008) and in O₂ sensing in fish gill neuroepithelial cells (Olson *et al.* 2008b), chromaffin cells (Perry *et al.* 2009) and heart (Whitfield *et al.* 2008). Given that oxygen sensing has been demonstrated in smooth muscle and cardiac muscle, it is entirely possible that this mechanism may also act in skeletal muscle. In fact, it has recently been shown that the two enzymes for H₂S production, cystathionine β-synthase and cystathionine λ-lyase, are expressed in the white muscle of rainbow trout (Perry *et al.* 2009). Therefore, the potential role of H₂S in O₂ sensing in skeletal muscles, and possibly other proposed O₂ sensing mechanisms, should form the basis of future investigation.

Alternatively, diffusion-limitation caused by localised hypoperfused regions of tissue, which might fall below the critical PO₂ at which diffusion of O₂ to the mitochondria begins to limit oxidative phosphorylation, may be responsible for the widely reported O₂-dependent pattern of VO₂ (Boutilier and St-Pierre 2002). This raises the possibility that our tissue slices were diffusion-limited due to inadequate rates of O₂ diffusion into the cells in the interior of the slices, which may have fallen below a critical O₂ tension. However, this is unlikely for several reasons: (1) the PO₂ (c.155 - air saturation) at the start of O₂ depletion treatment was 3.75-fold greater than the typical PO₂ value reported in skeletal muscle of about 40 mmHg *in vivo* (McKenzie *et al.* 2004), yet the same linear relationship between PO₂ and VO₂ persisted (data not shown) as between 0-125 mmHg. Therefore, it seems unlikely that diffusion was limiting VO₂ given that there was an excess of O₂ present relative to normoxia over our PO₂ range. A strong PO₂ gradient favouring O₂ entry at these high PO₂s, particularly in the tissues with high myoglobin concentrations, would have facilitated diffusion into the tissues. (2) When mitochondrial respiration was uncoupled in salmon tissues, VO₂ significantly increased at any given PO₂, a phenomenon not possible if diffusion was limiting VO₂. Furthermore, (3) lactate concentration significantly decreased while pH significantly increased, both favoured by the concentration gradients between the tissues and the well-buffered Ringers solution, at both PO₂s in the muscle energetics experiment which suggests that anaerobic glycolysis was not induced. Furthermore, the decline in lactate concentration suggests that any present at the start of the experiment either diffused out of the tissue or was oxidised during the incubation period. These data are not consistent with an anoxic core region in the tissue slices. Finally, (4) VO₂ by the isolated tissues in the current study matched or exceeded whole body rates of consumption. For example, reported temperature dependent resting VO₂ values by *Oncorhynchus* species range between about 35-90 ml O₂.kg⁻¹.h⁻¹ (Brett and Glass 1973; Bushnell *et al.* 1984; Kiceniuk and Jones 1977; Lee *et al.* 2003a) while our values for salmon tissues ranged up to 315 ml O₂.kg⁻¹.h⁻¹ over our PO₂ range (0-125 mmHg).

Given that muscle makes up more than half of the craniate body mass (Withers 1992a), the contribution from this tissue would have been considerable. Thus despite the fact that the various tissues studied would have made different contributions in intact animals - dependent on the mass of tissue - our values were likely in the same range as reported whole animal VO₂ values.

It is also possible that degradation of the tissue slices over time resulted in the decrease in VO₂, coincident with declining PO₂ over time. However, this too is unlikely as: (1) mitochondrial activity in slices continued at a steady rate over a 2 hour period (this was also the case in other tissues; data not shown). (2) When salmon cardiac muscle slices, chosen as a representative tissue, were subjected to a second PO₂ depletion treatment the resulting relationship between PO₂ and VO₂ was not significantly different from the initial (this was also the case in other tissues; data not shown). (3) When salmon red muscle tissue slices were incubated for one hour at either PO₂ in the muscle energetics experiment, key metabolites were maintained (glycogen, glucose and ADP) or even increased in concentration (ATP and creatine phosphate) while the reduction in NAD⁺ suggests flux to NADH (i.e. increased redox potential) and possibly increased donation of electrons for oxidative phosphorylation. It is worth noting that in the presence of cortisol and dexamethasone (glucocorticoid analog), rates of glycogen resynthesis were increased in white muscle slices (Frolow and Milligan 2004). Should the same processes be operating in red muscle, the presence of these hormones may have resulted in increased glycogen synthesis in the current study. (4) Similarly prepared tissue slices cut from white muscle in rainbow trout were shown previously to be viable for 2 hours in biochemical studies (Frolow and Milligan 2004; Kam and Milligan 2006). (5) Indicators of autolytic degradation in fish muscle (IMP, hypoxanthine and uric acid) (Aubourg *et al.* 2007) were decreased in both incubations relative to initial values.

Therefore, based on the evidence presented, it seems unlikely that O₂ diffusion-limitation or tissue degradation caused the observed coupling of VO₂ to PO₂. Instead, some kind of O₂ sensing mechanism may have triggered the observed decrease in VO₂. Coincident with this drop, ATP turnover was reduced in the muscle energetics experiment. Incubation of our representative tissue, (salmon red muscle) at 100 mmHg but not at 30 mmHg, resulted in an increase in ATP and creatine phosphate relative to the initial concentrations, relating to an increase in potential energy (a proxy of ATP turnover) (Connett 1988; Arthur *et al.* 1992). Furthermore, the increase in ATP:AMP ratio and ATP:IMP ratio relative to initial in the 100 mmHg treatment is suggestive of increased ATP turnover at higher PO₂. Considered together, the PO₂-dependence of VO₂ and the concentration of stores of potential energy and lack of ATP supplementation by anaerobic glycolysis at either PO₂ (30 or 100 mmHg) in red muscle suggests that ATP demand decreased with oxidative ATP supply.

Why do isolated cell cultures generally show oxyregulation? Intuitively, one might predict that diffusion distances might be the explanation, i.e. diffusion-limitation to VO₂ in intact tissues is due to large diffusion distances. However, oxyconformance has also been shown in cell cultures. For example, in isolated chick embryonic cardiac myocytes O₂-conformance of VO₂ to air saturation has been reported (Budinger *et al.* 1996). Similarly, VO₂ and other indicators of cellular energetics were shown to be PO₂-dependent in cultured rat hepatocytes in suspension over a wide PO₂ range (anoxia - air saturation) (Schumacker *et al.* 1993). The authors of this study suggest that the reason for this pattern in their work is due to the long time-course of their experiment. They suggest that the oxyregulation seen in cultures generally involves the rapid depletion of PO₂ and thus any O₂ sensing mechanism present might not be activated quickly enough to be observed. Another possible explanation for the oxyconformance of VO₂ is that biochemical pathways are mediated by the intracellular architecture (i.e. organelles, membranous networks, microfilaments, microtubules, channels, pumps, and motors) and possibly by extracellular domains in response to falling PO₂, as Hochachka (2003) suggests.

This possibility is highly plausible and may explain the oxyconformance reported in intact preparations (e.g. perfusion preparations) and *in vivo* versus the often highly disrupted situation typical of cell cultures maintained at supraphysiological O₂ tensions, which may not accurately reflect *in vivo* conditions. Certainly, isolated mitochondria, which are free of the intracellular architecture appear to operate maximally at very low PO₂s (Boutilier and St-Pierre 2002; Gnaiger 2003).

Of note is that the glycogen, creatine phosphate and ATP concentrations are about 5 to 10-fold less than that reported for anaesthetised and rapidly killed rainbow trout red muscle, immediately post-mortem (Saito *et al.* 1959; Richards *et al.* 2002a). The depleted creatine phosphate concentration in our muscle is consistent with the high creatine and creatinine concentrations I report. However, our low glycogen values are not mirrored by an elevated lactate concentration. In contrast to these data are the white muscle glycogen (16 $\mu\text{mol.g}^{-1}$), ATP (6 $\mu\text{mol.g}^{-1}$) and creatine phosphate (18 $\mu\text{mol.g}^{-1}$) concentrations from salmon harvested in exactly the same way as the current study (chapter 5). The reason for the relatively depleted concentrations of glycogen, ATP and creatine phosphate is unclear but may be associated with a relative hypoxia experienced by the red muscle, and consequent depletion of energy reserves, during transport of the fish or in the preparation of the tissues. This relative hypoxia may be due to hypoxaemia; a combination of decreased blood oxygenation and flow as a result of decreased ventilation frequency and heart rate in isoeugenol anaesthetised salmon (Hill and Forster 2004a; Rothwell *et al.* 2005) and/or the much greater mitochondrial density and metabolic activity of the red muscle relative to white muscle (Egginton and Siddel 1989; Luther *et al.* 1995), which would have depleted O₂ and metabolites more rapidly. However, given that lactate values were low suggest that glycogen reserves in this group of fish may have been low to begin with. This could possibly be due to the 48-168 hour fasting period prior to slaughter. Nevertheless, the fact that the concentrations of the metabolites in question were increased post-incubation suggests that the slices were not hypoxic during the incubation period.

Furthermore, despite the low initial concentrations in our tissue, the hypotheses being tested in this experiment were unaffected, since the change in concentration of key metabolites was used as a proxy of the ATP turnover. Consequently the absolute concentrations were of lesser importance.

Haem protein concentration in the tissues reflected in most part the concentration of myoglobin. This is supported by several facts. Firstly, the blood of all animals was heparinised before thorough exsanguination. Secondly, tissues were well rinsed and blotted. Thirdly, the very low haem protein concentrations reported for hagfish and fish white muscles (0.28 mg.g⁻¹ in hagfish, 0.26 mg.g⁻¹ in salmon, 0.12 mg.g⁻¹ in snapper) suggest little haemoglobin contamination, since these tissues have been shown to contain little or no myoglobin (Baldwin *et al.* 1991; Lurman *et al.* 2007). Therefore, if all the haem protein present in the white muscles was from haemoglobin then a maximum of 0.1-0.3 mg.g⁻¹ of haemoglobin was present in the samples. This is a trivial amount when considering the values for red and cardiac muscles which are as high as 14 mg.g⁻¹. However, highly vascularised tissues would have contained more haemoglobin, and could potentially have made a greater contribution to total haem protein concentration. The values I report for haem protein concentration (4-14 mg.g⁻¹ in cardiac muscles, 1-3.8 mg.g⁻¹ in red muscles, 0.1-0.9 mg.g⁻¹ in white muscles) are similar to published values for myoglobin concentration in a variety of tissues. For example, Wittenberg and Wittenberg (2003) report a range of 3.5-5.3 mg.g⁻¹ as typical of cardiac muscle and between 3.5-8.8 mg.g⁻¹ in skeletal muscles. Chicken hearts have been reported to contain between 1-5 mg.g⁻¹ myoglobin and typically less than 1 mg.g⁻¹ haemoglobin, reaching only 4 mg.g⁻¹ after induced haemorrhage (Kranen *et al.* 1999). In contrast to these and our data, O' Brien *et al.* (1992), who reported separating myoglobin and haemoglobin by differential ammonium sulphate precipitation, prior to determination using the orthotolidine/tertiary-butylhydroperoxide method, report rainbow trout white muscle values of 0.0047 mg.g⁻¹ myoglobin and 1.1 mg.g⁻¹ haemoglobin.

They also report values of 1.43 mg.g⁻¹ myoglobin and 12.9 mg.g⁻¹ haemoglobin for soleus and 5.5 mg.g⁻¹ myoglobin and 30.2 mg.g⁻¹ haemoglobin for cardiac muscle in rats. Based on our difficulty in separating haemoglobin and myoglobin and differences in the solubility of the haem proteins from different species outlined in the methods and the extremely high haemoglobin and low myoglobin values reported by O' Brien *et al.* (1992), it seems entirely possible that the ammonium sulphate precipitation, in eliminating haemoglobin, also removed significant concentrations of myoglobin, thus overestimating haemoglobin contamination. This is consistent with the conclusion of Lee-de Groot *et al.* (1998) who report similar problems with differential precipitation using this method. Also, Kranen *et al.* (1999), report that a significant quantity of myoglobin was precipitated using this method.

As might be expected, VO₂ by tissues corresponded with haem protein (myoglobin) concentration. For example, cardiac muscle VO₂ and haem protein concentrations were by far the greatest of the tissue types. Skeletal muscle VO₂ and haem protein concentration were intermediate, while the white muscles, which had very low haem protein concentration, had the lowest VO₂ rates. The presence of large quantities of myoglobin buffers the concentration of O₂ and facilitates flux to mitochondria (Artigue and Hyman 1976; Wittenberg *et al.* 1975; Wittenberg and Wittenberg 1987; Wittenberg and Wittenberg 2007), thus facilitating greater oxidative phosphorylation (Bailey *et al.* 1990; Meyer 2004).

I have demonstrated O₂-dependence of VO₂ in a number of tissues and ATP turnover in skeletal muscle from non-hibernating endo- and ectothermic species. The regulation of ATP supply-demand pathways by available O₂ in tissues (i.e. striated muscle and liver), thus reducing ATP supply with ATP demand pathways when hypoxia is experienced, could serve as an extremely important trait for species survival and adaptation. The oxyconformance of VO₂ differs from the response of vascular tissues to hypoxic challenge.

The oxyregulation observed in these tissues may relate to the critical role they play in delivering O₂ and metabolites around the body, and in synthesising and metabolising various humoral factors that likely translates to a basal metabolic requirement. The current study suggests that both the mechanisms associated with oxyregulation of VO₂ in vascular tissue and oxyconformance of VO₂ in the striated muscles appear to be conserved amongst vertebrates, and raises the question: is/are the sensing mechanism/s the same between vertebrates? If so, these phenomena may be able to be harnessed as a tool to control metabolic rate in tissues in a vast array of situations.

Chapter 4

Oxygen consumption, ventilation frequency and cytochrome c oxidase activity in blue cod (*Parapercis colias*) exposed to hydrogen sulphide or isoeugenol

4.1 Abstract

The effects of hydrogen sulphide (H₂S) and isoeugenol exposure on activity, oxygen consumption (VO₂) and ventilation frequency (Vf) in a teleost fish (blue cod) are reported. Effects of both compounds on cytochrome c oxidase activity *in vitro* compliment these data. In the H₂S treatment group (200 µM Na₂S) both resting VO₂ and Vf decreased, concurrent with narcosis and a loss of equilibrium, after 30 minutes of exposure. These events corresponded with a significant fall ($P<0.05$) in VO₂ (33%) and Vf (20%) by 15 minutes, both declining further to a nadir of 40% of resting values at 30 minutes. After flushing, VO₂ increased to resting levels, with Vf remaining significantly depressed ($P<0.05$) until 30 minutes of recovery. Recovery was accompanied by regained mobility and equilibrium and VO₂ and Vf were significantly increased ($P<0.05$) between 60-70 minutes, by 66% and 15% respectively. Isoeugenol anaesthetised fish (0.011 g.L⁻¹) reached stage 4-5 of anaesthesia accompanied by significant decreases ($P<0.05$) in VO₂ (45%) and Vf (25%) at 25 minutes, both parameters declining further to around 64% and 38% respectively by 35 minutes. Both VO₂ and Vf increased to around resting values after flushing, followed by a significant rise ($P<0.05$) in VO₂ by 45% and Vf by 25% between 30-35 minutes and 35-45 minutes of recovery respectively. Overall, VO₂ in relation to resting rate was reduced in the isoeugenol treated animals, while in H₂S treated fish, exposure was associated with a large oxygen debt, possibly a result of hypoxia or toxic effects. Cytochrome c oxidase activity was significantly greater ($P<0.001$) (about 9-fold) in red muscle than white muscle and gill lamellae. H₂S significantly reduced ($P<0.05$) cytochrome c oxidase activity between 69-79% at 20 µM and 77-97% at 200 µM Na₂S, while isoeugenol had no effect on activity in any tissue.

4.2 Keywords

Hydrogen sulphide, isoeugenol, oxygen-consumption, ventilation-frequency, cytochrome c oxidase, anaesthesia

4.3 Introduction

Hydrogen sulphide (H₂S) is present in the atmosphere and aquatic environments. It has long been recognised as a toxic compound, produced through geological and biological processes (e.g. an end product of certain anaerobic bacteria) and by industrial activity (Beauchamp *et al.* 1984). Acute administration of H₂S, mostly in toxicity studies, has identified complex IV of the mitochondrial electron transport chain, cytochrome c oxidase, as the primary target in mammals (Nicholls and Kim 1982; Khan *et al.* 1990; Dorman *et al.* 2002) and fish (Smith *et al.* 1976; Torrans and Clemens, 1982). This inhibition appears to be similar to that produced by carbon monoxide and cyanide (Szabó 2007).

Further to toxicity studies, H₂S has been identified as an energy source for many photo- and chemoautotrophic bacteria as well as animals such as the lugworm (*Arenicola marina*) (Goubern *et al.* 2007). H₂S is also used as a substrate for ATP generation by colonocyte mitochondria in humans (Goubern *et al.* 2007). H₂S is produced endogenously in vertebrate tissues from L-cysteine by two pyridoxyl 5'-phosphate-dependent enzymes: cystathionine β -synthase and cystathionine γ -lyase (Hosoki, *et al.* 1997; Szabó 2007). This discovery along with intensive research over recent decades has led to the recognition of the biological importance of H₂S in vertebrate tissues; roles have been identified in brain, gastrointestinal, reproductive, pulmonary, vascular and heart tissues (Dombkowski *et al.* 2005). For example, there is now strong evidence that the H₂S is involved in the oxygen sensing/signal-transduction cascade in hypoxic vasoconstriction and vasodilation in vertebrate smooth muscle (Dombkowski *et al.* 2004; Dombkowski *et al.* 2005; Dombkowski *et al.* 2006; Olson *et al.* 2006; Russell *et al.* 2007; Olson *et al.* 2008a; Olson 2008).

It has also been suggested that H₂S exposure can induce hypometabolism. Inhaled H₂S has been reported to produce a completely reversible state of hypometabolism in mice (reducing VO₂, VCO₂, heart rate and core body temperature) (Blackstone *et al.* 2005; Blackstone and Roth 2007; Haouzi *et al.* 2008; Volpato *et al.* 2008).

The original study by Blackstone *et al.* (2005) reported a 90% decrease in VO₂ after 6 hours of exposure to 80 ppm H₂S gas in mice. Subsequently, Blackstone and Roth (2007) reported that normally lethal levels of hypoxia (5% O₂) were survived for a 6.5 hour period in mice pre-treated with 150 ppm H₂S, with 100% mortality in control animals after only 20 minutes. These findings were received with much excitement; since should such effects be present in human tissues, the reduced metabolic rate could provide protection from ischemia-associated tissue damage (e.g. infarction) to organs as occurs after major trauma or cardiac arrest (Szabó 2007; Volpato *et al.* 2008). Interestingly, in addition to the potential to reduce metabolic rate and therefore ischemia associated infarction (Szabó 2007), it has recently been shown that H₂S is directly involved in oxygen sensing in the ischemia preconditioning response in rainbow trout hearts (*Oncorhynchus mykiss*) (Whitfield *et al.* 2008).

In a recent study H₂S-induced metabolic rate depression was reproduced in mice, but not in sedated sheep (Haouzi *et al.* 2008). The difference was attributed to size-related metabolic rate differences associated with endothermy. However, adult pigs showed a reduction in VO₂, VCO₂ and cardiac output (a fall in heart rate, but not stroke volume) on intra-venous H₂S (Na₂S) infusion (Simon *et al.* 2008). Conversely, piglets showed an increase in metabolic rate during H₂S inhalation (Li *et al.* 2008). These apparently conflicting responses to H₂S exposure between species need to be resolved.

In the aquaculture industry there is significant scope for an agent capable of decreasing activity and metabolic rate in animals before they are handled and slaughtered. Such an agent could help reduce the metabolic exhaustion and stress which is associated with increased pre-harvest activity (Johnston 1975; Milligan and Wood 1987; Milligan and McDonald 1988; Pagnotta and Milligan 1991; Milligan 1996; Schulte *et al.* 1992; Wang *et al.* 1994; Thomas *et al.* 1999).

Furthermore, an agent capable of reducing metabolic rate post-mortem that can rapidly cross the gill epithelia pre-harvest and be delivered to muscle tissue is highly appealing since maintaining tissue integrity by slowing autolytic degradation post-mortem has the potential to significantly improve product quality indicators and shelf-life. These kinds of improvements are evident in animals that have undergone “rested harvesting”. Rested harvesting following isoeugenol anaesthesia, mediated via a competitive blockade of neuromuscular transmission (Ingvast-Larsson *et al.* 2003), has been shown to greatly reduce activity, stress and metabolic exhaustion, resulting in significant improvements in quality indicators over conventional harvesting techniques (Jerrett *et al.* 1996; Sigholt *et al.* 1997; Jerrett and Holland 1998; Stehly and Gingerich 1999; Fletcher *et al.* 2003; Iversen *et al.* 2003; Black *et al.* 2004; Kiessling *et al.* 2004; Small 2004; Roth *et al.* 2006; Bagni *et al.* 2007; Bosworth *et al.* 2007; Ribas *et al.* 2007; Wilkinson *et al.* 2008; Tuckey *et al.* 2009a).

The current study examines the metabolic response of a teleost species, the blue cod (*Parapercis colias*), to acute H₂S exposure. Activity, VO₂ and ventilation frequency (Vf) before, during and after exposure are reported. For comparative purposes, the responses to isoeugenol anaesthesia were also assessed. The effects of the two compounds on cytochrome c oxidase activity in gill, red and white muscle in an *in vitro* study compliment these data. Furthermore, investigation of H₂S-induced exposure in a poikilothermic animal tests the hypothesis that a reduction in thermogenesis is the primary mechanism responsible for the hypometabolism reported in mammals.

4.4 Materials and methods

4.4.1 Animals

Adult mixed sex blue cod (*Parapercis colias* Forster) (379 ± 4 g; $n = 16$) were caught in baited cages set from the departmental research boat off Motunau beach, north Canterbury, New Zealand. Once captured, the fish were held in aerated seawater filled tanks while being transported back to the University's seawater aquaria (16°C) maintained on a 12:12 hour (light:dark) cycle. The animals proved particularly placid and fed from the hand after only 2 weeks. They were fed a mixed diet of squid, mussels and commercial fish pellets (Hagen, Mansfield, MA, USA) twice weekly. Animals were not fed within the 48 hours preceding an experiment. Animals were legally obtained, with a Ministry of Fisheries special permit. All manipulations described in this manuscript were approved by the University of Canterbury Animal Ethics Committee.

4.4.2 Respirometry

Approximately 12 hours before respirometry measurements, a fish was netted and placed into a customised perspex closed-box respirometer connected to an aerated reservoir of filtered seawater (see below for detail) and held in a temperature controlled room at acclimation temperature (16°C). The time between set-up and experimentation allowed the fish to recover from the disturbance associated with capture and settle in to its new surroundings. The set-up was covered with a black cotton sheet, so as to screen the fish. The respirometer was lit with a Leica CLS 150X fibre-optic light (Wetchar, Germany), that was switched on at least an hour prior to the initial resting rate measurements. This did not cause outward signs of discomfort. The light/dark cycle of the respirometer conformed to that in the holding aquarium.

The contents of the respirometer were mixed with two large magnetic stirrer bars, separated from the animal by a perspex grate and rotated by IKA-Werke lab disc (Staufen, Germany) magnetic stirrers. The change in the partial pressure of oxygen (PO₂) in the respirometer was measured with a Strathkelvin Instruments (Strathkelvin, Glasgow, Scotland) oxygen electrode (model IL1302) and meter (model 781), with the signal fed via a 4-channel bioamplifier into an ADInstruments Powerlab 4SP (Waverley, Australia) archiving on a PC laptop running Chart 5 software (ADInstruments). The change in PO₂ was used to calculate VO₂, according to the equation:

$$VO_2 = \frac{\Delta PO_2 \times \alpha O_2 \times V}{t \times M} \times 22.39$$

Where VO₂ is oxygen consumption (ml O₂.kg⁻¹.h⁻¹), ΔPO₂ is the change in the partial pressure of oxygen (mmHg, 1 mmHg = 0.133 kPa), αO₂ is the capacitance (seawater 1.66 μmol.l⁻¹.mmHg⁻¹), V is the volume of the respirometer (5.5 l), t is the time (hours), M is the mass of the fish (kg) and 22.39 is a constant used to convert moles to litres. Preliminary experiments showed that VO₂ and Vf were independent of PO₂ when >90 mmHg. As an increased ventilation rate and amplitude and a reflex bradycardia, due to stimulation of neuroepithelial cells, below a PO₂ of about 100 mmHg might have changed cardiorespiratory dynamics (Reid and Perry 2003), the PO₂ in the respirometer chamber was never allowed to drop below 100 mmHg.

4.4.3 Introduction of chemicals

The respirometer was connected to three independently controlled reservoirs (approximately 25 L each) filled with filtered seawater using Maxi-Jet MJ1000 water pumps (Aquarium Systems, Loreggia, Italy). With this arrangement, it was possible to switch between reservoirs and purge the contents of the respirometer by diverting its outflow to a drain pipe.

The set-up allowed sequential control, exposure and recovery VO₂ measurements to be made without moving the fish, with the seawater in the second and third reservoirs used to purge either H₂S or isoeugenol from the respirometer. Sequential dilution was achieved by flowing 25 L of fresh seawater through the respirometer. Any residual concentration of the chemicals in the respirometer were then further diluted when the contents were connected to the third reservoir. VO₂ in response to exposure to the chemicals was measured only after the resting rate had remained stable for at least 1 hour.

A 10 ppt stock solution of AQUI-S™ anaesthetic (AQUI-S NZ, Lower Hutt, New Zealand), containing isoeugenol, was introduced into the reservoir (total of 4 aliquots) every 5 minutes, creating a final concentration of 20 ppm AQUI-S™ (0.011 g.L⁻¹ isoeugenol). The concentration used was based on the manufacturer's recommendations. The respirometer chamber was then closed and the VO₂ measured for 40 minutes. After this time the contents of the chamber was purged and recovery VO₂ and Vf recorded until resting values were again restored. (n=5).

H₂S in solution was generated using hydrated sodium sulphide (Na₂S). A 1 M stock solution of Na₂S was introduced into the reservoir (total of 3 aliquots) every 5 minutes, creating a final concentration of 200 µM Na₂S. The aeration of the reservoir was ceased during mixing in order to avoid gassing off the H₂S in solution. The chamber was then closed and VO₂ measured for 30 minutes. Following this, the contents of the respirometer was purged and recovery VO₂ and Vf recorded until resting values were again restored (n=5). The concentration used was based on preliminary experiments, which showed the concentration to be effective in eliciting a hypometabolic response. Preliminary testing showed that the pH of seawater was unchanged at a final concentration of 200 µM Na₂S.

4.4.4 Ventilation frequency and activity

Gill opercula Vf per minute (cpm) was quantified by manual counts made from a video recording using a Canon MV400i video recorder (Lake Success, NY, USA) at 5 minute intervals. The video recorder was placed underneath the black cotton sheet during the set-up and remotely turned on at the commencement of an experiment. Changes in activity were noted throughout the course of the experiment via an externalised screen on the video recorder. The anaesthesia response in isoeugenol treated animals was assessed according to the scale developed by Summerfelt and Smith (1990).

4.4.5 Cytochrome c oxidase activity

Cytochrome c oxidase activity was measured by extracting the enzyme from fresh tissue and measuring its capacity to oxidise cytochrome c. The method is an adaptation of the methods of Cooperstein and Lazrow (1951) and Torrains and Clemens (1982). Animals (n=6) were restrained in a custom sling and killed by inserting the tip of an “iki jime” fish harvesting tool directly into the brain. Immediately after death, red muscle (pectoral fin muscle), white muscle (D-block) and gill lamellae were removed and placed in a Petri-dish and stored on ice. From these tissues, approximately 40 mg was mixed with 40 volumes of a 40 mM phosphate buffer containing 0.05 % Brij-58 (pH 7.4) in a 1.8 ml Nunc cryotube vial (Roskilde, Denmark). The tissue was homogenised by several bursts of a few seconds on a Heidolf Instruments DIAX 900 (Schwanbach, Germany) homogeniser on setting 3. The homogenate was centrifuged at 6,000 *g* for 5 minutes and the supernatant transferred into a microtube (Axygen, Union City, CA, USA). This extract was placed on ice and assayed immediately. For the assays, the extract was divided into 4 treatments in new microtubes; a control treatment, 2 concentrations of H₂S (20 and 200 µM Na₂S) and 1 of isoeugenol (0.011g.L⁻¹ (20 ppm AQUI-STM).

These treatments were prepared by diluting a minimal volume of a stock solution (6 µl into 300 µl) into the extracts, using distilled water for controls. The extracts were incubated for 10 minutes at 20 °C.

Cytochrome c oxidase activity was assessed by determining the rate at which a minimal volume of extract (5 µl (red muscle) or 20 µl (gill and white muscle)) oxidised a fully reduced (using 100 mM sodium dithionite) 15 µM cytochrome c solution (from horse heart) in a 40 mM phosphate buffer (pH 7.4) at 20 °C. Absorbance readings at 550 nm were made before and every 5 seconds after the addition of the extract for a 2 minute period on a Shimadzu Corporation UV-1700 PharmaSpec spectrophotometer (Shimadzu Scientific Instruments, Columbia, USA). The oxidation rate was calculated from the change in the optical density per minute ($\Delta OD \cdot \text{min}^{-1}$) from the initial linear portion of the oxidation kinetics. Oxidation rates in response to the treatments were expressed as a percentage of the control rate. Samples were measured in duplicate.

4.4.6 Chemicals

All chemicals listed in this manuscript were sourced from Sigma-Aldrich chemical company (St. Louis, MO, USA) unless otherwise stated.

4.4.7 Calculations and statistical analysis

All data were subjected to normality and equal variance testing prior to analysis. Changes in VO₂ and Vf over time were tested using one-way repeated measures ANOVA and Bonferroni post-hoc tests comparing exposure and recovery values to an averaged resting rate. Differences in cytochrome c oxidase activity were identified using one-way ANOVA with a Tukey's multiple comparison post-hoc test. Oxygen budgets were calculated by subtracting the mean resting VO₂ value (average of the 20 minutes prior to exposure) from the mean VO₂ on exposure to the chemical compounds and during recovery.

From this analysis, peaks were identified above and below the baseline (resting rate) and the areas of these peaks (ml O₂. kg⁻¹) calculated, giving an estimation of the depression or elevation in VO₂ relative to the resting rate. All analyses were performed using Prism 4.00 (Graphpad software, San Diego, CA, USA). The significance level used was P<0.05. All data appear as mean ± SEM.

4.5 Results

4.5.1 Isoeugenol respirometry

Prior to anaesthetic exposure, resting VO₂ and Vf in the isoeugenol group were around 55 ml O₂.kg⁻¹.h⁻¹ and 40 cpm respectively (fig 1). Animals gradually underwent changes typical of anaesthesia over the course of the 20 minute mixing period, reaching about stage 3 (Summerfelt and Smith 1990) by the time the respirometer was closed for VO₂ measurements. The animals did not show any notable discomfort or activity while becoming sedated. During exposure the fish entered the equivalent of stage 4-5, losing consciousness and equilibrium, but still showing limited ventilation. VO₂ had fallen significantly (P<0.05) by 25 minutes of exposure to 20 ppm isoeugenol, to around 30 ml O₂.kg⁻¹.h⁻¹, declining further by 40 minutes to 20 ml O₂.kg⁻¹.h⁻¹, representing falls of 45% and 64% respectively. Vf fell more rapidly, becoming significantly less (P<0.05) than the resting rate by 10 minutes of exposure at around 30 cpm, further declining to around 15 cpm by 35 minutes of exposure, representing drops of 25% and 38% respectively.

By the time the respirometer was completely flushed (15 minutes), both VO₂ and Vf had increased to resting values. This was followed by a progressive rise in VO₂, reaching a significantly elevated (P<0.05) value of around 80 ml O₂.kg⁻¹.h⁻¹ (45% increase) between 30-35 minutes from the start of the water change, the rate subsequently declining to resting values. During recovery, the fish regained consciousness and equilibrium.

Similarly, V_f rose progressively, reaching significance ($P < 0.05$) between 35-45 minutes of recovery at around 50 cpm (25% increase), the rate subsequently falling back to resting values.

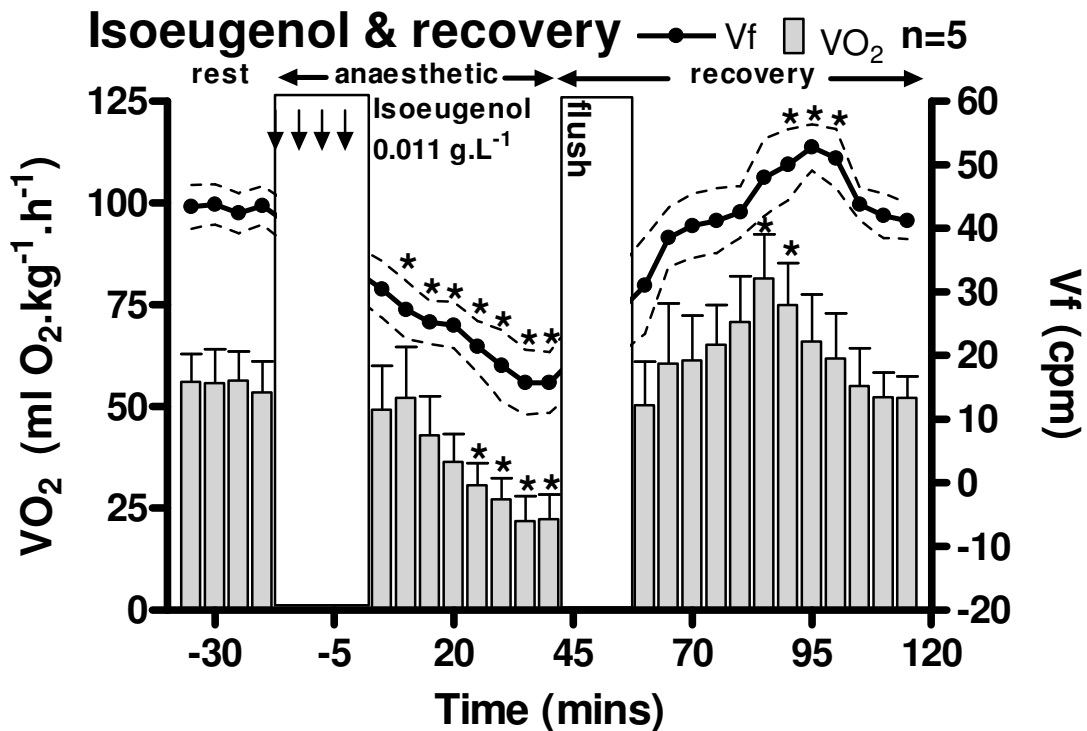


Figure 4.1. Oxygen consumption (VO_2 gray bars) and ventilation frequency (V_f black circles) in blue cod (*Paraperca colias*) exposed to 0.011 g.L^{-1} isoeugenol (20 ppm AQUI-STM). Arrows indicate the successive addition of aliquots of 5 ppm AQUI-STM (final concentration). * indicates a significant difference from an averaged resting value prior to exposure ($P < 0.05$) (one-way repeated measures ANOVA and Bonferroni post-hoc test). The white column post-exposure indicates the period of flushing the respirometer. Data are mean \pm SEM. $n=5$.

The estimated depression of VO_2 below the resting rate in response to isoeugenol exposure was greater than the estimated increase in consumption on recovery (fig 3A). Exposure to isoeugenol resulted in a decrease below resting VO_2 of $1187 \text{ ml O}_2.\text{kg}^{-1}$ over about 70 minutes, with an increase above the resting rate of $486 \text{ ml O}_2.\text{kg}^{-1}$ over about 45 minutes. This resulted in a net VO_2 of $-700 \text{ ml O}_2.\text{kg}^{-1}$ relative to the resting rate. Thus the oxygen not utilised during VO_2 depression was greater than the amount used during recovery.

4.5.2 H₂S respirometry

Prior to treatment, resting VO₂ and Vf in the H₂S group were around 45 ml O₂.kg⁻¹.h⁻¹ and 45 cpm respectively (fig 2). During the 15 minute mixing period the animals showed minor signs of discomfort (large opercular movements and changes in position within the respirometer). In preliminary experiments, this kind of activity did not result in a measurable change in VO₂. What followed the brief period of reactivity was apparent narcosis; the animals gradually decreased their activity and began to lose equilibrium. Animals had reached the equivalent narcotic state of stage 4-5 of anaesthesia by the time the chamber was flushed of H₂S (15 minutes). Changes in melanophores in the animal's skin resulted in a pronounced darkening during the mixing period, followed by lightening of the colouration during the exposure VO₂ measurements and the initial period of flushing. There was a significant fall in VO₂ at 15 minutes of 200 µM Na₂S exposure to around 30 ml O₂.kg⁻¹.h⁻¹, declining further to around 18 ml O₂.kg⁻¹.h⁻¹ by 30 minutes, representing decreases of 33% and 60% respectively. The fall in Vf was concomitant with VO₂, the rate being significantly lower (P<0.05) at 15 minutes of exposure at around 40 cpm, declining further to 20 cpm by 30 minutes of exposure, representing 20% and 60% drops respectively.

By the time the respirometer was completely flushed, VO₂ had increased again to resting levels, while Vf remained significantly depressed (P<0.05) until 30 minutes of recovery (including the flush). During recovery, the VO₂ progressively rose, becoming significantly elevated (P<0.05) between 60-75 minutes of recovery at around 75 ml O₂.kg⁻¹.h⁻¹ (66% increase) which then fell back to resting values. Similarly Vf was significantly elevated (P<0.05) at 52 cpm (15% increase) between 75-95 minutes, which subsequently declined to resting values. A darkening of the melanophores in the animal's skin occurred during this period. During recovery, the fish regained consciousness and equilibrium.

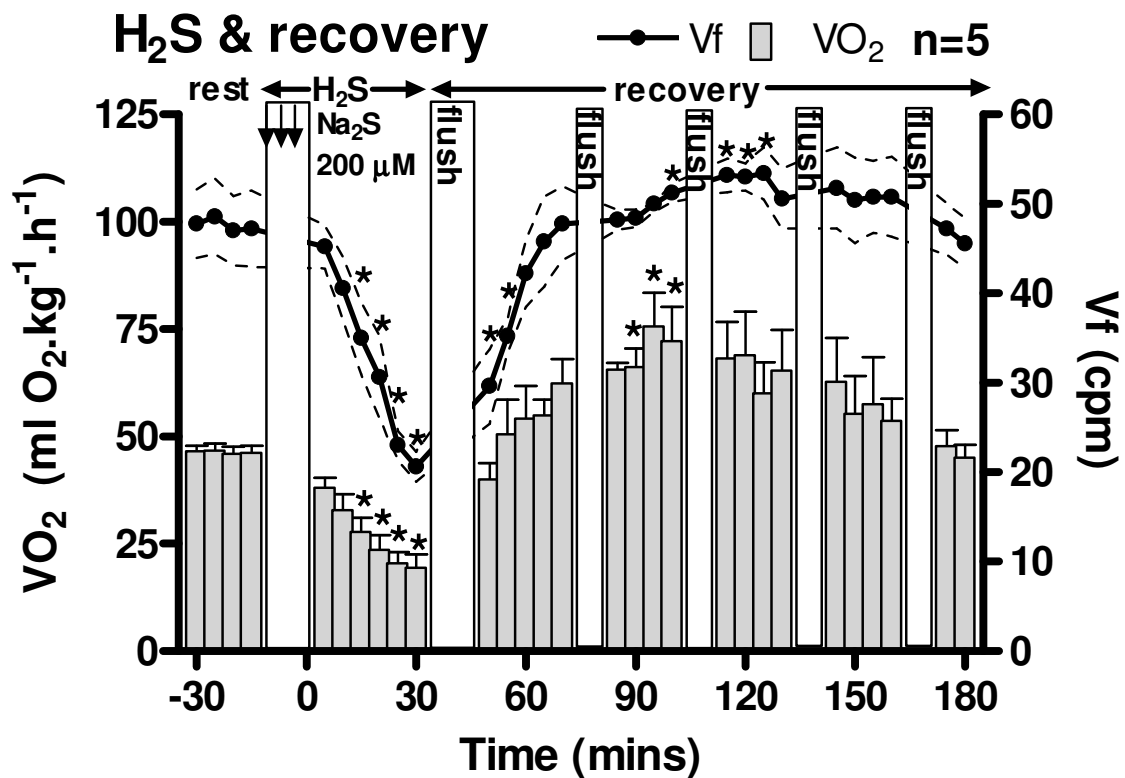


Figure 4.2. Oxygen consumption (VO_2 gray bars) and ventilation frequency (V_f black circles) in blue cod (*Parapercis colias*) exposed to 200 μM ppm Na_2S . Arrows indicate the successive addition of aliquots of 66 μM Na_2S (final concentration). * indicates a significant difference from an averaged resting value prior to exposure ($P < 0.05$) (one-way repeated measures ANOVA and Bonferroni post-hoc test). White columns post-exposure indicate periods of flushing the respirometer. Data are mean \pm SEM. $n=5$.

The degree of VO_2 suppression below resting rates in response to H_2S exposure was similar to the isoeugenol exposed group but on recovery the estimated oxygen usage exceeded the predicted debt (fig 3B). Exposure to H_2S resulted in a decrease below resting rate of 1220 $\text{ml O}_2 \cdot \text{kg}^{-1}$ over 70 minutes, with an increase above resting of 1871 $\text{ml O}_2 \cdot \text{kg}^{-1}$ over about 1½ hours. This resulted in a net VO_2 of +670 $\text{ml O}_2 \cdot \text{kg}^{-1}$ relative to the resting rate. Thus the oxygen utilisation for recovery exceeded that conserved by VO_2 depression.

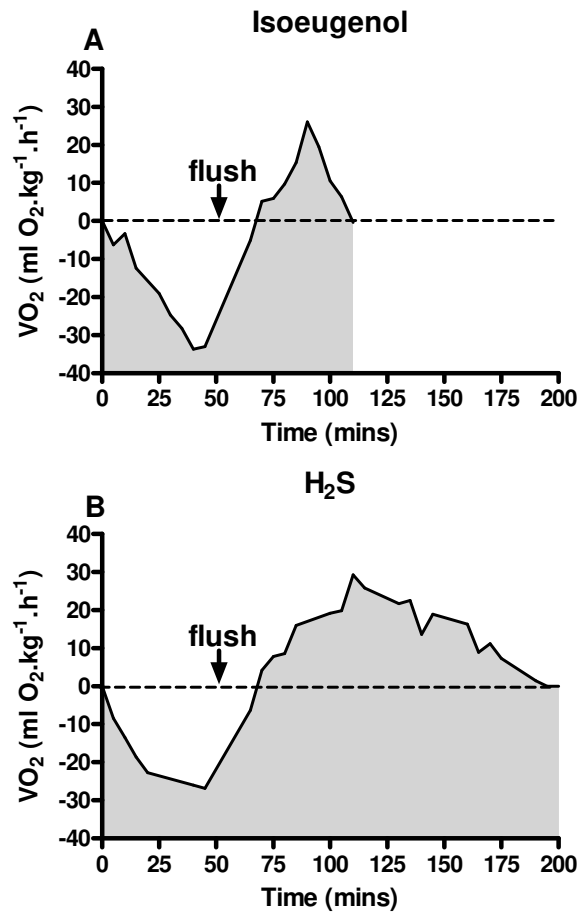


Figure 4.3. Estimated net oxygen consumption (VO_2) (ml $O_2 \cdot kg^{-1} \cdot h^{-1}$) relative to resting rate in blue cod (*Parapercis colias*). **A.** Response to 0.011 g.L⁻¹ isoeugenol (20 ppm AQUI-STM) exposure. Area below the line: 1187 ml $O_2 \cdot kg^{-1}$, area above the line 486 ml $O_2 \cdot kg^{-1}$, net area -700 ml $O_2 \cdot kg^{-1}$. **B.** Response to 200 μ M Na₂S exposure. Area below the line: 1220 ml $O_2 \cdot kg^{-1}$, area above the line 1871 ml $O_2 \cdot kg^{-1}$, net area +670 ml $O_2 \cdot kg^{-1}$. Arrows indicates the start of the initial flush period. Time zero is the start of exposure to either 0.011 g.L⁻¹ (20 ppm AQUI-STM) or 200 μ M Na₂S.

4.5.3 Cytochrome c oxidase activity

Enzyme activity in the tissue extracts rapidly and consistently decreased the optical density of the cytochrome c solution. The control rate ($0.424 \pm 0.045 \Delta\text{OD} \cdot \text{min}^{-1}$) for red muscle was significantly greater ($P < 0.001$) than both white muscle ($0.038 \pm 0.006 \Delta\text{OD} \cdot \text{min}^{-1}$) and gill ($0.077 \pm 0.011 \Delta\text{OD} \cdot \text{min}^{-1}$), representing 11- and 5.5-fold greater rates respectively (figure 4.4A). None of the rates were affected by exposure to $0.011 \text{ g} \cdot \text{L}^{-1}$ isoeugenol, at $105 \pm 17\%$ in red muscle (figure 4.4B), $101 \pm 10\%$ in white muscle (figure 4.4C) and $112 \pm 9\%$ in gill lamellae relative to the control rate (figure 4.4D). In contrast, red muscle extracts showed significantly inhibited ($P < 0.05$) oxidation rates of only $31 \pm 5\%$ and $24 \pm 3\%$ of the control rate in the presence of 20 and 200 μM Na₂S, respectively (figure 4.4B). White muscle extracts showed greater inhibition, to $29 \pm 5\%$ and $4 \pm 1\%$ of the control rate respectively (figure 4.4C). Gill extracts were inhibited the most at $21 \pm 5\%$ and $3 \pm 1\%$ of the control rate respectively (figure 4.4D).

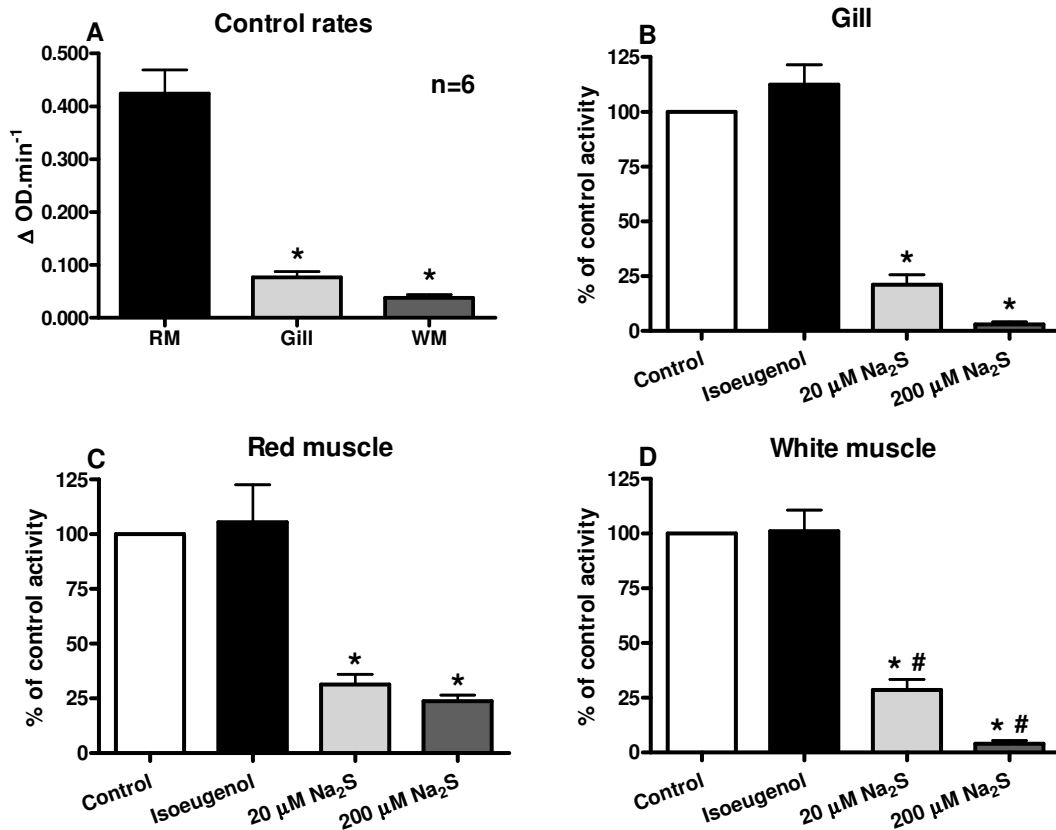


Figure 4.4. Cytochrome c oxidase activity in blue cod (*Parapercis colias*) tissues *in vitro*. **A.** Dilution-corrected rate ($\Delta OD \cdot \text{min}^{-1}$) of control cytochrome c oxidase oxidation of a fully reduced 15 μM cytochrome c solution by gill, red and white muscle extracts. * indicates significantly different from red muscle ($P < 0.001$) (One way-ANOVA with Tukey's post-hoc test). **B** gill, **C** red muscle and **D** white muscle cytochrome c oxidase activity (% of control) in response to incubation with 0.011 $\text{g} \cdot \text{L}^{-1}$ isoeugenol (20 ppm AQUI-S™) and 20 and 200 μM Na₂S. * indicates significantly different to control, bars which share # indicate a significant difference between treatments ($P < 0.05$) (one way-ANOVA with Tukey's post-hoc test). Data are mean \pm SEM.

4.6 Discussion

4.6.1 Physiological consequences of H₂S and isoeugenol exposure

The VO₂ and Vf of blue cod exposed to both 200 µM Na₂S (approximately 60 µM un-ionised H₂S gas at our water temperature and pH) and 0.011 g.L⁻¹ isoeugenol were significantly reduced, and activity declined as the animals became sedated. The anaesthesia produced in response to isoeugenol was similar to that previously reported (Stehly and Gingerich 1999; Iversen *et al.* 2003; Bosworth *et al.* 2007). Acute H₂S exposure also resulted in narcosis, equivalent to that seen in stage 4-5 of anaesthesia. These fish had lost equilibrium, were not reactive to stimuli, but still showed limited ventilation after 30 minutes of exposure. In both groups, flushing the chemical from the respirometer resulted first in a recovery to resting values, followed by a progressive increase in VO₂. In the isoeugenol group, Vf recovered to resting values by the time flushing was complete. The depression in Vf on isoeugenol exposure is consistent with previous reports (Hill and Forster 2004a; Rothwell *et al.* 2005). In H₂S exposed animals, Vf was depressed to a greater extent on exposure and for 30 minutes into recovery (flush and recovery). A depression in Vf was also reported in channel catfish (*Ictalurus punctatus*), showing a decrease from 140 to 88 cpm after 30 minutes of exposure to 6.4 µM un-ionised H₂S (Torrans and Clemens 1982). This and our findings are consistent with the decrease in ventilation reported in mammals (Blackstone *et al.* 2005; Blackstone and Roth 2007; Haouzi *et al.* 2008; Simon *et al.* 2008; Volpato *et al.* 2008).

A reversible reduction in VO₂ on H₂S exposure has been reported in mice (Blackstone *et al.* 2005; Blackstone and Roth 2007; Haouzi *et al.* 2008; Volpato *et al.* 2008) and pigs (Simon *et al.* 2008). The results of the current study indicate that H₂S and isoeugenol also rapidly and reversibly reduce metabolic rate (VO₂) in the blue cod. However, the time from the start of the flush period until resting VO₂ values were completely restored post-exposure differed for the two compounds; isoeugenol treated animals taking 1 hour and H₂S treated animals 2

hours (fig 3). Furthermore, there was a net VO₂ cost in excess of the estimated deficit in relation to the resting rate in the H₂S group. Conversely, the isoeugenol anaesthetised group showed a net saving in VO₂, as the estimated debt was not repaid. Similarly, a small decrease in VO₂ on exposure to isoeugenol is reported in the New Zealand spotty (*Notolabrus celiodotus*) for several hours post-anaesthesia, though this trend was not significant (Hill and Forster 2004b). This contrasted with the response to MS-222 and metomidate, in which no reduction in VO₂ was evident (Hill and Forster 2004b). Thus the finding that isoeugenol exposure can cause a reduction in VO₂ relative to the resting rate is to our knowledge, the first report of this phenomenon. The greater oxygen debt associated with the H₂S exposed animals may relate to the fact that respiration was depressed to a greater extent and for a longer period in these animals. Furthermore, in H₂S exposed animals, the prolonged rise in VO₂ during recovery may be evidence of a detoxification cost, e.g. H₂S oxidation to sulphate (SO₄²⁻) (Beauchamp *et al.* 1984), since previous work has shown that the metabolism of H₂S is oxygen dependent (Olson *et al.* 2008a). Whatever the explanation, it is clear that H₂S exposure does not induce hypometabolism in blue cod.

It is important to differentiate between a reduction in VO₂ and a state of hypometabolism. The decrease in VO₂ observed on H₂S exposure is likely associated with reduced aerobic ATP production. ATP supply under these conditions may be buffered by the creatine kinase pathway and supplemented by anaerobic glycolysis from glycogen stores (Hochachka 1985; Hochachka and McClelland 1997). These compensatory phenomena are elicited to satisfy ATP demand (Hochachka and Guppy 1987; Hochachka and McClelland 1997). As mentioned, the increase in VO₂ post-exposure in both groups suggests a detoxification cost of H₂S, but may also indicate recovery from anaerobic supplementation. For example, repayment of an oxygen debt was associated with burst-type activity in sockeye (*Oncorhynchus nerka*) and coho (*O. kisutch*) salmon (Lee *et al.* 2003), that resulted in a large anaerobic contribution to ATP supply.

Lactate accumulation in the blood of channel catfish exposed to 1.2 µM un-ionised H₂S for 30 minutes also suggests an anaerobic contribution to ATP supply (Torrans and Clemens 1982) in H₂S exposed animals.

Published studies have failed to comprehensively quantify VO₂ post H₂S exposure (Blackstone *et al.* 2005; Blackstone and Roth 2007; Haouzi *et al.* 2008; Simon *et al.* 2008; Volpato *et al.* 2008). From the limited data available, it appears that a large and prolonged rise in VO₂ does follow H₂S-exposure. Blackstone *et al.* (2005) report an increase above resting VO₂ of about 20%, 1-hour after a 6-hour 80 ppm H₂S exposure in mice. The rate immediately after exposure may well have been greater but is not quantified or discussed. Volpato *et al.* (2008) also show a 30% increase in VO₂, for a 15 minute period following a 30-minute exposure to 80 ppm in mice, the rate not returning to resting values by the termination of their experiment. Reliance on anaerobic ATP generation does not constitute a true hypometabolism. True hypometabolism is a two-phase process; an initial defense phase where the balanced suppression of ATP demand and supply pathways occurs (e.g. ion-channel arrest, glucose synthesis blockade, inhibition of anaerobic glycolysis, reduced mitochondrial proton leak), followed by a second phase involving longer-term strategies that involve the down-regulation of proteins and the activation of important genes (Hochachka and Guppy 1987; Hochachka *et al.* 1996; Gnaiger *et al.* 2000; St-Pierre *et al.* 2000; Boutilier 2001; Gnaiger 2003). Hypoperfusion and associated diffusion limitation of oxygen or some kind of oxygen sensing mechanism in skeletal muscle may contribute significantly to these processes (Boutilier and St-Pierre 2002).

The *in vitro* tissue cytochrome c oxidase activity experiment showed no effect of isoeugenol at 0.011 g.L⁻¹. In contrast, activities in all three tissues were significantly inhibited between 69-79% by 20 µM Na₂S and 77-97% by 200 µM Na₂S.

In channel catfish exposed for 30 minutes to a concentration of 6.4 µM unionised H₂S at 20°C cytochrome c oxidase activity was reduced in both brain (58%) and gill (61%) tissue (Torrans and Clemens 1982) and 30 minutes of exposure at a lower concentration and temperature resulted in even greater inhibition of cytochrome c oxidase activity in both the brain (60%) and gill (74%) due to a relative increase in unionised H₂S gas. It is worth noting that maximal inhibition was achieved within the first 5 minutes of exposure. Similarly, maximal inhibition was also achieved in blue cod tissues within the first 5 minutes of exposure *in vitro* (data not shown). Thus it is likely that H₂S inhibited mitochondrial function in tissues *in vivo* by interfering with cytochrome c oxidase, and could have contributed to the observed decline in VO₂ and consequently ATP supply. However, the presence of H₂S detoxification mechanisms in tissues (oxidation, methylation and reaction with metallo- or disulphide-containing proteins) (Beauchamp *et al.* 1984), and the fact that rainbow trout blood rapidly consumes H₂S (Whitfield *et al.* 2008), presumably eliminating endogenously produced H₂S, may have resulted in a rapid decrease in unionised H₂S *in vivo*. If this was the case, peripheral tissues would have been exposed to significantly lower concentrations of H₂S. Therefore, future work should examine both *in vivo* tissue H₂S concentrations and cytochrome c oxidase activity in response to H₂S exposure. Furthermore, the effects of H₂S exposure on fuel utilisation and ATP turnover should be fully elucidated before claims of hypometabolism in H₂S exposed animals can be validated.

4.6.2 Hypoxia and hypometabolism

Differences between H₂S exposure responses in mice and large mammals like sheep (Haouzi *et al.* 2008) have been explained as reflecting the very much larger body mass of these animals, with rapid heat loss in mice helping to reduce metabolic rate by decreasing the energy investment in thermogenesis. However, mice held at 35°C (near thermoneutrality) also showed reduced VO₂ when exposed to H₂S (Volpato *et al.* 2008).

Our studies on an ectothermic teleost fish are a further demonstration that the reduced VO₂ is not dependent on falling body temperature. However, even if a reversible hypometabolic state was induced in the blue cod, the over-compensation in VO₂ post-exposure suggests an overall metabolic cost (hypermetabolism) associated with exposure to H₂S. This is consistent with the hypermetabolism reported in piglets that inhaled H₂S (Li *et al.* 2008). Interestingly, the response to isoeugenol exposure is more suggestive of a hypometabolic state and even though there was some interpolation of data points during periods when the respirometry chamber was flushed, this is a potentially exciting discovery.

Oxygen availability is known to be involved with hypometabolic cascades in both cold- (West and Boutilier 1998; Platzack and Hicks 2001) and warm-blooded animals (Hochachka and Guppy 1987; Singer *et al.* 2002). Therefore, it is possible that some of the depression in VO₂ in both groups was due to decreased O₂ availability, since in the current study both groups showed a dramatic depression in Vf on exposure to the chemicals which likely resulted in decreased oxygen availability, due to oxyhaemoglobin desaturation. In H₂S exposed animals it is highly likely that this phenomenon persisted into the initial recovery period, given that Vf remained suppressed relative to the resting rate 30 minutes into the recovery period. In other studies, reduced Vf induced by H₂S exposure has been shown to result in compromised oxygen saturation of the blood. For example, reduced respiratory rate accompanied a drop in arterial PO₂ of 19 mmHg in mice that inhaled 80 ppm H₂S (Volpato *et al.* 2008). An even bigger decrease of 58 mmHg was reported in pigs who received 2 mg.kg⁻¹.h⁻¹ H₂S via i.v. infusion (Simon *et al.* 2008). Similarly, a reduced Vf results in hypoxaemia in isoeugenol anaesthetised fish (Hill and Forster 2004a). H₂S may have also directly affected the oxygen carrying capacity of the blood by the conversion of haemoglobin to sulfmethaemoglobin (Beauchamp *et al.* 1984).

Furthermore, acidosis of the blood by H₂S derived protons (H₂S in the blood would dissociate to form HS⁻, H⁺ and S₂⁻) as well as protons produced as a by-product of anaerobic glycolysis in tissues could have further reduced the oxygen carrying capacity of the blood.

H₂S also has direct effects on vascular tissues. It has been shown to act as a potent constrictor of the rainbow trout efferent branchial arteries (Dombkowski *et al.* 2005), lamprey dorsal aorta (Dombkowski *et al.* 2006) and hagfish efferent branchial arteries and dorsal aorta (Olson *et al.* 2008a) *in vitro*. Thus, the metabolic tissue hypoxia induced by interference with cytochrome c oxidase and likely reduction in the oxygen saturation and carrying capacity of the blood may have been further compounded by direct H₂S-induced vasoconstriction, resulting in reduced blood flow to tissues. Further to these direct effects, teleosts typically release catecholamines during hypoxia, which also constricts the systemic vasculature (Sandblom and Axelsson 2005; Sandblom and Axelsson 2006). Furthermore, it has recently been reported that H₂S directly stimulates catecholamine release via membrane depolarisation followed by Ca²⁺-mediated exocytosis from chromaffin cells in veins and anterior kidneys in rainbow trout (Perry *et al.* 2009). The observation that melanophores in the skin darkened and then lightened in our H₂S exposed animals may be an indication of the presence of catecholamines in the bloodstream, since injection of catecholamines in fish is associated with both melanophore expansion and contraction, the predominant response being contraction (darkening) (Bagnara and Hadley 1973; Mazeaud and Mazeaud 1981). Catecholamines are released from autonomic nerves that are intimately associated with melanophores, and in rainbow trout the severing of these nerves resulted in the expansion of melanophores, lightening the colour of the skin (Bagnara and Hadley 1973; Mazeaud and Mazeaud 1981). Therefore, it is possible that the lightening in colour following the initial darkening may have represented the loss of autonomic nervous control.

The additive effects of direct H₂S vasoactivity (Dombkowski *et al.* 2004; Dombkowski *et al.* 2005; Dombkowski *et al.* 2006; Olson *et al.* 2008a) and that induced by hypoxia, via circulating catecholamines and possibly through a direct action on the smooth muscle (Olson *et al.* 2001; Russell *et al.* 2001; Smith *et al.* 2001; Russell *et al.* 2007; Olson *et al.* 2008a) may have resulted in a profound decrease in tissue blood flow in our animals.

Recent evidence suggest that H₂S itself directly mediates oxygen-sensing in neuroepithelial cells in fish gills, which trigger many of the responses to hypoxia typical in teleost fish including bradycardia (Olson *et al.* 2008b). Olson *et al.* (2008b) report that intrabuccal injection of H₂S produced a transient dose-dependent bradycardia, which was similar to the hypoxic response in rainbow trout. Furthermore, Torrains and Clemens (1982) also reported bradycardia in catfish exposed to H₂S. Thus H₂S may have directly activated gill neuroepithelial cell responses and produced bradycardia in our animals.

Isoeugenol exposure slowed heart rate, cardiac output, stroke volume and reduced central blood pressure during anaesthesia and resulted in catecholamine release following anaesthesia in Chinook salmon. These effects were attributed to hypoxaemia i.e. reduced PO₂ in the dorsal aortic blood (Hill and Forster 2004a; Rothwell *et al.* 2005). The decreased blood flow and pressure coupled with hypoxaemia (Hill and Forster 2004a; Rothwell *et al.* 2005), and the reduced metabolic rate (current study) on isoeugenol anaesthesia strongly implicate reduced oxygen supply in initiating a reduction in VO₂. Interestingly, high cut-surface muscle pH values (7.5-7.6) are typically reported in animals that have been rested harvested with isoeugenol, indicating that energy supply has not been supplemented anaerobically (Black *et al.* 2004; Forgan and Forster 2008; Tuckey *et al.* 2009). Considered together these data suggest an overall reduction in metabolic rate, and therefore ATP demand, upon anaesthesia with isoeugenol that is coupled to oxygen supply.

Hypoxic hypometabolism has been reported in a number of fish species. For example, hypoxia-induced hypometabolism has been reported in goldfish (*Carassius auratus*) (van Ginneken *et al.* 2004). Furthermore, evidence of blood flow dependent VO₂ is common in the literature, with many studies showing that VO₂ and oxygen delivery are stoichiometric (Hochachka and Guppy 1987; Hochachka and McClelland 1997; Boutilier 2001). In our laboratory, I have shown this to be the case in fish muscle; VO₂ was oxygen delivery dependent below a critical oxygen delivery in a perfused Chinook salmon tail preparation (Forgan and Forster 2008). These data suggest that oxygen supply may be the signal to reduce aerobic ATP demand in hypoxia challenged animals. Thus it is likely that reduced oxygen delivery contributed to the decreased VO₂ observed in blue cod exposed to both isoeugenol and H₂S. Furthermore, it is possible that the blocking of neuromuscular transmission may have resulted in a reduced oxygen demand due to a reduction in tonic activity in the muscle tissue, contributing to the reduced debt associated with isoeugenol anaesthesia.

4.6.3 Narcotic properties of H₂S

Could H₂S be used as a narcotic agent? It certainly produced a rapid state of immobilisation in the blue cod. This is consistent with earlier reports of sedation in mammals (Blackstone *et al.* 2005; Blackstone and Roth 2007; Haouzi *et al.* 2008; Volpato *et al.* 2008). In addition, the complete recovery from sub-lethal H₂S exposure of mice (Blackstone *et al.* 2005; Blackstone and Roth 2007; Haouzi *et al.* 2008; Volpato *et al.* 2008), rats (Khan *et al.* 1990; Dorman *et al.* 2002) and fish (Smith *et al.* 1976; Torrains and Clemens 1982, current study) is good evidence that the compound is rapidly and effectively metabolised and has no apparent long-term effects. Cytochrome c oxidase activity had fully recovered by about 6 hours in channel catfish exposed to 1.2 µM un-ionised H₂S for 30 minutes (Torrains and Clemens 1982). Surprisingly, in preliminary experiments to the current study fish exposed for 30 minutes to H₂S concentrations as high as 500 µM recovered well after exposure, reaching good condition scores.

The presence of the previously mentioned detoxification mechanisms of H₂S in tissues also gives H₂S potential as a reversible narcotic agent. Detoxification processes may explain the exceptionally rapid removal of H₂S in the extremophile Mexican cave fish (*Poecilia mexicana*) which can live in concentrations of H₂S as high as 300 µM (Tobler *et al.* 2006), a concentration that is lethally toxic to most fishes on prolonged exposure (Smith *et al.* 1976).

4.6.4 Summary

I have demonstrated changes in the metabolic rate of a teleost species following exogenous H₂S exposure for the first time. The dramatic fall in VO₂ and Vf on exposure to 200 µM Na₂S is compensated for by an excess VO₂ and Vf on recovery. The drop in VO₂ and Vf is similar to that induced by isoeugenol anaesthesia, though in this treatment there was a net reduction in VO₂ relative to resting rate and a quicker time to recover Vf. Cytochrome c oxidase activity was not compromised by isoeugenol at a concentration of 0.011 g.L⁻¹ *in vitro* in gill lamellae, red and white muscle. In contrast, a concentration of 20 µM Na₂S resulted in an approximately 70% reduction in activity, while 200 µM Na₂S resulted in an almost complete inhibition in all three tissues. The results suggest that the reduction in VO₂ on H₂S exposure is not a true hypometabolism. However, I have identified that H₂S has narcotic properties in fish.

Chapter 5

Post-mortem calorimetric and biochemical profiles of Chinook salmon (*Oncorhynchus tshawytscha*) white muscle following rested and exhausted harvesting

5.1 Abstract

I report calorimetric and biochemical profiles of anoxic post-mortem white muscle from Chinook salmon subjected to rested and exhausted harvesting regimens at their acclimation temperature (10°C). Rested animals were undisturbed and anaesthetised with 0.012 g.L⁻¹ isoeugenol prior to harvest. Power output was significantly greater in the rested group at the time of death and for 7 hours post-mortem ($P < 0.01$). The muscle of these animals had a high metabolic rate at the time of death, at around 400 $\mu\text{W.g}^{-1}$, which declined rapidly over the first 12 hours to 15 $\mu\text{W.g}^{-1}$. Exhausted animals were forced to swim and were then crowded before capture. In this group the initial power output was $< 10 \mu\text{W.g}^{-1}$. In both groups there was an exothermic event, occurring between 4 and 6 hours post-mortem amounting to a rise of around 35 $\mu\text{W.g}^{-1}$. A single-phase exponential decay model ($R^2 = 0.98$; intercept 417 $\mu\text{W.g}^{-1} \mu\text{mol.g}^{-1}$; half-time 2.3 hours) appropriately described the net power output of the rested profile when the data from exhausted fish were subtracted. Rested animals had significantly higher ($P < 0.05$) initial cut surface pH (7.5 vs 6.7), tissue glycogen (16 vs 2 $\mu\text{mol.g}^{-1}$), creatine phosphate (18 vs 0.1 $\mu\text{mol.g}^{-1}$), ATP (6 vs 3.5 $\mu\text{mol.g}^{-1}$) and potential energy (30 vs 7 $\mu\text{mol.g}^{-1}$) than the exhausted group, which had significantly elevated ($P < 0.05$) tissue concentrations of lactate (43 vs 18 $\mu\text{mol.g}^{-1}$) and glucose (5 vs 2 $\mu\text{mol.g}^{-1}$). Both groups showed a rapid depletion in metabolites post-mortem, with significant drops ($P < 0.05$) in many by the first hour. However, potential energy in the form of ATP, glycogen and creatine phosphate pools remained elevated for an extended period post-mortem in rested animals while catabolites further down the chain such as inosine, hypoxanthine and uric acid accumulated at similar rates in both groups.

5.2 Keywords

Muscle, calorimetry, anaerobic-metabolism, ATP, isoeugenol, energetics

5.3 Introduction

Seafood, primarily fish, constitutes about 20% of the animal protein consumed by humans worldwide (Zabel *et al.* 2003). The activity of the skeletal muscle of these animals at the time of harvest influences the energy charge of the tissue which can greatly affect the period of cell viability before rigor mortis sets in and autolytic degradation begins (Fletcher *et al.* 2003; Black *et al.* 2004; Bosworth *et al.* 2007). White muscle is typically recruited for predatory and escape behaviours (Johnston and Ward 1975; Bone 1978; Peake and Farrell 2004) and possesses large carbohydrate stores which are utilised for anaerobic energy generation (Johnston 1975; Moyes *et al.* 1989; Milligan 1996). The stores of carbohydrate, creatine phosphate and ATP are readily depleted by pre-mortem activity (Johnston 1975; Milligan and Wood 1987; Milligan and McDonald 1988; Pagnotta and Milligan 1991; Milligan 1996; Schulte *et al.* 1992; Wang *et al.* 1994; Thomas *et al.* 1999). Thus it is desirable to use harvest regimens that conserve the energy generating potential in tissues. White muscle from fish that are rested harvested, frequently combining pre-harvest anaesthesia, invariably has a higher cut-surface pH and extended pre-rigor period and shows improvements in a host of other indicators of meat quality (e.g. texture, colour, gaping, drip loss) (Jerrett *et al.* 1996; Sigholt *et al.* 1997; Jerrett and Holland 1998; Stehly and Gingerich 1999; Fletcher *et al.* 2003; Iversen *et al.* 2003; Black *et al.* 2004; Kiessling *et al.* 2004; Small 2004; Roth *et al.* 2006; Bagni *et al.* 2007; Bosworth *et al.* 2007; Ribas *et al.* 2007; Wilkinson *et al.* 2008; Tuckey *et al.* 2009a). These characteristics are highly desirable since they are associated with freshness and perceived quality of consumed items. To this end, the application of anaesthetics safe for human consumption in the aquaculture industry is being increasingly explored (e.g. Stehly and Gingerich 1999; Bosworth *et al.* 2007; Tuckey *et al.* 2009a; Tuckey *et al.* 2009b).

Extending viability in tissues is underpinned by knowledge of post-mortem metabolism and biochemistry, particularly relating to energy stores and how they are used in the essentially anoxic conditions associated with the loss of blood supply upon death. Quantifying post-mortem metabolism and energetics in harvested tissue is fundamental to the process of understanding tissue degradation. This understanding could help in the development of strategies to maximise harvest returns via handling protocols that slow the progression of autolysis. The aim of the current study was to measure metabolic activity and biochemical changes in post-mortem white muscle in a commercially harvested teleost species, Chinook salmon, subjected to two quite different harvest regimens. The first was a simulation of the exercise, crowding and netting procedures typical of some commercial aquaculture facilities (exhausted harvest). The second was a controlled anaesthesia with isoeugenol, involving the competitive blockade of neuromuscular transmission (Ingvast-Larsson *et al.* 2003), before harvest with minimal “burst-type” activity and associated stress (rested harvest). I used anoxic isothermal calorimetry to evaluate the effects of exhausted and rested harvesting on anaerobic metabolic rate post-mortem. These data were correlated with a parallel longitudinal study measuring glucose, glycogen, lactate, creatine compounds, ATP and other important purine nucleotides, nucleosides and related bases. From these values, adenylate ratios to ATP, the total nucleotide pool, potential energy (Connett 1988; Arthur *et al.* 1992) and K-values (Aubourg *et al.* 2007) were calculated. Correlation analysis between power output and the metabolites link changes observed in the two datasets. Both studies were performed within one degree of acclimation temperature (10°C) to minimise the effect of temperature change on the post-mortem physiology.

5.4 Materials and Methods

5.4.1 Animals

Female Chinook salmon (*Oncorhynchus tshawytscha*, Walbaum) (mass 1.898 ± 0.111 kg; fork length 51 ± 1 cm; condition factor 1.41 ± 0.04 ; $n = 28$) were obtained from a local freshwater salmon farm (Isaac Salmon Farm, Canterbury, New Zealand). The animals were transferred from commercial raceways, where they had been fed up until the time of transfer with Reliance Stock Feeds salmon pellets (CRT, Dunedin, New Zealand), into an 1800 L holding tank which had a continuous flow of high quality bore-water (a constant 11°C). These fish were left undisturbed for a minimum of 48 hours and were used within 1 week of transfer into the holding tanks. The animals were not fed after transfer to the holding tanks. All manipulations described in this manuscript were approved by the University of Canterbury Animal Ethics Committee.

5.4.2 Exhausted harvest

Individual fish were forced to swim in their holding tanks for 5 minutes by chasing them with a large net. An individual fish was then manoeuvred into one quarter of the tanks volume using a wooden board, netted and placed into 20 L of water (11°C) in an insulated transport container. The water was then gassed with 100% oxygen for 5 minutes and the air-space in the container filled with oxygen and the animals transported to the University. Immediately on arrival (<25 minutes), the animals were restrained in a custom sling and killed by inserting the tip of an “iki jime” fish harvesting tool directly into the brain. Immediately after death, approximately 1 ml a 0.9% NaCl solution containing heparin sulphate ($2500 \text{ IU}\cdot\text{ml}^{-1}\cdot\text{kg}^{-1}$) was injected into the dorsal aorta through the roof of the mouth, and allowed to circulate briefly before the animal was exsanguinated by cutting the ventral aorta, allowing it to bleed into the water.

5.4.3 Rested harvest

The fish were anaesthetised to stage 4-5 (not reactive to stimuli, but still showing limited ventilation: Summerfelt and Smith 1990) with AQUI-S™ (AQUI-S NZ, Lower Hutt, New Zealand) at a concentration of 22 ppm (0.012 g.L^{-1} isoeugenol). Without alerting the animals, a concentrated stock solution of anaesthetic was gradually introduced into the holding tank gravimetrically and mixed with a Maxi-Jet MJ1000 water pump (Aquarium Systems, Loreggia, Italy). The animals were subsequently transported and killed in the same way as the exhausted fish, except in this case the holding tank water contained 22 ppm AQUI-S™.

5.4.4 Muscle biopsy

Immediately after death, both fillets were removed from the carcass and skinned. A custom cylindrical stainless steel biopsy tool was then used to cut $c.1 \text{ cm}^3$ cylindrical muscle plugs from the D-block, 5 cm from the cephalad end of the fillet and stored in sterile glass vials. If necessary, the samples were trimmed to approximately 1 cm^3 . The total preparation time did not exceed 10 minutes and all equipment was made sterile prior to use.

5.4.5 Calorimetry

Anaerobic power output (μW) was measured in rested and exhausted white muscle tissue biopsies over a 24-hour period at 10°C . Three replicate white muscle biopsies were weighed and placed into sterile, pre-cooled, lidded Hasteloy® ampoules in a nitrogen filled bag and then placed into one of 3 chambers, from which the power output was compared to a fourth reference ampoule containing 1 cm^3 distilled water, in a multi-cell differential scanning calorimeter (MC-DSC) (Calorimetry Sciences Corporation, South Provo, Utah, USA) in isothermal (10°C) mode.

The power output was recorded every 10 seconds over a 24-hour period using Cpcalc v.2.2.0.9 software (Calorimetry Sciences Corporation). The instrument took twenty minutes to equilibrate after the samples were inserted. These twenty minutes of data are not included in our analyses. The ten minutes taken in the preparation of the biopsies has been added to the calorimetry equilibration time, resulting in a 30 minute period from the time of death for which no power output values are shown. The raw power output from the samples was corrected by subtracting the background power output of 1 cm³ of distilled water at 10°C. Values are expressed per gram of tissue.

5.4.6 Biochemical profile experiment

Removal of subsamples from the calorimeter whilst recording would have affected the temperature equilibration of the instrument and given erroneous readings. Therefore, a parallel experiment was conducted to accompany the calorimetry. In this longitudinal experiment, animals were harvested and muscle biopsies were prepared in exactly the same way as described for the two regimens above, except that four animals from each treatment were harvested on the same day. An initial sample, representing time zero, was rapidly freeze-clamped between two large aluminium blocks cooled in liquid nitrogen, then wrapped in aluminium foil and stored at -80°C. A further ten samples, corresponding to 1,2,3,4,5,6,7,8,12 and 24 hours post-mortem, were simultaneously placed into 1.7 ml microtubes (Axygen, Union City, CA, USA) in a bag filled with nitrogen. Samples were stored in racks in an insulated temperature controlled box held at $10.0 \pm 0.5^\circ\text{C}$ with a Tropicool XC3000A (Christchurch, New Zealand) temperature control unit with flow through nitrogen. At the designated time the appropriate 4 samples were removed and frozen in the way described above. The temperature in the box was logged using a HOBOTM H8 Pro Series (Onset Computer Corporation, Bourne, MA, USA) temperature logger and analysed using BoxCar v3.6 software (Onset Computer Corporation, Bourne, MA, USA).

5.4.7 Cut surface pH

Immediately after the muscle biopsies were removed, a transaxial cut was made through the two unused parts of the fillets. Using a Sensorex model 450C surface pH electrode (Garden Grove, CA, USA) with Radiometer model PHM84 pH meter (Copenhagen, Denmark) the initial cut surface pH of the white muscle was measured; mean of 6 measurements (a dorsal, medial and ventral measurement from each side of the fillet) from the freshly cut surfaces. At each subsequent time point during the experiment, an additional cut surface pH measurement was recorded from a freshly-cut muscle biopsy; this time splitting the tissue biopsy with a scalpel blade and taking an average of the two freshly cut surfaces.

5.4.8 Tissue extraction

5.4.8.1 Creatine compounds, purine nucleotides and nucleosides and related bases

The frozen 1 cm³ muscle biopsy was ground in a porcelain pestle and mortar with liquid nitrogen. Approximately 100 mg of frozen powder was placed into a 1.8 ml Nunc cryotube vial (Roskilde, Denmark) with a pre-cooled spatula. Approximately 1.5 ml of ice cold 0.4 N perchloric acid was added and the powder homogenised for c.1 minute using a Heidolf Instruments DIAX 900 (Schwanbach, Germany) homogeniser on setting 6. The homogeniser blade was rinsed with 100 µl of perchloric acid and the mass made up to 1.80 g using perchloric acid. The extract was centrifuged at 6000 *g* for 5 minute and the supernatant transferred into a 1.7 ml microtube and neutralised (pH 7) with 2 M K₂CO₃. The extract was frozen at -80°C until assayed (within 2 weeks).

5.4.8.2 *Glucose, glycogen and lactate*

Muscle samples were prepared in the same way as described above except that the extraction medium consisted of 500 μl of ice-cold 0.6 N perchloric acid mixed in a ratio of 7:3 with absolute methanol and the mass was made up to 0.80 g. This homogenate was frozen at -80°C until assayed (within 2 weeks). On thawing the extracts for analysis, a subsample was removed for the glycogen assay. This sample was neutralised with 2 M K_2CO_3 . The remaining unneutralised homogenate was centrifuged at 10 000 g for 5 minutes. The supernatant was then neutralised in a new microtube using 2 M K_2CO_3 and further diluted (1-fold) with distilled water. Glucose and lactate concentrations were determined in this extract.

5.4.9 *Assays*

5.4.9.1 *Glucose and glycogen assay*

Glucosyl units were determined in the glucose and glycogen extracts using a modified version of the method of Keppler and Decker (1974). Glycogen extracts were diluted with five volumes of a 200 mM acetate buffer (120 mM sodium acetate and 80 mM glacial acetic acid, pH 4.8) containing $2\text{ g}\cdot\text{ml}^{-1}$ amyloglucosidase and incubated for 2.5 hours in a shaking water-bath heated to 37°C . Following this, the samples were stored on ice until assayed. Glucosyl units were measured in both extracts using the hexokinase method, employing a Roche Gluco-quant Glucose/HK assay kit (Mannheim, Germany) adapted for use in cuvettes. In this method the production of NADPH is stoichiometric with glucose conversion. The NADPH was quantified using a Shimadzu Corporation UV-1700 PharmaSpec spectrophotometer (Shimadzu Scientific Instruments, Columbia, USA) at 340 nm.

Net glycogen-derived glucosyl units were determined by subtracting the tissue glucose concentration from the glycogen values. All samples were measured in duplicate.

5.4.9.2 Lactate assay

L-lactate in the neutralised and diluted muscle extracts was determined using the L-lactate dehydrogenase method, utilising a Megazyme L-lactic acid assay kit (Wicklow, Ireland). Here NADH production is stoichiometric with the L-lactate dehydrogenation, with NADH measured as described above. All samples were measured in duplicate.

5.4.9.3 Creatine compounds, purine nucleotides and nucleosides and related bases

Creatine compounds, purine nucleosides and nucleotides and related bases were separated by ion-pair reversed phase high performance liquid chromatography (HPLC) and quantified using UV-Vis detection on a Shimadzu Scientific Instruments SIL-10A with a reversed phase 5 μm ODS (C18) 250 x 4.6 mm column protected with a C18 SecurityGuard guard column (both Phenomenex Inc., Torrance, CA, USA) based on the methods of Fürst and Hallstrom (1992) and Tuckey *et al.* (2009a). The neutralised muscle extracts were centrifuged at 10,000 *g* and a 20 μl subsample injected onto the column. The column oven was held constant at 32 °C and sample cooler at 2 °C. A solvent gradient was run between two mobile phases over a 50 minute period: mobile phase A (MPA) (0.05 M phosphate buffer (NaH_2PO_4) containing 2 $\text{g}\cdot\text{L}^{-1}$ of HPLC grade tetrabutylammonium bisulfate (ion-pair reagent) (Fluka, ex Sigma Aldrich Chemical Co.) (pH 5.5)) and mobile phase B (MPB) (75% MPA and 25% acetonitrile, pH 5.5).

System flow was maintained at 1 ml.min⁻¹ throughout the gradient cycle, which began with 100% MPA for 5 minutes followed by a 20 minute gradient to 70% MPB. This was held for 3 minutes followed by a 2 minute gradient back to 100% MPA. The column was then equilibrated with 100% MPA for a further 20 minutes, totalling 50 minutes. Dual wavelength UV-Vis detection was used to accurately quantify the absorbance of both the creatine compounds (214 nm) and the other compounds (254 nm). Peak areas were calculated and adjusted with Shimadzu post-run software and compared to standards of known concentration. All values were corrected for dilution factor. All samples were measured in duplicate.

5.4.10 Nucleotide ratios and total pool, K-values and potential energy

ATP:ADP, ATP:AMP and ATP:IMP ratios were calculated from the chromatography nucleotide data. The total nucleotide pool was calculated in $\mu\text{mol.g}^{-1}$ as the sum of ATP, ADP, AMP, IMP, NAD⁺, inosine, hypoxanthine and uric acid. K-values were calculated using equation 1 (Aubourg *et al.* 2007).

$$\text{K-value (\%)} = \frac{\text{inosine} + \text{hypoxanthine}}{\text{ATP} + \text{ADP} + \text{AMP} + \text{IMP} + \text{inosine} + \text{hypoxanthine}} \times 100 \quad \text{eq. 1}$$

Potential energy was calculated using equation 2 (Connett 1988; Arthur *et al.* 1992).

$$\text{Pe } (\mu\text{mol.g}^{-1}) = \text{creatine phosphate} + 2[\text{ATP}] + \text{ADP} \quad \text{eq. 2}$$

Where Pe is the cell potential energy, phosphate bond state or energetic state, since ATP has 2 and ADP and creatine phosphate have 1 available phosphate for phosphorylation (Connett 1988; Arthur *et al.* 1992).

5.4.11 Chemicals

All chemicals listed in this manuscript were sourced from Sigma-Aldrich chemical company (St. Louis, MO, USA) unless otherwise stated.

5.4.12 Statistical analysis

All data were subjected to normality and equal variance testing prior to analysis. Differences from the initial value (time zero, except for power output where 1 hour was used) within groups for the calorimetric and biochemical profiles, pH, ratios (log 10), K-values and total nucleotide pool were determined by one-way repeated measures ANOVA followed by a Dunnett's post-hoc test. Differences between the rested and exhausted treatments were determined using two-way repeated measures ANOVA and Bonferroni post-hoc test, examining all comparisons. For comparison between the calorimetry data and the biochemical data, a smoothed value representing power output at each hour was used for analysis. Exhausted muscle calorimetry values were subtracted from the rested calorimetry values and the resulting net power output was fitted with a single-phase exponential decay curve. Correlations between power output and all of the metabolites and correlations between other relevant metabolites were calculated using Pearson r correlation analysis. All analysis was performed in Prism 4.00 (Graphpad software, San Diego, CA, USA). The significance level used was $P < 0.05$ but actual P-values or greater significance is shown where appropriate. All data appear as mean \pm SEM, except the power output data which appears as mean \pm 95% CI.

5.5 Results

5.5.1 Harvest regimen associated activity

Animals subjected to the exhausted harvest protocol produced the "burst-type" swimming behaviour typical of salmonids (e.g. Johnston and Ward 1975).

Fish displayed this behaviour for a variable amount of time, typically being unwilling to swim beyond about 4 minutes. The fish were relatively inactive when netted and handled after this treatment, although some fish continued to struggle. Animals subjected to the rested harvest regimen underwent anaesthesia without any “burst-type” swimming. While being netted and handled the fish remained immobile but ventilated steadily.

5.5.2 Calorimetry

The rested muscle produced a vastly different power output profile than the exhausted muscle. From an initial rate of around $400 \mu\text{W}\cdot\text{g}^{-1}$, power output from the rested group declined exponentially over a 12 hour period to $15 \mu\text{W}\cdot\text{g}^{-1}$, the rate dropping significantly after the first hour of storage post-mortem ($P < 0.001$) (figure 5.1A). There was a clear exothermic event superimposed over the decline in power output between 4 and 6 hours. Muscle from exhausted animals had a very low initial power output ($< 10 \mu\text{W}\cdot\text{g}^{-1}$), rising significantly ($P < 0.01$) to around $35 \mu\text{W}\cdot\text{g}^{-1}$ at 5 and 6 hours post-mortem before progressively decreasing, mirroring the exothermic event in the rested muscle (figure 5.1A). Rested and exhausted treatments were significantly different for the first 7 hours of storage ($P < 0.001$). The exothermic event present in both treatments was removed by subtracting the exhausted profile from the rested profile, resulting in a net power output that was well described by a single-phase exponential decay model ($R^2 = 0.98$) (figure 5.1B). The predicted power output from this model at time zero is $417 \mu\text{W}\cdot\text{g}^{-1}$, reducing with a half time of 2.3 hours.

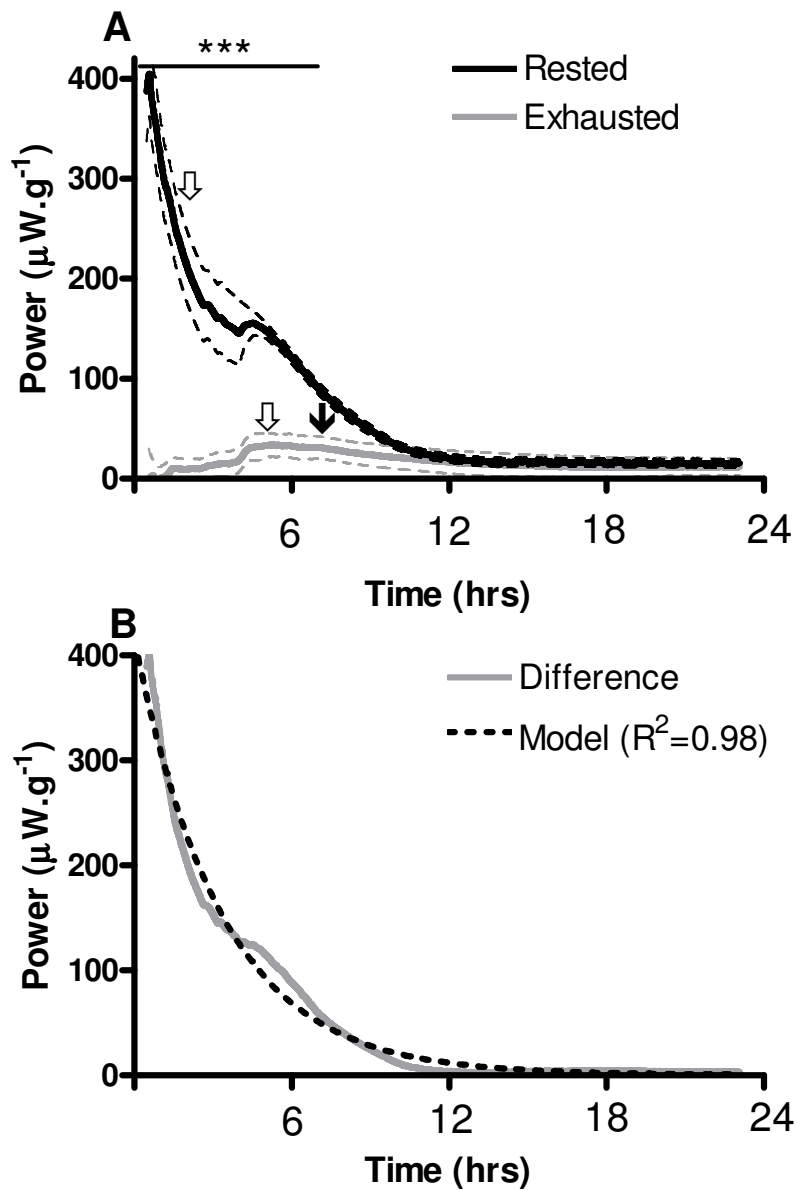


Figure 5.1. Power output of anoxic salmon white muscle at 10°C over a 24-hour period. **A.** Rested (black line) and exhausted (grey line) power output. Dashed lines are 95% CI. *** indicates significantly different between datasets ($P<0.001$) (two-way repeated measures ANOVA with Bonferroni post-test). White arrows indicate the first significant change in power output from the initial time (1 hour) in the dataset. The black arrow indicates the time at which values were no longer significantly elevated above initial values. Both $n=8$. **B.** Difference between the rested and exhausted treatments (grey line) and a single-phase exponential decay model fitted to these data ($y=417\cdot\exp(-8.366\cdot 10^{-5}\cdot x) + 0.5582$, half-time 2.3 hours, $R^2=0.98$) (dashed black line).

5.5.3 Biochemical profiles

5.5.3.1 Glycogen, glucose, lactate and pH

The concentration of glycogen at the time of death in the rested group was $16 \mu\text{mol.g}^{-1}$, which declined significantly by the first-hour post-mortem to $7 \mu\text{mol.g}^{-1}$ ($P < 0.01$), reaching a value close to zero by 3 hours (figure 5.2A). Exhausted muscles at time zero had $<2 \mu\text{mol.g}^{-1}$ of glycogen, which declined significantly by 2 hours post-mortem to a value close to zero ($P < 0.01$). The rested and exhausted treatments were significantly different from each other at time zero and 1 and 2 hours post-mortem ($p < 0.001$). The time zero muscle glucose concentration was significantly elevated in exhausted animals at $5 \mu\text{mol.g}^{-1}$ versus $2 \mu\text{mol.g}^{-1}$ in the rested group ($P < 0.001$) (figure 5.2B). Glucose concentration in the rested group did not change significantly from the initial value at any time point but the elevated initial concentration in the exhausted tissue had significantly dropped from its initial high value by 1 hour post-mortem ($P < 0.05$). In both groups the concentration remained around $2\text{--}4 \mu\text{mol.g}^{-1}$ after this time. Lactate rose significantly ($P < 0.01$) by 1 hour in both groups from a time zero value of 18 and $43 \mu\text{mol.g}^{-1}$ to a plateau of around 55 and $65 \mu\text{mol.g}^{-1}$ in rested and exhausted groups respectively (both $P < 0.01$) (figure 5.2C). Rested and exhausted treatments were significantly different at time zero and 1, 2 and 4 hours post-mortem ($P < 0.01$). Consistent with the rise in lactate in both groups, the pH fell to a plateau from around 7.5 and 6.7 to 6.4 and 6.0 in rested and exhausted groups respectively, by 3 hours post-mortem, the fall being significant by 1 hour in both groups ($P < 0.01$). The pH of rested muscle was significantly greater than that of exhausted muscle at time zero and at 1, 2 and 3 hours post-mortem ($P < 0.05$).

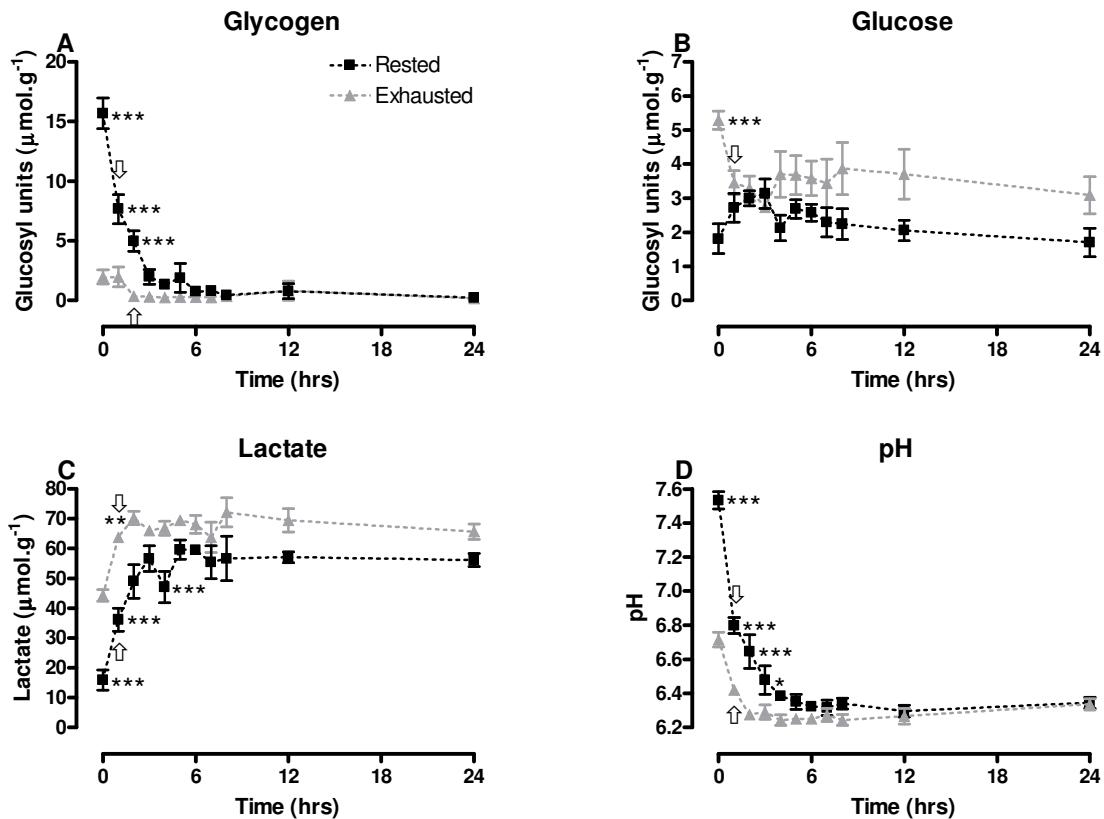


Figure 5.2. Metabolite profiles from rested (black squares) and exhausted (grey triangles) anoxic white muscle at 10°C over a 24-hour period post-mortem. **A.** Glycogen. **B.** Glucose. **C.** Lactate. **D.** pH. * is $P < 0.05$, ** is $P < 0.01$, *** is $P < 0.001$ (two-way repeated measures ANOVA with Bonferroni post-test). White arrows indicate the first significant change in concentration from time zero of the dataset. Data are mean \pm SEM. All $n = 4$.

5.5.3.2 Creatine phosphate, creatine, creatinine and potential energy

The time zero concentration of creatine phosphate in rested tissue was 18 $\mu\text{mol.g}^{-1}$, which declined significantly ($P < 0.01$) by the first hour of storage to just less than 5 $\mu\text{mol.g}^{-1}$ and became undetectable by 12 hours post-mortem (figure 5.3A). In contrast, the exhausted group concentration at time zero was 0.1 $\mu\text{mol.g}^{-1}$, and was undetectable by 3 hours post-mortem. The rested group concentration was significantly higher at time zero and at 1 hour of storage than in the exhausted muscle ($P < 0.01$).

Potential energy decreased significantly ($P < 0.01$) in rested and exhausted groups from an initial concentration of 30 and 7 $\mu\text{mol.g}^{-1}$ to 9 and 3 $\mu\text{mol.g}^{-1}$ respectively at 1 hour post-mortem (figure 5.3B). Rested tissue potential energy was significantly greater than exhausted tissue at time zero, 1 and 2 hours post-mortem ($P < 0.01$). There were no significant changes in the creatine concentration relative to time zero in either group, remaining around 70 $\mu\text{mol.g}^{-1}$ (figure 5.3C). Furthermore, no difference between groups was detected at any time. Similarly, there were no significant changes in creatinine concentration relative to time zero in either group, remaining around 20 $\mu\text{mol.g}^{-1}$ with no differences detected between groups (figure 5.3D).

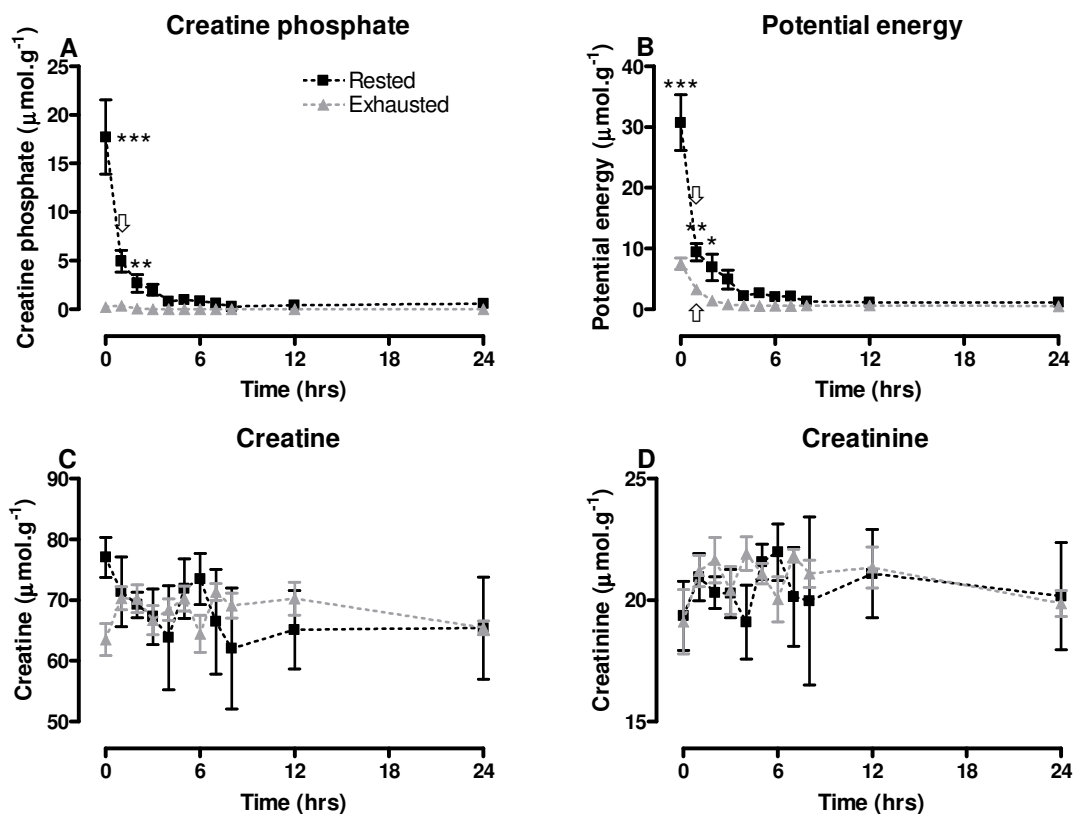


Figure 5.3. Metabolite profiles from rested (black squares) and exhausted (grey triangles) anoxic white muscle at 10°C over a 24-hour period post-mortem. **A.** Creatine phosphate. **B.** Potential energy. **C.** Creatine. **D.** Creatinine. * is $P < 0.05$, ** is $P < 0.01$, *** is $P < 0.001$ (two-way repeated measures ANOVA with Bonferroni post-test). White arrows indicate the first significant change in concentration from time zero of the dataset. Data are mean \pm SEM. All $n = 4$.

5.5.3.3 ATP, ADP, AMP and NAD⁺

In both groups the concentration of ATP, ADP and NAD⁺ declined rapidly over the first 6 hours post-mortem (figure 5.4). Initial ATP concentrations in rested and exhausted groups declined significantly from 6 $\mu\text{mol.g}^{-1}$ and 3.2 $\mu\text{mol.g}^{-1}$ to 1.8 and 0.9 $\mu\text{mol.g}^{-1}$ respectively by 1 hour post-mortem ($P < 0.01$). ATP concentration (figure 5.4A) was significantly greater in the rested group at 1 and 3 hours post-mortem ($P < 0.05$). ADP concentration declined almost identically in both groups from around 1 $\mu\text{mol.g}^{-1}$ at time zero to around 0.4 $\mu\text{mol.g}^{-1}$ after 24 hours (figure 5.4B). The concentration of ADP in the rested group was significantly lower by 2 hours and in the exhausted group by 3 hours ($P < 0.01$). There were no significant differences in concentrations between the 2 groups at any time (figure 5.4B). AMP significantly increased ($P < 0.01$) in concentration from 100 nmol.g^{-1} to 300 nmol.g^{-1} by 1 hour post-mortem in the rested group, returning to the initial concentration by 7 hours post-mortem (figure 5.4C). In contrast, the exhausted group values were not significantly different from the time zero concentration at any time post-mortem, remaining at around 100 nmol.g^{-1} . The rested group had a significantly elevated AMP concentration at 4 and 6 hours post-mortem ($P < 0.01$). In both groups, there was a significant decline in NAD⁺ from an initial concentration of 550 nmol.g^{-1} to 280 nmol.g^{-1} by 1 hour post-mortem ($P < 0.01$), declining further to $< 50 \text{ nmol.g}^{-1}$ after 24 hours (figure 5.4D). No difference in NAD⁺ concentration was detected between groups at any time point.

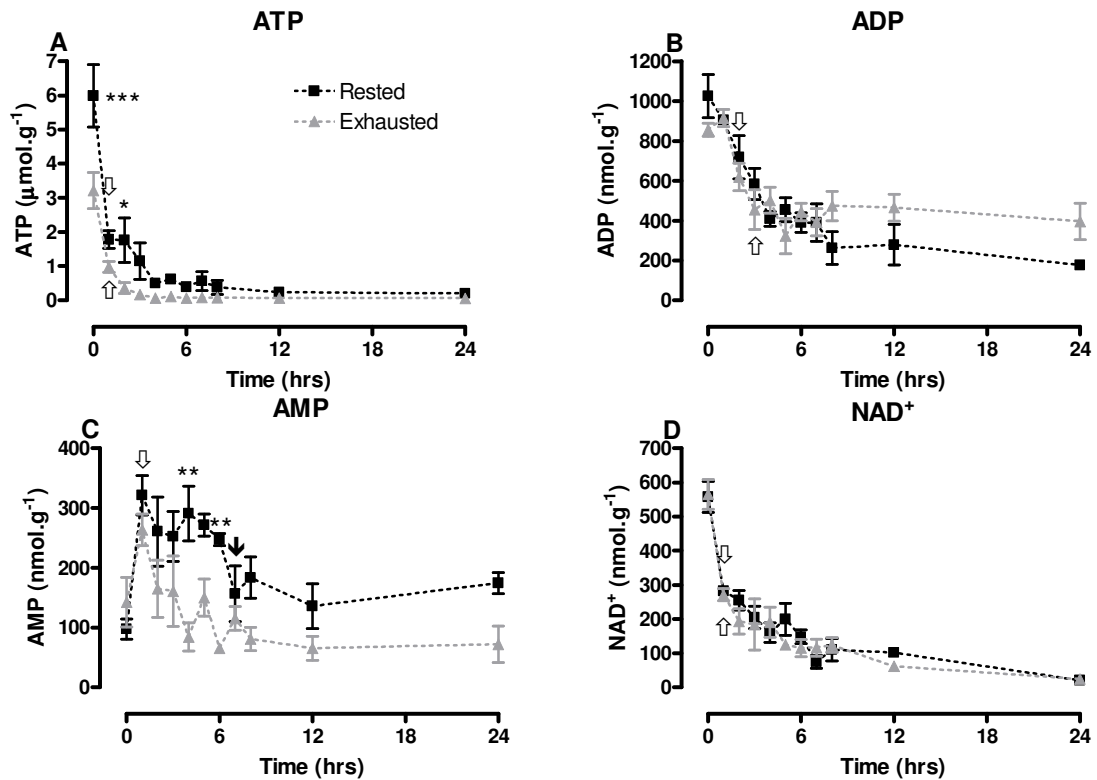


Figure 5.4. Metabolite profiles from rested (black squares) and exhausted (grey triangles) anoxic white muscle at 10°C over a 24-hour period post-mortem. **A.** ATP. **B.** ADP. **C.** AMP. **D.** NAD⁺. * is $P < 0.05$, ** is $P < 0.01$, *** is $P < 0.001$ (two-way repeated measures ANOVA with Bonferroni post-test). White arrows indicate the first significant change in concentration from time zero of the dataset. Data are mean \pm SEM. All $n = 4$.

5.5.3.4 IMP, inosine, hypoxanthine and uric acid

IMP concentration in the rested group rose significantly ($P < 0.01$) from just less than $2 \mu\text{mol.g}^{-1}$ at time zero to $5.5 \mu\text{mol.g}^{-1}$ at 1 hour post-mortem, before gradually declining to initial concentrations by 12 hours (figure 5.5A). IMP concentration in the exhausted group also increased significantly ($P < 0.01$) between time zero and 1 hour, from $3.5 \mu\text{mol.g}^{-1}$ to $6 \mu\text{mol.g}^{-1}$, declining to initial concentrations by 24 hours. IMP concentration was significantly higher ($P < 0.05$) in rested tissue at 2 and 4 hours post-mortem. Inosine was undetectable at time zero, significantly increasing in concentration above the initial by 3 hours post-mortem in both groups ($P < 0.01$), rising to values around $4 \mu\text{mol.g}^{-1}$ by 24 hours (figure 5.5B). There was no difference detected between treatments at any time. Hypoxanthine was also undetectable at time zero in both the rested and exhausted groups (figure 5.5C). The concentration then gradually increased, becoming significantly elevated by 4 hours post-mortem ($P < 0.01$). By 24 hours the exhausted group had accumulated significantly ($P < 0.01$) more hypoxanthine than the rested group, at 450 versus 350 nmol.g^{-1} respectively. Uric acid concentration changed in a similar manner to inosine and hypoxanthine, significantly increasing ($P < 0.01$) from undetectable concentrations at time zero to 500 nmol.g^{-1} by 3 hours, further increasing to $1.5 \mu\text{mol.g}^{-1}$ by 24 hours in both groups (figure 5.5D).

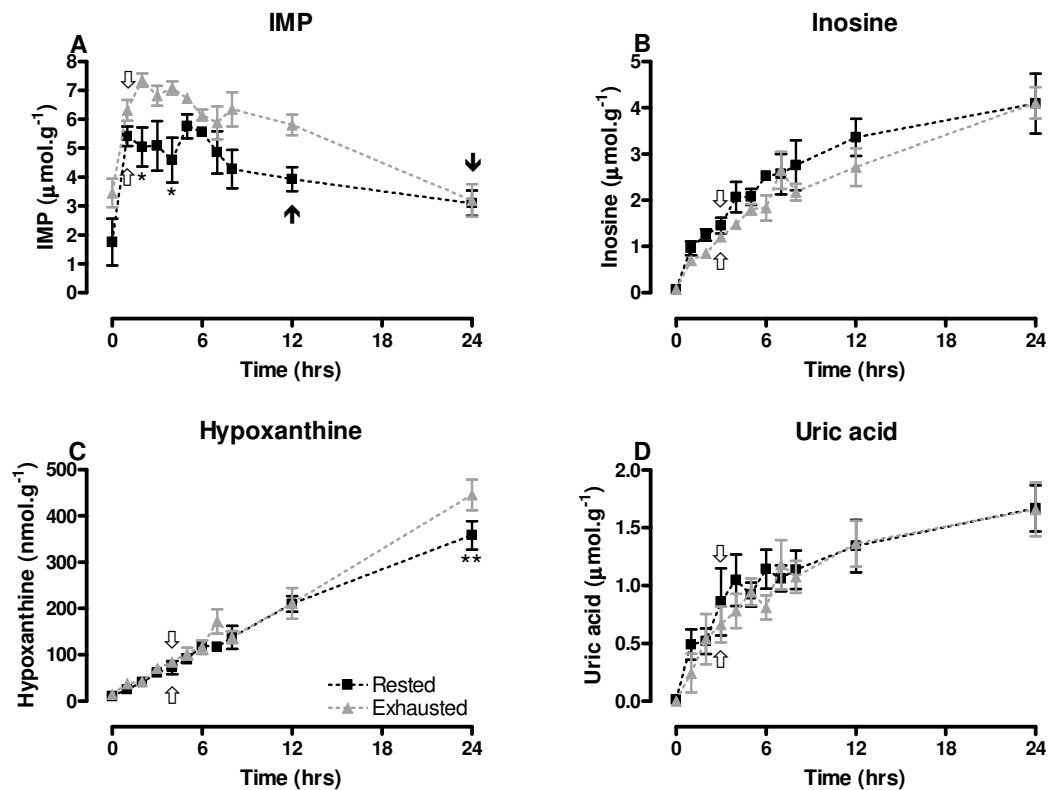


Figure 5.5. Metabolite profiles from rested (black squares) and exhausted (grey triangles) anoxic white muscle at 10°C over a 24-hour period post-mortem. **A.** IMP. **B.** Inosine. **C.** Hypoxanthine. **D.** Uric acid. * is $P < 0.05$, ** is $P < 0.01$, *** is $P < 0.001$ (two-way repeated measures ANOVA with Bonferroni post-test). White arrows indicate the first significant change in concentration from time zero of the dataset. Black arrows indicate a return to initial concentration. Data are mean \pm SEM. All $n = 4$.

5.5.4 Nucleotide ratios and total pool, *K*-values and correlations

The total nucleotide pool in both the rested and exhausted groups remained at a constant concentration of around 10 μM over the 24 hour period post-mortem, with no difference determined between treatments at any time (figure 5.6A). For both treatments the ratios of ATP to ADP, AMP and IMP all showed a significant decline ($P < 0.01$) over the first hour post-mortem (Figures 6B, 6C, 6D). At time zero all three ratios were significantly lower (all $P < 0.01$) in the exhausted muscles.

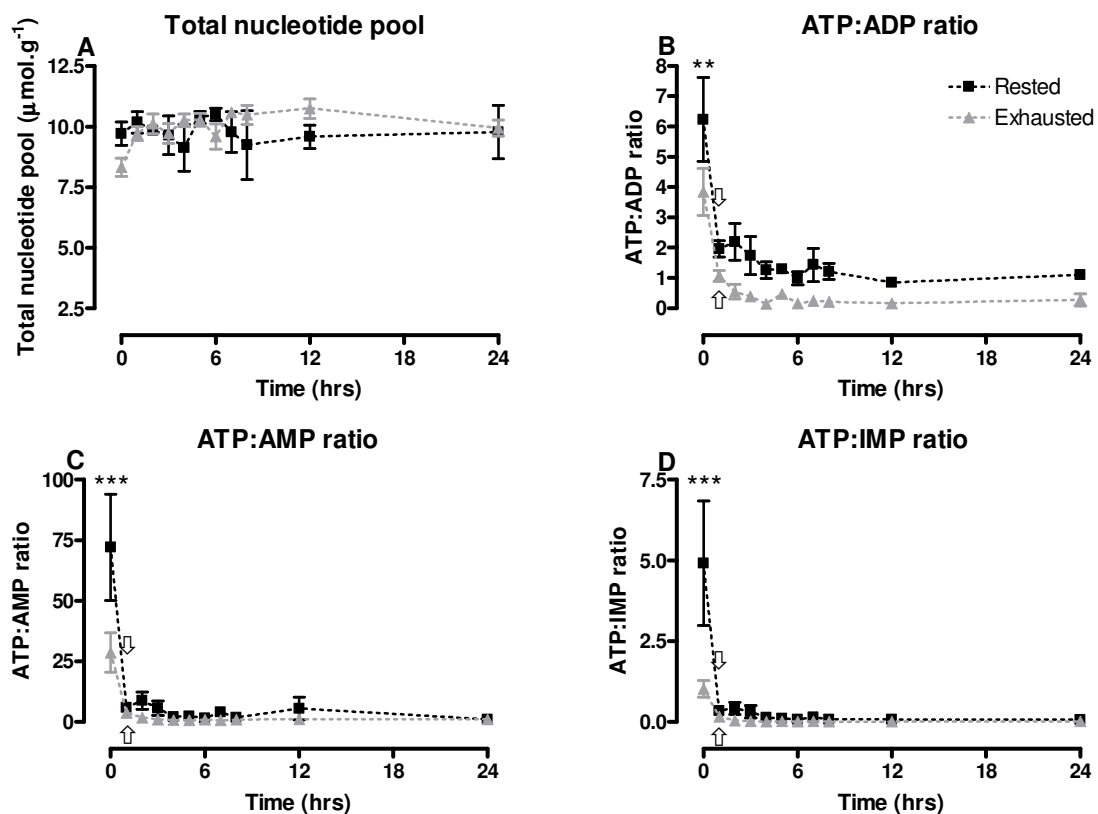


Figure 5.6. Ratios between selected metabolites and the total nucleotide pool from rested (black squares) and exhausted (grey triangles) anoxic salmon white muscle at 10 °C over a 24-hour period post-mortem. **A.** Total nucleotide pool. **B.** ATP:ADP. **C.** ATP:AMP. **D.** ATP:IMP. * is $P < 0.05$, ** is $P < 0.01$, *** is $P < 0.001$ (two-way repeated measures ANOVA with Bonferroni post-test on the log 10 of ratios). White arrows indicate the first significant change in concentration from time zero of the dataset. Data are mean \pm SEM. All $n=4$.

The K-values in both groups rose from an initial value of 0% to a peak of around 55% by 24 hours, becoming significantly greater ($P < 0.01$) than the initial by 2 and 3 hours in the rested and exhausted groups respectively. K-values in the exhausted treatment were significantly lower ($P < 0.05$) than in the rested group at 12 hours post-mortem.

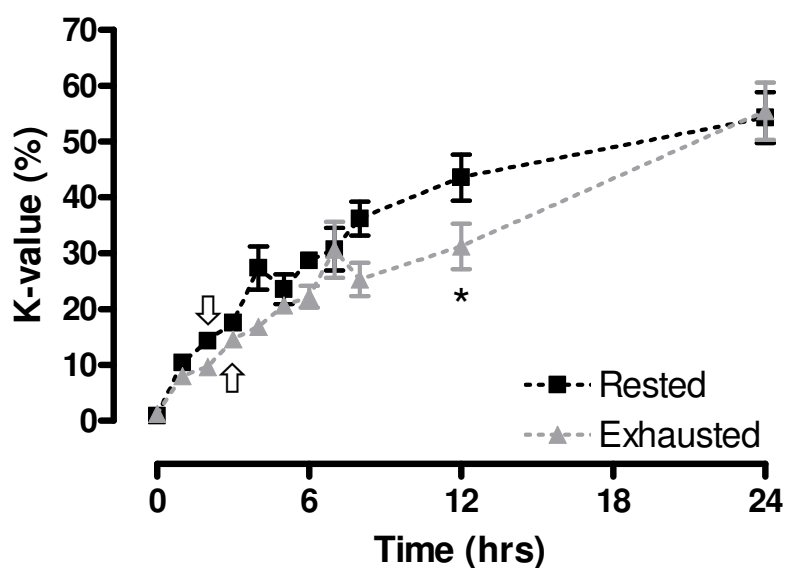


Figure 5.7. K-values from rested (black squares) and exhausted (grey triangles) anoxic salmon white muscle at 10°C over a 24-hour period. * signifies $P < 0.05$ (two-way repeated measures ANOVA with Bonferroni post-test). White arrows indicate the first significant change in K-value of the dataset. Data are mean \pm SEM. $n=4$.

Correlations between metabolites and power output from 1 hour onwards are summarised in table 5.1. The only metabolites that did not significantly correlate ($P > 0.05$) with power output in the rested group were creatine, creatinine and the total nucleotide pool. In contrast, only changes in pH, ATP, creatine phosphate and potential energy were significantly correlated ($P < 0.05$) with power output in the exhausted muscles; although in these the correlations were all negative. A second series of correlation analyses is presented in table 5.2, and includes time zero. In these correlations, declines in glycogen were significantly correlated ($P < 0.0001$) with falling pH, lactate and ATP in both groups.

Conversely, there is an inverse correlation between lactate and pH in both groups. The decline in ATP concentration was significantly correlated ($P < 0.0001$) with a fall in pH, creatine phosphate, ADP and NAD^+ in both groups. Changes in ATP and IMP were inversely correlated ($P < 0.05$) in rested but not exhausted animals, while changes in ATP and AMP were not correlated in either group.

Table 5.1. Correlation analysis between metabolic power output and metabolite concentrations, K-values, total nucleotide pool and potential energy in rested and exhausted anoxic salmon white muscle at 10°C from 1 to 24 hours. * is $P < 0.05$, ** is $P < 0.01$, *** is $P < 0.001$. The Pearson r coefficient ranges from -1 to +1, corresponding to a perfect negative and positive correlation respectively. $n=4$.

Correlate	Rested				Exhausted			
	Pearson r	P-value	Summary	r^2	Pearson r	P-value	Summary	r^2
Glycogen	0.91	0.0002	**	0.84	0.45	0.1884	ns	0.21
Glucose	0.73	0.0170	*	0.53	-0.61	0.0587	ns	0.38
Lactate	-0.76	0.0110	*	0.56	0.31	0.3790	ns	0.09
pH	0.89	0.0005	**	0.80	-0.76	0.0100	*	0.58
ATP	0.89	0.0004	**	0.80	-0.69	0.0253	*	0.49
Creatine phosphate	0.91	0.0002	**	0.83	-0.66	0.0300	*	0.44
Creatine	0.55	0.0960	ns	0.31	-0.06	0.8700	ns	<0.01
Creatinine	0.10	0.7910	ns	<0.01	-0.01	0.9880	ns	<0.01
ADP	0.97	<0.0001	***	0.94	-0.76	0.0110	*	0.56
AMP	0.87	0.0011	**	0.76	-0.55	0.0940	ns	0.31
NAD^+	0.92	0.0001	***	0.86	-0.44	0.2020	ns	0.19
Hypoxanthine	-0.82	0.0037	**	0.67	0.03	0.9288	ns	<0.01
Inosine	-0.93	<0.0001	***	0.87	0.27	0.4600	ns	0.07
Uric acid	-0.92	0.0001	***	0.85	0.35	0.3190	ns	0.12
IMP	0.71	0.0217	*	0.50	0.09	0.8050	ns	0.01
Total nucleotide pool	0.33	0.3449	ns	0.11	0.33	0.3510	ns	0.11
K-values	-0.93	0.0001	***	0.86	0.19	0.5800	ns	0.04
Potential energy	0.93	<0.0001	***	0.86	-0.71	0.0209	*	0.51

Table 5.2. Correlation analysis between selected metabolites in rested and exhausted anoxic salmon white muscle at 10°C over 24 hours. * is $P < 0.05$, ** is $P < 0.01$, *** is $P < 0.001$. $n=4$.

Correlate	Rested				Exhausted			
	Pearson r	P-value	Summary	r^2	Pearson r	P-value	Summary	r^2
Glycogen vs pH	0.99	<0.0001	***	0.99	0.82	0.0010	**	0.68
Glycogen vs Lactate	-0.96	<0.0001	***	0.92	-0.69	0.0170	*	0.48
Glycogen vs ATP	0.98	<0.0001	***	0.95	0.82	0.0020	**	0.67
Lactate vs pH	-0.96	<0.0001	***	0.92	-0.095	<0.0001	***	0.9
ATP vs pH	0.99	<0.0001	***	0.96	0.098	<0.0001	***	0.96
ATP vs Creatine phosphate	0.99	<0.0001	***	0.98	0.66	0.0300	*	0.43
ATP vs ADP	0.85	0.0011	*	0.71	0.76	0.0060	*	0.58
ATP vs AMP	-0.35	0.3010	ns	0.12	0.35	0.2890	ns	0.124
ATP vs NAD	0.95	<0.0001	***	0.90	0.095	<0.0001	***	0.89
ATP vs IMP	-0.61	0.0480	*	0.37	-0.52	0.0960	ns	0.28

5.6 Discussion

The power output and metabolite concentrations in the muscles of anaesthetised animals of the rested group contrasted starkly with those in the exhausted group. An initial power output of approximately $400 \mu\text{W}\cdot\text{g}^{-1}$ in the rested group declined exponentially over 12 hours (figure 5.1A). Conversely, the exhausted group exhibited a low ($<10 \mu\text{W}\cdot\text{g}^{-1}$) and relatively unchanging power output. This difference in power output suggests an extended period of metabolic activity post-mortem in the white muscle of animals that were rested harvested. In the rested group, the metabolic rate showed a positive correlation with changes in the concentration of glucose, glycogen, pH, lactate, ADP, AMP, IMP and NAD^+ as well as the derived parameter, potential energy (a proxy of ATP turnover; Connett *et al.* 1988; Arthur *et al.* 1992) (table 5.1). Similarly, the concentration of lactate, inosine, hypoxanthine and uric acid, as well as the K-values showed a negative correlation with power output. These data suggest that the concentrations of key metabolites such as ATP, ADP, creatine phosphate and stores of glycogen, which are elevated in the rested treatment, contribute to the total power output (figures 5.2A, 5.3A, 5.4A and 5.4B). Thus, the decline in power output represents a loss in energy stores.

Despite the elevated metabolic rate reported here, it is clear that from the time of death the muscles in both groups have begun losing high energy compounds as the myocytes become unable to regenerate metabolites and redox potential, presumably leading to autolysis. In viable cells, ATP, ADP, NAD^+ and creatine phosphate do not fluctuate greatly in concentration, despite large changes in ATP turnover (Hochachka and M^cClelland 1997). For example, in a study using a perfused dog gastrocnemius preparation, creatine phosphate, inorganic phosphate and ATP concentrations showed no measurable changes in concentration despite an 18-fold change in the rate of ATP turnover (Hogan *et al.* 1992).

This phenomenon is known as the stability paradigm (Hochachka 1999) and is thought to be facilitated by the three-dimensional intracellular structure within cells that constrains metabolite behaviour, increasing the rates of reactions dramatically (Hochachka 2003). However, measurable changes in the concentrations of ATP, creatine phosphate and glycogen have been induced by pre-mortem activity in fish (Johnston 1975; Milligan and Wood 1987; Milligan and McDonald 1988; Pagnotta and Milligan 1991; Milligan 1996; Schulte *et al.* 1992; Wang *et al.* 1994; Thomas *et al.* 1999). Furthermore, during anoxia, van den Thillart *et al.* (1989) demonstrated that after creatine phosphate stores were exhausted by 85%, ATP fell and IMP accumulated in crucian carp (*Carassius carassius*) and goldfish (*Carassius auratus*) muscle. Thus high energy demand and environmental/metabolic hypoxia in fish muscle *in vivo* is associated with a decline in tissue ATP and other metabolite concentrations.

In the current study, ATP fell rapidly in both groups concurrent with a drop in glycogen and creatine phosphate (figures 5.2A, 5.3A and 5.4A). Thus ATP concentration was dependent on the concentration of these two metabolites. Therefore, there is no evidence from our data that creatine phosphate, via the creatine kinase pathway, or anaerobic glycolysis maintained ATP concentration. Of note is the very low concentration of creatine phosphate and glycogen in the exhausted group, which indicates that much of the capacity to provide rapid ADP phosphorylation had been compromised by pre-mortem activity. Consequently ATP concentration fell more rapidly. The similar falls in the ATP:ADP, ATP:AMP and ATP:IMP ratios reflects in most part the rapid fall in ATP concentration in both treatments (figures 5.6B, 5.6C and 5.6D). The ATP:ADP ratio is consistently lower in the exhausted group, reflecting the lower ATP concentrations in exhausted muscle over the course of the experiment. Differences in the ATP:AMP and ATP:IMP ratio are diminished at 1 hour post-mortem in both treatments due to the fall in ATP but also the pronounced rise in AMP and IMP post-mortem, which is suggestive of depleted ATP stores and impaired ATP supply.

The potential contributions of intracellular lipid and protein to ATP generation in our study are unknown, but certainly failed to bolster ATP concentrations. Lipid is favoured for oxidation during sustained aerobic locomotion (Richards *et al.* 2002a; Kieffer *et al.* 1998) and in aerobic recovery from exhaustive exercise (Richards *et al.* 2002b), which would have been impossible under the anoxic conditions of our study. Similarly, protein oxidation could not have contributed to ATP generation.

Interestingly, there is a clear exothermic event in the power output profiles of both groups at around 4 hours. The timing of this event suggests that it is not directly associated with energy metabolism. Instead it is likely to be associated in some way with the loss of cell viability following death. If the event was associated with energy metabolism, I would have expected the event to have registered earlier in the exhausted group, in which ATP and creatine phosphate concentrations fell to minimal values between 1 and 3 hours, well before the rested muscle. Further to this, the negative correlation between ATP, creatine phosphate and potential energy in the exhausted muscle represents an interaction with increased power output in this tissue over time due to the exothermic event. This is a further demonstration that the event is not directly associated with energy metabolism, since it seems unlikely that an increasing power output would accompany completely depleted energy stores. Instead, a variety of autolytic processes might be responsible for the exothermic event; for example, the folding and unfolding of proteins involves enthalpy changes (Prabhu and Sharp 2005). Conformational changes can be influenced by the hydrogen ion concentration, but this can be ruled out as the pH fell much more rapidly in the exhausted group (figure 5.2D). ADP and NAD^+ also plateaued at 4 hours in both rested and exhausted muscle (figures 5.4B and 4D). By 4 hours the concentration of ADP was reduced to one third and the concentration of NAD^+ reduced to one sixth the concentration at one hour post-mortem. Perhaps the concentrations of ADP and NAD^+ at this time critically restrict the production of ATP through substrate and reducing capacity limitations respectively. It is possible that bacterial proliferation contributed to the exothermic event/s.

However, the chances of a bacterial contribution were low for several reasons: the biopsies were prepared using sterile instruments, the ampoules were sterilised and the samples were kept in a nitrogen atmosphere during the course of the experiment, which would preclude the proliferation of aerobic bacteria. In addition, the appearance at 4 hours and disappearance at 6 hours of the exothermic event is not consistent with the exponential growth typical of bacteria.

To eliminate the effects of the exothermic event/s on metabolic rundown, the exhausted data was subtracted from the rested data at corresponding time points (figure 5.1B). The single-phase exponential curve fitted to the net power output, exhibited a much better fit of the data (R^2 0.98) than before subtraction ($R^2=0.77$). This analysis demonstrates that any remaining energy relating to metabolic power output in rested muscle has effectively disappeared by 12 hours, with the time to halving of power output estimated as 2.3 hours. From the curve I estimated a starting metabolic output (intercept) in rested muscle of $417 \mu\text{W} \cdot \text{g}^{-1}$. I presume this to be an anaerobic metabolic rate in the tissue at the time of death, although it could be elevated by tissue damage associated with the preparation of the biopsies. For example, tissue wounding of plant tissue increases metabolic power output (Wadsö *et al.* 2004).

Similar to our findings, an exponential decline in metabolic rate has been reported in adult, infantile and neonatal rat myocardial tissue over a 3.5 hour period (Mühlfeld *et al.* 2005). The metabolic rates were significantly higher in neonatal and infantile rat hearts, declining exponentially from around 4.5 and $2.5 \text{ mW} \cdot \text{g}^{-1}$ (dry weight) to around $1 \text{ mW} \cdot \text{g}^{-1}$ and $400 \mu\text{W} \cdot \text{g}^{-1}$ respectively over 90 minutes. The authors term these “dying curves”. Of interest is that these authors report a period before the exponential decline of about 10 minutes where metabolic rate drops more slowly, indicating that tissue homeostasis may have been partially sustained. There is no evidence of this in our data, although I could not measure metabolic power output reliably over the first 30 minutes. Another study (Conley *et al.* 2001) that has identified an exponential decline in anaerobic power output makes for an interesting comparison.

These authors report a non-sustainable power output by human legs during cycling of >800 W that decreases exponentially over a 5 minute period. This trend is attributed to creatine phosphate and glycogen availability in the “effectively hypoxic/anoxic skeletal leg muscles”. These data corroborate our results and are supportive of the idea that reduced ATP supply from anaerobic glycolysis and ADP phosphorylation, via the creatine kinase pathway, contribute to an exponential decline in metabolic rate (power output) in muscle.

Interestingly, the initial estimated resting power output for our salmon white muscle is in the same range as values recorded for whole fish. In goldfish held at 20°C in a flow-through calorimeter the normoxic power output was 400 $\mu\text{W}\cdot\text{g}^{-1}$, falling to 250 $\mu\text{W}\cdot\text{g}^{-1}$ during exposure to 3% of the normoxic PO_2 (van Ginneken *et al.* 2004). Tilapia (*Tilapia mossambica*) at the same temperature had a power output of 448 $\mu\text{W}\cdot\text{g}^{-1}$ in light conditions and 317 $\mu\text{W}\cdot\text{g}^{-1}$ in the dark (van Ginneken *et al.* 1997). Similar values are also reported in experiments using a constantly perfused myocardial calorimetry apparatus measuring aerobic power output in hibernator and non-hibernator mammalian myocardial tissue slices (Ikomi-Kumm *et al.* 1994). These values ranged between about 500 $\mu\text{W}\cdot\text{g}^{-1}$ -2 mW $\cdot\text{g}^{-1}$, and were temperature (20 and 37°C) and hibernation-state dependent. Interestingly, their lowest values are close to our predicted anaerobic metabolic rate of 417 $\mu\text{W}\cdot\text{g}^{-1}$ at time zero.

Contrasting with the rapid rundown of metabolic rate in salmon white muscle, brain tissue slices from the anoxia-tolerant crucian carp showed only a one-third decrease of anaerobic heat production over an 18 hour period from 600 to 400 $\mu\text{W}\cdot\text{g}^{-1}$, which were then capable of recovery to oxygenated levels (Johansson *et al.* 1995). The extraordinary hypoxia tolerance and fermentation of pyruvate to ethanol in this animal (Hochachka 1985) may explain this phenomenal observation. At the lower end of the spectrum, maximum power output that the working, perfused hagfish heart could maintain solely through anaerobic metabolism was estimated at 280 $\mu\text{W}\cdot\text{g}^{-1}$, and in this case the heart was able to export lactate as it was produced (Forster 1991).

At the other extreme, a report by Beddow *et al.* (1995) of power outputs of between 21-24 mW.g⁻¹ in sea scorpion (*Myxocephalus scorpius*) white muscle during “C-shaped fast-starts” greatly exceeds our values. These measurements are in close agreement with Johnson and Johnston (1991), although Franklin and Johnston (1997) reported 3-fold lower maximal power outputs values in the Antarctic fish *Notothenia coriiceps*. These relatively high values from teleost fish are sustainable only for extremely brief periods, and their relationship to resting metabolic rate is not clear.

Glycogen fell over the first 4 hours concurrent with but not stoichiometric with the rise in lactate concentration (figure 5.2C). The source of the additional lactate in the exhausted animals is not clear as there were only around 5 µmol.g⁻¹ glucose glucosyl units and 2 µmol.g⁻¹ glycogen glucosyl units present in the tissue immediately post-mortem, and yet lactate concentration increased by close to 25 µmol.g⁻¹, which would require 12.5 µmol.g⁻¹ glucose. The rise in the rested group is also 20% higher than predicted if glucose was its only source. This discrepancy may reflect substrate recruitment from other, unknown sources since glucose concentrations do not fall to zero at 4 hours, remaining between 2 and 4 µmol.g⁻¹. Our high lactate values, which were as high as 70 µmol.g⁻¹ in the exhausted treatment, may have exceeded the rested values due to lipid and/or protein oxidation, which generates glyceraldehyde and pyruvate respectively, before death. These metabolites could later have been converted to lactate. High tissue lactate values (up to 80 µmol.g⁻¹) in post-mortem muscle have also been reported in white muscle of yellow-eyed mullet (*Aldrichetta forsteri*) and New Zealand snapper (*Pagrus auratus*) in a hyperoxic hyperbaric atmosphere (Black *et al.* 2004) and in thawed tissue following frozen storage in Chinook salmon (Cook *et al.* 2009), which were all greater than predicted by carbohydrate stores. Investigation of the source of the additional lactate could form the basis of future work.

AMP increased greatly over the first 5 hours post-mortem in rested tissue, the exhausted tissue producing less (figure 5.4C). This event could represent a significant means of managing hypoxia in muscle. Recently, Jibb and Richards (2008) have demonstrated an AMP concentration-dependent activation of AMP-activated protein kinase (AMPK) in hypoxic goldfish. AMPK is known to have a multitude of effects in white muscle, many of which can enhance anaerobic ATP generation and may also play a role in metabolic rate suppression by decreasing protein synthesis (Jibb and Richards 2008). If these same processes are activated in salmon muscle it is possible that some of the decline in metabolic rate, and by inference ATP supply, may be attributable to AMPK activity, while the enzyme remained viable.

Inosine, hypoxanthine and uric acid concentrations showed a progressive rise over 24 hours, while IMP concentrations peaked over the first 2 hours in both groups (figure 5.5) and then gradually declined. Hypoxanthine was significantly lower after 24 hours and IMP dropped significantly quicker in the rested group, but the general trend is similar in both groups and must therefore reflect the time of death more than the pre-harvest treatment. Consistent with these trends, Aubourg *et al.* (2007) reported increases in the concentrations of inosine and hypoxanthine and a sharp drop in IMP over the first 24 hours of storage at 2 °C in coho salmon (*Oncorhynchus kisutch*) white muscle fillets. The relatively stable total nucleotide pool (figure 5.6A) in both groups over time gives us confidence in our analytical methods.

The K-value represents the ratio of the sum of hypoxanthine and inosine to a pool of relevant ATP related compounds, and is frequently used as an indicator of freshness in fish muscle (Aubourg *et al.* 2007). The K-value in both groups in the current study rises from zero to 55% over 24 hours, the exhausted group being significantly lower at 12 hours (Figure 5.7). The K-value in our study was greatly influenced by the inosine concentration in the tissue; the inosine values being approximately 10-fold higher than those of hypoxanthine.

The end K-value of 55% after only 24 hours is markedly greater than the 30% reported in coho salmon after 24 hours (Aubourg *et al.* 2007), which suggests a greater rate of autolysis. This may reflect the relatively small size of the tissue biopsies used in the current study (1 cm³).

Consistent with this idea is other work in our laboratory (Tuckey *et al.* 2009a), which has shown that whole fillets retained potential energy in the form of glycogen, creatine phosphate and ATP longer than the small muscle biopsies used in the current study, despite this preparation being maintained at 5°C warmer than the current experiment. The slower depletion of high energy metabolites and pH illustrates a potentially important finding: that processing of muscle tissue (i.e. filleting, portioning) should be left to the latest possible time to maintain maximal metabolite stores. However, a difference to note was that the muscle in the Tuckey *et al.* (2009a) study was kept in a chamber with circulating air. Thus, there was the potential for aerobic metabolism to occur in the tissues immediately adjacent to and in direct contact with the air which could contribute to ATP production. Secondly, exposure of uncovered tissue to circulating air over the period of the experiment could have dehydrated the fillets, thus artificially elevating metabolite concentrations. Tuckey *et al.* (2009a) report some other differences to note. Creatine phosphate concentrations in particular are much higher at time zero in our study. This difference might be due to differences in sample preparation or harvesting technique, or possibly differences in the metabolic state of the fish used. Inosine concentrations were also considerably higher in the current study (up to 5 µmol.g⁻¹ versus a maximum of 0.025 µmol.g⁻¹, relating to K-values of between 10–30% by 24 hours). Consistent with this, our hypoxanthine and uric acid concentrations were considerably lower; a maximum of 0.4 µmol.g⁻¹ vs 0.6 µmol.g⁻¹ and 1.5 µmol.g⁻¹ vs 5 µmol.g⁻¹ respectively by 24 hours. Since uric acid, the end-point of adenylate degradation is not accounted for in the K-value equation, elevated K-values were calculated in our study, even though the sum of these three metabolites was similar between studies.

For this reason it seems appropriate to include uric acid in this calculation of adenylate depletion in future work, since it is the ultimate end-product of adenylate degradation. As to why there was a delayed conversion of inosine to hypoxanthine and uric acid (catalytic sequence: ATP - ADP - AMP - IMP - inosine - hypoxanthine - xanthine - uric acid) in the current study is uncertain, although the aforementioned differences between preparations may have played a role.

Temperature differences may also partially explain the relatively rapid rate of K-value increase in the current study. The storage temperature in our study was 8°C warmer than the coho muscle in the Aubourg *et al.* (2007) study. This would have accelerated biochemical reactions by mass action effects. Assuming a conservative Q_{10} of 2, the estimated K-value of coho at 10°C would be 48%, close to our value (55%). Had I maintained our preparation at refrigeration temperature, I would have expected a much slower rate of metabolism and associated metabolite depletion. Active behavioural selection of cold temperature is used as an adaptive strategy for metabolic rate suppression in ectotherms, e.g. aestivating frogs (Boutilier 2001b). Furthermore, a refrigeration temperature of about 4-5°C would be approximately half the acclimation temperature, which is reported to be optimal for post-mortem white muscle storage (Jerrett *et al.* 2000; Jerrett *et al.* 2002). Our data further highlights the importance of rapidly chilling tissues to slow metabolite depletion.

Further to the positive effects of rested harvesting in maintaining metabolic rate and energy charge in muscle (current study), this practice has been shown to reduce cortisol secretion and lactate accumulation in stressed channel catfish (*Ictalurus punctatus*) (confined, low oxygen conditions) (Small 2004), retard spoilage in Chinook salmon (Fletcher *et al.* 2003) and improve meat quality indicators in Atlantic salmon (*Salmo salar*) (Kiessling *et al.* 2004). Thus the additive effects of rested harvesting have a significant impact on the quality, freshness and shelf-life of harvested products. Furthermore, products from animals that have been killed in a way that is as humane as possible allows them to be marketed to customers who value such efforts (North *et al.* 2008). This market looks set to increase greatly in the future (North *et al.* 2008).

Thus additional research into the beneficial effects of the use of rested harvesting in the aquaculture industry is warranted. The food grade approval in several countries (New Zealand, Australia and Chile) of isoeugenol and promising results suggesting that it may enhance the activity of antimicrobial compounds used in food preservation (Abourashed *et al.* 2008), inhibit lipid oxidation in fish white muscle (Tuckey *et al.* 2009b) and potentially kill gram negative bacteria, like the related molecule eugenol (Gill and Holley 2006) make it an appealing compound for use in the rested harvesting of fish.

In summary, I have studied the anaerobic metabolism and energetics in the white muscle of a commercially harvested teleost (Chinook salmon) subjected to different harvest regimens. I measured anaerobic metabolic rate using calorimetry and key metabolites associated with anaerobic energy production. The effect of harvest regimen was pronounced; the anaesthetised and rested animals having a markedly elevated metabolic rate and concentration of metabolites above the exhausted group for a period post-mortem. The exponential decline in anaerobic metabolic rate from the rested group was highly correlated with exponential declines in ATP, creatine phosphate and glycogen concentrations which were the most likely source of the observed differences between treatments. These data corroborate earlier reports that harvesting associated with little pre-mortem activity can retain energy stores thus extending metabolic activity in muscle.

Chapter 6

Oxygen dependency of hydrogen sulfide-mediated vasoconstriction in cyclostome aortas

Contributions to the work presented in Chapter 6

The work presented in chapter 6 was done collaboratively. During a sabbatical visit by Professor Ken Olson to the University of Canterbury in late 2007, a joint research project was initiated involving Ken Olson, Ryan Dombkowski, Malcolm Forster and Myself with the aim of publishing our results. I planned and executed all the vessel oxygen consumption experiments (figures 6.5 and 6.6) and contributed to the myography studies on hagfish vessels (figure 6.3A). The primary responsibility for the preparation of the manuscript fell to Ken Olson. However, I contributed to the writing of the manuscript and responses to referees comments post-review. The published article is included in appendix 3.

6.1 Abstract

Hydrogen sulfide (H₂S) has been proposed to mediate hypoxic vasoconstriction (HVC), however, other studies suggest the vasoconstrictory effect indirectly results from an oxidation product of H₂S. Here we examined the relationship between H₂S and O₂ in isolated hagfish and lamprey vessels that exhibit profound hypoxic vasoconstriction. In myographic studies, H₂S (Na₂S) dose-dependently constricted dorsal aortas (DA) and efferent branchial arteries (EBA) but did not affect ventral aortas or afferent branchial arteries; effects similar to those produced by hypoxia. Sensitivity of H₂S-mediated contraction in hagfish and lamprey DA was enhanced by hypoxia. HVC in hagfish DA was enhanced by the H₂S precursor cysteine and inhibited by amino-oxyacetate, an inhibitor of the H₂S-synthesising enzyme, cystathionine β-synthase, and unaffected by propargyl glycine, an inhibitor of cystathionine λ-lyase. Oxygen consumption (MO₂) of hagfish DA was constant between a PO₂ of 15 and 115 mmHg, decreased when PO₂ < 15 mmHg, and increased if PO₂ exceeded 115 mmHg (1 mmHg = 0.133 kPa). 10 μmol.l⁻¹ H₂S increased and concentrations above 100 μmol.l⁻¹ H₂S decreased MO₂. Consistent with the effects on HVC, cysteine increased and amino-oxyacetate and hydroxylamine, an inhibitor of pyridoxyl 5'-phosphate-dependent enzymes, decreased MO₂. These results show that H₂S is a monophasic vasoconstrictor of specific cyclostome vessels and because hagfish lack vascular NO, and vascular sensitivity to H₂S was enhanced at low PO₂, it is unlikely that H₂S contractions are mediated by either an H₂S-NO interaction or an oxidation product of H₂S. These experiments provide additional support for the hypothesis that the metabolism of H₂S is involved in oxygen sensing/signal transduction in vertebrate vascular smooth muscle.

6.2 Keywords

Hypoxic-vasoconstriction, oxygen-sensing, vascular smooth muscle, H₂S

6.3 Introduction

Hypoxic vasoconstriction (HVC) was first observed in the mammalian pulmonary vasculature by von Euler and Liljestrand (von Euler and Liljestrand 1946) and it is now generally accepted that in mammals this response is unique to the pulmonary circulation, whereas hypoxic vasodilation (HVD) is the prominent response of systemic vessels (Weir and Archer 1995). Although HVC and HVD may be modulated by endothelial-derived and/or circulating substances (Félétou *et al.* 1995; Jacobs and Zeldin 2001; Kerkhof *et al.* 2001; Liu *et al.* 2001; Aaronson *et al.* 2002; Deussen *et al.* 2006), the basic responses are intrinsic to the vascular smooth muscle cell (Madden *et al.* 1992). In non-mammalian vertebrates, HVC has been observed in both systemic and respiratory conductance vessels (Olson *et al.* 2001; Russell *et al.* 2001; Smith *et al.* 2001; Russell *et al.* 2007) and HVC appears to be an intrinsic response of vascular smooth muscle cells in the cyclostome dorsal aorta as well (Olson *et al.* 2001). HVD has only recently been systematically examined in non-mammalian vertebrates (Russell *et al.* 2007) and while it is common in systemic vessels it is not necessarily the predominant response.

How vascular smooth muscle cells “sense” hypoxia and transduce this into a mechanical response, either HVC or HVD, is unknown. We recently proposed that the metabolism of hydrogen sulphide (H₂S) is involved in the O₂-sensing signal transduction process. Our model is based on the balance between constitutive cellular production of vasoactive H₂S and its oxidation to inactive products by available O₂ (Olson *et al.* 2006). Furthermore, this model appears to be applicable to both HVC and HVD and evidence for an H₂S-mediated hypoxic relaxation has even been observed in the trout urinary bladder (Dombkowski *et al.* 2006).

There is also relatively little information on the mechanism through which H₂S elicits mechanical responses in the vasculature. H₂S-mediated vasodilation has been demonstrated in mammalian systemic vessels and at least part of this response is due to H₂S opening of ATP sensitive potassium (K_{ATP}) channels on the vascular smooth muscle cell and to release of nitric oxide (NO) from the endothelium (Zhao *et al.* 2001; Zhao and Wang 2002; Wang *et al.* 2004). H₂S-mediated vasoconstriction has been demonstrated in mammalian pulmonary vessels (Olson *et al.* 2006) and in a variety of both pulmonary and systemic vessels from non-mammalian vertebrates (Dombkowski *et al.* 2005). Although it is unlikely that H₂S contractions are mediated through either K_{ATP} channels or endothelial-derived vasoconstrictor substances, the mechanism/s of H₂S-mediated vasoconstriction is unknown.

Recently, Koenitzer *et al.* (2007) examined the effects of H₂S on rat thoracic aortas at high (200 $\mu\text{mol.l}^{-1}$, ~150 mmHg) and low (40 $\mu\text{mol.l}^{-1}$, ~30 mmHg) partial pressures of O₂ (PO₂) and showed that vascular relaxation was more sensitive to H₂S at low oxygen concentration ([O₂]) and that H₂S-mediated contractions were present at high, but not low [O₂]. They postulated that the decreased sensitivity of the H₂S-mediated vasorelaxation at high [O₂] was due to the combined effect of rapid oxidation (and therefore inactivation) of vasodilatory H₂S plus the generation of a vasoconstrictor oxidation product of H₂S that would compete with the H₂S relaxation. Thus H₂S does not directly produce vasoconstriction. The identity of this oxidation product was not determined.

There are other possible explanations for the results of Koenitzer *et al.* (2007) that seem equally or more plausible. First, Koenitzer *et al.* (2007) examined rat aortas and these vessels relax when exposed to either hypoxia or lower (and perhaps more physiological?) concentrations of H₂S and thus a contraction would not normally be expected. Second, our theory of H₂S metabolism in vascular O₂ sensing predicts that as [O₂] falls, endogenous [H₂S] increases.

Thus at low PO₂ we would expect greater sensitivity to exogenous H₂S when applied against a background of elevated endogenous H₂S, consistent with the observations of Koenitzer *et al.* (2007). Furthermore, we also think that H₂S directly produces vasoconstriction in vessels that exhibit hypoxic vasoconstriction (e.g. hagfish and lamprey aortas) because it seems unlikely to us that cellular concentrations of an oxidation product of H₂S would be increasing when PO₂ is falling.

In the present study we examined the interaction between [O₂] and [H₂S] in the dorsal aorta of the most ancient extant craniate, the hagfish. This vessel was chosen because it has a mono-phasic, [O₂]-dependent HVC that is endothelium independent, and does not involve K_{ATP} channels, products of lipoxygenase, cyclooxygenase, cytochrome P₄₅₀ enzyme activity, or α adrenergic, muscarinic, nicotinic, purinergic or serotonergic receptors (Olson *et al.* 2001). If our hypotheses that H₂S directly produces vasoconstriction and that endogenous H₂S increases when PO₂ falls is correct, we expect to see an increased sensitivity of H₂S-constriction at low [O₂], not an unmasking of H₂S relaxation. We also provide additional evidence for H₂S metabolism in the O₂ sensing mechanism by examining the contribution of its precursor, cysteine, and the effects of inhibitors of H₂S synthesis on HVC. The effects of H₂S, cysteine and enzyme inhibitors on vessel O₂ consumption (MO₂) were measured to determine whether H₂S exposure increased MO₂ and inhibitors decreased it. For comparison, we examined the O₂ sensitivity of H₂S contraction in lamprey aortas. These vessels are identical to hagfish aortas in their response to hypoxia (Olson *et al.* 2001) and evidence for the role of H₂S in O₂ sensing has been described (Olson *et al.* 2006).

6.4 Materials and Methods

6.4.1 Animals

New Zealand hagfish, (*Eptatretus cirrhatus* Forster 1122 ± 165 g, n=26) were collected in Akaroa Harbour, New Zealand, and held in 14 °C seawater aquaria at the University of Canterbury, Christchurch, NZ for at least 1 week prior to use. They were anaesthetised in a combination of AQUI-STM (200 ppm; Lower Hutt, New Zealand), benzocaine (400 ppm) and MS-222 (400 ppm). The ventral and dorsal aortas (VA and DA) and afferent and efferent branchial arteries (ABA and EBA) were removed cleaned of excess fat and blood and placed in 4 °C hagfish Hepes saline until use (within 1–2 days). The saline was changed daily prior to use.

Sea lamprey (*Petromyzon marinus* Linnaeus 130–450 g) were captured by the US Geological Survey, Biological Resources Division, in Michigan during the spring-summer spawning migration and airlifted to Indiana University School of Medicine–South Bend (IUSM-SB). They were housed in 500 l rectangular tanks in aerated, flowing well water (15 °C), and exposed to a 12 h:12 h light:dark photoperiod. They were not fed. Lamprey were anaesthetised in benzocaine (1:5000, wt:vol), and the vessels were dissected out and placed in Cortland buffered saline at 4 °C until use.

Chinook salmon (*Oncorhynchus tshawytscha* Walbaum) were obtained from a nearby hatchery (NZ), anaesthetised with 22 ppm AQUI-STM in their holding tanks and then killed by pithing the brain and proximal spinal cord. The ventral aorta and afferent branchial arteries were rapidly excised and stored at 4 °C in freshwater salmon Ringer's solution; the dorsal aorta is firmly attached to the vertebral column and cannot be removed intact.

Experimental procedures were approved by the University of Canterbury's Animal Ethics Committee and the IUSM-SB IACUC.

6.4.2 Myography

Vessels were cut transaxially into 3–4 mm long segments, mounted on 280 μ m diameter stainless-steel hooks and suspended in 20 ml, water-jacketed (12°C) smooth muscle chambers and gassed with room air. Tension was measured with Grass FT03C force displacement transducers (Grass Instruments, West Warwick, RI, USA) and collected electronically using Biopac model MP35 (Biopac Systems Inc., Goleta, CA, USA), or measured with MLT0210 isometric force transducers (ADInstruments, Castle Hill, Waverley, NSW, Australia) using Powerlab® systems with bridge amplifiers (ADInstruments). Data were archived at 2 Hz on notebook computers. A resting tension of 500 ± 50 mg (Olson *et al.* 2001) was applied to the vessels for 45–60 min prior to experimentation. Vessels were maximally contracted with the acetylcholine analog carbamylcholine chloride (carbachol, $10 \mu\text{mol.l}^{-1}$; figure 6.1) until tension plateaued (30–45 min), then rinsed four times with buffer and resting tension re-established over the ensuing 60 min. They were then contracted a second time with $10 \mu\text{mol.l}^{-1}$ carbachol, the rinse repeated, and the vessels were allowed to stabilise and resting tension re-established for the next 1–2 h. The tension produced by the second application of carbachol was used as the reference contraction for subsequent experiments.

6.4.3 Protocols

6.4.3.1 Carbachol dose-response

Cumulative carbachol dose–response curves were initially obtained for efferent branchial arteries (figure 6.1) and dorsal aortas (not shown). Carbachol at $10 \mu\text{mol.l}^{-1}$ produced maximum contraction in both vessels. Therefore, carbachol at this concentration was used twice at the beginning of experiments, first for initial activation and second for a reference contraction.

A third carbachol (10 $\mu\text{mol.l}^{-1}$) was also applied at the end of many experiments to determine if other treatments had non-specific effects on vascular reactivity.

6.4.3.2 Effect of H₂S on buffer pH

The dissolution of Na₂S in water produces H₂S and HS⁻ (collectively referred to in this study as H₂S) and increases pH. Because extracellular alkalinity can contract vascular smooth muscle independently of other exogenous stimuli (Smith *et al.* 2006), the buffering capacity of Hepes samples over the range of 1 $\mu\text{mol.l}^{-1}$ to 10 mmol.l^{-1} H₂S was measured in triplicate using an Orion 911600 semi-micro pH electrode (Beverly, MA USA) and a PHM 84 pH meter (Radiometer, Copenhagen, Denmark).

6.4.3.3 H₂S dose-dependent responses

Cumulative H₂S dose-response curves (1 $\mu\text{mol.l}^{-1}$ to 1 mmol.l^{-1}) were obtained for otherwise unstimulated, normoxic (gassed with room air; 21% O₂) dorsal aortas and efferent branchial arteries. To determine if H₂S relaxed vessels, a second series of experiments was conducted with the vessels pre-contracted with 150 mmol.l^{-1} KCl or 0.3 $\mu\text{mol.l}^{-1}$ carbachol prior to the H₂S doses. In pilot studies, H₂S had no effect on ventral aortas or afferent branchial arteries (n=4) and these vessels were not examined further.

6.4.3.4 Effect of PO₂ on H₂S responses

The effect of graded hypoxia on the H₂S dose response of hagfish dorsal aortas was examined by initially gassing groups of vessels with either 100% room air (PO₂=157 mmHg), 6% air/94% N₂ (PO₂=10 mmHg), or 100% N₂ (PO₂<1 mmHg) for 20–30 min prior to and during the H₂S treatments (1 mmHg=0.133 kPa). The air/N₂ mixture was controlled with a Wöstoff type 1M 300/a-F gas mixing pump (H. Wöstoff, Bochum, Germany).

The PO₂ was measured in one myograph chamber using a Microelectrodes MI-730 oxygen electrode and meter (Bedford, NH).

The effect of moderate hypoxia on the H₂S dose response of lamprey dorsal aortas was examined using the following protocol. Vessels were contracted twice with 80 mmol.l⁻¹ KCl, washed twice after each contraction, and then vigorously gassed with 100% N₂ to produce a maximal HVC. After recovery (normoxia) the flow of N₂ was reduced to produce HVC that was 20 ± 6% of the maximal HVC. This is equivalent to a bath PO₂ of 20–30 mmHg (Olson *et al.* 2001). Cumulative doses of H₂S (10 nmol.l⁻¹-1 mmol.l⁻¹) were applied during this moderate hypoxia.

6.4.3.5 Involvement of H₂S mechanisms in hagfish hypoxic vasoconstriction

The involvement of H₂S in hagfish HVC was examined by measuring the response of hypoxia-contracted (100% N₂) aortas to serial additions of the substrate for H₂S synthesis: L-cysteine (0.1, 1 and 10 mmol.l⁻¹), amino-oxyacetate (AOA; 0.1, 1 and 4 mmol.l⁻¹), an inhibitor of cystathionine β synthase (CBS), D,L-propargylglycine (PPG; 0.1, 1 and 4 mmol.l⁻¹), an inhibitor of cystathionine λ-lyase (CSE), or hydroxylamine (0.01, 0.1 and 1 mmol.l⁻¹), a general inhibitor of pyridoxyl 5'-phosphate-dependent enzymes. Following a standard carbachol (10 μmol.l⁻¹) contraction the vessels were thoroughly washed and gassed with 100% N₂ for 20–30 min until the hypoxic contraction stabilised. Cumulative doses of cysteine or inhibitors were applied during the hypoxic contraction followed by a final application of 10 μmol.l⁻¹ carbachol. Vessels were not washed prior to the final carbachol application. The effects of hypoxia, cysteine, inhibitors and final carbachol were normalised relative to the reference carbachol contraction.

6.4.4 Oxygen consumption

6.4.4.1 Oxygen consumption by hagfish dorsal aortas

Hagfish dorsal aortas used in the MO₂ experiments were stored and maintained in hagfish Hepes buffer containing gentamycin sulphate (200 µg.ml⁻¹) to reduce the potential for micro-organisms to contribute to MO₂ (Rudin *et al.* 1970). Four to six aortas, 3–8 mm long, were freed of any remaining connective tissue and fat and threaded onto a 280 µm diameter stainless steel wire frame. They were placed into 1 ml of either air-saturated or reduced [O₂] (PO₂ ~60 mmHg) Hepes buffer in model RC300 respirometers (Strathkelvin Instruments, Glasgow, Scotland) fitted with IL 1302 O₂ electrodes and maintained at 12 °C. The electrode signal was fed into a Strathkelvin model 781 O₂ meter and then via a Powerlab 4SP to a notebook running Chart 5 software (both ADInstruments). Treatments were introduced into the respirometer via a small slot in the electrode holder with a 50 µl Hamilton syringe (Hamilton Co., Reno, Nevada, USA) fitted with a length of polythene tubing (Portex Ltd, Hythe, Kent, England; OD 0.61 mm, ID 0.28 mm). Oxygen consumption was determined from the equation:

$$MO_2 = \frac{\Delta PO_2 \times \alpha O_2 \times V}{t \times M}$$

where MO₂ is the rate of oxygen consumption (mmol O₂.mg⁻¹.min⁻¹), ΔPO₂ is the change in PO₂ during the treatment period (mmHg), αO₂ is the solubility of O₂ in seawater (1.72 mmol O₂.l⁻¹.mmHg⁻¹; hagfish plasma has very similar ionic composition), V is the volume of the respirometer (l), t is the time (minutes) between PO₂ measurements and M is the mass (mg) of the vessels in the respirometer.

The relationship between PO₂ and MO₂ was measured in vessels that were allowed to deplete the oxygen content from air saturation (PO₂ ~155 mmHg) down to zero.

These experiments showed that the vessels could efficiently regulate their MO₂ between a PO₂ of 15 and 115 mmHg (see Results). Subsequent experiments on the effects of H₂S, cysteine and inhibitors of H₂S production were performed between 40 and 60 mmHg PO₂ where MO₂ was otherwise independent of PO₂.

A cumulative H₂S concentration–MO₂ response was established for 1 µmol.l⁻¹–1 mmol.l⁻¹ H₂S in both uncontracted and carbachol (100 µmol.l⁻¹)-contracted vessels.

The effects of the H₂S precursor, L cysteine (1 and 10 mmol.l⁻¹) and inhibitors of H₂S production, AOA and HA (both 10 µmol.l⁻¹–1 mmol.l⁻¹), on MO₂ were also determined.

6.4.4.2 Oxygen consumption by salmon vessels

In the initial studies on hagfish vessels it became evident that contracting the vessels with carbachol had no effect on MO₂. This was unexpected as it has been shown that contracting mammalian vessels increases MO₂ (Koenitzer *et al.* 2007). To determine whether this was an actual physiological difference or an experimental artefact, we repeated the studies with ventral aortas and afferent branchial arteries isolated from Chinook salmon using the general protocol described above for hagfish vessels. Storage and preparation of the salmon vessels for respirometry was identical to that described below for hagfish.

6.4.5 Chemicals

The composition of hagfish Hepes-buffered saline was (in mmol.l⁻¹): 497.95 NaCl, 8.05 KCl, 5.10 CaCl₂, 9.00 MgCl₂, 3.04 MgSO₄, 3.00 Hepes [N-(2-hydroxyethyl)piperazine-N'-(2-ethane-sulfonic acid)] acid form, 6.99 Hepes sodium salt, 5.55 glucose, pH 7.8. The composition of lamprey Cortland saline was (in mmol.l⁻¹): 124 NaCl, 3 KCl, 2 CaCl₂, 0.57 MgSO₄, 12 NaHCO₃, 0.09 NaH₂PO₄, 1.8 Na₂HPO₄, 5.5 glucose, pH 7.8.

The composition of salmon Ringer was (in mmol.l⁻¹; 136.89 NaCl; 2.11 KCl; 0.99 MgCl₂; 1.30 CaCl₂; 3.00 Hepes acid form; 6.99 Hepes sodium salt; 0.30 sodium glutamate; 0.40 L-glutamine; 0.02 sodium aspartate; 0.05 DL-carnitine; 10.00 glucose, pH 7.6. AOA was purchased from ACROS Organics (Morris Plains, NJ, USA) all other chemicals were purchased from Sigma Chemical Co. (St Louis, MO, USA).

6.4.6 Calculations and statistical analysis

Concentration response curves were expressed as a percentage of the maximal response. Vessel responses were normalised to the second carbachol contraction produced prior to experimentation. At the end of an experiment the vessel was blotted on paper towelling and weighed. This value was used to normalise vessel tension to wet mass, i.e. mg tension.g⁻¹ wet mass. Because the hypoxic responses of individual vessels were reproducible (Olson *et al.* 2001), each vessel served as its own control and treatment effects were statistically examined by paired t-test or repeated measures tests. Student's t-test and analysis of variance (ANOVA) were used for comparisons between vessels. Significant differences in rates of MO₂ and responses to drugs were determined using a repeated measures ANOVA. Where significant differences were calculated between means, Tukey's post-hoc tests were used to determine differences between treatments. Paired Student's t-tests were used to detect differences between carbachol-treated and -untreated vessels in the MO₂ data (controls and at each concentration of H₂S). Significance was assumed when P<0.05. All analyses were performed in Prism 4.00 (Graphpad software, San Diego, CA, USA). Results are presented as mean ± SEM.

6.5 Results

6.5.1 Carbachol dose-response of hagfish efferent branchial arteries

Carbachol produced a dose-dependent contraction of efferent branchial arteries (figure 6.1) with an EC₅₀ of $0.275 \pm 0.148 \mu\text{mol.l}^{-1}$ (n=4). Peak force was achieved at a concentration of $10 \mu\text{mol.l}^{-1}$ carbachol.

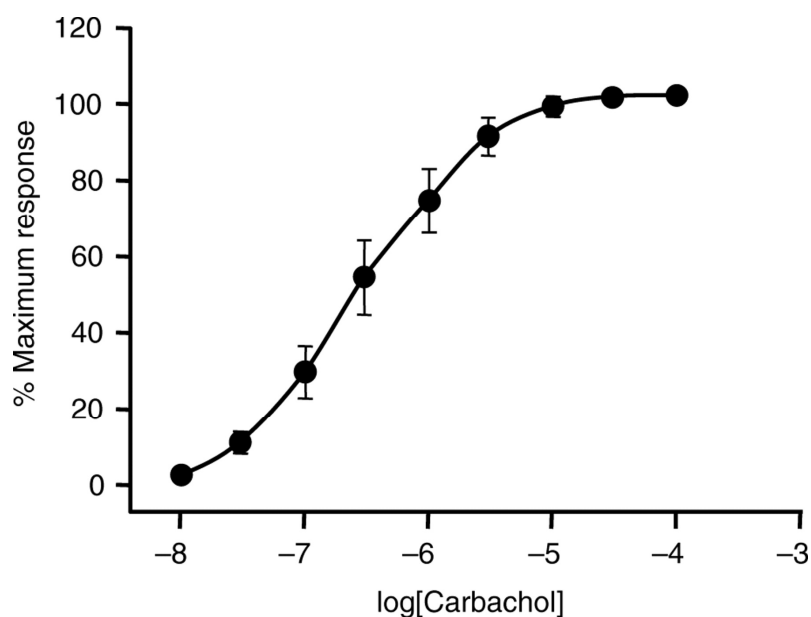


Figure 6.1. Cumulative carbachol dose-response curve for efferent branchial arteries (mean \pm SEM; n=4).

6.5.2 Effects of H₂S on pH

The effects of increasing concentrations of H₂S on pH of hagfish Hepes buffer is shown in figure 6.2. Buffering was very efficient between $1 \mu\text{mol.l}^{-1}$ and 1 mmol.l^{-1} H₂S and increased less than 0.3 pH units between 1 mmol.l^{-1} and 3 mmol.l^{-1} H₂S. However, pH increased nearly 2.5 units between 3 and 10 mmol.l^{-1} H₂S. H₂S contractions appeared to be independent of pH between $1 \mu\text{mol.l}^{-1}$ and 1 mmol.l^{-1} H₂S, but concentrations above 1 mmol.l^{-1} alkalinised the medium and this appeared to greatly augment H₂S contractions.

H₂S concentrations were limited in subsequent experiments to 1 mmol.l⁻¹ in order to minimise the possibility of pH interference and to avoid complications that might result from changes in ionic strength or composition due to increasing the buffering capacity, or titration.

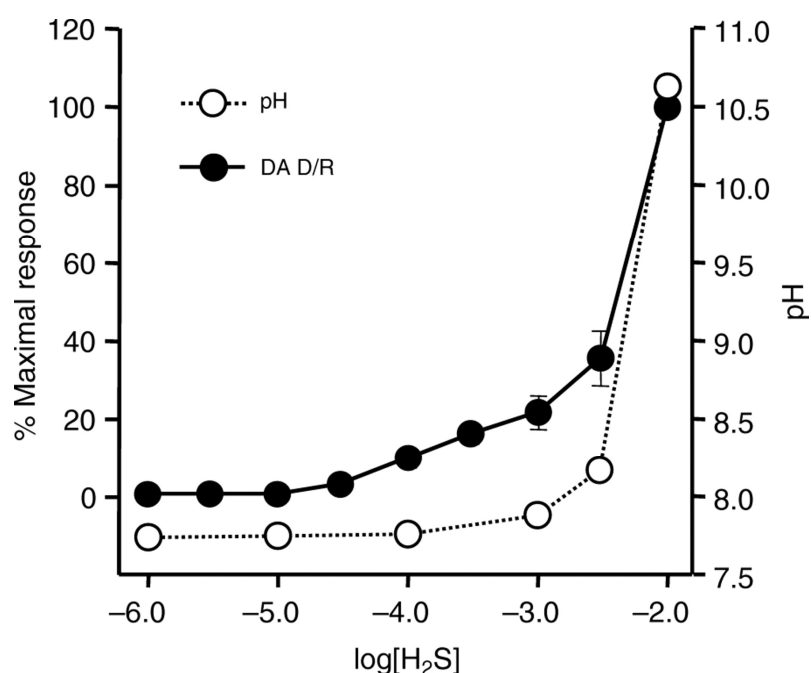


Figure 6.2. Effects of H₂S (administered as Na₂S) on buffer pH (open circles, n=2) and contraction of dorsal aortas (filled circles, n=4). pH is relatively stable at an [H₂S] of ≤1 mmol.l⁻¹, but higher concentrations produce increasing alkalinity and appear to augment aortic contraction.

6.5.3 Vascular effects of H₂S

H₂S produced dose-dependent contractions in otherwise unstimulated dorsal aortas and efferent branchial arteries of hagfish (figure 6.3) but had no effect on ventral aortas or afferent branchial arteries data (not shown). H₂S produced essentially identical dose dose-dependent contractions in KCl (150 mmol.l⁻¹, n=4) and carbachol (0.3 μmol.l⁻¹, n=4) pre-contracted dorsal aortas and in carbachol (0.3 μmol.l⁻¹, n=4) pre-contracted efferent branchial arteries (data not shown for pre-contracted vessels). There was no obvious H₂S-mediated relaxation in either pre-contracted or otherwise unstimulated vessels.

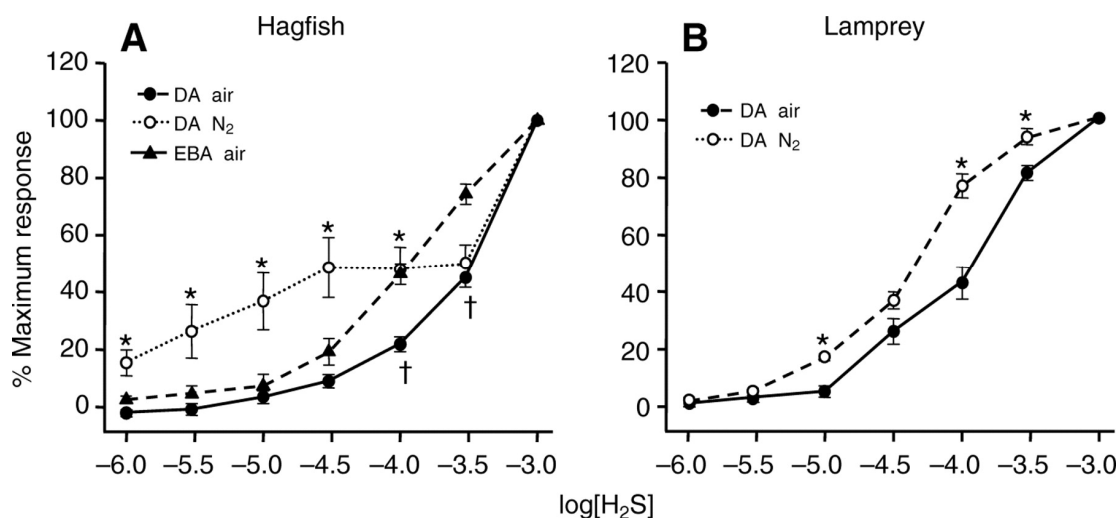


Figure 6.3. (A) H₂S dose–response curves for hagfish dorsal aortas (filled circles; $n=22$) and efferent branchial arteries (filled triangles; $n=8$) gassed with room air, and dorsal aortas gassed with 100% nitrogen (open circles; $n=10$). Aortas gassed with nitrogen were significantly (*) more sensitive to low concentrations of H₂S than air gassed aortas and appear to have a two-phase response to H₂S. H₂S at 100 and 300 $\mu\text{mol.l}^{-1}$ produces a significantly greater response in normoxic efferent branchial arteries than normoxic dorsal aortas (†). (B) H₂S dose–response curves for lamprey dorsal aortas gassed with room air (filled circles; $n=8$) or during moderate hypoxia (open circles; $n=8$). Hypoxic vessels were significantly (*) more sensitive to H₂S. Values are means \pm SEM.

6.5.4 Effect of PO_2 on H₂S responses of hagfish and lamprey dorsal aortas

Hagfish dorsal aortas gassed with 100% N₂ were significantly more sensitive to low H₂S concentrations than aortas gassed with room air and the H₂S dose–response curve of hypoxic (anoxic) vessels appeared to have two components (figure 6.3). H₂S-mediated contractions of hagfish aortas gassed with 6% air/94% N₂ (data not shown) were not significantly different from aortas gassed with room air. H₂S produced dose-dependent contractions of lamprey dorsal aortas (figure 6.3). Moderate hypoxia increased H₂S sensitivity between 10 and 300 $\mu\text{mol.l}^{-1}$ H₂S (P -value at 30 $\mu\text{mol.l}^{-1}$ H₂S was 0.053).

Hypoxia did not affect the magnitude of the 1 mmol.l⁻¹ H₂S contraction which in hypoxia was $41 \pm 5\%$ and in normoxia $43 \pm 4\%$ of a 80 mmol.l⁻¹ KCl contraction. H₂S at concentrations between 10 nmol.l⁻¹ to 1 μ mol.l⁻¹ did not affect either normoxic or hypoxic vessels (not shown).

6.5.5 Involvement of H₂S mechanisms in hagfish hypoxic vasoconstriction

In these experiments vessels were contracted with 10 μ mol.l⁻¹ carbachol, washed, then continuously contracted with by gassing with 100% N₂. During the hypoxic contraction, the vessels were given cumulative additions of cysteine or inhibitors and this was followed, without washing the vessels, by 10 μ mol.l⁻¹ carbachol.

The effect of L-cysteine, a substrate for H₂S synthesis, on hypoxic contractions of hagfish dorsal aortas is shown in figure 6.4, top left panel. 100 μ mol l⁻¹ cysteine produced a consistent, but statistically non-significant increase in the force of the N₂ contraction. Increasing cysteine to 1 mmol.l⁻¹ significantly ($P < 0.05$) contracted the vessels to approximately double that in the original N₂ contraction. Raising cysteine to 10 mmol.l⁻¹ produced an immediate relaxation back to the pre-cysteine (N₂) tension ($P < 0.05$). The carbachol (10 μ mol.l⁻¹) contraction at the end of the experiment, in the presence of N₂ and 10 mmol.l⁻¹ cysteine, was not significantly different from the reference carbachol contraction ($90 \pm 14\%$ of reference, $n=7$).

The effect of the cystathionine β -synthase (CBS) inhibitor, amino oxyacetate (AOA), on hypoxic vasoconstriction of the dorsal aorta is shown in figure 6.4 top right panel. Hypoxic contractions were unaffected by 100 μ mol.l⁻¹ and 1 mmol l⁻¹ AOA. 4 mmol l⁻¹ AOA completely inhibited the hypoxic contraction ($P < 0.05$). The carbachol (10 μ mol l⁻¹) contraction at the end of the experiment, in the presence of 4 mmol l⁻¹ AOA, was not significantly different from the reference carbachol contraction ($111 \pm 12\%$ of reference, $n=8$).

As shown in figure 6.4, lower left panel, the cystathionine λ -lyase (CSE) inhibitor, propargyl glycine (PPG; between 100 $\mu\text{mol.l}^{-1}$ and 4 mmol.l^{-1}) had no effect on the hypoxic contraction. A carbachol (10 $\mu\text{mol.l}^{-1}$) contraction at the end of the experiment, in the presence of PPG, was similarly unaffected ($104 \pm 7\%$ of reference, $n=8$).

Hydroxylamine (HA), an uncoupler of pyridoxyl 5'-phosphate-dependent enzymes including CBS and CSE, at 10 $\mu\text{mol.l}^{-1}$ significantly increased the force of the N₂ contraction (figure 6.4, lower right panel). Increasing HA to 100 $\mu\text{mol.l}^{-1}$ and 1 mmol.l^{-1} produced slight, but statistically non-significant, further increases in tension. The carbachol (10 $\mu\text{mol.l}^{-1}$) contraction at the end of the experiment, in the presence of HA, was not significantly different from the reference carbachol contraction ($103 \pm 12\%$ of reference, $n=8$).

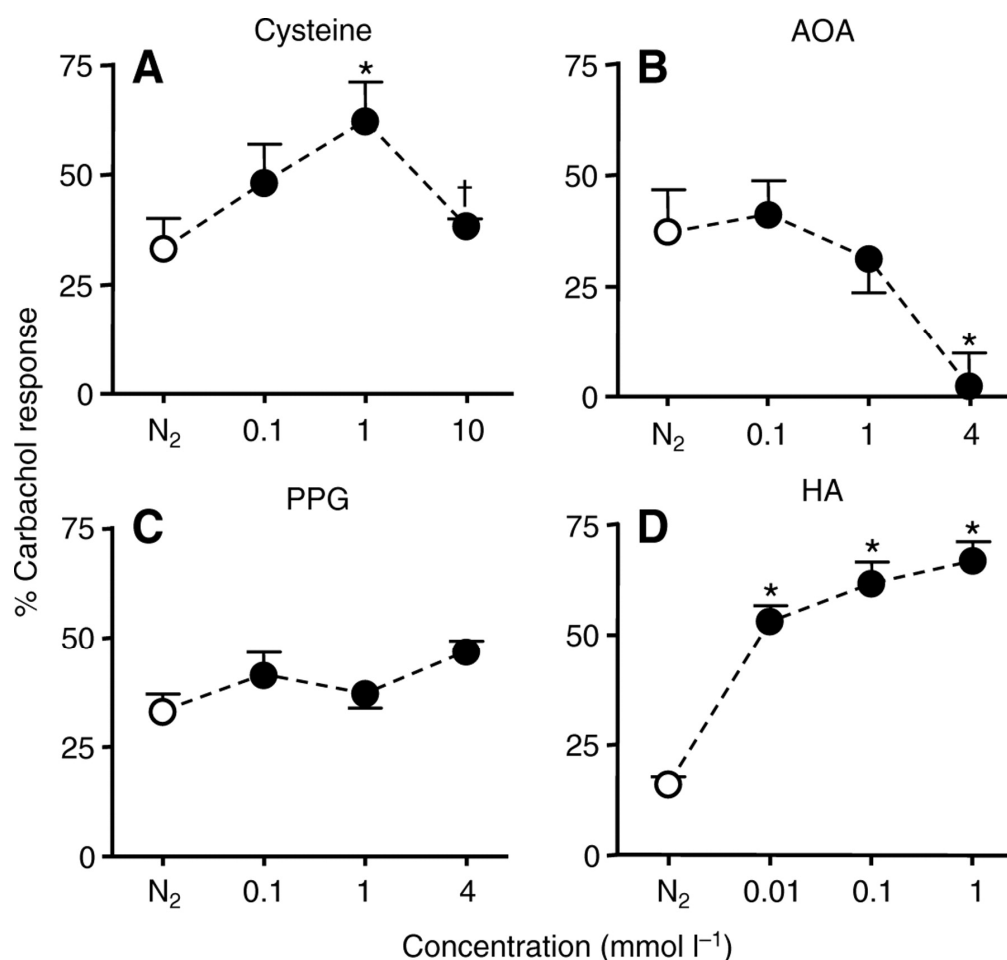


Figure 6.4. Effects of (A) L-cysteine, the substrate for H₂S synthesis, (B) the cystathionine β -synthase inhibitor, amino-oxyacetate (AOA), (C) the cystathionine λ -lyase inhibitor, propargyl glycine (PPG) and (D) an uncoupler of pyridoxyl 5'-phosphate-dependent enzymes, hydroxylamine (HA) on hypoxic (100% N₂) vasoconstriction of hagfish dorsal aorta. Vessels were continuously contracted with N₂ then given cumulative additions of cysteine or inhibitors followed by 10 $\mu\text{mol.l}^{-1}$ carbachol (CBC). Values are expressed as the average tension (mean \pm SEM) as the percentage of the reference carbachol contraction (100%; dashed line). Hypoxic contractions (N₂) were generally \sim 30% of the reference carbachol contraction. Cysteine at 1 mmol.l^{-1} approximately doubled the force of the original N₂ contraction, whereas raising cysteine to 10 mmol.l^{-1} relaxed the vessels back to the original N₂ level (* significant increase from N₂; † significant decrease from 1 mmol.l^{-1} cysteine; n=7). Hypoxic contractions were unaffected by 100 $\mu\text{mol.l}^{-1}$ and 1 mmol.l^{-1} AOA. At 4 mmol.l^{-1} AOA, the hypoxic contraction was completely inhibited (*; n=8). PPG did not significantly affect the N₂ contraction (n=8). HA, 10 $\mu\text{mol.l}^{-1}$ HA significantly (*) increased the force of the N₂ contraction and tension was maintained at 100 $\mu\text{mol.l}^{-1}$ and 1 mmol.l^{-1} (n=8).

6.5.6 Vessel MO_2

The relationship between PO_2 and oxygen consumption (MO_2) in uncontracted and carbachol pre-contracted hagfish dorsal aortas is shown in figure 6.5A. MO_2 was well maintained around $2.4 \text{ pmol.mg}^{-1}.\text{min}^{-1}$ between 15 and 115 mmHg, but PO_2 doubled between 115 and 155 mmHg and fell to zero as PO_2 approached zero. MO_2 fell to 90% of the regulated rate at a PO_2 of 12 mmHg and the PO_2 at which the regulated MO_2 fell to half (P_{50}) was 3 mmHg. Pre treating hagfish aortas with $100 \text{ }\mu\text{mol.l}^{-1}$ carbachol did not significantly affect MO_2 . MO_2 was also well regulated in unstimulated salmon vessels between 15 and 115 mmHg PO_2 but the rate of oxygen consumption per unit tissue mass was five times that of hagfish aortas (figure 6.5B). Pre-treating salmon vessels with $100 \text{ }\mu\text{mol.l}^{-1}$ carbachol nearly doubled MO_2 at all but the lowest PO_2 .

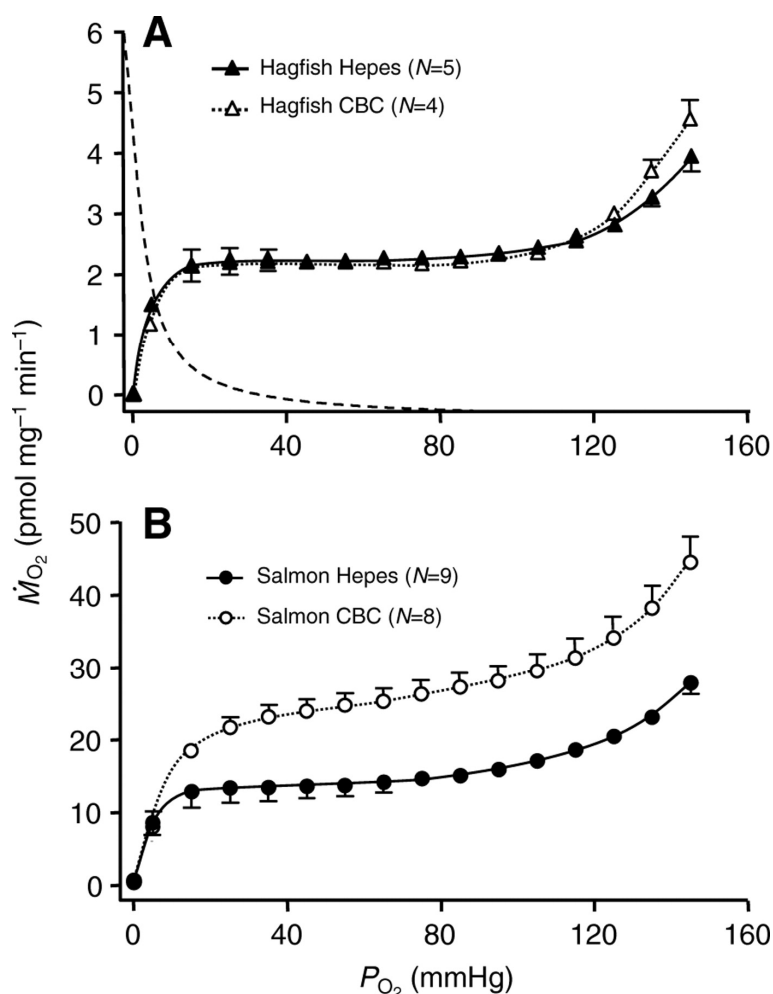


Figure 6.5. Effect of P_{O_2} on oxygen consumption (\dot{M}_{O_2}) by hagfish dorsal aortas (A) and salmon vessels (B). \dot{M}_{O_2} is tightly regulated in unstimulated hagfish aortas (filled triangles) between a P_{O_2} of 15 and 115 mmHg (1 mmHg=0.133 kPa), but varies with P_{O_2} at either extreme. At a P_{O_2} of 12 mmHg \dot{M}_{O_2} falls to 90% of the regulated level and \dot{M}_{O_2} is halved at 3 mmHg (P_{50}). \dot{M}_{O_2} was not affected by pre-contracting hagfish aortas with 100 $\mu\text{mol.l}^{-1}$ carbachol (CBC; open triangles). \dot{M}_{O_2} was also regulated in unstimulated salmon vessels (B; filled circles) between a P_{O_2} of 15 and 115 mmHg; however, per unit tissue mass it was five times greater than that of hagfish aortas. Pre-treatment of salmon vessels with 100 $\mu\text{mol.l}^{-1}$ carbachol nearly doubled \dot{M}_{O_2} at all P_{O_2} (open circles). Mean \pm SEM; n indicates the number of groups of 4–6 vessels per group in each experiment (standard error not shown when within the symbol). Broken line shows the P_{O_2} dependency of hypoxic contraction in hagfish dorsal aortas [redrawn from Olson *et al.* (Olson *et al.* 2001)].

The effects of H₂S, cysteine, AOA and HA on MO₂ are summarised in figure 6.6. 10 µmol.l⁻¹ H₂S significantly stimulated MO₂ whereas 100 µmol.l⁻¹ and 1 mmol.l⁻¹ significantly inhibited MO₂. A 12-fold increase in MO₂ was produced by 10 mmol.l⁻¹ cysteine; in many experiments 1 mmol.l⁻¹ cysteine often appeared to increase MO₂ as well, although this was not statistically significant. MO₂ was inhibited by either 10 mmol.l⁻¹ AOA or 10 mmol.l⁻¹ HA. Other concentrations of AOA (10 µmol.l⁻¹–1 mmol.l⁻¹) and HA (10 µmol.l⁻¹–1 mmol.l⁻¹) did not significantly affect MO₂. Precontraction with 100 µmol.l⁻¹ carbacol did not significantly affect MO₂ in vessels treated with 10 µmol.l⁻¹, 100 µmol.l⁻¹ or 1 mmol.l⁻¹ H₂S (figure 6.6), 10 mmol.l⁻¹ cysteine, 10 mmol.l⁻¹ AOA or 10 mmol.l⁻¹ HA (n=5 for all; data not shown), although MO₂ of vessels in 10 µmol.l⁻¹ H₂S was significantly greater than MO₂ of vessels in 100 µmol.l⁻¹ H₂S (figure 6.6).

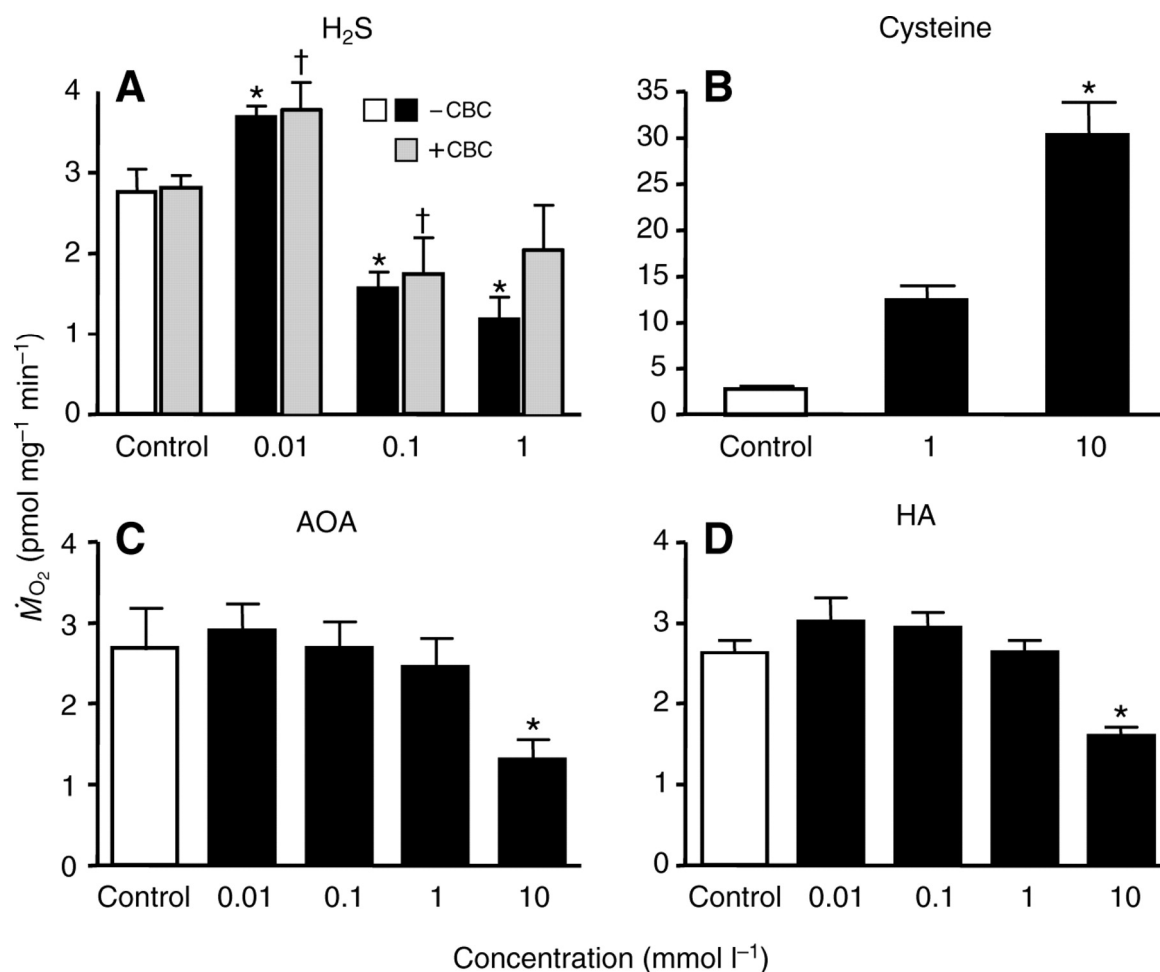


Figure 6.6. Effect of (A) H₂S (as Na₂S), (B) the substrate for H₂S synthesis, L-cysteine (cysteine), and inhibitors of H₂S production, (C) amino-oxyacetate (AOA) and (D) hydroxylamine (HA), on oxygen consumption (MO₂) by hagfish dorsal aortas. MO₂ was stimulated by 10 μmol.l⁻¹ H₂S and 10 mmol.l⁻¹ cysteine and inhibited by 100 μmol.l⁻¹ and 1 mmol.l⁻¹ H₂S and by 10 mmol.l⁻¹ AOA and 10 mmol.l⁻¹ HA. Carbachol (100 μmol.l⁻¹) pre-treatment (+CBC) did not affect MO₂ at any [H₂S] compared to untreated (–CBC) vessels, although MO₂ was significantly different between 10 μmol.l⁻¹ and 100 μmol.l⁻¹ H₂S in carbachol pretreated vessels. Mean ± SEM; n=7 (H₂S), 5 (cysteine), 4 (AOA), 4 (HA) groups of 4–6 vessels per group; *significantly different from respective control; † significantly different from +CBC control.

6.6 Discussion

The present studies support our hypotheses that, (1) H₂S directly produces vasoconstriction, and (2) the metabolism of H₂S is involved in the oxygen sensing and/or signal transduction cascade in hypoxic vasoconstriction of the hagfish aorta.

6.6.1 H₂S as a vasoconstrictor

As shown in figure 6.3, the H₂S sensitivity in both hagfish and lamprey aortas increased when PO₂ was decreased. Hagfish vessels gassed with 100% N₂ responded to 1 $\mu\text{mol.l}^{-1}$ H₂S, whereas 100 $\mu\text{mol.l}^{-1}$ H₂S was required to contract vessels gassed with room air (figure 6.3). Similarly, the apparent H₂S thresholds for hypoxic (PO₂ ~20–30 mmHg) and normoxic lamprey vessels were 10 and 30 $\mu\text{mol.l}^{-1}$ H₂S, respectively (figure 6.3). Furthermore, the H₂S dose–response curves for both animals were left-shifted in low PO₂. Thus although the effect of hypoxia on the H₂S response of lamprey vessels was less dramatic than that of hagfish vessels (probably because the hypoxia was less severe), the basic responses were, nevertheless, quite similar. As described below, these results support the hypothesis that H₂S has direct vasoconstrictory activity in specific vessels.

Koenitzer *et al.* (2007) observed a bi-phasic effect of H₂S on rat aortas; low H₂S concentrations produced dilation and high concentrations (1 mmol.l⁻¹) produced contraction. They also found that H₂S-mediated dilation of rat aortas became more sensitive to H₂S at low PO₂. These authors (Koenitzer *et al.* 2007) suggested that the H₂S-mediated vasoconstriction of aortas gassed with room air was due to an oxidation product of H₂S, not H₂S itself, and that the reason rat aortas became more sensitive to H₂S during hypoxia was because in the absence of this putative oxidation product there was no offsetting constrictory stimulus to compete with the direct H₂S dilation. Our findings argue against these hypotheses.

First, H₂S only constricted hagfish and lamprey dorsal aortas and therefore the increased sensitivity observed at low PO₂ could not be due to removal of a competing (in this case dilatory) process. Second, it seems unlikely that production of this hypothetical vasoconstrictory oxidation product of H₂S would increase when the vessels were gassed with 100% N₂. An alternative, and we think more plausible, explanation for the increased H₂S sensitivity, and one that is consistent with our (Olson *et al.* 2006) hypothesis of H₂S involvement in HVC (see below), is that when PO₂ falls endogenous H₂S increases. Therefore, less exogenous H₂S is required for vasoconstriction.

Ali *et al.* (2006) and Kubo *et al.* (2007) observed the opposite effects of Koenitzer *et al.* (2007), i.e. low H₂S concentrations (<200 µmol.l⁻¹) contracted, and elevated H₂S concentrations (200–1600 µmol.l⁻¹) relaxed rat aortic rings. They attributed the low-dose H₂S contraction to H₂S combining with NO and thereby removing the tonic NO-mediated vasodilation (Ali *et al.* 2006), or directly inhibiting endothelial nitric oxide synthase (Kubo *et al.* 2007). This also is unlikely to occur in either hagfish or lamprey dorsal aortas because, (1) there is at present no evidence for endothelial NO production by either of these vessels (Olson *et al.* 2001), (2) exogenous NO produces a modest contraction in the ventral aorta of the hagfish, *Myxine glutinosa* (Evans and Harrie 2001), and (3) NO synthesis from L-arginine and O₂ would be expected to be reduced during prolonged hypoxia. Our studies suggest that H₂S may directly constrict specific vessels and that this response is an intrinsic property of the smooth muscle cells. Clearly, however, variations in this response can be achieved through H₂S interactions with other vasoregulatory mechanisms.

6.6.2 H₂S metabolism in O₂ sensing

Our model of the role of H₂S metabolism in oxygen sensing and/or signal transduction appears to accommodate both hypoxic vasoconstriction (HVC) and hypoxic vasodilation (HVD) in vertebrate smooth muscle (Olson *et al.* 2006).

This model is based on the balance between H₂S production by vascular tissue and its inactivation through oxidation, and it provides a simple and rapid mechanism that couples the concentration of a vasoactive molecule directly to PO₂. The model is supported by observations that the responses of a wide variety of vessels (either constriction, dilation or multi-phasic) to hypoxia and H₂S are identical, H₂S is constitutively produced by blood vessels, cysteine the metabolic precursor of H₂S, augments HVC and inhibitors of H₂S production inhibit HVC and HVD. The present study provides additional support for the involvement of H₂S in HVC in hagfish vessels.

6.6.3 Similarity of vascular responses to H₂S and hypoxia

The responses of New Zealand hagfish vessels to H₂S are in many respects similar to those produced by hypoxia. H₂S and hypoxia (Olson *et al.* 2001), appear to be exclusively vasoconstrictory in hagfish dorsal aortas and efferent branchial arteries because they consistently contracted both un-stimulated and pre-contracted vessels. Conversely, neither H₂S nor hypoxia produced a sustained response in ventral aortas or afferent branchial arteries. H₂S and hypoxic (Olson *et al.* 2001) contractions of aortas and efferent branchial arteries were also unaffected by pre-contraction with KCl. Furthermore, because KCl pre-contraction presumably depolarises smooth muscle cells it is likely that the mechanism of H₂S excitation is independent of cell depolarisation; evidence for depolarisation independent HVC in these vessels has also been presented previously (Olson *et al.* 2001). This is in contrast to the H₂S-mediated relaxation of rat aorta (Zhao *et al.* 2001; Zhao and Wang 2002) and trout efferent branchial arteries (Dombkowski *et al.* 2004) where elevated KCl partially inhibits the response. Collectively, these findings suggest that H₂S contraction and HVC have a common, or at least similar, excitation pathway in hagfish vessels.

This is consistent with other studies (Olson *et al.* 2001; Dombkowski *et al.* 2004; Dombkowski *et al.* 2005; Olson *et al.* 2006; Russell *et al.* 2007) that have shown that the vascular response to hypoxia is identical to that of H₂S irrespective of whether this response is contraction, relaxation, multi-phasic, or, as in the case of hagfish ventral aorta and afferent branchial arteries, no response at all. We have also observed identical hypoxic and H₂S responses in trout urinary bladder (Dombkowski *et al.* 2006) and thus hypoxia and H₂S appear to have a common, or at least similar excitation pathway in vertebrate smooth muscle in general.

6.6.4 Metabolic coupling of HVC to H₂S production

Cysteine, which is presumed to be the precursor of H₂S production in animals (Julian *et al.* 2002) increases the magnitude of HVC at lower concentrations (figure 6.4) suggesting that it increases tissue production of H₂S. This is consistent with a cysteine-enhanced HVC in lamprey dorsal aortas and bovine pulmonary arteries and enhanced HVD observed in rat thoracic aortas (Olson *et al.* 2006). Further elevation of the cysteine concentration (10 mmol.l⁻¹) inexplicably reduced the HVC in hagfish dorsal aorta. This may be due to a feedback-type inhibitory effect of cysteine on H₂S production, as we (R.D., S. Head, N. Whitfield and K.O., unpublished observation) have also observed elevated cysteine (10 mmol.l⁻¹ or 100 mmol.l⁻¹) inhibition of H₂S production in homogenised bovine heart or trout vessels, respectively, which is consistent with feedback inhibition. Alternatively, cysteine at a concentration of 10 mmol.l⁻¹ may be toxic to smooth muscle cells. However, the fact that carbachol contractions on top of 10 mmol.l⁻¹ cysteine were not significantly different from the reference contractions, suggests that cytotoxicity of cysteine at 10 mmol.l⁻¹ is unlikely, and the reason for this inhibition remains to be identified.

The effects of inhibitors of H₂S production provide additional evidence for H₂S signaling in hypoxic responses. As shown in figure 6.4, AOA, an inhibitor of CBS completely inhibited HVC in hagfish aortas, whereas the CSE inhibitor, PPG, was ineffective (figure. 6.4).

This suggests that HVC in the hagfish dorsal aorta is dependent upon H₂S synthesis via CBS. This is in contrast to mammalian systemic vessels where CSE, but not CBS, catalyses H₂S production (Hosoki *et al.* 1997; Zhao *et al.* 2003). We (Olson *et al.* 2006) have also shown that inhibition of CSE, but not CBS, blocked HVD in rat aortas, whereas inhibition of CBS, but not CSE, blocked HVC in bovine pulmonary arteries. Interestingly, in trout, H₂S produces a tri-phasic relaxation-contraction-relaxation (Dombkowski *et al.* 2004) and these vessels appear to possess both CBS and CSE (G. Yang, R. Wang and K.O., unpublished observation). These studies not only support the hypothesis of H₂S as a vascular O₂ sensor but they also provide additional evidence that different enzymes for H₂S production, CBS and CSE, may mediate HVC and HVD, respectively in different vessels.

Contractions produced by carbachol while hagfish dorsal aortas were exposed to AOA or PPG were not significantly different from the reference contraction produced by carbachol in the absence of inhibitors. Thus the inhibitory effect of AOA on HVC could not be due to general inhibition of the contractile apparatus. Separate H₂S and ligand mediated responses have also been observed in other vessels (Dombkowski *et al.* 2004; Olson *et al.* 2006), indicating that the pathway for H₂S activation is not shared with some of the more common ligand-mediated mechanisms.

It is not clear why hydroxylamine potentiated HVC in hagfish aortas, although a non-specific effect seems likely. Hydroxylamine inhibits at least 100 enzymes that use pyridoxyl 5'-phosphate as a co-enzyme (Kery *et al.* 1999; Tang *et al.* 2005) including CBS and CSE. Although we expected it to act in a manner similar to AOA and inhibit vasoconstriction, it was the most potent constrictor tested, on a molar basis. Interestingly, despite turning the vasa vasorum brown, probably as a result of an action on haem groups (Canty and Driedzic 1987; Nichols and Weber 1989), and contracting the vessels, the vessels remained viable and the response to the final carbachol exposure was not diminished.

6.6.5 Effect of PO₂ on MO₂

As shown in figure 6.5, hagfish aortas display a remarkable ability to maintain O₂ consumption (MO₂) over a wide range of ambient PO₂ (~15–115 mmHg). It is not clear why the vessels lose their regulatory ability when PO₂ exceeds ~115 mmHg, but this may be near the maximum PO₂ these vessels encounter in the wild, i.e. in air-saturated seawater (inspired PO₂ of 156 mmHg), arterial PO₂ was 109 mmHg (Forster *et al.* 1992). When PO₂ falls below ~15 mmHg, MO₂ also falls.

The PO₂ over which MO₂ decreases is quite similar to the PO₂ at which HVC increases (dashed line in figure 6.5). The PO₂ at which MO₂ begins to decrease in hagfish dorsal aortas (15 mmHg) is somewhat less than the 20 mmHg critical PO₂ (PO₂ at which MO₂ was reduced by 5%) in isolated rat aortas (Koenitzer *et al.* 2007). However, the MO₂ for rat aortas (78 pmol.mg⁻¹.min⁻¹ (Koenitzer *et al.* 2007)) is 32.5 times greater than the MO₂ for hagfish aortas (2.4 pmol.mg⁻¹.min⁻¹). Even assuming a Q₁₀ of 2.4, the 25°C temperature difference between our study and that of Koenitzer *et al.* (2007) would only account for a six-fold difference in MO₂. In fact, these differences would probably be even greater if the O₂ solubility coefficients were accounted for; mammalian (human) plasma at 37°C is 1.26 µmol.l⁻¹.mmHg⁻¹ and seawater (with the same osmolarity of hagfish plasma) at 12°C is 1.72 µmol.l⁻¹.mmHg⁻¹ (Boutilier *et al.* 1984).

Koenitzer *et al.* (2007) also showed that MO₂ more than doubled when rat aortas were contracted with phenylephrine. We did not find any difference in MO₂ between uncontracted and contracted hagfish aortas, perhaps because MO₂ was so low to begin with, or more likely because once hagfish aortas are contracted they are able to maintain tension with little additional energy expenditure. The latter point may be related to the hypoxia tolerance of hagfish vessels where hypoxic contractions can be sustained for 8 hours of continuous gassing with 100% N₂ (Olson *et al.* 2001).

Many non-mammalian vertebrates, especially the more “primitive” ones are considerably more hypoxia tolerant than mammals because of their ability to downregulate cellular metabolism and balance ATP demand with ATP supply (Boutilier 2001a). Hypoxia tolerance varies across hagfish species and interestingly, *E. cirrhatus* does not voluntarily tolerate an ambient PO₂ of less than 45 mmHg (82 µmol.l⁻¹) at 11 °C (Forster 1992). Clearly, the lack of an increase in MO₂ was not due to the technique used as carbachol nearly doubled MO₂ in salmon.

Despite the elevated metabolic rate of rat aortas, the tension (in mg tension.mg⁻¹ wet mass) produced by KCl contraction of rat aortas, which varies from 240 (Olson *et al.* 2001) to 720 (Resende *et al.* 2004) is only 2.5–7.5 times greater than a KCl contraction of hagfish dorsal aorta (94 ± 12, n=4; data from this study). Thus it appears in rat vessels that either more oxygen is consumed for noncontractile-related activities, or that force development is energetically less efficient.

6.6.6 Relationship between MO₂ and H₂S production

In many organisms, MO₂ is affected by H₂S. At low [H₂S], O₂ often increases because of the use of H₂S in mitochondrial ATP synthesis or for H₂S detoxification; at elevated [H₂S], O₂ consumption often decreases because of H₂S inhibition of mitochondrial cytochrome c oxidase (Grieshaber and Völkel 1998), or perhaps even a general metabolic depression (Blackstone *et al.* 2005). H₂S also affects MO₂ in un-contracted hagfish aortas (figure 6.6) in a manner consistent with that described by Grieshaber and Völkel (1998). An increase in MO₂ is also predicted by our (Olson *et al.* 2006) model of H₂S oxidation by blood vessels as a mechanism to inactivate H₂S during normoxia. Higher (100 µmol.l⁻¹ and 1 mmol.l⁻¹) [H₂S] inhibits MO₂ (figure 6.3) but not tension development (figures 6.2 and 6.3).

This likely reflects the inherently low energy cost of force development, consistent with our observation that MO₂ does not change even during maximal carbachol contraction and it also provides a mechanism for sustaining HVC even when mitochondrial energy production is compromised.

The increase in MO₂ produced by cysteine and the decrease in MO₂ produced by AOA (figure 6A) are also consistent with a positive and negative effect on H₂S production by hagfish dorsal aortas. It is not clear why 10 mmol.l⁻¹ cysteine appeared to decrease tension, yet increase MO₂. This suggests that H₂S oxidation continues, although the mechanism that causes contraction is subject to feedback inhibition. However, other explanations are also plausible, i.e. the experimental conditions were different (anoxia in myograph studies, PO₂ ~40-50 mmHg in H₂S studies), this cysteine concentration is near the threshold for both processes, or there are temporal differences in responses. The effects of hydroxylamine on MO₂ do not correlate with its effects on tension and may also be nonspecific as it inhibits many other enzymes (Zollner 1989).

Chapter 7

Final discussion

7.1 Important findings and implications of this thesis

7.1.1 Summary of thesis

The five discreet but related studies presented in this thesis have investigated several aspects of the physiology and biochemistry of whole animals, perfused and isolated tissues from fishes and other relevant vertebrates. Important fundamental questions about tissue metabolism and energy supply and utilisation in relation to O₂ supply and applied questions relating to commercial harvesting and post-mortem muscle physiology were addressed. Metabolism in various tissues exposed to anoxia, hypoxia, normoxia and hyperoxia under a range of conditions was shown to be O₂ supply dependent in intact (chapter 2) and isolated (chapter 3) preparations. Changes in respiratory parameters of animals exposed to isoeugenol and H₂S were marked and superficially similar (chapter 4). Harvest protocol had pronounced effects on white muscle anaerobic metabolic rate and energetics post-mortem (chapter 5). Finally, we showed that H₂S is directly involved in vascular O₂ sensing in two phylogenetically ancient chordates (chapter 6).

7.1.2 Metabolic rates in perfused and isolated tissues

I developed a viable isolated muscle perfusion preparation for the study of metabolic processes. I matched O₂ delivery with utilisation, by manipulating perfusate O₂ capacitance and flow, and in so doing ensured our preparation was not hypoxic. O₂ capacitance was manipulated with great effect by the addition of red blood cells (RBCs) to our freshwater teleost Ringer. Similar delivery gains were not achievable simply by increased flow as vascular pressure rose beyond physiological values, resulting in oedema. Varying O₂ delivery revealed two distinct phases to utilisation by the preparation; O₂-dependent and -independent phases.

The independence of VO_2 above certain delivery rates suggests that the upper limit to VO_2 with increased O_2 delivery relates to a minimum oxidative ATP demand to maintain homeostasis. This may also be interpreted as a direct supply-utilisation relationship that was saturated above a critical rate of O_2 delivery. In unstimulated muscle supplied with Ringer containing RBCs, there was a very small change in cut surface muscle pH (0.05 pH units) over the 2 hour period of perfusion, which suggests that there was only a small contribution to energy supply by anaerobic glycolysis (Robb 2008). This implies that the preparation received adequate O_2 to satisfy basal energy requirements. These data correlate well with O_2 delivery independence of VO_2 in these preparations. It was only for intense muscle work that anaerobic glycolysis, indicated by a drop in cut surface tissue pH of 0.53 pH units (an almost doubling of the hydrogen ion concentration), contributed substantially to ATP supply. Thus it seems that a minimum oxidative energy requirement to maintain basal rates was necessary, and that the relationship was supply dependent until that contribution was attained. However, when muscle ATP demand was exceeded during simulated exercise, substrate level phosphorylation was essential to maintaining ATP supply.

It is possible that the dependency seen below the critical O_2 delivery in the perfused salmon tail was due to a decline in the PO_2 rather than O_2 delivery, since the O_2 tension prevailing in the venous outflow was greater and the preparation was never delivery dependent with RBCs present. Tissues that were perfused with RBC-free Ringer rapidly reduced the PO_2 of the solution, in some cases from 90 to <5% O_2 saturation (data not shown), and were often below the critical O_2 delivery at physiological flow and pressure. In contrast, venous outflow PO_2 was only reduced to around 60% saturation in RBC-enriched Ringer (data not shown) due to the increase in capacitance. Thus, it is likely that some peripheral tissues would have been exposed to very low PO_2 s when perfused with RBC-free Ringer. Thus the presence of in RBCs in the Ringer both maintained the PO_2 and increased the rate of O_2 delivery to tissues.

It is possible that there is a different relationship between PO_2 and the delivery of O_2 with respect to sensing, although I were unable to resolve this based on these data alone.

Our data from the perfusion work raised the question: what effect does PO_2 have on metabolic rate? Resting tissue PO_2 s have been shown to be low (15-60 mmHg, Marcinek *et al.* 2003; McKenzie *et al.* 2004). Thus, the PO_2 in tissues subjected to hypoperfusion during exercise or environmental and/or metabolic hypoxia must be even lower. In these situations, does ATP demand decrease to match the decrease in supply or does anaerobic glycolysis bolster ATP supply? To answer this question, I investigated the effect of PO_2 on the metabolic rate in isolated cardiovascular tissues and skeletal muscles below, within and above the physiological PO_2 range. What I found was unexpected: in striated muscles and liver tissue preparations from a number of vertebrates, VO_2 was directly proportional to PO_2 , well above measured tissue PO_2 s. The PO_2 -dependence of VO_2 and estimated ATP-turnover and the lack of supplementation of ATP supply by anaerobic glycolysis at low or high PO_2 (30 or 100 mmHg) in skeletal muscle suggested that ATP demand decreases with ATP-supply. Thus I can infer that the O_2 supply-utilisation relationship observed in the striated muscles and liver accompany a suppressed ATP demand. However, it is possible that the opposite is the case; high PO_2 increased ATP turnover, regardless of demand. Either way, O_2 availability was crucial for ATP turnover over a wide PO_2 range.

The obvious potential for tissue degradation in our experimental model was initially of concern. Therefore, I investigated whether mitochondrial activity was affected by exposure time. This revealed viable, and unchanged, mitochondrial function over the two hour period of incubation. To test whether tissue degradation was occurring, tissues exposed to a PO_2 depletion treatment were reoxygenated and subjected to a second depletion treatment. This revealed that the PO_2 -dependent rates were unchanged. When metabolite pools were determined in our model tissue, I showed constant or increased concentrations of ATP and other volatile metabolites.

Furthermore, metabolites produced through the degradation of tissue adenylate pools (IMP, inosine, hypoxanthine and uric acid), did not accumulate but actually decreased in concentration. Diffusion-limitation to VO_2 was also deemed unlikely as an explanation for the observed phenomenon in the striated muscles. The most compelling evidence for this argument is the lack of activation of anaerobic glycolysis and the uncoupling of muscle mitochondria which resulted in a VO_2 increase at any given PO_2 above about 15 mmHg in all the representative tissues. Increased VO_2 could not occur under these circumstances if it was limited by a maximum rate of diffusion into the tissue. These findings are not suggestive of either tissue degradation or an anoxic core region (i.e. diffusion limitation) in the tissue at the PO_2 s investigated. Thus, our data suggest that in the quiescent striated muscle of several vertebrate taxa, it is the PO_2 that determines that rate at which O_2 is used and that the mechanism is highly conserved between taxa. Is this a mechanism for dealing with tissue hypoxia in non-vital tissues in vertebrates? Are only certain tissues, such as striated muscle, able to change their energy requirements in this way?

The relative O_2 -independence in the metabolic rate of the vasculature (smooth muscle, connective tissue and endothelium) contrasted with the striated muscles. The metabolically active vascular tissue performs many vital roles in the body. It mediates the transport of O_2 and metabolites around the body by manipulating blood flow (Opie 1998). Furthermore, it is responsible for the synthesis of numerous humoral factors (Friesenecker 2007) which no doubt explains the exceptional ability to increase VO_2 when uncoupled. Thus I can deduce from our data that this tissue has a basal requirement that must be maintained at all times and is defended well down to low PO_2 . This kind of metabolic regulation is known in other tissues critical for survival, such as brain tissue, even during anoxia (Johansson *et al.* 1995).

It could be that the difference between oxyregulation in the vasculature and oxyconformance in striated muscle was the result of diffusion-limitation, since the vascular tissue preparation had a shorter O_2 diffusion path. Based on our results, this is unlikely.

Nevertheless, evidence of oxyregulation in isolated cells (e.g. Wilson *et al.* 1979; Rumsey *et al.* 1990) supports the hypothesis that diffusion is limiting to VO_2 in intact tissues, since isolated cells have a short diffusion path for O_2 compared to the situation in intact tissue. However, conflicting reports are found in the literature. For example, VO_2 and other indicators of cellular energetics were shown to be PO_2 -dependent in cultured rat hepatocytes in suspension over a wide PO_2 range (i.e. up to air saturation) over a longer time course than typically reported for such studies (2 hours vs <40 minutes) (Schumacker *et al.* 1993). This observation may well be the result of some kind of sensing mechanism, as these cells in suspension were certainly not diffusion-limited in the upper PO_2 range. Thus the time course of our depletion experiments (1-2 hours) may have played a key factor in the activation and transduction of any signalling mechanisms that may have been effected. Of significant importance is that hagfish, fish and rats do not enter hypometabolic states, yet their tissues (liver and striated muscle) respond to O_2 availability (Schumacker *et al.* 1993; current study), suggesting the response may be a highly conserved mechanism to deal with localised tissue hypoxia. However, just how these observations relate to tissues *in vivo* is unclear, since the PO_2 s at which these changes begin to occur are in some cases well above measured tissue values.

Is it possible that tissue PO_2 is maintained at low concentrations by the vasculature to restrict tissue metabolism? In the current study the vasculature of all species had a relatively low O_2 demand, relative to the other tissues. This conflicts with some recent, but questionable evidence from mammals that suggested that vessels may partition O_2 away from the tissues. The extremely high VO_2 values in vessels reported using phosphorescence quenching microscopy, for example Shibata *et al.* (2005) who reported values of between $28.8\text{--}64.8 \text{ L O}_2\cdot\text{kg}^{-1}\cdot\text{h}^{-1}$ in the quiescent first order arterioles in rat cremaster muscle, have now been largely discredited due to the discovery of methodological errors that overestimated the PO_2 gradient between vessels and tissues (Golub *et al.* 2008). Our study is a further demonstration that vessels do not partition O_2 away from tissues by their own high rates of consumption.

Nevertheless it is possible that tissue PO_2 s are maintained low by changes in smooth muscle tone that restrict blood flow.

The idea that skeletal muscle and liver can downregulate ATP requirement is highly plausible. However, how does the heart manage this phenomenon when it must constantly work? Given its constant energy needs, one might assume that there would be a basal level of energy supply that must be maintained at all costs. This continual requirement for energy may be satisfied by uninterrupted blood flow since by necessity the heart receives a constant supply of O_2 from the blood via the internal route and in some hearts via the coronary circulation. Since many fish species lack a coronary blood supply, the importance of maintaining O_2 supply to the myocardium via the internal route may be even more critical. Given that blood flow through the heart is continual, it is likely that it is never completely deprived of O_2 as other tissues almost certainly are under certain conditions. Nevertheless, during times of extreme hypoxia, the supplementation of ATP supply by anaerobic glycolysis may be extremely important in the fish heart (Farrell 2007). Certainly, the protective effect of catecholamines on myocardial function during hypoxia (Gamperl *et al.* 1998), implies a response to dysfunction, and may suggest ATP supply is compromised with decreased O_2 availability i.e. a direct relationship between the supply of O_2 and ATP production. Theoretically, a supply-utilisation relationship in the heart could actually be of benefit during exercise since increased blood flow, and consequently O_2 delivery, to the cardiac muscle would occur during elevated heart rate, although this is likely to be negated by working tissues extracting more O_2 from the blood. Nonetheless, this could be of great significance in hearts which lack a coronary circulation, since increased blood flow through the heart is the only means to increase O_2 delivery.

Our *in vitro* studies in chapters 2 and 3 raise many important questions, the most pertinent: does the control of metabolic rate reside at the cellular level in the vasculature, but depend on blood supply in skeletal muscle and organs? Answering this question is of fundamental importance in future studies (discussed below).

7.1.3 The effects of anaesthesia, narcosis and harvest technique on animals and tissues

Metabolic responses to anaesthesia with isoeugenol and exposure to H₂S on VO₂, Vf and activity were investigated in a teleost (blue cod). This gave us important information on the metabolic cost of both anaesthesia, a common practice in the aquaculture industry, and H₂S exposure, which is reported to induce hypometabolism in mammals (Blackstone *et al.* 2005; Blackstone and Roth 2007; Volpato *et al.* 2008). With respect to the latter, I shed light on important questions relating to previously reported H₂S induced metabolic changes. Our experiment showed that the decrease in VO₂ associated with H₂S exposure was not a true hypometabolism and that a reduction in VO₂ was not dependent on a reduction in core body temperature. This study also revealed several other interesting findings, which are discussed below.

Based on available evidence I can deduce that animals exposed to H₂S were likely hypoxic. It has been shown that H₂S interferes with cytochrome c oxidase causing metabolic hypoxia, depresses Vf and triggers a bradycardia in fish (Torrans and Clemens 1982; current study). During hypoxia in fish, a reflex bradycardia, mediated by parasympathetic acetylcholine release, is usually triggered, which is generally compensated for by an increase in stroke volume; thus cardiac output is maintained (Reid and Perry 2003; Sandblom and Axelsson 2005; Sandblom and Axelsson 2006; Farrell 2007). It has been previously assumed that bradycardia and hypertension may enhance gas transfer at the gill, though this has recently been disproved in rainbow trout; instead hyperventilation appears to be the primary mechanism for enhancing gas transfer (Perry and Desforges 2006). However, bradycardia may improve myocardial O₂ uptake, due to a prolonged residence time in the heart, improve contractility and reduce cardiac O₂ demand (Farrell 2007). However, with the reduced Vf that followed H₂S exposure in our fish, it is likely that the unaltered flow (if there was stroke volume compensation) was delivering blood with a decreased O₂ saturation.

Furthermore, during hypoxia vascular smooth muscle contraction, mediated by α -adrenergic receptor stimulation by sympathetic nerves and/or catecholamines, results in a rise in systemic vascular resistance which leads to reduced blood flow to peripheral tissues (Perry and Desforges 2006). In chapter 4 I present evidence that catecholamines were likely present in the blood of H₂S exposed animals.

Furthermore, I argue that direct vascular effects should not be disregarded in the interpretation of studies applying H₂S to animals (Torrans and Clemens 1982; Blackstone *et al.* 2005; Blackstone and Roth 2007; Haouzi *et al.* 2008; Li *et al.* 2008; Simon *et al.* 2008; Volpato *et al.* 2008; current study). H₂S has been shown to act in a concentration-dependent triphasic manner (relaxation-contraction-relaxation) in rainbow trout efferent branchial arteries *in vitro*, with the predominant response being contraction (Dombkowski *et al.* 2004). Similarly, the hagfish (Olson *et al.* 2008a) and lamprey (Dombkowski *et al.* 2005) dorsal aortas show a dose-dependent constriction in response to H₂S. Should H₂S exposure have resulted in increased vasoconstriction in the blue cod, this may have resulted in decreased blood flow to peripheral tissues and consequently compounded tissue hypoxia. In addition to the impaired ventilatory response and the likely hypoxia-induced increase in systemic vascular resistance, a direct H₂S induced vasoconstriction would have greatly affected tissue O₂ delivery. Metabolic hypoxia associated with inhibited cytochrome c oxidase activity likely further compromised ATP supply. Thus I can deduce that it is highly likely that the reduced VO₂ in H₂S exposed animals was attributable to reduced O₂ delivery to tissues - the result of decreased blood O₂ content and increased peripheral vascular resistance induced by hypoxia - and the ability of mitochondria to utilise O₂. Therefore the possibility that H₂S exposure results in systemic hypoxia should be the focus of future work.

When blue cod were exposed to H_2S , VO_2 was decreased and animals entered a state of narcosis which is suggestive of hypometabolism. However, the large detoxification cost or O_2 debt associated with H_2S exposure appears to have overridden any hypometabolic response that may have been triggered by H_2S , since the recovery VO_2 by far exceeded the depression in VO_2 compared with the resting rate. Inhibiting cytochrome c oxidase activity and V_f may simply decrease ATP supply but not demand. Thus information on ATP turnover would be useful in interpreting future studies. Lactate accumulation in the blood of channel catfish (Torrans and Clemens 1982) exposed to H_2S suggests that aerobic ATP supply was inadequate to satisfy ATP demand. Nonetheless, some component of the reduced VO_2 in the current study may have been associated with a reduced ATP demand, possibly mediated through decreased O_2 supply, inhibited oxidative phosphorylation or via O_2 sensing. However, H_2S as applied in the current study, does not appear to be capable of inducing any useful metabolic depression in blue cod. On the other hand, the narcosis identified could potentially prove useful.

During isoeugenol anaesthesia, fish show a CNS mediated reduction in V_f , which reduces gas transfer across the gills that results in hypoxaemia, and show a transient depression in cardiovascular parameters (heart rate, cardiac output, stroke volume and dorsal aortic pressure) (Hill and Forster 2004a). Given that hyperventilation is the primary way of improving blood O_2 saturation during hypoxia in fish (Perry and Desforges 2006), the impaired V_f response coupled with reduced blood flow during isoeugenol anaesthesia may have rendered the animals' tissues hypoxic in a similar way as H_2S exposed animals. However, this may have been in part mitigated by the direct vasorelaxant effect of isoeugenol (Rothwell and Forster 2005). Nonetheless, reduced O_2 delivery was again implicated in a reduced VO_2 .

Interestingly while both groups of animals showed a reduced VO_2 , the isoeugenol anaesthetised animals showed a net reduction in VO_2 relative to the resting rate, when the depression in VO_2 on anaesthesia and rise during recovery were accounted for. When accounting for O_2 debt repayment in coho and sockeye salmon exercised at critical swimming speed, excess post-exercise oxygen consumption (EPOC) attributable to anaerobically-fuelled swimming was almost stoichiometric with the increase in O_2 utilisation above the routine resting rate on recovery (Lee *et al.* 2003b). Based on this finding, and if an unchanged resting ATP demand in our study is assumed, the O_2 used on recovery from hypoxia (if solely attributable to recovery from anaerobic metabolism) would be expected to approximately equal the amount that it is depressed relative to the resting rate. Thus, I have shown a depression in metabolic rate from resting conditions. In the discussion in chapter 4 it is suggested that this may be associated with hypoxia rather than a direct action of isoeugenol, although clearly both possibilities deserve consideration. Two lines of evidence suggest that a direct action of isoeugenol on muscle VO_2 is unlikely. First, cytochrome c oxidase activity was unchanged by exposure to isoeugenol. Secondly, white muscle slice VO_2 was unaffected by isoeugenol between concentrations of $0.0054\text{--}0.54\text{ g.L}^{-1}$ ($n=2$; data not shown). This contrasts with H_2S exposed muscle slices that showed an inhibition of VO_2 over a wide range of concentrations ($n=2$; data not shown).

Further to the studies on the metabolic responses of intact animals to isoeugenol anaesthesia and H_2S exposure, the effects of harvest protocol (i.e. anaesthetised and rested and exhausted harvesting) on post-mortem metabolism and tissue degradation were investigated. The results revealed a far greater metabolic rate (power output) and elevated metabolite concentrations in anoxic fish white muscle post-mortem in rested harvested animals versus those slaughtered in a simulated commercial harvest.

Our study contributes important information on metabolic rate, key metabolites and energetics post-mortem and furthers earlier findings (Jerrett *et al.* 1996; Sigholt *et al.* 1997; Jerrett and Holland 1998; Stehly and Gingerich 1999; Fletcher *et al.* 2003; Iversen *et al.* 2003; Black *et al.* 2004; Kiessling *et al.* 2004; Small 2004; Roth *et al.* 2006; Bagni *et al.* 2007; Bosworth *et al.* 2007; Ribas *et al.* 2007; Wilkinson *et al.* 2008; Tuckey *et al.* 2009a) that show rested harvesting is associated with an increased pre-rigor period, greater energy stores and improvements in tissue quality indicators. The improvements in tissue energy stores associated with rested harvesting were pronounced, but I showed that inevitably energy supply decreased consistently once O₂ supply from the bloodstream was removed. Creatine phosphate and anaerobic glycolysis only had a limited ability to support ATP supply under these conditions. The activation of anaerobic glycolysis in a failed bid to maintain tissue ATP supply in anoxic tissue, contrasts with the perfused salmon tail which showed virtually no anaerobic glycolysis (a drop of 0.05 pH units, versus a drop of 1 pH unit by 2 hours in the biopsies post-mortem). Thus, effecting prolonged metabolic viability in unperfused tissues, following typical and rested harvesting still remains a challenge.

It is possible that the rapid rundown in metabolic rate and energetic state observed in both groups relates to the size of the biopsies used and/or ambient O₂ availability, since Tuckey *et al.* (2009a), who stored whole fillets at a higher temperature than I used, but in air, showed a tissue pH drop of only 0.4 pH units after 2 hours. Furthermore, slower pH changes corresponded with a less rapid decline in the concentrations of creatine phosphate and ATP than I report. With respect to biopsy size, our study has identified a potentially important finding which suggests that processing of muscle tissue should be delayed until immediately before sale, with regard to fresh products to ensure the retention of high-energy metabolites.

With respect to the possibility of ambient O₂ contributing to energy supply, it is clear from other work that increased ambient O₂ can enhance the ATP concentration in stored post-mortem fillets (Black *et al.* 2004), although the effects of supraphysiological O₂ tension may be damaging (e.g. free radical damage).

7.1.4 H₂S: an emerging O₂ sensor

Investigation of the response of the vasculature to hypoxia and H₂S in the ancestral chordates, the hagfish and lamprey, strengthened the case for the involvement of H₂S in the O₂-sensing/signal transduction cascade involved in HVC and HVD in smooth muscle and that this mechanism evolved very early in the chordate lineage (Dombkowski *et al.* 2004; Dombkowski *et al.* 2005; Dombkowski *et al.* 2006; Olson *et al.* 2006; Russell *et al.* 2007; Olson *et al.* 2008a; Olson 2008). Critically, the study demonstrated the O₂-dependence of the mechanism, and thus O₂-sensing in this way in vascular tissue seems highly plausible. Of great interest is that the VO₂ in hagfish vessels was O₂-independent over a wide range in PO₂, which disappeared with low PO₂ conditions. This coincides with increased HVC below the critical PO₂ in these vessels and increased H₂S-induced constriction which suggest that endogenously produced H₂S was likely contributing to vasoconstriction. That VO₂ decreased in response to a specific inhibitor for the H₂S producing enzyme, cystathionine β-synthase, and increased on exposure to the H₂S precursor, cysteine, further supports the involvement of H₂S in the O₂-sensing/signal transduction cascade in the smooth muscle of vertebrates. The results were in accordance with the findings of Koenitzer *et al.* (2007) in rats, which showed a similar vasorelaxation and vasoconstriction to both hypoxia and H₂S exposure, except I applied a different interpretation to the results; that H₂S itself and not an H₂S-NO interaction or an oxidation product of H₂S induces HVC and HVD.

7.2 Future work

7.2.1 O₂-sensing and diffusion limitation

Hypoxia, be it environmental or metabolic is a potential threat to most animals (Olson 2008). A lot of research has focussed on how hypoxia affects metabolic processes and how this signal is sensed and transduced in cells. Early models proposed for O₂ sensing, involving a sensor with fixed properties that feeds information back to a central controller also with fixed properties, have proven to be too simplistic (Cherniack 2003). Instead it has been recognised that sensors and control systems are plastic, changing with maturation and with altered internal and environmental conditions (Cherniack 2003). It is possible that multiple sensors may operate in tissues with different thresholds, sensitivities and dynamics with different and in some cases overlapping targets (Cherniack 2003). Certainly different O₂-sensing mechanisms in a variety of tissues have been proposed, although many of the models proposed for O₂-sensing and signal transduction cascades are unresolved and there is very little consensus between research groups (Aaronson *et al.* 2006; Olson 2008). The multiplicity of proposed O₂-sensing mechanisms suggests that they may have evolved several times and now constitute multiple systems for dealing with hypoxia or that many of these mechanisms may be either modulators of or even peripheral to one fundamental process (Olson 2008). In chapter 6 we report further evidence to suggest that H₂S is universally involved in O₂-sensing in smooth muscle. Could H₂S be associated with O₂ sensing/signal transduction in other tissues and could this signal effect a reduction in VO₂?

Interestingly in addition to a role in mediating hypoxic vasoactivity, H₂S is involved in O₂ sensing in neuroepithelial (Olson *et al.* 2008b) and chromaffin cells (Perry *et al.* 2009).

In addition, it has been demonstrated that H₂S is involved in O₂ sensing in the rainbow trout heart and mediates the ischaemic-preconditioning response (Whitfield *et al.* 2008) typically associated with the priming of respiratory and metabolic responses in animals and reduced infarction size and oxidative stress in cardiac and skeletal muscle (Miquel *et al.* 1992; Pang *et al.* 1995; Routley *et al.* 2002; Nelson *et al.* 2005). Furthermore, the enzymes responsible for H₂S synthesis are reported from multiple tissues in mammals and fish (Szabó 2007; Perry *et al.* 2009). Recently, mRNA expression of the enzymes responsible for H₂S synthesis, cystathionine β -synthase and cystathionine γ -lyase, in the liver, spleen, brain, anterior and posterior kidney, anterior and posterior cardinal vein and white muscle were reported in rainbow trout (Perry *et al.* 1999). Thus, the presence of H₂S production in white muscle suggests that it is theoretically possible that H₂S could be involved in O₂ sensing/signal transduction in this tissue, although many other biological roles of H₂S are known (Dombkowski *et al.* 2005; Szabó 2007). The Olson *et al.* (2006) model predicts that with falling PO₂, H₂S concentration increases. Thus in tissues expressing H₂S-producing enzymes, H₂S concentration could increase during hypoxia. An H₂S-induced decline in VO₂ could be effected by interrupting oxidative phosphorylation by interference with cytochrome c oxidase or via the downregulation of ATP demand pathways or both.

A PO₂ dependent decline in VO₂ and ATP turnover is typical of animals during hypometabolic states (Hochachka and Guppy 1987; Boutilier and St Pierre 2002) in peripheral tissues such as skeletal muscle and liver, possibly the result of O₂ sensing mechanisms (Boutilier *et al.* 1997; West and Boutilier 1998; Hochachka and McClelland 1997; Boutilier 2001a; Boutilier 2001b). However, O₂ dependence and O₂ sensing phenomena in species that are not subject to periods of hypometabolism are relatively unexplored. I have demonstrated in a number of these species that VO₂ and energetic state is PO₂-dependent in several tissues that must undergo large-scale changes in O₂ flux and that the relationship is not limited by diffusion.

However, I did not show any evidence of mechanisms that may trigger such an effect, which would compliment the current study well. In future work, the presence of O₂ sensing mechanisms in peripheral tissues such as skeletal muscle could be investigated with special reference to the role of H₂S.

In the current study (Olson *et al.* 2008a) and others (Dombkowski *et al.* 2004; Dombkowski *et al.* 2005; Dombkowski *et al.* 2006; Olson *et al.* 2006; Russell *et al.* 2007; Olson 2008), H₂S has been implicated in both HVD and HCV in the vertebrate smooth muscle. Expression and translation of H₂S-producing enzymes in the vascular tissue of the hagfish, lamprey and other vertebrates would strengthen these data and build on information from mammals (Hosoki *et al.* 1997; Szabó 2007) and fish (Perry *et al.* 2009) and should form the basis of future work. Another major focus of subsequent studies should be the identification of the pathway/s associated with alterations in the mechanical activity of smooth muscle which are effected by H₂S and hypoxia. This would involve the systematic testing of proposed and novel hypoxia-mediated signal transduction pathways in conjunction with the H₂S mediated O₂ sensing model (Olson *et al.* 2006). The creation of a gene-knockout model seems like an appealing way to test some these unknowns, but the physiological changes associated with this may be complex and may not reveal underlying mechanisms. Instead, it would possibly be more appropriate to look at changes in gene expression in animals with functional H₂S machinery intact. Incorporation of one or more of the other sensing mechanisms identified into the H₂S model (Olson *et al.* 2006) could potentially link key changes in cells during hypoxia and could resolve some of the controversies surrounding existing models.

Recent work (Whitfield *et al.* 2008) suggests that that H₂S is an autocrine or paracrine vascular signal and that it is unlikely that H₂S operates as a humoral factor in the blood. However, unknowns as to whether H₂S is carrier bound or locally activated remain (Olson 2008). Thus, future work should try and address the possibility that haemoglobin is in some way involved in the transport of H₂S around the body.

Certainly, there is an interaction between haemoglobin and H₂S (Beauchamp *et al.* 1984; Szabó 2007), although whether this mechanism is involved in the transport of H₂S to distant tissues remains unknown. The possibility that a blood-borne factor carries H₂S could be tested using an isolated perfusion preparation, either diluting the blood or removing it completely and investigating the effects of H₂S application and hypoxia on tissue H₂S delivery. Furthermore, the effect of H₂S on peripheral resistance could be tested in this way or using microperfusion techniques.

The revised methods reported for *in vivo* phosphorescence quenching microscopy by Golub *et al.* (2008), offer exciting possibilities for non-invasive *in situ* measurements of VO₂ and intravascular, interstitial and intracellular PO₂s in a variety of tissues. Another promising technology for the measurement of *in vivo* tissue and vascular PO₂ and VO₂ are the fibre-optic probes of various kinds (employing a range of spectro- and fluoroscopic methods) which can be used to measure tissue myoglobin and blood haemoglobin saturation as well as to directly measure tissue and vascular PO₂ (e.g. Marcinek *et al.* 2003; McKenzie *et al.* 2004). Furthermore, these techniques can be combined with isotopes and magnetic resonance spectroscopy (MRS) of tissues to determine metabolite concentrations (e.g. creatine phosphate, ATP, ADP) (Marcinek *et al.* 2003) to get a complete picture of O₂ dynamics and energetic state *in vivo*. These methods could be applied to our situation, allowing us to explore our *in vitro* observations in living animals, since clearly *in vivo* studies would remove any methodological uncertainties associated with our *in vitro* findings.

I have recently acquired a fibre-optic system and subsequent studies will further investigate our current findings and test new hypotheses relating to O₂-dependence. Future work will involve the direct interrogation of muscle PO₂ and VO₂ in the isolated salmon tail preparation or in living animals, in a bid to further investigate some of the observations from the current studies. This will be done with the concurrent measurement of changes in key metabolites to elucidate changes in metabolic pathway activation.

The use of these methods to further explore the role of O₂ supply and utilisation will contribute to our *in vitro* data and potentially resolve the conflicting reports of oxyregulation and oxyconformance of cellular respiration and metabolic processes in the literature. These studies could be effectively combined with molecular techniques to examine changes in gene expression and translation, e.g. hypoxia inducible factors and enzymes associated with both anaerobic and aerobic energy supply.

7.2.2 Anaesthesia, rested harvesting and hypometabolism

The fundamental improvement in tissue quality through a reduction in exhaustion and stress, which is associated with extended shelf-life and improvements in meat quality indicators in rested harvested fish using anaesthetics, is now well recognised in the aquaculture industry (Jerrett *et al.* 1996; Sigholt *et al.* 1997; Jerrett and Holland 1998; Stehly and Gingerich 1999; Fletcher *et al.* 2003; Iversen *et al.* 2003; Black *et al.* 2004; Kiessling *et al.* 2004; Small 2004; Roth *et al.* 2006; Bagni *et al.* 2007; Bosworth *et al.* 2007; Ribas *et al.* 2007; Wilkinson *et al.* 2008; Tuckey *et al.* 2009a). Further to this, the greater metabolic rate and concentration of key metabolites identified in the muscle of fish that were rested harvested in the current study demonstrate that significant improvements in post-mortem metabolic scope are also achievable.

Further to this, the discovery in the current study that isoeugenol anaesthesia may induce a relative hypometabolism (reduced VO₂), may be beneficial when fish are crowded and handled pre-slaughter, since energy reserves are finite and PO₂ may rapidly deplete under these conditions. Along with the established benefits of anaesthesia, the saving in energy stores and requirements could be additive. But does this reduced metabolic rate result in reduced tissue metabolism post-mortem? Current evidence (discussed above) does not suggest this to be the case, although this is not conclusive. This possibility could be explored further in a number of ways.

Firstly, the preliminary experiments using tissue slices could be further extended; VO_2 on exposure to various concentrations of isoeugenol could be finalised. Along with tissue VO_2 measurements, changes in calorimetric and biochemical profiles of incubated tissues could be examined. Secondly, similar parameters could be measured in the isolated salmon tail model to examine changes in tissues from unanaesthetised animals perfused with isoeugenol post-mortem. The possibility that the reduction in VO_2 on exposure to isoeugenol is a result of hypoxia and/or reduced blood flow could also be explored in future work. This could be investigated using indicators of blood flow (e.g. fluorescently dyed microspheres), fibre-optic techniques and/or other minimally invasive techniques (e.g. phosphorescence quenching microscopy) to measure tissue PO_2 and VO_2 , accompanied by the quantification of key metabolites (e.g. ATP, creatine phosphate, glycogen, lactate, pH) in muscle in tissue preparations and/or intact animals.

In future work, VO_2 measurements on H_2S exposure should accompany changes in cardiovascular parameters and blood catecholamine concentrations, with particular reference to the direct cardiovascular effects reported in other studies (e.g. Dombkowski *et al.* 2004; Dombkowski *et al.* 2005; Dombkowski *et al.* 2006; Li *et al.* 2008; Simon *et al.* 2008; Volpato *et al.* 2008; Whitfield *et al.* 2008; Perry *et al.* 2009). As with isoeugenol exposed animals, H_2S exposed animals could be examined for tissue hypoxia by measuring changes in tissue PO_2 and blood flow which could be combined with biochemical analyses. The mechanisms and consequences of acute exposure should also be fully elucidated (i.e. physiological and toxic effects).

Studies using controlled harvests to highlight the physiological consequences of traditional harvesting practices, which can sometimes be violent and result in severe exhaustion, have demonstrated the poor quality of the majority of harvested fish muscle, particularly in the wild-fishing sector. Can rested harvesting principles be applied in the fishing industry? Certainly, improvements in tissue quality could be achieved by the modification or complete overhaul of fishing practices associated with certain species.

One case study in particular is worthy of discussion: the live capture of schools of southern blue-fin tuna (*Thunnus macoyii*) in the southern-ocean, which are enclosed in a net-pen and towed back to shore for on-growing. This kind of fishing provides radically different quality muscle than if the fish were caught and slaughtered at sea. Furthermore, a reduction in bycatch of non-target species is a positive outcome. Even if animals were not translocated, they could be allowed to recover from any metabolic exhaustion associated with capture, a process that can be enhanced by low-velocity swimming (Milligan *et al.* 2000). Potentially, these animals could be anaesthetised, by enclosing the net with a barrier of some kind before harvest. While labour intensive, the additional costs of this kind of activity could be recouped by the higher prices attainable for these rested harvested animals. The example given demonstrates that live capture, particularly of high-value species, is economically viable, although whether this is achievable with other species is uncertain. For example, how can the deleterious effects of large changes in pressure, as is the case for deep-water species, be mitigated?

Nevertheless, if a fundamental change in the quality, shelf-life and welfare of harvested animals is to be effected, radically different methods of harvesting are required in most instances. Just as each species has a unique physiology associated with its life-history, the harvest method used to catch these animals should be individually tailored to reduce metabolic exhaustion and stress. Thus, future work should explore novel and innovative ways to catch fish and apply rested harvesting principles since these measures can reduce the physiological extremes associated with harvest. While there are many challenges in this regard, the gains in product quality, and associated capital gain, should drive this kind of research.

References

- Aaronson, P. I., Robertson, T. P., Knock, G. A., Becker, S., Lewis, T. H., Snetkov, V. and Ward, J. P.** (2006). Hypoxic pulmonary vasoconstriction: mechanisms and controversies. *Journal of Physiology* **570**, 53-58.
- Aaronson, P. I., Robertson, T. P. and Ward, J. P. T.** (2002). Endothelium-derived mediators and hypoxic pulmonary vasoconstriction. *Respiratory Physiology and Neurobiology* **132**, 107-120.
- Abourashed, E. A., Galal, A. M., Shebl, A. M. and J. S. Mossa.** (2008). Enhancing effect of isoeugenol on the antimicrobial activity of isoniazid, 6-paradol and 6-shogaol. *Journal of Herbs, Spices and Medicinal Plants* **13**, 92-100.
- Ali, M. Y., Ping, C. Y., Mok, Y. Y., Ling, L., Whiteman, M., Bhatia, M. and Moore, P. K.** (2006). Regulation of vascular nitric oxide *in vitro* and *in vivo*; a new role for endogenous hydrogen sulphide? *British Journal of Pharmacology* **149**, 625-634.
- Arthur, P. G., Hogan, M. C., Bebout, D. E., Wagner, P. D. and Hochachka, P. W.** (1992). Modelling the effects of hypoxia on ATP turnover in exercising muscle. *Journal of Applied Physiology* **73**, 737-742.
- Artigue, R. S. and Hyman, W. A.** (1976). The effect of myoglobin on the oxygen concentration in skeletal muscle subjected to ischemia. *Annals of Biomedical Engineering* **4**, 128-137.
- Aubourg, S. P., Quitral, V., Larrain, M. A., Rodriguez, A., Gomez, J., Maier, I. and Vinagre, J.** (2007). Autolytic degradation and microbial activity in farmed coho salmon (*Oncorhynchus kisutch*) during chilled storage. *Food Chemistry* **104**, 369-375.
- Bagnara, J. T. and Hadley, M. E.** (1973). Chromatophore control II. In *Chromatophores and color change: the comparative physiology of animal pigmentation*, pp. 202. Englewood Cliffs: Prentice-Hall inc.
- Bagni, M., Civitareale, C., Priori, A., Ballerini, A., Finoia, M., Brambilla, G. and Marino, G.** (2007). Pre-slaughter crowding stress and killing procedures affecting quality and welfare in sea bass (*Dicentrarchus labrax*) and sea bream (*Sparus aurata*). *Aquaculture* **263**, 52-60.

Bailey, J. R., Sephton, D. H. and Driedzic, W. R. (1990). Oxygen uptake by isolated perfused fish hearts with differing myoglobin concentrations under hypoxic conditions. *Journal of Molecular and Cellular Cardiology* **22**, 1125-1134.

Baldwin, J., Davison, W. and Forster, M. E. (1991). Anaerobic glycolysis in the dental retractor muscles of the New Zealand hagfish *Eptatretus cirrhatus* during feeding. *Journal of Experimental Zoology* **260**, 295-301.

Ballantyne, J. S. and Chamberlin, M. E. (1988). Adaptation and evolution of mitochondria: osmotic and ionic considerations. *Canadian Journal of Zoology* **66**, 1028-1035.

Barron, M. G., Tarr B. D., and Hayton W. L. (1987). Temperature-dependence of cardiac output and regional blood flow in rainbow trout, *Salmo gairdneri* Richardson. *Journal of Fish Biology* **31**, 735-744.

Beauchamp, R., Bus, J., Popp, J., Boreiko, C. and Andjelkovich, D., (1984). A critical review of hydrogen sulfide toxicity. *CRC Critical Reviews in Toxicology* **13**, 25-97.

Beddow, T. A., Leuween, J. L. V. and Johnston, I. A. (1995). Swimming kinetics of fast starts are altered by temperature acclimation in the marine fish *Myxocephalus scorpius*. *Journal of Experimental Biology* **198**, 203-208.

Berlin, G., Challoner, K. and Woodson, R. (2002). Low-O₂ affinity erythrocytes improve performance of ischemic myocardium. *Journal of Applied Physiology* **92**, 1267-1276.

Black, S., Jerrett, A. and Forster, M. (2004). Extension of the pre-rigor period in ischemic white muscle from yellow-eye mullet (*Aldrichetta forsteri*) and the New Zealand snapper (*Pagrus auratus*) as affected by hyperbaric oxygen treatment. *Journal of Food Science* **69**, 297-302.

Blackstone, E., Morrison, M. and Roth, M. (2005). H₂S induces a suspended animation-like state in mice. *Science* **308**, 518.

Blackstone, E. and Roth, M. (2007). Suspended animation-like state protects mice from lethal hypoxia. *Shock* **27**, 370-372.

Bockman, E. L. (1983). Blood flow and oxygen consumption in active soleus and gracilis muscles in cats. *American Journal of Physiology* **244**, H546-H551.

Bone, Q. (1978). Locomotor muscle. In *Fish Physiology*, vol. 7 (eds. Hoar, W. S. and Randall, D. J.), pp. 361-424. New York: Academic Press.

- Bone, Q.** (1988). General organisation of the locomotor system. In *Physiology of the elasmobranch fishes*, (ed. Shuttleworth, T. J.), pp. 100-122. Berlin: Springer-Verlag.
- Bosworth, B. G., Small, B. C., Gregory, D., Kim, J., Black, S. E. and Jerrett, A. R.** (2007). Effects of rested-harvest using the anesthetic AQUI-S™ on channel catfish, *Ictalurus punctatus*, physiology and fillet quality. *Aquaculture* **262**, 302-318.
- Boutilier, R. G.** (2001a). Mechanisms of cell survival in hypoxia and hypothermia. *Journal of Experimental Biology* **204**, 3171-3181.
- Boutilier, R. G.** (2001b). Mechanisms of metabolic defence against hypoxia in hibernating frogs. *Respiration Physiology* **128**, 365-377.
- Boutilier, R. G., Donohoe, P. H., Tattersall, G. J. and West, T. G.** (1997). Hypometabolic homeostasis in overwintering aquatic amphibians. *Journal of Experimental Biology* **200**, 387-400.
- Boutilier, R. G., Heming, T. A. and Iwama, G. K.** (1984). Physiochemical parameters for use in fish respiratory physiology. In *Fish Physiology*, Vol. X, Gills, Part A (ed. Hoar, W.S. and Randall, D.J.), pp. 401-430. Orlando: Academic Press.
- Boutilier, R. G. and St-Pierre, J.** (2002). Adaptive plasticity of skeletal muscle energetics in hibernating frogs: mitochondrial proton leak during metabolic depression. *Journal of Experimental Biology* **205**, 2287-2296.
- Brand, M. D.** (2003). Approximate yield of ATP from glucose, designed by Donald Nicholson. *Biochemistry and Molecular Biology Education* **31**, 2-4.
- Brett, J. R. and Glass, N. R.** (1973). Metabolic rates and critical swimming speeds of sockeye salmon (*Oncorhynchus nerka*) in relation to size and temperature. *Journal of the Fisheries Research Board of Canada* **30**, 379-387.
- Buck, L. T. and Hochachka, P. W.** (1993). Anoxic suppression of Na⁺-K⁺-ATPase and constant membrane potential in hepatocytes: support for channel arrest. *American Journal of Physiology* **265**, R1020-R1025.
- Buck, L. T., Hochachka, P. W., Schön, A. and Gnaiger, E.** (1993). Microcalorimetric measurement of reversible metabolic suppression induced by anoxia in isolated hepatocytes. *American Journal of Physiology* **265**, R1014-R1019.

Budinger, G. R. S., Chandel, N., Shao, Z. H., Li, C. Q., Melmed, A., Becker, L. B. and Schumacker, P. T. (1996). Cellular energy utilization and supply during hypoxia in embryonic cardiac myocytes. *American Journal of Physiology* **270**, L44-L53.

Buerk, D. G. and Lahiri, S. (2003). Effects of nitric oxide on carotid body oxygen consumption at low PO₂. In *Oxygen sensing: responses and adaptation to hypoxia*, vol. 175 (eds. Lahiri, S., Sesenza, G. L. and Prabhakar, N. R.), pp. 395-409. New York: Marcel-Dekker.

Bushnell P. G., Steffensen, J. F. and Johansen, K. (1984). Oxygen consumption and swimming performance in hypoxia-acclimated rainbow trout, *Salmo gairdneri*. *Journal of Experimental Biology* **113**, 225-235.

Campbell, N. A., Reece, J. B. and Mitchell, L. G. (1999a). Sensory and motor mechanisms. In *Biology*, (ed. Mulligan, E.), pp. 992-1081. New York: Addison Wesley Longman, Inc.

Campbell, N. A., Reece, J. B. and Mitchell, L. G. (1999b). Cellular respiration: harvesting chemical energy. In *Biology*, (ed. Mulligan, E.), pp. 147-165. New York: Addison Wesley Longman, Inc.

Canty, A. A. and Driedzic, W. R. (1987). Evidence that myoglobin does not support heart performance at maximal levels of oxygen demand. *Journal of Experimental Biology* **128**, 469-473.

Champe, P. C., Harvey, R. A. and Ferrier, D. R. (2008). Bioenergetics and oxidative phosphorylation. In *Lippincott's illustrated reviews: Biochemistry.*, (eds. Champe, P. C. and Harvey, R. A.), Philadelphia: Woltes Kluwer/Lippincott Williams & Wilkins.

Cherniack, N. (2003). Foreword. In *Oxygen sensing: responses and adaptations to hypoxia*, (eds. Lahiri, S., Semenza, G. L. and Prabhakar, N. R.), pp. 776. New York: Dekker, Marcel Inc.

Clark, M. (1999). Fisheries for orange roughy (*Hoplostethus atlanticus*) on seamounts in New Zealand. *Ocean Acta* **22**, 593-602.

Clements, J. D. and Rees, D. (1998). Preservation of inherent contractility in isolated gut segments from herbivorous and carnivorous marine fish. *Journal of Comparative Physiology B* **168**, 61-72.

- Cleto, C. L., Vandenberghe, A. E., MacLean, D. W., Pannunzio, P., Tortorelli, C., Meedel, T. H., Satou, Y., Satoh, N. and Hastings, K. E. M.** (2003). Ascidian larva reveals ancient origin of vertebrate-skeletal-muscle troponin I characteristics in chordate locomotory muscle. *Molecular Biology and Evolution* **20**, 2113-2122.
- Conley, K. E., Kemper, W. F. and Crowther, G. J.** (2001). Limits to sustainable muscle performance: interaction between glycolysis and oxidative phosphorylation. *Journal of Experimental Biology* **204**, 3189-3194.
- Connett, R. J.** (1988). Analysis of metabolic control: new insights using scaled creatine kinase model. *American Journal of Physiology* **254**, R949-R959.
- Cook, D. G., Holland, A. J., Jerrett, A. R. and Forster, M. E.** (2009). The effect of harvest treatment on biochemical properties of farmed Chinook salmon (*Oncorhynchus tshawytscha*) during frozen and thawed storage. *Journal of Food Science* **74**, 543-548.
- Cooperstein, S. J. and Lazrow, A.** (1951). A microspectrophotometric method for the determination of cytochrome oxidase. *Journal of Biological Chemistry* **18**, 665-670.
- Deussen, A., Brand, M., Pexa, A. and Weichsel, J.** (2006). Metabolic coronary flow regulation-current concepts. *Basic Respiratory Cardiology* **101**, 453-464.
- Dombkowski, R. A., Russell, M. J. and Olson, K. R.** (2004). Hydrogen sulfide as an endogenous regulator of vascular smooth muscle tone in trout. *American Journal of Physiology* **286**, R678-R685.
- Dombkowski, R. A., Russell, M. J., Schulman, A. A., Doellman, M. M. and Olson, K. R.** (2005). Vertebrate phylogeny of hydrogen sulfide vasoactivity. *American Journal of Physiology* **288**, R243-R252.
- Dombkowski, R. A., Doellman, M. M., Head, S. K. and Olson, K. R.** (2006). Hydrogen sulfide mediates hypoxia-induced relaxation of trout urinary bladder smooth muscle. *Journal of Experimental Biology* **209**, 3234-3240.
- Dorman, D. C., Moulin, F. J. M., McManus, B. E., Mahle, K. C., James, R. A. and Struve, M. F.** (2002). Cytochrome oxidase inhibition induced by acute hydrogen sulfide inhalation: correlation with tissue sulfide concentrations in the rat brain, liver, lung, and nasal epithelium. *Toxicological Science* **65**, 18-25.
- Dunn, J. F. and Hochachka, P. W.** (1986). Metabolic responses of trout (*Salmo gairdneri*) to acute environmental hypoxia. *Journal of Experimental Biology* **123**, 229-242.

- Dunn, J. F., Davison, W., Maloiy, G. M. O., Hochachka, P. W. and Guppy, M.** (1981). An ultrastructural and histochemical study of the axial musculature of the African lungfish. *Cell and Tissue Research* **220**, 599-609.
- Egginton, S. and Sidell, B. D.** (1989). Thermal acclimation induces adaptive changes in subcellular structure of fish skeletal muscle. *American Journal of Physiology* **256**, R1-R9.
- Egginton, S., Turek, Z. and Hoofd, L. J. C.** (1988). Differing patterns of capillary distribution in fish and mammalian skeletal muscle. *Respiration Physiology* **74**, 383-396.
- Evans, D. H. and Harrie, A. C.** (2001). Vasoactivity of the ventral aorta of the American eel (*Anguilla rostrata*), Atlantic hagfish (*Myxine glutinosa*), and sea lamprey (*Petromyzon marinus*). *Journal of Experimental Zoology* **289**, 273-284.
- Farrell, A. P.** (1996). Features heightening cardiovascular performance in fishes, with special reference to tunas. *Comparative Biochemistry and Physiology A* **113**, 61-67.
- Farrell, A. P.** (2007). Tribute to P.L. Lutz: a message from the heart - why hypoxic bradycardia in fishes? *Journal of Experimental Biology* **210**, 1715-1725.
- Féférou, M., Girard, V. and Canet, E.** (1995). Different involvement of nitric oxide in endothelium-dependent relaxation of porcine pulmonary artery and vein: Influence of hypoxia. *Journal of Cardiovascular Pharmacology* **25**, 665-673.
- Fields, H. A.** (1988). Fermentative adaptations to lack of oxygen. *Canadian Journal of Zoology* **66**, 1036-1040.
- Fletcher, G. C., Corrigan, V. K., Summers, G., Leonard, M. J., Jerrett, A. R. and Black, S. E.** (2003). Spoilage of rested harvested king salmon (*Oncorhynchus tshawytscha*). *Journal of Food Science* **68**, 2810-2816.
- Flood, P. R.** (1965). The skeletal muscle fibre types of *Myxine glutinosa* L. related to those of other chordates. *Acta Reg. Soc. Sci. Litt. Gothenburg Zool.* **8**, 17-20.
- Flood, P. R.** (1979). The vascular supply of three fibre types in the parietal trunk muscle of the Atlantic hagfish (*Myxine glutinosa* L.): a light microscopic quantitative analysis and an evaluation of various methods to express capillary density relative to fibre types. *Microvascular Research* **17**, 53-70.
- Forgan, L. G. and Forster, M. E.** (2007). Effects of potential mediators of an intestinal brake mechanism on gut motility in Chinook salmon, (*Oncorhynchus tshawytscha*). *Comparative Biochemistry and Physiology C* **146**, 343-347.

Forgan, L. G. and Forster, M. E. (2008). Oxygen consumption and blood flow distribution in perfused skeletal muscle of Chinook salmon. *Journal of Comparative Physiology B* **179**, 359-368.

Forster, M. E. (1991). Myocardial oxygen consumption and lactate release by the hypoxic hagfish heart. *Journal of Experimental Biology* **156**, 583-590.

Forster, M. E., Davison, W., Axelsson, M. and Farrell, A. P. (1992). Cardiovascular responses to hypoxia in the hagfish, *Eptatretus cirrhatus*. *Respiration Physiology* **88**, 373-386.

Franklin, C. E. and Johnston, I. A. (1997). Muscle power output during escape responses in an Antarctic fish. *Journal of Experimental Biology* **200**, 703-712.

Friesenecker, B. (2007). Does the vessel wall partition oxygen away from the tissue? *Antioxidants and Redox Signaling* **9**, 985-989.

Frolow, J. and Milligan, C. L. (2004). Hormonal regulation of glycogen metabolism in white muscle slices from rainbow trout (*Oncorhynchus mykiss* Walbaum). *American Journal of Physiology* **287**, R1344-R1353.

Furchgott, R. F., Carvalho, M. H., Khan, M. T. and Matsunaga, K. (1987). Evidence for endothelium-dependent vasodilation by acetylcholine. *Journal of Vascular Research* **24**, 145-149.

Furchgott, R. F. and Zawadzki, J. V. (1980). The obligatory role of endothelial cells in the relaxation of arterial smooth muscle by acetylcholine. *Nature* **288**, 373-376.

Fürst, W. and Hallstrom, S. (1992). Simultaneous determination of myocardial nucleotides, nucleosides, purine bases and creatine phosphate by ion-pair high performance liquid chromatography. *Journal of Chromatography* **578**, 39-44.

Gamperl, A. K., Vijayan, M. M., Pereira, C. and Farrell, A. P. (1998). Beta-receptors and stress protein 70 expression in hypoxic myocardium of rainbow trout and chinook salmon. *American Journal of Physiology* **43**, R428-R436.

Gardiner, B. (1999). Fishes. In *The Marshall illustrated encyclopaedia of dinosaurs and prehistoric animals*, (ed. Palmer, D.), pp. 18-45. London: Marshall Publishing Ltd.

- Gill, A. O. and Holley, R. A.** (2006). Disruption of *Escherichia coli*, *Listeria monocytogenes* and *Lactobacillus sakei* cellular membranes by plant oil aromatics. *International Journal of Food Microbiology* **108**, 1-9.
- Gilles-Gonzalez, M. A.** (2003). Biochemistry and physiological importance of heme proteins as oxygen sensors. In *Oxygen sensing: responses and adaptation to hypoxia*, vol. 175 (eds. Lahiri, S., Sesenza, G. L. and Prabhakar, N. R.), pp. 7-21. New York: Marcel Dekker.
- Gnaiger, E.** (2003). Oxygen conformance of cellular respiration - a perspective of mitochondrial physiology. In *Hypoxia: through the Lifecycle*, (eds. Roach, R. C. *et al.*), pp 39-55. Kluwer: New York.
- Gnaiger, E., Mendez, G. and Hand, S. C.** (2000). High phosphorylation efficiency and depression of uncoupled respiration in mitochondria under hypoxia. *Proceedings of the National Academy of Sciences of the United States of America* **97**, 11080-11085.
- Golub, A. S., Barker, M. C. and Pittman, R. N.** (2008). Microvascular oxygen tension in the rat mesentery. *American Journal of Physiology* **294**, H21-H28.
- Goolish, E.** (1991). Aerobic and anaerobic scaling in fish. *Biological Reviews* **66**, 33-56.
- Goubern, M., Andriamihaja, M., Nübel, T., Blachier, F. and Bouillaud, F.** (2007). Sulfide, the first inorganic substrate for human cells. *FASEB Journal* **21**, 1699-1706.
- Greer-Walker, M. and Pull, G. A.** (1975). A survey of red and white muscle in marine fish. *Journal of Fish Biology* **7**, 295-300.
- Grieshaber, M. K. and Völkel, S.** (1998). Animal adaptations for tolerance and exploitation of poisonous sulfide. *Annual Reviews in Physiology* **60**, 33-53.
- Griffith, T. M., Henderson, A. H., Edwards, H. D. and Lewis, M. J.** (1984). Isolated perfused rabbit coronary artery and aortic strip preparations: the role of endothelium-derived relaxant factor. *Journal of Physiology* **351**, 13-24.
- Guerrero, F., Theron, M. and Sebert, P.** (2000). *In vitro* reactivity of ventral aorta to acetylcholine and noradrenaline in yellow freshwater eel (*Anguilla anguilla* L.) acclimatized to 10.1 MPa hydrostatic pressure. *Canadian Journal of Physiology and Pharmacology* **78**, 897-903.

- Guppy, M. and Withers, P.** (1999). Metabolic depression in animals: physiological perspectives and biochemical generalizations. *Biological Reviews of the Cambridge Philosophical Society* **74**, 1-40.
- Griffith, R. W.** (1994). The life of the first vertebrates. *Bioscience* **44**, 408-416.
- Hamid R., Rotshteyn Y., Rabadi L., Parikh R. and Bullock P.** (2004). Comparison of alamar blue and MTT assays for high through-put screening. *Toxicology In Vitro* **18**, 703-710.
- Haouzi, P., Notet, V., Scheneul, B., Chalon, B., Sponne, I., Ogier, V. and Bihain, B.** (2008). H₂S induced hypometabolism in mice is missing in sedated sheep. *Respiratory Physiology and Neurobiology* **160**, 109-115.
- Hardisty, M. W.** (1979). The skeleton and muscular system. In *Biology of the Cyclostomes*, (ed. Hardisty, M. W.), pp. 122-137. London: Chapman and Hall.
- Hemmingsen, A. M.** (1960). Energy metabolism as related to body size and respiratory surfaces, and its evolution. *Reports of Steno Memorial Hospital* **9**, 1-110.
- Hill J. V. and Forster M. E.** (2004a). Cardiovascular responses of Chinook salmon (*Oncorhynchus tshawytscha*) during rapid anaesthetic induction and recovery. *Comparative Biochemistry and Physiology C* **137**, 167-177.
- Hill, J. V. and Forster, M. E.** (2004b). The effects of settlement and anaesthesia on oxygen consumption in the New Zealand spotty (*Notolabrus celidotus*) measured in an automated flow-through respirometry system. *New Zealand Natural Sciences* **29**, 39-48.
- Hjemdahl, P., Belfrage, E. and Daleskog, M.** (1979). Vascular and metabolic effects of circulating epinephrine and norepinephrine. *Journal of Clinical Investigation* **64**, 1221-1228.
- Hochachka, P. W.** (1980). Living without oxygen: closed and open systems in hypoxia tolerance. London: Harvard University Press.
- Hochachka, P. W.** (1985). Fuels and pathways as designed systems for support of muscle work. *Journal of Experimental Biology* **115**, 149-164.
- Hochachka, P. W.** (1999). The metabolic implications of intracellular circulation. *Proceedings of the National Academy of Sciences of the United States of America* **96**, 12233-12239.

- Hochachka, P. W.** (2003). Intracellular convection, homeostasis and metabolic regulation. *Journal of Experimental Biology* **206**, 2001-2009.
- Hochachka, P. W. and Guppy, M.** (1987). Metabolic arrest and control of biological time. Cambridge, Mass: Harvard University Press.
- Hochachka, P. W. and McClelland, G. B.** (1997). Cellular metabolic homeostasis during large-scale change in ATP turnover rates in muscles. *Journal of Experimental Biology* **200**, 381-386.
- Hochachka, P. W. and Mommsen T. P.** (1983). Protons and anaerobiosis. *Science* **219**, 1391-1398.
- Hochachka, P. W., Buck, L. T., Doll, C. J. and Land, S. C.** (1996). Unifying theory of hypoxia tolerance: molecular/metabolic defence and rescue mechanisms for surviving oxygen lack. *Proceedings of the National Academy of Sciences of the United States of America* **93**, 9493-9498.
- Hogan, M. C., Arthur, P. G., Bebout, D. E., Hochachka, P. W. and Wagner, P. D.** (1992). Role of O₂ in regulating tissue respiration in dog muscle working *in situ*. *Journal of Applied Physiology* **73**, 728-736.
- Hosoki, R., Matsuki, N. and Kimura, H.** (1997). The possible role of hydrogen sulfide as an endogenous smooth muscle relaxant in synergy with nitric oxide. *Biochemical and Biophysical Research Communications* **237**, 527-531.
- Ikomi-Kumm, J., Monti, M., Hanson, A. and Johansson, B. W.** (1994). Microcalorimetric study on myocardial metabolism in a hibernator and two nonhibernators at 20 °C and 37 °C. *Cryobiology* **31**, 133-143.
- Ingvast-Larsson, J. C., Axén, V. C. and Kiessling, A. K.** (2003). Effects of isoeugenol on *in vitro* neuromuscular blockade of rat phrenic nerve-diaphragm preparations. *American Journal of Veterinary Research* **64**, 690-693.
- Iversen, M., Finstad, B., McKinley, R. S. and Eliassen, R. A.** (2003). The efficacy of metomidate, clove oil, AQUI-STM and Benzoak® as anaesthetics in Atlantic salmon (*Salmo salar* L.) smolts, and their potential stress-reducing capacity. *Aquaculture* **221**, 549-566.
- Jacobs, E. R. and Zeldin, D. C.** (2001). The lung HETEs and (EETs) up. *American Journal of Physiology* **280**, H1-H10.
- Janssen, G.** (2003). Factors affecting the *in vitro* performance of tissue from Chinook salmon. M.Sc. thesis, University of Canterbury, Christchurch.

- Jerrett, A. R. and Holland, J.** (1998). Rigor tension development in excised 'rested', 'partially exercised' and 'exhausted' Chinook salmon white muscle. *Journal of Food Science* **63**, 48-52.
- Jerrett, A. R., Law, R. A., Holland, A. J., Cleaver, S. E. and Ford, S. C.** (2000). Optimum postmortem chilled storage temperature for summer and winter acclimated, rested Chinook salmon (*Oncorhynchus tshawytscha*) white muscle. *Journal of Food Science* **65**, 750-755.
- Jerrett, A. R., Law, R. A., Holland, A. J. and Black, S. E.** (2002). Profiles of New Zealand snapper (*Pagrus auratus*) postmortem metabolism as affected by acclimated temperature and postmortem storage temperature. *Journal of Food Science* **67**, 2843-2850.
- Jerrett, A. R., Stevens, J. and Holland, A. J.** (1996). Tensile properties of white muscle in rested and exhausted chinook salmon (*Oncorhynchus tshawytscha*). *Journal of Food Science* **61**, 527-532.
- Jibb, L. A. and Richards, J. G.** (2008). AMP-activated protein kinase activity during metabolic rate depression in the hypoxic goldfish, *Carassius auratus*. *Journal of Experimental Biology* **211**, 3111-3122.
- Johansson, D., Nilsson, G. E. and Tornblom, E.** (1995). Effects of anoxia on energy metabolism in crucian carp brain slices studied with microcalorimetry. *Journal of Experimental Biology* **198**, 853-859.
- Johnston, I. A.** (1975). Anaerobic metabolism in the carp (*Carassius carassius* L.). *Comparative Biochemistry and Physiology B* **51**, 235-241.
- Johnston, I. A.** (1991). Muscle action during locomotion: a comparative perspective. *Journal of Experimental Biology* **160**, 167-185.
- Johnson, T. P. and Johnston, I. A.** (1991). Power output of fish muscles performing oscillatory work: effects of acute and seasonal temperature change. *Journal of Experimental Biology* **157**, 409-423.
- Johnston, I. A. and Ward, P. S.** (1975). Studies on the swimming musculature of the rainbow trout I. Fiber types. *Journal of Fish Biology* **7**, 451-458.
- Jones, J. A.** (1995). Red blood cell substitutes: current status. *British Journal of Anaesthesiology* **74**, 697-703.
- Julian, D., Statile, J. L., Wohlgemuth, S. E. and Arp, A. J.** (2002). Enzymatic hydrogen sulfide production in marine invertebrate tissues. *Comparative Biochemistry and Physiology A* **133**, 105-115.

- Kam, J. C. and Milligan, C. L.** (2006). Fuel use during glycogenesis in rainbow trout (*Oncorhynchus mykiss* Walbaum) white muscle studied *in vitro*. *Journal of Experimental Biology* **209**, 871-880.
- Kasting, J. F.** (1993). Earth's early atmosphere. *Science* **259**, 920-926.
- Keppler, D. and Decker, K.** (1974). Glycogen: determination with amyloglucosidase. In *Methods of Enzymatic Analysis*, (ed. Bergmeyer, H. V.), pp. 1127-1131. New York: Academic Press.
- Kerkhof, C. J., Van Der Linden, P. J. and Sipkema, P.** (2002). Role of myocardium and endothelium in coronary vascular smooth muscle responses to hypoxia. *American Journal of Physiology* **282**, H1296-H1303.
- Kery, V., Poneleit, L., Meyer, J. D., Manning, M. C. and Kraus, J. P.** (1999). Binding of pyridoxyl 5'-phosphate to the heme protein human cystathionine β -synthase. *Biochemistry* **38**, 2716-2724.
- Khan, A., Schuler, M., Prior, M., Yong, S., Coppock, R., Florence, L. and Lillie, L.** (1990). Effects of Hydrogen sulfide exposure on lung mitochondrial respiratory chain enzymes in rats. *Toxicology and Applied Pharmacology* **103**, 482-490.
- Kieffer, J. D., Alsop, D. and Wood, C. M.** (1998). A respirometric analysis of fuel use during aerobic swimming at different temperatures in rainbow trout (*Oncorhynchus mykiss*). *Journal of Experimental Biology* **201**, 3123-3133.
- Kiessling, A., Espe, M., Ruohonen, K. and Mørkøre, T.** (2004). Texture, gaping and colour of fresh and frozen Atlantic salmon as affected by pre-harvest iso-eugenol or CO₂ slaughter. *Aquaculture* **236**, 645-657.
- Kiceniuk J. W. and Jones, D. R.** (1977). Oxygen transport system in trout (*Salmo gairdneri*) during exercise. *Journal of Experimental Biology* **69**, 247-261.
- Koenitzer, J. R., Isabell, T. S., Patel, H. D., Benavides, G. A., Dickinson, D. A., Patel, R. P., Darley-USmar, V. M., Lancaster, J. R., Doeller, J. E. and Kraus, D. W.** (2007). Hydrogen sulfide mediates vasoactivity in an O₂-dependent manner. *American Journal of Physiology* **292**, H1953-H1960.
- Kolář, F. and Janský, L.** (1984). Oxygen consumption in rat skeletal muscle at various rates of oxygen delivery. *Cellular and Molecular Life Sciences* **40**, 353-354.

- Kolok A. S., Spooner, R. M. and Farrell, A. P.** (1993). The effects of exercise on the cardiac output and blood flow distribution of the largescale sucker *Catostomus macrocheilus*. *Journal of Experimental Biology* **183**, 301-321.
- Kosan, R. L. and Burton, A. C.** (1966). Oxygen consumption of arterial smooth muscle as a function of active tone and passive stretch. *Circulation Research* **18**, 79-88.
- Koslow, J. A.** (1997). Seamounts and the ecology of deep-sea fisheries. *American Scientist* **85**, 168–176.
- Koslow, J. A.** (2000). Continental slope and deep-sea fisheries: implications for a fragile ecosystem. *ICES Journal of Marine Science* **57**, 548–557.
- Kranen, R. W., van Kuppevelt, T. H., Goedhart, H. A., Veerkamp, C. H., Lambooy, E. and Veerkamp, J. H.** (1999). Hemoglobin and myoglobin content in muscles of broiler chickens. *Poultry Science* **78**, 467-476.
- Kubo, S., Doe, I., Kurokawa, Y., Nishikawa, H. and Kawabata, A.** (2007). Direct inhibition of endothelial nitric oxide synthase by hydrogen sulfide: contribution to dual modulation of vascular tension. *Toxicology* **232**, 138-146.
- Kuznetsov, A., Lassnig, B. and Margreiter, R.** (1998). Diffusion limitation of oxygen versus ADP in permeabilized muscle fibers. In *Biothermokinetics in the post-genomic era*, (eds. Larsson, C., Pålman, I. L. and Gustafsson, L.), pp. 273-276. Göteborg: Chalmers Reproservice.
- Laberee, K. and Milligan, C. L.** (1999). Lactate transport across sarcolemmal vesicles isolated from rainbow trout white muscle. *Journal of Experimental Biology* **202**, 2167-2175.
- Lahiri, S., Prabhakar, N. R. and Forster, R. E.** (2000). Oxygen sensing: molecule to man. New York: Kluwer Academic/Plenum Publishers.
- Lauder, G. V.** (2006). Locomotion. In *The physiology of fishes*, (eds. Evans, D. H. and Claiborne, J. B.), pp. 3-46. Boca Ranton, Florida: CRC Press.
- Leary, S. C., Lyons, C. N., Rosenberger, A. G., Ballantyne, J. S., Stillman, J. and Moyes, C. D.** (2003). Fiber-type differences in muscle mitochondrial profiles. *American Journal of Physiology* **285**, R817-R826.
- Lee, C. G., Devlin, R. H. and Farrell, A. P.** (2003a). Swimming performance, oxygen consumption and excess post-exercise oxygen consumption in adult transgenic and ocean-ranched coho salmon. *Journal of Fish Biology* **62**, 753-766.

- Lee, C. G., Farrell, A. P., Lotto, A., Hinch, S. G. and Healey, M. C.** (2003b). Excess post-exercise oxygen consumption in adult sockeye (*Oncorhynchus nerka*) and coho (*O. kisutch*) salmon following critical speed swimming. *Journal of Experimental Biology* **206**, 3253-3260.
- Lee-de Groot, M. B. E., des Tombe, A. and van der Laarse, W. J.** (1998). Calibrated histochemistry of myoglobin concentration in cardiomyocytes. *The Journal of Histochemistry and Cytochemistry* **46**, 1077-1084.
- Li, J., Zhang, G., Cai, S. and Redington, A.N.,** (2008). Effects of inhaled hydrogen sulfide on metabolic rate in anesthetized, paralyzed, and mechanically ventilated piglets. *Pediatric Critical Care Medicine* **9**, 110-112.
- Lindqvist, A., Dreja, K., Sward, K. and Hellstrand, P.** (2002). Effects of oxygen tension on energetics of cultured vascular smooth muscle. *American Journal of Physiology* **283**, H110-H117.
- Liu, Q., Sham, J. S., Shimoda, L. A. and Sylvester, J. T.** (2001). Hypoxic constriction of distal porcine pulmonary arteries: endothelium and endothelin dependence. *American Journal of Physiology* **280**, L856-L865.
- Lurman, G. J., Koschnick, N., Pörtner, H-O. and Lucassen, M.** (2007) Molecular characterisation and expression of Atlantic cod (*Gadus morhua*) myoglobin from two populations held at two different acclimation temperatures. *Comparative Biochemistry and Physiology A*, **148** 681-689.
- Luther, P. K., Munro, P. M. G. and Squire, J. M.** (1995). Muscle ultrastructure in the teleost fish. *Micron* **26**, 431-459.
- Madden, J. A., Vadula, M. S. and Kurup, V. P.** (1992). Effects of hypoxia and other vasoactive agents on pulmonary and cerebral artery smooth muscle cells. *American Journal of Physiology* **263**, L384-L393.
- Mallard, T.** (2008). Bill to improve aquaculture development passes, (ed. Ministry of the Environment): New Zealand Government <http://feeds/beehive/govt.nz/speech/bill+help+aquaculture+development+passes>. Accessed in March 2009.
- Marcinek, D. J., Ciesielski, W. A., Conley, K. E. and Schenkman, K. A.** (2003). Oxygen regulation and limitation to cellular respiration in mouse skeletal muscle *in vivo*. *American Journal of Physiology* **285**, H1900-H1908.
- McKenzie, D. J., Aota, S. and Randall, D. J.** (1991). Ventilatory and cardiovascular responses to blood pH, plasma Pco₂, blood O₂ content, and catecholamines in an air-breathing fish, the bowfin *Amia calva*. *Physiological Zoology* **64**, 432-450.

- McKenzie, D. J., Wong, S., Randall, D.J., Egginton, S., Taylor E. W. and Farrell A. P.** (2004). The effects of sustained exercise and hypoxia upon oxygen tensions in the red muscle of rainbow trout. *Journal of Experimental Biology* **207**, 3629-3637.
- Mazeaud, M. M. and Mazeaud, F.** (1981). Adrenergic responses to stress in fish. In *Stress and fish*, (ed. Pickering, A. D.), pp. 367. London: Academic Press.
- Meyer, R. A.** (2004). Aerobic performance and the function of myoglobin in human skeletal muscle. *American Journal of Physiology* **287**, R1304-R1305.
- Milligan, C. L.** (1996). Metabolic recovery from exhaustive exercise in rainbow trout. *Comparative Biochemistry and Physiology A* **113**, 51-60.
- Milligan, C. L., Hooke, G. B. and Johnson, C.** (2000). Sustained swimming at low velocity following a bout of exhaustive exercise enhances metabolic recovery in rainbow trout. *Journal of Experimental Biology* **203**, 921-926.
- Milligan, C. L. and McDonald, D. G.** (1988). *In vivo* lactate kinetics at rest and during recovery from exhaustive exercise in coho salmon (*Oncorhynchus kisutch*) and starry flounder (*Platichthys stellatus*). *Journal of Experimental Biology* **135**, 119-131.
- Milligan, C. L. and Wood, C. M.** (1987). Effects of strenuous activity on intracellular and extracellular acid-base status and H⁺ exchange with the environment in the inactive benthic starry flounder *Platichthys stellatus*. *Physiological Zoology* **60**, 37-53.
- Millot, J. and Anthony, J.** (1958). Squelette, muscles et formations de soutien. In *Anatomie de Latimeria chalumnae*, vol. 1 (eds. Millot, J. and Anthony, J.), Paris.
- Miquel, J., de Juan, E. and Sevilla, I.** (1992). Oxygen-induced mitochondrial damage and aging. In *Free Radicals and Aging*, (eds. Emerit, I. and Chance, B.), pp. 49-57. Basel: Birkhauser.
- Mosmann, T.** (1983). Rapid colorimetric assay for cellular growth and survival: application to proliferation and cytotoxicity assays. *Journal of Immunological Methods* **65**, 55-63.
- Moyes, C. D., Buck, L. T., Hochachka, P. W. and Suarez, R. K.** (1989). Oxidative properties of carp red and white muscle. *Journal of Experimental Biology* **143**, 321-331.

Moyes, C. D. and Hood, D. A. (2003). Origins and consequences of mitochondrial variation in skeletal muscle. *Annual Review of Physiology* **65**, 177-201.

Moyes, C. D. and West, T. G. (1995). Exercise metabolism in fish. In *Biochemistry and Molecular Biology*, vol. 4 (eds. Hochachka, P. and Mommsen, T. P.), pp. 367-392. Amsterdam: Elsevier.

Mühlfeld, C., Singer, D., Engelhart, N., Richter, J. and Schmeiedl, A. (2005). Electron microscopy of the postnatal rat heart (*Rattus norvegicus*). *Comparative Biochemistry and Physiology A* **141**, 310-318.

Nelson, S. K., Bose, S., Rizeq, M. and McCord, J. M. (2005). Oxidative stress in organ preservation: a multifaceted approach to cardioplegia. *Biomedicine and Pharmacotherapy* **59**, 149-157.

Neumann, P., Holeton, G. F. and Heisler, N. (1983). Cardiac output and regional blood flow in gills and muscles after exhaustive exercise in rainbow trout (*Salmo gairdneri*). *Journal of Experimental Biology* **105**, 1-14.

Nicholls, P. and Kim, J. M. (1982). Sulphide as an inhibitor and electron donor for the cytochrome c oxidase system. *Canadian Journal of Biochemistry* **60**, 613-623.

Nichols, J. W. and Weber, L. J. (1989). Comparative oxygen affinity of fish and mammalian myoglobins. *Journal of Comparative Physiology Part B* **159**, 205-209.

North, B. P., Ellis, T. E., Bron, J., Knowles, T. G. and Turnbull, J. F. (2008). The use of stakeholder focus groups to identify indicators for the on-farm assessment of trout welfare. In *Fish welfare*, (ed. Branson, E. J.), pp. 243-266. Oxford: Blackwell Publishing Ltd.

O'Brien, P., Shen, H., McCutcheon, L. J., O'Grady, M., Byrne, P. J., Ferguson, H. W., Mirsalami, M. S., Julian, R. J., Sargeant, J. M. and Tremblay, R. R. M. (1992). Rapid, simple and sensitive microassay for skeletal and cardiac myoglobin and hemoglobin: use in various animals indicates functional role of myohemoproteins. *Molecular and Cellular Biochemistry* **112**, 45-52.

Olson, K. R. (2002). Gill circulation: Regulation of perfusion distribution and metabolism of regulatory molecules. *Journal of Experimental Zoology* **293**, 320-335.

Olson, K. R. (2008). Hydrogen sulfide and oxygen sensing: implications in cardiorespiratory control. *Journal of Experimental Biology* **211**, 2727-2734.

- Olson, K. R., Dombkowski, R. A., Russell, M. J., Doellman, M. M., Head, S. K., Whitfield, N. L. and Madden, J. A.** (2006). Hydrogen sulfide as an oxygen sensor/transducer in vertebrate hypoxic vasoconstriction and hypoxic vasodilation. *Journal of Experimental Biology* **209**, 4011-4023.
- Olson, K. R. and Farrell, A. P.** (2006). The cardiovascular system. In *The physiology of fishes*, vol. 3 (eds. Evans, D. H. and Claiborne, J. B.), pp. 119-152. Boca Raton, Florida: CRC Press.
- Olson, K. R., Forgan, L. G., Dombkowski, R. A. and Forster, M. E.** (2008a). Oxygen dependency of hydrogen sulfide-mediated vasoconstriction in cyclostome aortas. *Journal of Experimental Biology* **211**, 2205-2213.
- Olson, K. R., Healey, M., Qin, J., Skovgaard, N., Vulesevic, B., Duff, D. W., Whitfield, N. L., Yang, G., Wang, R. and Perry, S. F.** (2008b). Hydrogen sulfide as an oxygen sensor in trout gill chemoreceptors. *American Journal of Physiology* **295**, R669-R680.
- Olson, K. R., Russell, M. J. and Forster, M. E.** (2001). Hypoxic vasoconstriction of cyclostome systemic vessels: the antecedent of hypoxic pulmonary vasoconstriction? *American Journal of Physiology* **280**, R198-R206.
- Olson, K. R. and Villa, J.** (1991). Evidence against nonprostanoid endothelium-derived relaxing factor(s) in trout vessels. *American Journal of Physiology* **260**, R925-R933.
- Opie, L. H.** (1998). Introductory cardiovascular concepts. In *The heart: from cell to circulation*, (ed. Swan, K.), pp. 3-16. New York: Lippincott - Raven.
- Pagnotta, A. and Milligan, C. L.** (1991). The role of blood glucose in the restoration of muscle glycogen during recovery from exhaustive exercise in rainbow trout (*Oncorhynchus mykiss*) and winter flounder (*Pseudopleuronectes americanus*). *Journal of Experimental Biology* **161**, 489-508.
- Pang, C. Y., Yang, R. Z., Zhong, A., Xu, N., Forrest, C. R. and Boyd, B.** (1995). Acute ischemic preconditioning protects against skeletal muscle infarction in the pig. *Cardiovascular Research* **29**, 782-788.
- Paul, R. J.** (1980). Chemical energetics of vascular smooth muscle. In *Handbook of Physiology volume 2: The cardiovascular system part 2*, vol. 2 (eds. Bohr, D. H., Somlyuo, A. P. and Sparks, H. V.), Baltimore: Waverly Press.
- Peake, S. J. and Farrell, A. P.** (2004). Locomotory behaviour and post-exercise physiology in relation to swimming speed, gait transition and metabolism in free-swimming smallmouth bass (*Micropterus dolmieu*). *Journal of Experimental Biology* **207**, 1563-1575.

- Perry, S. F. and Desforbes, P. R.** (2006). Does bradycardia or hypertension enhance gas transfer in rainbow trout (*Oncorhynchus mykiss*)? *Comparative Biochemistry and Physiology A* **144**, 163-172.
- Perry, S. F., Davie P. S., Daxboeck, C., Ellis, A. G. and Smith, D. G.** (1984). Perfusion methods for the study of gill physiology. In *Fish Physiology*, (eds Hoar, W. S. and Randall, D. J.), Academic Press, New York, pp 325-388.
- Perry, S. F. and Farrell, A. P.** (1989). Perfused preparations in comparative respiratory physiology. In *Techniques in comparative respiratory physiology: an experimental approach*, (eds Bridges, C. R. and Butler, P. J.), pp 223-257. Cambridge: Cambridge University Press.
- Perry, S. F., McNeill, B., Elia, E., Nagpal, A. and Vulesevic, B.** (2009). Hydrogen sulfide stimulates catecholamine secretion in rainbow trout (*Oncorhynchus mykiss*). *American Journal of Physiology* **296**, R133-R140.
- Platzack, B. R., Hicks, J. W.** (2001). Reductions in systemic oxygen delivery induce a hypometabolic state in the turtle (*Trachemys scripta*). *American Journal of Physiology* **281**, R1295-R1301.
- Pozeg, Z. I., Thebaud, B., Tyrell, B. D., Michelakis, E. D. and Archer, S. L.** (2003). Mitochondria as vascular oxygen sensors: the redox hypothesis of vascular O₂ sensing. In *Oxygen sensing: responses and adaptation to hypoxia*, vol. 175 (eds Lahiri S., Sesenza, G. L. and Prabhakar, N. R.), pp. 523-552. New York: Marcel-Dekker.
- Prabhu, N. V. and Sharp, K. A.** (2005). Heat capacity in proteins. *Annual Reviews in Physical Chemistry* **56**, 521-548.
- Qiu, Y., Sutton, L. and Riggs, A. F.** (1998). Identification of myoglobin in human smooth muscle. *Journal of Biological Chemistry* **273**, 23426-23432.
- Reid, S. G. and Perry, S. F.** (2003). Peripheral O₂ chemoreceptors mediate humoral catecholamine secretion from fish chromaffin cells. *American Journal of Physiology* **284**, R990-R999.
- Resende, A. C., Tabellion, A., Nadaud, S., Lartaud, I., Bagrel, D., Faure, S., Atkinson, J. and Capdeville-Atkinson, C.** (2004). Incubation of rat aortic rings produces a specific reduction in agonist-evoked contraction: effect of age of donor. *Life Sciences* **76**, 9-20.
- Ribas, L., Flos, R., Reig, L., MacKenzie, S., Barton, B. A. and Tort, L.** (2007). Comparison of methods for anaesthetizing Senegal sole (*Solea senegalensis*) before slaughter: Stress responses and final product quality. *Aquaculture* **269**, 250-258.

Richards, J. G., Mercado, A. J., Clayton, C. A., Heigenhauser, G. J. F. and Wood, C. M. (2002a). Substrate utilization during graded aerobic exercise in rainbow trout. *Journal of Experimental Biology* **205**, 2067-2077.

Richards, J. G., Heigenhauser, G. J. F. and Wood, C. M. (2002b). Lipid oxidation fuels recovery from exhaustive exercise in white muscle of rainbow trout. *American Journal of Physiology* **282**, R89-R99.

Robb, D. H. F. (2008). Welfare of fish at harvest. In *Fish welfare*, (ed. Branson, E. J.), pp. 217-240. Oxford: Blackwell Publishing Ltd.

Roberts, C. (2002). Deep impact: the rising toll of fishing in the deep sea *Trends in Ecology and Evolution* **17**, 242-245.

Rome, L. C. (1994). The mechanical design of the muscular system. In *Comparative vertebrate exercise physiology: unifying physiological principles*, (ed. Jones, J. H.), pp. 125-179. San Diego: Academic Press.

Roth, B., Slinde, E. and Arildsen, J. (2006). Pre or post mortem muscle activity in Atlantic salmon (*Salmo salar*). The effect on rigor mortis and the physical properties of flesh. *Aquaculture* **257**, 504-510.

Rothwell, S. E. and Forster M. E. (2005). Anaesthetic effects on the hepatic portal vein and on the vascular resistance of the tail of the Chinook salmon (*Oncorhynchus tshawytscha*). *Fish Physiology and Biochemistry* **31**, 11-21.

Rothwell, S. E., Black, S. E., Jerrett, A. R. and Forster, M. E. (2005). Cardiovascular changes and catecholamine release following anaesthesia in Chinook salmon (*Oncorhynchus tshawytscha*) and snapper (*Pagrus auratus*). *Comparative Biochemistry and Physiology A* **140**, 289-298.

Routley, M. H., Nilsson, G. E. and Renshaw, G. M. C. (2002). Exposure to hypoxia primes the respiratory and metabolic responses of the epaulette shark to progressive hypoxia. *Comparative Biochemistry and Physiology A* **131**, 313-321.

Ruderman, N. B., Kemmer, F. W., Goodman, M. N. and Berger, M. (1980). Oxygen consumption in perfused skeletal muscle. *Biochemical Journal* **190**, 57-64.

Rudin, A., Healy, A., Phillips, C. A., Gump, D. W. and Forsyth, B. R. (1970). Antibacterial activity of gentamycin sulphate in tissue culture. *Applied Microbiology* **20**, 989-990.

- Rumsey, W. L., Schlosser, C., Nuutinen, E. M., Robiolio, M. and Wilson, D. F.** (1990). Cellular energetics and the oxygen dependence of respiration in cardiac myocytes isolated from adult rat. *Journal of Biological Chemistry* **265**, 15392-15402.
- Russ, G. R.** (1991). Coral reef fisheries: effects and yields. In *The ecology of fishes on coral reefs*, (ed. Sale, P. F.), San Diego: Academic Press.
- Russell, M. J., Dombkowski, R. A. and Olson, K. R.** (2007). Effects of hypoxia on vertebrate blood vessels. *Journal of Experimental Zoology A* **309**, 55-63.
- Russell, M. J., Pelaez, N. J., Packer, C. S., Forster, M. E. and Olson, K. R.** (2001). Intracellular and extracellular calcium utilization during hypoxic vasoconstriction of cyclostome aortas. *American Journal of Physiology* **281**, R1506-R1513.
- Saito, T., Arai, K. and Yajima, T.** (1959). Changes in purine nucleotides of red lateral muscle of rainbow trout. *Nature* **184**, 1415-1415.
- Sandblom, E. and Axelsson, M.** (2005). Effects of hypoxia on the venous circulation in rainbow trout (*Oncorhynchus mykiss*). *Comparative Biochemistry and Physiology A* **140**, 233-239.
- Sandblom, E. and Axelsson, M.** (2006). Adrenergic control of venous capacitance during moderate hypoxia in the rainbow trout (*Oncorhynchus mykiss*): role of neural and circulating catecholamines. *American Journal of Physiology* **291**, R711-R718.
- Satchell, G. H.** (1991) Physiology and form of fish circulation. Cambridge: Cambridge University Press.
- Schenkman, K., Beard, D., Ciesielski, K. and Feigl, E.** (2003). Comparison of buffer and red blood cell perfusion of guinea pig heart oxygenation. *American Journal of Physiology* **285**, H1819-H1825.
- Schopf, J. W.** (1978). The evolution of the earliest cells. *American Scientist* **239**, 111-138.
- Schulte, P. M., Moyes, C. D. and Hochachka, P. W.** (1992). Integrating metabolic pathways in post-exercise recovery of white muscle. *Journal of Experimental Biology* **166**, 181-195.
- Schumacker, P. T., Chandel, N. and Agusti, A. G. N.** (1993). Oxygen conformance of cellular respiration in hepatocytes. *American Journal of Physiology* **265**, L395-L402.

- SeaFIC.** (2009). Industry fact file 2009: Seafood Industry Council of New Zealand Limited. <http://www.seafood.co.nz/factfile>. Accessed in March 2009.
- Sharpe, R. L. and Milligan, C. L.** (2003). Lactate efflux from sarcolemmal vesicles isolated from rainbow trout *Oncorhynchus mykiss* white muscle is via simple diffusion. *Journal of Experimental Biology* **206**, 543-549.
- Shibata, M., Ichioka, S. and Kamiya, A.** (2005). Estimating oxygen consumption rates of arteriolar walls under physiological conditions in rat skeletal muscles. *American Journal of Physiology* **289**, H295-H230.
- Shiels, H. A. and Farrell, A. P.** (1997). The effect of temperature and adrenaline on the relative importance of the sarcoplasmic reticulum in contributing Ca^{2+} to force development in isolated ventricular trabeculae from rainbow trout. *Journal of Experimental Biology* **200**, 1607-1621.
- Sigholt, T., Erikson, U., Rustad, T., Johansen, S., Nordtvedt, T. S. and Seland, A.** (1997). Handling stress and storage temperature affect meat quality of farmed-raised Atlantic salmon (*Salmo salar*). *Journal of Food Science* **62**, 898-905.
- Simon, F., Giudici, R., Duy, C., Schelzig, H., Öter, S., Gröger, M., Wachter, U., Vogt, J., Speit, G., Szabó, C., Radermacher, P. and Calzia, E.** (2008). Hemodynamics and metabolic effects of hydrogen sulfide during porcine ischemia/reperfusion injury. *Shock* **30**, 359-364.
- Singer, D.** (2004). Metabolic adaptation to hypoxia: cost and benefit of being small. *Respiratory Physiology and Neurobiology* **141**, 215-228.
- Singer, D., Ince, A. and Hallmann, B.** (2002). Oxygen supply, body size, and metabolic rate at the beginning of mammalian life. *Thermochimica Acta* **394**, 253-259.
- Small, B. C.** (2004). Effect of isoeugenol sedation on plasma cortisol, glucose, and lactate dynamics in channel catfish, *Ictalurus punctatus* exposed to three stressors. *Aquaculture* **283**, 469-481.
- Small, S. A., MacDonald, C. and Farrell, A. P.** (1990). Vascular reactivity of the coronary artery in rainbow trout (*Oncorhynchus mykiss*). *American Journal of Physiology* **258**, R1402-R1410.
- Smith, L., Oseid, D., Adelman, I. and Broderus, S.** (1976). Effect of hydrogen sulfide on fish and invertebrates: Part 1. Acute and chronic toxicity studies. *Ecological Research Series*, EPA **600/3-76-062a**.

- Smith, M. P., Dombkowski, R. A., Wincko, J. T. and Olson, K. R.** (2006). Effect of pH on trout blood vessels and gill vascular resistance. *Journal of Experimental Biology* **209**, 2586-2594.
- Smith, M. P., Russell, M. J., Wincko, J. T. and Olson, K. R.** (2001). Effects of hypoxia on isolated vessels and perfused gills of rainbow trout. *Comparative Biochemistry and Physiology A* **130**, 171-181.
- Sonveaux, P., Lobysheva, I. I., Feron, O. and McMahon, T. J.** (2007). Transport and peripheral bioactivities of nitrogen oxides carried by red blood cell hemoglobin: role in oxygen delivery. *Physiology* **22**, 97-112.
- Stary, M. and Hogan, M. C.** (1999). Effect of varied extracellular PO₂ on muscle performance in *Xenopus* single skeletal muscle fibers. *Journal of Applied Physiology* **86**, 1812-1816.
- Stehly, G. R. and Gingerich, W. H.** (1999). Evaluation of AQUI-S (efficacy and minimum toxic concentration) as a fish anaesthetic/sedative for public aquaculture in the United States. *Aquaculture Research* **30**, 365-372.
- Steinlechner-Maran, R., Eberl, T., Kunc, M., Margreiter, R. and Gnaiger, E.** (1996). Oxygen dependence of respiration in coupled and uncoupled endothelial cells. *American Journal of Physiology* **271**, C2053-C2061.
- St-Pierre, J., Brand, M. D. and Boutilier, R. G.** (2000). The effect of metabolic depression on proton leak rate in mitochondria from hibernating frogs. *Journal of Experimental Biology* **203**, 1469-1476.
- Summerfelt, R. C. and Smith, L. S.** (1990). Anesthesia, surgery, and related techniques. In *Methods for Fish Biology*, (eds Schreck, C. B. and Moyle P. B.), pp 213-272. Bethesda: American Fisheries Society.
- Sutherland, F. and Hearse, D.** (2000). The isolated blood and perfusion fluid perfused heart. *Pharmacology Research* **41**, 613-627.
- Szabó, C.** (2007). Hydrogen sulphide and its therapeutic potential. *Nature Reviews - Drug Discovery* **6**, 917-935.
- Takashima, F. and Hibiya, T.** (1995). Muscle. In *An atlas of fish histology: normal and pathological features*, (eds. Takashima, F. and Hibiya, T.), pp. 24-31. Stuttgart: Gustav Fisher Verlag.
- Tang, G., Wu, L. and Wang, R.** (2005). The effect of hydroxylamine on K_{ATP} channels in vascular smooth muscle and underlying mechanisms. *Molecular Pharmacology* **67**, 1723-1731.

Thomas, P. M., Pankhurst, N. W. and Bremner, H. A. (1999). The effect of stress and exercise on post-mortem biochemistry of Atlantic salmon and rainbow trout. *Journal of Fish Biology* **54**, 1177-1196.

Tobler, M., Schlupp, I., Heubel, K., Reisch, R., León, F., Giere, O. and Plath, M. (2006). Life on the edge: hydrogen sulfide and the fish communities of a Mexican cave and surrounding waters. *Extremophiles* **10**, 577-585.

Torrans, E. and Clemens, H. (1982). Physiological and biochemical effects of acute exposure of fish to hydrogen sulfide. *Comparative Biochemistry and Physiology C* **71**, 183-190.

Tucker, V.A. (1967). Method for oxygen content and dissociation curves on microliter blood samples. *Journal of Applied Physiology* **23**, 410-414.

Tuckey, N. P. L. (2008). Technologies for tissue preservation: the role of endogenous antioxidants in preserving tissue function in Chinook salmon, *Oncorhynchus tshawytscha*. Ph.D. thesis, University of Canterbury, Christchurch.

Tuckey, N. P. L., Forster, M. E. and Gieseg, S. P. (2009a). The effects of rested harvesting on muscle metabolite concentrations and K-values in chinook salmon (*Oncorhynchus tshawytscha*) fillets during storage at 15°C. *Aquaculture* **In press**.

Tuckey, N. P. L., Forster, M. E. and Gieseg, S. P. (2009b). Lipid oxidation is inhibited by isoeugenol exposure in chinook salmon (*Oncorhynchus tshawytscha*) fillets during storage at 15°C. *Journal of Food Science* **74**, 333-338.

Turner N., Hulbert A. J. and Else P. L. (2006). Limits to physical performance and metabolism across species. *Current Opinion in Clinical and Nutritional Medical Care* **9**, 691-696.

van den Thillart, G., Waarde, A., Muller, H. J., Erkelens, C., Addink, A. D. F. and Lugtenburg, J. (1989). Fish muscle energy metabolism measured by *in vivo* ³¹P-NMR during anoxia and recovery. *American Journal of Physiology* **256**, R922-R929.

van Ginneken, V. J. T., Addink, A. D. F., van den Thillart, G. E. E. J. M., Körner, F., Noldus, L. and Buma, M. (1997). Metabolic rate and level of activity determined in tilapia (*Oreochromis mossambicus* Peters) by direct and indirect calorimetry and videomonitoring. *Thermochimica Acta* **291**, 1-13.

van Ginneken, V. J. T., Snelderwaard, P., van den Linden, R., van den Reijden, N., van den Thillart, G. E. E. J. M. and Kramer, K. (2004). Coupling of heart rate with metabolic depression in fish: a radiotelemetric and calorimetric study. *Thermochimica Acta* **414**, 1-10.

Volpato, G., Searles, R., Yu, B., Scherrer-Crosbie, M., Bloch, K. Ichinose, F. and Zapol, W. (2008). Inhaled hydrogen sulfide: a rapidly reversible inhibitor of cardiac and metabolic function in the mouse. *Anesthesiology* **108**, 659-668.

von Euler, U. S. and Liljestrand, G. (1946). Observations on the pulmonary arterial blood pressure in the cat. *Acta Physiology Scandania* **12**, 301-320.

Wadsö, L., Gomez, F., Sjöholm, I. and Rocculi, P. (2004). Effect of tissue wounding on the results from calorimetric measurements of vegetable respiration. *Thermochimica Acta* **422**, 89-93.

Wang, R., Cheng, Y. and Wu, L. (2004). The role of hydrogen sulfide as an endogenous vasorelaxant factor. In *Signal Transduction and the Gasotransmitters*, (ed. Wang, R.), pp. 323-332. Totowa, NJ: Humana Press.

Wang, Y., Heigenhauser, G. J. and Wood, C. M. (1994). Integrated responses to exhaustive exercise and recovery in rainbow trout white muscle: acid-base, phosphogen, carbohydrate, lipid, ammonia, fluid volume and electrolyte metabolism. *Journal of Experimental Biology* **195**, 227-258.

Weir, E. K. and Archer, S. L. (1995). The mechanism of acute hypoxic pulmonary vasoconstriction: the tale of two channels. *FASEB Journal* **9**, 183-189.

Wells, R. M. G and Weber, R. E. (1991). Is there an optimal haematocrit for rainbow trout, *Oncorhynchus mykiss* (Walbaum)? An interpretation of recent data based on blood viscosity measurements. *Journal of Fish Biology* **38**, 53-65.

West, T. G. and Boutilier, R. G. (1998). Metabolic suppression in anoxic frog muscle. *Journal of Comparative Physiology B* **168**, 273-280.

Weston, A. H. (1972). The effects of isoprenaline and phenylephrine on oxygen consumption in isolated smooth muscle. *British Journal of Pharmacology* **45**, 95-103.

Whalen, W. J., Buerk, D. and Thuning, C. A. (1973). Blood flow-limited oxygen consumption in resting cat skeletal muscle. *American Journal of Physiology* **224**, 763-768.

Whitfield, N. L., Kreimier, E. L., Verdial, F. C., Skovgaard, N. and Olson, K. (2008). Reappraisal of H₂S/sulphide concentration in vertebrate blood and its potential significance in ischemic preconditioning and vascular signalling. *American Journal of Physiology* **294**, R1930–R1937.

- Wilkinson, R. J., Paton, N. and Porter, M. J. R.** (2008). The effects of pre-harvest stress and harvest method on the stress response, rigor onset, muscle pH and drip loss in barramundi (*Lates calcarifer*). *Aquaculture* **282**, 26-32.
- Wilson, D. F., Ereciska, M., Drown, C. and Silver, I. A.** (1979). The oxygen dependence of cellular energy metabolism. *Archives of Biochemistry and Biophysics* **195**, 485-493.
- Wilson, D. F., Mokashi, A., Lahiri, S. and Vinogradov, S. A.** (2000). Tissue PO₂ and mitochondrial enzymes: cytochrome c oxidase as an oxygen sensor. In *Oxygen sensing: molecule to man*, vol. 475 (eds. Lahiri, S., Prabhakar, N. R. and Forster, R. E.), pp. 259-264. New York: Kluwer Academic/Plenum Publishers.
- Wilson, R. W. and Egginton S.** (1994). Assessment of maximal sustainable swimming performance in rainbow trout (*Oncorhynchus mykiss*). *Journal of Experimental Biology* **192**, 299-305.
- Withers, P.** (1992a). Cell movement. In *Comparative animal physiology*, pp.393-447. Fort Worth: Saunders College Publishing.
- Withers, P.** (1992b). Circulation. In *Comparative animal physiology*, pp.665-726. Fort Worth: Saunders College Publishing.
- Wittenberg, B. A. and Wittenberg, J. B.** (1987). Myoglobin-mediated oxygen delivery to mitochondria of isolated cardiac myocytes. *Proceedings of the National Academy of Sciences* **84**, 7503-7507.
- Wittenberg, J. B. and Wittenberg, B. A.** (2003). Myoglobin function reassessed. *Journal of Experimental Biology* **206**, 2011-2020.
- Wittenberg, J. B. and Wittenberg, B. A.** (2007). Myoglobin-enhanced oxygen delivery to isolated cardiac mitochondria. *Journal of Experimental Biology* **210**, 2082-2090.
- Wittenberg, B. A., Wittenberg, J. B. and Caldwell, P. R. B.** (1975). Role of myoglobin in the oxygen supply to red skeletal muscle. *Journal of Biological Chemistry* **250**, 9038-9043.
- Wood, C. M. and Shelton, G.** (1975). Physical and adrenergic factors affecting systemic vascular resistance in the rainbow trout: a comparison with branchial vascular resistance. *Journal of Experimental Biology* **63**, 505-523.

Yang, T. H. and Somero, G. H. (1993). Effects of feeding and food deprivation on oxygen consumption, muscle protein concentration and activities of energy metabolism enzymes in muscle and brain of shallow-living (*Scorpaena guttata*) and deep-living (*Sebastolobus alascanus*) scorpaenid fishes. *Journal of Experimental Biology* **181**, 213-232.

Zabel, R. W., Harvey, C. J., Katz, S. L., Good, T. P. and Levin, P. S. (2003). Ecologically sustainable yield: marine conservation requires a new ecosystem based concept for fisheries management that looks beyond sustainable yield for individual species. *American Scientist* **92**, 150-158.

Zhao, W. and Wang, R. (2002). H₂S-induced vasorelaxation and underlying cellular and molecular mechanisms. *American Journal of Physiology* **283**, H474-H480.

Zhao, W., Zhang, J., Lu, Y. and Wang, R. (2001). The vasorelaxant effect of H₂S as a novel endogenous K_{ATP} channel opener. *EMBO Journal* **20**, 6008-6016.

Zhao, W., Ndisang, J. F. and Wang, R. (2003). Modulation of endogenous production of H₂S in rat tissues. *Canadian Journal of Physiology and Pharmacology* **81**, 848-853.

Zollner, H. (1989). Handbook of Enzyme Inhibitors. Weinheim: VCH Verlagsgesellschaft.

Appendix 1

Conference presentations and abstracts

Conference 1:

An oral presentation was given by me at the annual meeting of the **Australian and New Zealand Society for Comparative Physiology and Biochemistry (ANZSCP)** in Perth, Australia in December 2007.

Talk title:

Oxygen dependence of hydrogen sulfide-mediated vasoconstriction in the hagfish dorsal aorta

Leonard G. Forgan, Kenneth R. Olson, and Malcolm E. Forster

Abstract

Hydrogen sulfide (H_2S) is a vasoregulatory molecule that has been shown to be a mediator of hypoxic vasoconstriction (HVC) and dilation (HVD) in vertebrates. The mechanism by which this vasoactivity is effected is not completely understood. A novel hypothesis for H_2S mediated vasoactivity and the relationship between H_2S and O_2 is presented in the most primitive extant vertebrate, the hagfish. In myographic studies, hypoxia produced HVC. H_2S dose-dependently constricted dorsal aortas (DA) and efferent branchial arteries but did not affect either the ventral aorta or afferent branchial arteries. HVC in the hagfish DA was enhanced by the H_2S precursor cysteine and inhibited by aminooxy acetate (AOA), an inhibitor of the H_2S -synthesizing enzyme, cystathionine β -synthase. HVC was unaffected by propargyl glycine, an inhibitor of cystathionine λ -lyase (an H_2S -synthesizing enzyme). The hagfish DA was found to regulate oxygen consumption (MO_2) over a physiological PO_2 range; MO_2 was constant between PO_2 of 15 and 115 mmHg, but decreased when $PO_2 < 15$ mmHg and increased when PO_2 exceeded 115 mmHg. Treatment with 10 μM H_2S increased MO_2 , whereas MO_2 fell when $H_2S \geq 100 \mu M$. Consistent with the effects on HVC, cysteine increased and AOA decreased MO_2 . These results show that H_2S is a monophasic vasoconstrictor of hagfish vessels and provides evidence for the hypothesis that H_2S production is dependant on oxygen availability.

Conference 2:

A poster was presented by me at the annual meeting of the **Society for Experimental Biology (SEB)** in Marseille, France in July 2007.

Poster title:

Oxygen dependent and independent metabolic rates in fish muscles

Leonard G. Forgan and Malcolm E. Forster

Abstract

The relationship between oxygen delivery and utilisation by vertebrate skeletal muscle cells has received much attention over the years. The internal and external tissue partial pressure of oxygen (PO_2) and its relationship to tissue oxygen consumption (VO_2) is also an intensely investigated area, yet many unknowns remain and most studies are confined to mammalian systems. Using an isolated salmon tail skeletal muscle preparation, it was shown that with increased capacitance of the perfusate for oxygen, by the addition of red blood cells and an increased flow rate, VO_2 was supply-dependent until a plateau was reached. This plateau was increased post-stimulation. Further to this, using a tissue slice preparation, we show oxyconformance of VO_2 in the striated muscle of rats, two species of teleost and a cyclostome. Rates of VO_2 were shown to differ significantly between skeletal muscle sub-types (red, white and cardiac). These data contrast with a vascular preparation that oxyregulated VO_2 over a wide PO_2 range in all four species. The mitochondrial uncouplers DNP and FCCP significantly increased VO_2 in striated and smooth muscle preparations. These data suggest that oxygen utilisation in skeletal muscle is primarily determined by PO_2 . The finding that the oxyregulation of VO_2 seen in salmon vasculature can be greatly increased by uncoupling is noteworthy and suggests that a large scope to increase in VO_2 is present in the tissue. The oxyconformance of VO_2 reported here for primitive vertebrates is similar to that observed in mammalian skeletal muscle preparations.

Conference 3:

An oral presentation was given by Professor Ken Olson at the **Federation of American Societies for Experimental Biology (FASEB) - Experimental Biology (EB)** meeting in San Diego, USA in April 2008.

Talk title:

Oxygen dependency of hydrogen sulfide-mediated vasoconstriction in cyclostome aortas

Kenneth R. Olson, Leonard G. Forgan, Ryan A. Dombkowski and Malcolm E. Forster

Abstract

Hydrogen sulfide (H_2S) is a vasoregulatory molecule and recent evidence suggests it may be an O_2 sensor for hypoxic vasoconstriction (HVC). Here we examined H_2S - O_2 interactions in hagfish vessels. In myographic studies, H_2S (Na_2S) dose-dependently constricted dorsal aortas (DA) and efferent branchial arteries (EBA) but did not affect ventral aorta or afferent branchial arteries; hypoxia produces similar responses. Hypoxia enhanced DA sensitivity to H_2S . HVC in DA was augmented by the H_2S precursor cysteine and inhibited by aminooxy acetate (AOA), an inhibitor of the H_2S -synthesizing enzyme, CBS. HVC was unaffected by propargyl glycine, the CSE inhibitor. DA O_2 consumption (MO_2) was constant between PO_2 15–115 mmHg, but decreased when $\text{PO}_2 < 15$ mmHg and increased after PO_2 exceeded 115 mmHg. 10 μM H_2S increased MO_2 , whereas MO_2 fell when $[\text{H}_2\text{S}] > 100$ μM . Consistent with the effects on HVC, cysteine increased and AOA decreased MO_2 . These results show that H_2S is a monophasic vasoconstrictor of specific cyclostome vessels and because hagfish lack vascular NO, and vascular sensitivity was enhanced at low PO_2 , it is unlikely that H_2S contractions are mediated by either H_2S -NO interaction or an oxidation product of H_2S . They also support the hypothesis that H_2S metabolism is an O_2 sensor in vertebrate vascular smooth muscle.

Appendix 2

Forgan and Forster (2008). *J. Comp. Physiol. B* **179**: 359-368

Oxygen dependency of hydrogen sulfide-mediated vasoconstriction in cyclostome aortas

Kenneth R. Olson^{1,*}, Leonard G. Forgan², Ryan A. Dombkowski³ and Malcolm E. Forster²

¹Indiana University School of Medicine—South Bend, 1234 Notre Dame Avenue, South Bend, IN 46617, USA,

²School of Biological

Sciences, University of Canterbury, Private Bag 4800, Christchurch 8020, New Zealand and ³Department of Biology, Saint Mary's

College, Notre Dame, IN 46556, USA

*Author for correspondence (e-mail: kolson@nd.edu)

Accepted 10 April 2008

SUMMARY

Hydrogen sulfide (H₂S) has been proposed to mediate hypoxic vasoconstriction (HVC), however, other studies suggest the

vasoconstrictory effect indirectly results from an oxidation product of H₂S. Here we examined the relationship between H₂S and

O₂ in isolated hagfish and lamprey vessels that exhibit profound hypoxic vasoconstriction. In myographic studies, H₂S (Na₂S)

dose-dependently constricted dorsal aortas (DA) and efferent branchial arteries (EBA) but did not affect ventral aortas or afferent

branchial arteries; effects similar to those produced by hypoxia. Sensitivity of H₂S-mediated contraction in hagfish and lamprey

DA was enhanced by hypoxia. HVC in hagfish DA was enhanced by the H₂S precursor cysteine and inhibited by amino-oxyacetate,

an inhibitor of the H₂S-synthesizing enzyme, cystathionine β -synthase. HVC was unaffected by propargyl glycine, an inhibitor of

cystathionine β -lyase. Oxygen consumption ($\dot{M}O_2$) of hagfish DA was constant between 15 and 115 mmHg P_{O2} (1 mmHg=0.133 kPa), decreased when P_{O2} <15 mmHg, and increased after P_{O2} exceeded 115 mmHg. 10 μ mol l⁻¹

H₂S increased and

100 μ mol l⁻¹ H₂S decreased $\dot{M}O_2$. Consistent with the effects on HVC, cysteine increased and amino-oxyacetate decreased $\dot{M}O_2$.

These results show that H₂S is a monophasic vasoconstrictor of specific cyclostome vessels and because hagfish lack vascular

NO, and vascular sensitivity to H₂S was enhanced at low P_{O2}, it is unlikely that H₂S contractions are mediated by either H₂S–NO

interaction or an oxidation product of H₂S. These experiments also provide additional support for the hypothesis that the

metabolism of H₂S is involved in oxygen sensing/signal transduction in vertebrate vascular smooth muscle.

Key words: hypoxic vasoconstriction, oxygen sensing, vascular smooth muscle.

The original publication is available at www.springerlink.com

Appendix 3

Olson, Forgan, Dombkowski and Forster (2008). *J. Exp. Biol.* **211**: 2205-2213

Oxygen dependency of hydrogen sulfide-mediated vasoconstriction in cyclostome aortas

Kenneth R. Olson^{1,*}, Leonard G. Forgan², Ryan A. Dombkowski³ and Malcolm E. Forster²

¹Indiana University School of Medicine–South Bend, 1234 Notre Dame Avenue, South Bend, IN 46617, USA, ²School of Biological Sciences, University of Canterbury, Private Bag 4800, Christchurch 8020, New Zealand and ³Department of Biology, Saint Mary's College, Notre Dame, IN 46556, USA

*Author for correspondence (e-mail: kolson@nd.edu)

Accepted 10 April 2008

SUMMARY

Hydrogen sulfide (H₂S) has been proposed to mediate hypoxic vasoconstriction (HVC), however, other studies suggest the vasoconstrictory effect indirectly results from an oxidation product of H₂S. Here we examined the relationship between H₂S and O₂ in isolated hagfish and lamprey vessels that exhibit profound hypoxic vasoconstriction. In myographic studies, H₂S (Na₂S) dose-dependently constricted dorsal aortas (DA) and efferent branchial arteries (EBA) but did not affect ventral aortas or afferent branchial arteries; effects similar to those produced by hypoxia. Sensitivity of H₂S-mediated contraction in hagfish and lamprey DA was enhanced by hypoxia. HVC in hagfish DA was enhanced by the H₂S precursor cysteine and inhibited by amino-oxyacetate, an inhibitor of the H₂S-synthesizing enzyme, cystathionine β -synthase. HVC was unaffected by propargyl glycine, an inhibitor of cystathionine λ -lyase. Oxygen consumption (\dot{M}_{O_2}) of hagfish DA was constant between 15 and 115 mmHg P_{O_2} (1 mmHg=0.133 kPa), decreased when P_{O_2} <15 mmHg, and increased after P_{O_2} exceeded 115 mmHg. 10 μ mol l⁻¹ H₂S increased and ≥ 100 μ mol l⁻¹ H₂S decreased \dot{M}_{O_2} . Consistent with the effects on HVC, cysteine increased and amino-oxyacetate decreased \dot{M}_{O_2} . These results show that H₂S is a monophasic vasoconstrictor of specific cyclostome vessels and because hagfish lack vascular NO, and vascular sensitivity to H₂S was enhanced at low P_{O_2} , it is unlikely that H₂S contractions are mediated by either H₂S–NO interaction or an oxidation product of H₂S. These experiments also provide additional support for the hypothesis that the metabolism of H₂S is involved in oxygen sensing/signal transduction in vertebrate vascular smooth muscle.

Key words: hypoxic vasoconstriction, oxygen sensing, vascular smooth muscle.

INTRODUCTION

Hypoxic vasoconstriction (HVC) was first observed in the mammalian pulmonary vasculature by von Euler and Liljestrand (von Euler and Liljestrand, 1946) and it is now generally accepted that in mammals this response is unique to the pulmonary circulation, whereas hypoxic vasodilation (HVD) is the prominent response of systemic vessels (Weir and Archer, 1995). Although HVC and HVD may be modulated by endothelial-derived and/or circulating substances (Félétou et al., 1995; Jacobs and Zeldin, 2001; Kerkhof et al., 2001; Liu et al., 2001; Aaronson et al., 2002; Deussen et al., 2006), the basic responses are intrinsic to the vascular smooth muscle cell (Madden et al., 1992). In non-mammalian vertebrates, HVC has been observed in both systemic and respiratory conductance vessels (Olson et al., 2001; Russell et al., 2001; Smith et al., 2001; Russell et al., 2007) and HVC appears to be an intrinsic response of vascular smooth muscle cells in the cyclostome dorsal aorta as well (Olson et al., 2001). HVD has only recently been systematically examined in non-mammalian vertebrates (Russell et al., 2007) and while it is common in systemic vessels it is not necessarily the predominant response.

How vascular smooth muscle cells 'sense' hypoxia and transduce this into a mechanical response, either HVC or HVD, is unknown. We recently proposed that the metabolism of H₂S is involved in the O₂-sensing signal transduction process. Our model is based on the balance between constitutive cellular production of vasoactive hydrogen sulfide (H₂S) and its oxidation to inactive products by available O₂ (Olson et al., 2006). Furthermore, this model appears

to be applicable to both HVC and HVD and evidence for a H₂S-mediated hypoxic relaxation has even been observed in the trout urinary bladder (Dombkowski et al., 2006).

There is also relatively little information on the mechanism through which H₂S elicits mechanical responses in the vasculature. H₂S-mediated vasodilation has been demonstrated in mammalian systemic vessels and at least part of this response is due to H₂S opening of ATP sensitive potassium (K_{ATP}) channels on the vascular smooth muscle cell and to release of nitric oxide (NO) from the endothelium (Zhao et al., 2001; Zhao and Wang, 2002; Wang et al., 2004). H₂S-mediated vasoconstriction has been demonstrated in mammalian pulmonary vessels (Olson et al., 2006) and in a variety of both pulmonary and systemic vessels from non-mammalian vertebrates (Dombkowski et al., 2005). Although it is unlikely that H₂S contractions are mediated through either K_{ATP} channels or endothelial-derived vasoconstrictor substances, the mechanism(s) of H₂S-mediated vasoconstriction is unknown.

Recently, Koenitzer et al. (Koenitzer et al., 2007) examined the effects of H₂S on rat thoracic aortas at high (200 μ mol l⁻¹, ~150 mmHg) and low (40 μ mol l⁻¹, ~30 mmHg) partial pressures of O₂ and showed that vascular relaxation was more sensitive to H₂S at low oxygen concentration ([O₂]) and that H₂S-mediated contractions were present at high, but not low [O₂]. They postulated that the decreased sensitivity of the H₂S-mediated vasorelaxation at high [O₂] was due to the combined effect of rapid oxidation (and therefore inactivation) of vasodilatory H₂S plus the generation of a

vasoconstrictor oxidation product of H_2S that would compete with the H_2S relaxation. Thus H_2S does not directly produce vasoconstriction. The identity of this oxidation product was not determined.

There are other possible explanations for the results of Koenitzer et al. (Koenitzer et al., 2007) that seem equally or more plausible. First, Koenitzer et al. (Koenitzer et al., 2007) only examined rat aortas and these vessels relax when exposed to either hypoxia or lower (and perhaps more physiological?) concentrations of H_2S and thus a contraction would not normally be expected. Second, our theory of H_2S metabolism in vascular O_2 sensing predicts that as $[\text{O}_2]$ falls, endogenous $[\text{H}_2\text{S}]$ increases. Thus at low P_{O_2} we would expect greater sensitivity to exogenous H_2S when applied against a background of elevated endogenous H_2S , consistent with the observations of Koenitzer et al. (Koenitzer et al., 2007). Furthermore, we also think that H_2S directly produces vasoconstriction in vessels that exhibit hypoxic vasoconstriction (e.g. hagfish and lamprey aortas) because it seems unlikely to us that cellular concentrations of an oxidation product of H_2S would be increasing when P_{O_2} is falling.

In the present study we examined the interaction between $[\text{O}_2]$ and $[\text{H}_2\text{S}]$ in the dorsal aorta of the most ancient extant craniate, the hagfish. This vessel was chosen because it has a mono-phasic, $[\text{O}_2]$ -dependent HVC that is endothelium independent, and does not involve K_{ATP} channels, products of lipoxygenase, cyclooxygenase, cytochrome P_{450} enzyme activity, or α -adrenergic, muscarinic, nicotinic, purinergic or serotonergic receptors (Olson et al., 2001). If our hypotheses that H_2S directly produces vasoconstriction and that endogenous H_2S increases when P_{O_2} falls is correct, we expect to see an increased sensitivity of H_2S -constriction at low $[\text{O}_2]$, not an unmasking of H_2S relaxation. We also provide additional evidence for H_2S metabolism in the O_2 sensing mechanism by examining the contribution of its precursor, cysteine, and the effects of inhibitors of H_2S synthesis on HVC. The effects of H_2S , cysteine and enzyme inhibitors on vessel O_2 consumption were measured to determine whether H_2S exposure increased \dot{M}_{O_2} and inhibitors decreased it. For comparison, we examined the O_2 sensitivity of H_2S contraction in lamprey aortas. These vessels are identical to hagfish aortas in their response to hypoxia (Olson et al., 2001) and evidence for the role of H_2S in O_2 sensing has been described (Olson et al., 2006).

MATERIALS AND METHODS

Animals

New Zealand hagfish, *Eptatretus cirrhatus* Forster (1122±165 g, $N=26$) were collected in Akaroa Harbour, New Zealand, and held in 14°C seawater aquaria at the University of Canterbury, Christchurch, NZ for at least 1 week prior to use. They were anesthetized in a combination of AQUI-STM (200 p.p.m.; Lower Hutt, New Zealand), benzocaine (400 p.p.m.) and MS-222 (400 p.p.m.). The ventral and dorsal aortas (VA and DA) and afferent and efferent branchial arteries (ABA and EBA) were removed cleaned of excess fat and blood and placed in 4°C hagfish Hepes saline until use (within 1–2 days). The saline was changed daily prior to use.

Sea lamprey (*Petromyzon marinus* L.; 130–450 g) were captured by the US Geological Survey, Biological Resources Division, in Michigan during the spring-summer spawning migration and airlifted to Indiana University School of Medicine–South Bend (IUSM-SB). They were housed in 500 l rectangular tanks in aerated, flowing well water (15°C), and exposed to a 12 h:12 h light:dark photoperiod. They were not fed. Lamprey were anesthetized in

benzocaine (1:5000, wt:vol), and the vessels were dissected out and placed in Cortland buffered saline at 4°C until use.

Salmon (*Oncorhynchus tshawytscha* Walbaum) were obtained from a nearby hatchery, anaesthetized with 22 p.p.m. AQUI-STM in their holding tanks and then killed by pithing the brain and proximal spinal cord. The ventral aorta and afferent branchial arteries were rapidly excised and stored at 4°C in freshwater salmon Ringer's solution; the dorsal aorta is firmly attached to the vertebral column and cannot be removed intact. Storage and preparation of the salmon vessels for respirometry was identical to that described below for hagfish.

Experimental procedures were approved by the University of Canterbury's Animal Ethics Committee and the IUSM-SB IACUC.

Myography

Vessels were cut transaxially into 3–4 mm long segments, mounted on 280 μm diameter stainless-steel hooks and suspended in 20 ml, water-jacketed (12°C) smooth muscle chambers and bubbled with room air. Tension was measured with Grass FT03C force-displacement transducers (Grass Instruments, West Warwick, RI, USA) and collected electronically using Biopac model MP35 (Biopac Systems Inc., Goleta, CA, USA), or measured with MLT0210 isometric force transducers (ADInstruments, Castle Hill, Waverley, NSW, Australia) using Powerlab[®] systems with bridge amplifiers (ADInstruments). Data were archived at 2 Hz on notebook computers. A resting tension of 500±50 mg (Olson et al., 2001) was applied to the vessels for 45–60 min prior to experimentation. Vessels were maximally contracted with the acetylcholine analog carbamylcholine chloride (carbachol, 10 $\mu\text{mol l}^{-1}$; Fig. 1) until tension plateaued (30–45 min), then rinsed four times with buffer and resting tension re-established over the ensuing 60 min. They were then contracted a second time with 10 $\mu\text{mol l}^{-1}$ carbachol, the rinse repeated, and the vessels were allowed to stabilize and resting tension re-established for the next 1–2 h. The tension produced by the second application of carbachol was used as the reference contraction for subsequent experiments.

Protocols

Carbachol dose response

Cumulative carbachol dose–response curves were initially obtained for efferent branchial arteries (Fig. 1) and dorsal aortas (not shown). Carbachol at 10 $\mu\text{mol l}^{-1}$ produced maximum contraction in both

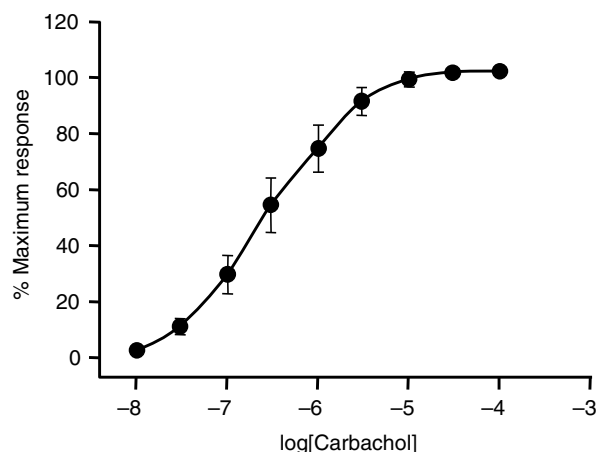


Fig. 1. Cumulative carbachol dose–response curve for efferent branchial arteries (mean ± s.e.m.; $N=4$).

vessels. Therefore, carbachol at this concentration was used twice at the beginning of experiments, first for initial activation and second for a reference contraction. A third carbachol (10 $\mu\text{mol l}^{-1}$) was also applied at the end of many experiments to determine if other treatments had non-specific effects on vascular reactivity.

Effect of H₂S on buffer pH

The dissolution of Na₂S in water produces H₂S and HS⁻ (collectively referred to in this study as H₂S) and increases pH. Because extracellular alkalinity can contract vascular smooth muscle independently of other exogenous stimuli (Smith et al., 2006), the buffering capacity of Hepes samples over the range of 1 $\mu\text{mol l}^{-1}$ to 10 mmol l^{-1} H₂S was measured in triplicate using an Orion 911600 semi-micro pH electrode (Beverly, MA USA) and a PHM 84 pH meter (Radiometer, Copenhagen, Denmark).

H₂S dose-dependent responses

Cumulative H₂S dose-response curves (1 $\mu\text{mol l}^{-1}$ to 1 mmol l^{-1}) were obtained for otherwise unstimulated, normoxic (bubbled with room air; 21% O₂) dorsal aortas and efferent branchial arteries. To determine if H₂S relaxed vessels, a second series of experiments were conducted with the vessels pre-contracted with 150 mmol l^{-1} KCl or 0.3 $\mu\text{mol l}^{-1}$ carbachol prior to the H₂S doses. In pilot studies, H₂S had no effect on ventral aortas or afferent branchial arteries ($N=4$) and these vessels were not examined further.

Effect of P_{O₂} on H₂S responses

The effect of graded hypoxia on the H₂S dose response of hagfish dorsal aortas was examined by initially aerating groups of vessels with either 100% room air ($P_{\text{O}_2}=157$ mmHg), 6% air/94% N₂ ($P_{\text{O}_2}=10$ mmHg), or 100% N₂ ($P_{\text{O}_2}<1$ mmHg) for 20–30 min prior to and during the H₂S treatments (1 mmHg=0.133 kPa). The air/N₂ mixture was controlled with a Wöstoff type 1M 300/a-F gas mixing pump (H. Wöstoff, Bochum, Germany). The P_{O_2} was measured in one myograph chamber using a Microelectrodes MI-730 oxygen electrode and meter (Bedford, NH).

The effect of moderate hypoxia on the H₂S dose response of lamprey dorsal aortas was examined using the following protocol. Vessels were contracted twice with 80 mmol l^{-1} KCl, washed twice after each contraction, and then vigorously bubbled with 100% N₂ to produce a maximal HVC. After recovery (normoxia) the flow of N₂ was reduced to produce HVC that was 20±6% of the maximal HVC. This is equivalent to a bath P_{O_2} of 20–30 mmHg (Olson et al., 2001). Cumulative doses of H₂S (10 nmol l^{-1} –1 mmol l^{-1}) were applied during this moderate hypoxia.

Involvement of H₂S mechanisms in hagfish hypoxic vasoconstriction

The involvement of H₂S in hagfish HVC was examined by measuring the response of hypoxia-contracted (100% N₂) aortas to serial additions of the substrate for H₂S synthesis: L-cysteine (0.1, 1 and 10 mmol l^{-1}), amino-oxyacetate (AOA; 0.1, 1 and 4 mmol l^{-1}), an inhibitor of cystathionine β -synthase (CBS), D,L-propargylglycine (PPG; 0.1, 1 and 4 mmol l^{-1}), an inhibitor of cystathionine λ -lyase, or hydroxylamine (0.01, 0.1 and 1 mmol l^{-1}), a general inhibitor of pyridoxyl 5'-phosphate-dependent enzymes. Following a standard carbachol (10 $\mu\text{mol l}^{-1}$) contraction the vessels were thoroughly washed and gassed with 100% N₂ for 20–30 min until the hypoxic contraction stabilized. Cumulative doses of cysteine or inhibitors were applied during the hypoxic contraction followed by a final application of 10 $\mu\text{mol l}^{-1}$ carbachol. Vessels were not washed prior to the final carbachol. The effects of hypoxia, cysteine, inhibitors

and final carbachol were normalized relative to the reference carbachol contraction.

Oxygen consumption by hagfish dorsal aortas

Hagfish dorsal aortas used in the oxygen consumption (\dot{M}_{O_2}) experiments were stored and maintained in hagfish Hepes buffer containing gentamicin sulfate (200 $\mu\text{g ml}^{-1}$) to reduce the potential for micro-organisms to contribute to \dot{M}_{O_2} (Rudin et al., 1970). Four to six aortas, 3–8 mm long, were freed of any remaining connective tissue and fat and threaded onto a 280 μm diameter stainless steel wire frame. They were then placed into 1 ml of either air-saturated or reduced [O₂] (P_{O_2} ~60 mmHg) Hepes buffer in model RC300 respirometers (Strathkelvin Instruments, Glasgow, Scotland) fitted with IL 1302 oxygen electrodes and maintained at 12°C. The electrode signal was fed into a Strathkelvin model 781 O₂ meter and then *via* a Powerlab 4SP to a notebook running Chart 5 software (both ADInstruments). Treatments were introduced into the respirometer *via* a small slot in the electrode holder with a 50 μl Hamilton syringe (Hamilton Co., Reno, Nevada, USA) fitted with a length of polythene tubing (Portex Ltd, Hythe, Kent, England; o.d. 0.61 mm, i.d. 0.28 mm). Oxygen consumption was determined from the equation:

$$\dot{M}_{\text{O}_2} = \Delta P_{\text{O}_2} \frac{60 \times \alpha_{\text{O}_2} \times V}{t \times M},$$

where \dot{M}_{O_2} is the rate of oxygen consumption ($\text{mmol O}_2 \text{ mg}^{-1} \text{ min}^{-1}$), ΔP_{O_2} is the change in P_{O_2} during the treatment period (in mmHg), α_{O_2} is the solubility of O₂ in seawater (in $\text{mmol O}_2 \text{ l}^{-1} \text{ mmHg}^{-1}$; hagfish plasma has very similar ionic composition), V is the volume of the respirometer (in l), t is the time (in s) between P_{O_2} measurements and M is the mass of the vessels in the respirometer (in mg).

The relationship between P_{O_2} and \dot{M}_{O_2} was measured in vessels that were allowed to deplete the oxygen content from air saturation (P_{O_2} ~155 mmHg) down to zero. These experiments showed that the vessels could efficiently regulate their \dot{M}_{O_2} between a P_{O_2} of 15 and 115 mmHg (see Results). Subsequent experiments on the effects of H₂S, cysteine and inhibitors of H₂S production were performed between 40 and 60 mmHg P_{O_2} where \dot{M}_{O_2} was otherwise independent of P_{O_2} .

A cumulative H₂S concentration– \dot{M}_{O_2} response was established for 1 $\mu\text{mol l}^{-1}$ –1 mmol l^{-1} H₂S in both un-contracted and carbachol (100 $\mu\text{mol l}^{-1}$)-contracted vessels. The effects of the H₂S precursor, L-cysteine (1 and 1 mmol l^{-1}) and inhibitors of H₂S production, AOA and HA (both 10 $\mu\text{mol l}^{-1}$ –1 mmol l^{-1}), on \dot{M}_{O_2} were also determined.

Oxygen consumption by salmon vessels

In the initial studies on hagfish vessels it became evident that contracting the vessels with carbachol had no effect on oxygen consumption. This was unexpected as it has been shown that contracting mammalian vessels increases oxygen consumption (Koenitzer et al., 2007). To determine whether this was an actual physiological difference or an experimental artifact, we repeated the studies with ventral aortas and afferent branchial arteries isolated from chinook salmon using the general protocol described above for hagfish vessels.

Chemicals

The composition of hagfish Hepes-buffered saline was (in mmol l^{-1}): 497.95 NaCl, 8.05 KCl, 5.10 CaCl₂, 9.00 MgCl₂, 3.04 MgSO₄, 3.00 Hepes [*N*-(2-hydroxyethyl)piperazine-*N'*-(2-ethane-sulfonic acid)]

acid form, 6.99 Hepes sodium salt, 5.55 glucose, pH 7.8. The composition of lamprey Cortland saline was (in mmol l⁻¹): 124 NaCl, 3 KCl, 2 CaCl₂, 0.57 MgSO₄, 12 NaHCO₃, 0.09 NaH₂PO₄, 1.8 Na₂HPO₄, 5.5 glucose, pH 7.8. The composition of salmon Ringer was (in mmol l⁻¹): 136.89 NaCl; 2.11 KCl; 0.99 MgCl₂; 1.30 CaCl₂; 3.00 Hepes acid form; 6.99 Hepes sodium salt; 0.30 sodium glutamate; 0.40 L-glutamine; 0.02 sodium aspartate; 0.05 DL-carnitine; 10.00 glucose, pH 7.6. AOA was purchased from ACROS Organics (Morris Plains, NJ, USA) all other chemicals were purchased from Sigma Chemical Co. (St Louis, MO, USA).

Calculations

Concentration response curves were expressed as a percentage of the maximal response. Vessel responses were normalized to the second carbachol contraction produced prior to experimentation. At the end of an experiment the vessel was blotted on paper toweling, weighed and vessel tension was normalized to wet mass, i.e. mg tension g⁻¹ wet mass. Because the hypoxic responses of individual vessels were reproducible (Olson et al., 2001), each vessel served as its own control and treatment effects were statistically examined by paired *t*-test or repeated measures tests. Results are presented as mean ± s.e.m. Student's *t*-test and analysis of variance (ANOVA) were used for comparisons between vessels. Significance was assumed when *P* ≤ 0.05.

Significant differences in rates of \dot{M}_{O_2} and responses to drugs were determined using a repeated measures ANOVA. Where significant differences were calculated between means, Tukey's *post-hoc* tests showed which means were significantly different from each other. Paired Student's *t*-tests were used to detect differences between carbachol-treated and -untreated vessels in the \dot{M}_{O_2} data (controls and at each concentration of H₂S). Significance was assumed when *P* ≤ 0.05. All analyses were performed in Prism 4.00 (Graphpad software, San Diego, CA, USA).

RESULTS

Carbachol dose response of hagfish efferent branchial arteries

Carbachol produced a dose-dependent contraction of efferent branchial arteries (Fig. 1) with an EC₅₀ of 0.275 ± 0.148 μmol l⁻¹ (*N* = 4). Peak force was achieved at a concentration of 10 μmol l⁻¹ carbachol.

Effects of H₂S on pH

The effects of increasing concentrations of H₂S on pH of hagfish Hepes buffer is shown in Fig. 2. Buffering was very efficient between 1 μmol l⁻¹ and 1 mmol l⁻¹ H₂S and increased less than 0.3 pH unit between 1 mmol l⁻¹ and 3 mmol l⁻¹ H₂S. However, pH increased nearly 2.5 units between 3 and 10 mmol l⁻¹ H₂S. H₂S contractions appeared to be independent of pH between 1 μmol l⁻¹ and 1 mmol l⁻¹ H₂S, but concentrations above 1 mmol l⁻¹ alkalinized the medium and this appeared to greatly augment H₂S contractions. H₂S concentrations were limited in subsequent experiments to 1 mmol l⁻¹ in order to minimize the possibility of pH interference and to avoid complications that might result from changes in ionic strength or composition due to increasing the buffering capacity, or titration.

Vascular effects of H₂S

H₂S produced dose-dependent contractions in otherwise unstimulated dorsal aortas and efferent branchial arteries of hagfish (Fig. 3) but had no effect on ventral aortas or afferent branchial arteries (not shown). H₂S produced essentially identical dose-

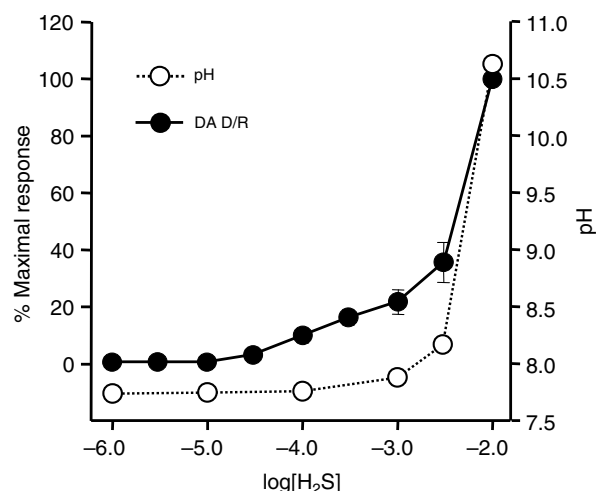


Fig. 2. Effects of H₂S (administered as Na₂S) on buffer pH (open circles, *N* = 2) and contraction of dorsal aortas (filled circles, *N* = 4). pH is relatively stable at an [H₂S] of ≤ 1 mmol l⁻¹, but higher concentrations produce increasing alkalinity and appear to augment aortic contraction.

dependent contractions in KCl (150 mmol l⁻¹, *N* = 4) and carbachol (0.3 μmol l⁻¹, *N* = 4) pre-contracted dorsal aortas and in carbachol (0.3 μmol l⁻¹, *N* = 4) pre-contracted efferent branchial arteries (data not shown for pre-contracted vessels). There was no obvious H₂S-mediated relaxation in either pre-contracted or otherwise unstimulated vessels.

Effect of P_{O₂} on H₂S responses of hagfish and lamprey dorsal aortas

Hagfish dorsal aortas bubbled with 100% N₂ were significantly more sensitive to low H₂S concentrations than aortas bubbled with room air and the H₂S dose-response curve of hypoxic (anoxic) vessels appeared to have two components (Fig. 3). H₂S-mediated contractions of hagfish aortas bubbled with 6% air/94% N₂ (data not shown) were not significantly different from aortas bubbled with room air.

H₂S produced dose-dependent contractions of lamprey dorsal aortas (Fig. 3). Moderate hypoxia increased H₂S sensitivity between 10 and 300 μmol l⁻¹ H₂S (*P* value at 30 μmol l⁻¹ H₂S was 0.053). Hypoxia did not affect the magnitude of the 1 mmol l⁻¹ H₂S contraction which in hypoxia was 41 ± 5% and in normoxia 43 ± 4% of a 80 mmol l⁻¹ KCl contraction. H₂S at concentrations between 10 nmol l⁻¹ to 1 μmol l⁻¹ did not affect either normoxic or hypoxic vessels (not shown).

Involvement of H₂S mechanisms in hagfish hypoxic vasoconstriction

In these experiments vessels were contracted with 10 μmol l⁻¹ carbachol, washed, then continuously contracted with 100% N₂ aeration. During the hypoxic contraction, the vessels were given cumulative additions of cysteine or inhibitors and this was followed, without washing the vessels, by 10 μmol l⁻¹ carbachol.

The effect of L-cysteine, a substrate for H₂S synthesis, on hypoxic contractions of hagfish dorsal aortas is shown in Fig. 4, top left panel. 100 μmol l⁻¹ cysteine produced a consistent, but statistically insignificant increase in the force of the N₂ contraction. Increasing cysteine to 1 mmol l⁻¹ significantly (*P* < 0.05) contracted the vessels to approximately double that in the original N₂

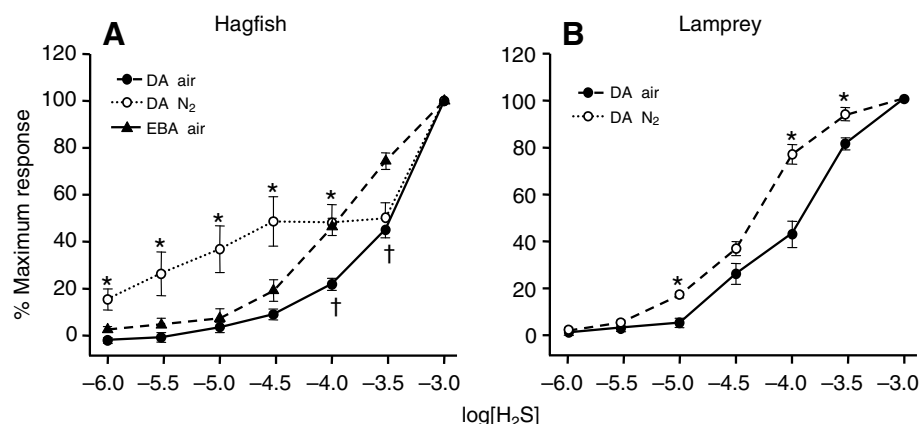


Fig. 3. (A) H₂S dose–response curves for hagfish dorsal aortas (filled circles; *N*=22) and efferent branchial arteries (filled triangles; *N*=8) bubbled with room air, and dorsal aortas bubbled with 100% nitrogen (open circles; *N*=10). Aortas bubbled with nitrogen were significantly (*) more sensitive to low concentrations of H₂S than air-bubbled aortas and appear to have a two-phase response to H₂S. H₂S at 100 and 300 $\mu\text{mol l}^{-1}$ produces a significantly greater response in normoxic efferent branchial arteries than normoxic dorsal aortas (*). (B) H₂S dose–response curves for lamprey dorsal aortas bubbled with room air (filled circles; *N*=8) or during moderate hypoxia (open circles; *N*=8). Hypoxic vessels were significantly (*) more sensitive to H₂S. Values are means \pm s.e.m.

contraction. Raising cysteine to 10 mmol l^{-1} produced an immediate relaxation back to the pre-cysteine (N₂) level ($P<0.05$). The carbachol (10 $\mu\text{mol l}^{-1}$) contraction at the end of the experiment, in the presence of N₂ and 10 mmol l^{-1} cysteine, was not significantly different from the reference carbachol contraction ($90\pm14\%$ of reference, *N*=7).

The effect of the cystathionine β -synthase (CBS) inhibitor, amino-oxyacetate (AOA), on hypoxic vasoconstriction of the dorsal aorta is shown in Fig. 4 top right panel. Hypoxic contractions were unaffected by 100 $\mu\text{mol l}^{-1}$ and 1 mmol l^{-1} AOA. 4 mmol l^{-1} AOA completely inhibited the hypoxic contraction ($P<0.05$). The carbachol (10 $\mu\text{mol l}^{-1}$) contraction at the end of the experiment, in the presence of 4 mmol l^{-1} AOA, was not significantly different from the reference carbachol contraction ($111\pm12\%$ of reference, *N*=8).

As shown in Fig. 4, lower left panel, the cystathionine λ -lyase (CSE) inhibitor, propargyl glycine (PPG; between 100 $\mu\text{mol l}^{-1}$ and 4 mmol l^{-1}) had no effect on the hypoxic contraction. A carbachol (10 $\mu\text{mol l}^{-1}$) contraction at the end of the experiment, in the presence of PPG, was similarly unaffected ($104\pm7\%$ of reference, *N*=8).

Hydroxylamine (HA), an uncoupler of pyridoxyl 5'-phosphate-dependent enzymes including CBS and CSE, at 10 $\mu\text{mol l}^{-1}$ significantly increased the force of the N₂ contraction (Fig. 4, lower right panel). Increasing HA to 100 $\mu\text{mol l}^{-1}$ and 1 mmol l^{-1} produced slight, but statistically insignificant, further increases in tension. The carbachol (10 $\mu\text{mol l}^{-1}$) contraction at the end of the experiment, in the presence of HA, was not significantly different from the reference carbachol contraction ($103\pm12\%$ of reference, *N*=8).

Vessel O₂ consumption

The relationship between P_{O_2} and oxygen consumption (\dot{M}_{O_2}) in uncontracted and carbachol pre-contracted hagfish dorsal aortas is shown in Fig. 5A. \dot{M}_{O_2} was well maintained around 2.4 $\mu\text{mol mg}^{-1} \text{min}^{-1}$ between 15 and 115 mmHg P_{O_2} but doubled between 115 and 155 mmHg and fell to zero as P_{O_2} approached zero. \dot{M}_{O_2} fell to 90% of the regulated rate at a P_{O_2} of 12 mmHg and the P_{O_2} at which the regulated \dot{M}_{O_2} fell to half (P_{50}) was 3 mmHg. Pre-treating hagfish aortas with 100 $\mu\text{mol l}^{-1}$ carbachol did not significantly affect \dot{M}_{O_2} . \dot{M}_{O_2} was also well-regulated in unstimulated salmon vessels between 15 and 115 mmHg P_{O_2} but the rate of oxygen consumption per unit tissue mass was five times that of hagfish aortas (Fig. 5B). Pre-treating salmon vessels with 100 $\mu\text{mol l}^{-1}$ carbachol nearly doubled \dot{M}_{O_2} at all but the lowest P_{O_2} .

The effects of H₂S, cysteine, AOA and HA on \dot{M}_{O_2} are summarized in Fig. 6. 10 $\mu\text{mol l}^{-1}$ H₂S significantly stimulated \dot{M}_{O_2} whereas 100 $\mu\text{mol l}^{-1}$ and 1 mmol l^{-1} significantly inhibited \dot{M}_{O_2} . A 12-fold increase in \dot{M}_{O_2} was produced by 10 mmol l^{-1} cysteine; in many experiments 1 mmol l^{-1} cysteine often appeared to increase \dot{M}_{O_2} as well, although this was not statistically significant. \dot{M}_{O_2} was inhibited by either 10 mmol l^{-1} AOA or 10 mmol l^{-1} HA. Other concentrations of AOA (10 $\mu\text{mol l}^{-1}$ –1 mmol l^{-1}) and HA (10 $\mu\text{mol l}^{-1}$ –1 mmol l^{-1}) did not significantly affect \dot{M}_{O_2} . Pre-contraction with 100 $\mu\text{mol l}^{-1}$ carbachol did not significantly affect \dot{M}_{O_2} in vessels treated with 10 $\mu\text{mol l}^{-1}$, 100 $\mu\text{mol l}^{-1}$ or 1 mmol l^{-1} H₂S (Fig. 6), 10 mmol l^{-1} cysteine, 10 mmol l^{-1} AOA or 10 mmol l^{-1} HA (*N*=5 for all; data not shown), although \dot{M}_{O_2} of vessels in 10 $\mu\text{mol l}^{-1}$ H₂S was significantly greater than \dot{M}_{O_2} of vessels in 100 $\mu\text{mol l}^{-1}$ H₂S (Fig. 6).

DISCUSSION

The present studies support our hypotheses that, (1) H₂S directly produces vasoconstriction, and (2) the metabolism of H₂S is involved in the oxygen sensing and/or signal transduction cascade in hypoxic vasoconstriction of the hagfish aorta.

H₂S as a vasoconstrictor

As shown in Fig. 3, the H₂S sensitivity in both hagfish and lamprey aortas increased when P_{O_2} was decreased. Hagfish vessels bubbled with 100% N₂ responded to 1 $\mu\text{mol l}^{-1}$ H₂S, whereas 100 $\mu\text{mol l}^{-1}$ H₂S was required to contract vessels bubbled with room air (Fig. 3). Similarly, the apparent H₂S thresholds for hypoxic (P_{O_2} ~20–30 mmHg) and normoxic lamprey vessels were 10 and 30 $\mu\text{mol l}^{-1}$ H₂S, respectively (Fig. 3). Furthermore, the H₂S dose–response curves for both animals were left-shifted in low P_{O_2} . Thus although the effect of hypoxia on the H₂S response of lamprey vessels was less dramatic than that of hagfish vessels (probably because the hypoxia was less severe), the basic responses were, nevertheless, quite similar. As described below, these results support the hypothesis that H₂S has direct vasoconstrictory activity in specific vessels.

Koenitzer et al. (Koenitzer et al., 2007) observed a bi-phasic effect of H₂S on rat aortas; low H₂S concentrations produced dilation and high concentrations (1 mmol l^{-1}) produced contraction. They also found that H₂S-mediated dilation of rat aortas became more sensitive to H₂S at low P_{O_2} . These authors (Koenitzer et al., 2007) suggested that the H₂S-mediated vasoconstriction of aortas bubbled with room air was due to an oxidation product of H₂S, not H₂S itself, and that the reason rat aortas became more sensitive to H₂S during hypoxia

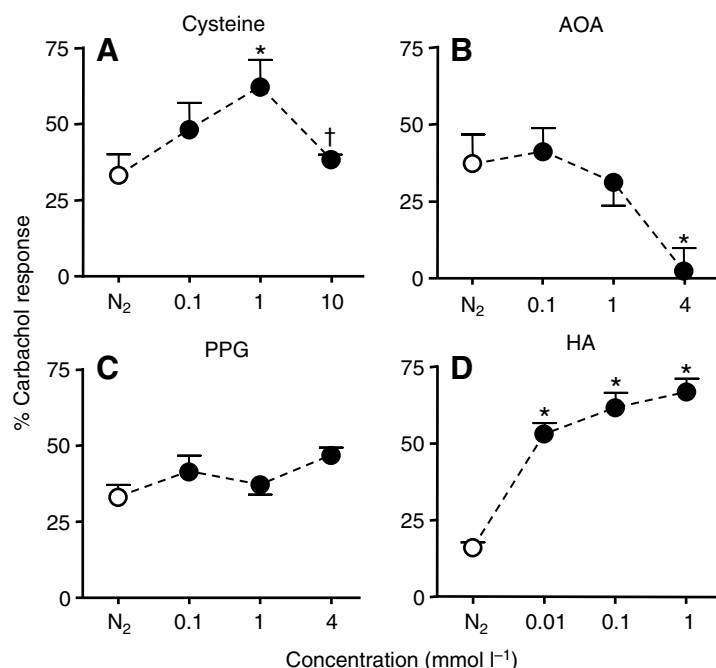


Fig. 4. Effects of (A) L-cysteine, the substrate for H₂S synthesis, (B) the cystathionine β -synthase inhibitor, amino-oxoacetate (AOA), (C) the cystathionine λ -lyase inhibitor, propargyl glycine (PPG) and (D) an uncoupler of pyridoxyl 5'-phosphate-dependent enzymes, hydroxylamine (HA) on hypoxic (100% N₂) vasoconstriction of hagfish dorsal aorta. Vessels were continuously contracted with N₂ then given cumulative additions of cysteine or inhibitors followed by 10 μ mol l⁻¹ carbachol (CBC). Values are expressed as the average tension (mean \pm s.e.m.) as the percentage of the reference carbachol contraction (100%; dashed line). Hypoxic contractions (N₂) were generally ~30% of the reference carbachol contraction. Cysteine at 1 mmol l⁻¹ approximately doubled the force of the original N₂ contraction, whereas raising cysteine to 10 mmol l⁻¹ relaxed the vessels back to the original N₂ level (* significant increase from N₂; † significant decrease from 1 mmol l⁻¹ cysteine; $N=7$). Hypoxic contractions were unaffected by 100 μ mol l⁻¹ and 1 mmol l⁻¹ AOA. At 4 mmol l⁻¹ AOA, the hypoxic contraction was completely inhibited (*; $N=8$). PPG did not significantly affect the N₂ contraction ($N=8$). HA, 10 μ mol l⁻¹ HA significantly (*) increased the force of the N₂ contraction and tension was maintained at 100 μ mol l⁻¹ and 1 mmol l⁻¹ ($N=8$).

was because in the absence of this putative oxidation product there was no offsetting constrictory stimulus to compete with the direct H₂S dilation. Our findings argue against these hypotheses. First, H₂S only constricted hagfish and lamprey dorsal aortas and therefore the increased sensitivity observed at low P_{O_2} could not be due to removal of a competing (in this case dilatory) process. Second, it seems unlikely that production of this hypothetical vasoconstrictory oxidation product of H₂S would increase when the vessels are bubbled with 100% N₂. An alternative, and we think more plausible, explanation for the increased H₂S sensitivity, and one that is consistent with our (Olson et al., 2006) hypothesis of H₂S involvement in HVC (see below), is that when P_{O_2} falls endogenous H₂S increases. Therefore, less exogenous H₂S is required for vasoconstriction.

Ali et al. (Ali et al., 2006) and Kubo et al. (Kubo et al., 2007) observed the opposite effects of Koenitzer et al. (Koenitzer et al., 2007), i.e. low H₂S concentrations (<200 μ mol l⁻¹) contracted, and elevated H₂S concentrations (200–1600 μ mol l⁻¹) relaxed rat aortic rings. They attributed the low-dose H₂S contraction to H₂S combining with NO and thereby removing the tonic NO-mediated vasodilation (Ali et al., 2006), or directly inhibiting endothelial nitric oxide synthase (Kubo et al., 2007). This also is unlikely to occur in either hagfish or lamprey dorsal aortas because, (1) there is at present no evidence for endothelial NO production by either of these vessels (Olson et al., 2001), (2) exogenous NO produces a modest contraction in the ventral aorta of the hagfish, *Myxine glutinosa* (Evans and Harrie, 2001), and (3) NO synthesis from L-arginine and O₂ would be expected to be reduced during prolonged hypoxia. Our studies suggest that H₂S may directly constrict specific vessels and that this response is an intrinsic property of the smooth muscle cells. Clearly, however, variations in this response can be achieved through H₂S interactions with other vasoregulatory mechanisms.

H₂S metabolism in O₂ sensing

Our model of the role of H₂S metabolism in oxygen sensing and/or signal transduction appears to accommodate both hypoxic vasoconstriction (HVC) and hypoxic vasodilation (HVD) in vertebrate smooth muscle (Olson et al., 2007). This model is based

on the balance between H₂S production by vascular tissue and its inactivation through oxidation, and it provides a simple and rapid mechanism that couples the concentration of a vasoactive molecule directly to P_{O_2} . The model is supported by observations that the responses of a wide variety of vessels (either constriction, dilation or multi-phasic) to hypoxia and H₂S are identical, H₂S is constitutively produced by blood vessels, cysteine the metabolic precursor of H₂S, augments HVC and inhibitors of H₂S production inhibit HVC and HVD. The present study provides additional support for the involvement of H₂S in HVC in hagfish vessels.

Similarity of vascular responses to H₂S and hypoxia

The responses of New Zealand hagfish vessels to H₂S are in many respects similar to those produced by hypoxia. H₂S and hypoxia (Olson et al., 2001), appear to be exclusively vasoconstrictory in hagfish dorsal aortas and efferent branchial arteries because they consistently contracted both un-stimulated and pre-contracted vessels. Conversely, neither H₂S nor hypoxia produced a sustained response in ventral aortas or afferent branchial arteries. H₂S and hypoxic (Olson et al., 2001) contractions of aortas and efferent branchial arteries were also unaffected by pre-contraction with KCl. Furthermore, because KCl pre-contraction presumably depolarizes smooth muscle cells it is likely that the mechanism of H₂S excitation is independent of cell depolarization; evidence for depolarization-independent HVC in these vessels has also been presented previously (Olson et al., 2001). This is in contrast to the H₂S-mediated relaxation of rat aorta (Zhao et al., 2001; Zhao and Wang, 2002) and trout efferent branchial arteries (Dombkowski et al., 2004) where elevated KCl partially inhibits the response. Collectively, these findings suggest that H₂S contraction and HVC have a common, or at least similar, excitation pathway in hagfish vessels. This is consistent with other studies (Olson et al., 2001; Dombkowski et al., 2004; Dombkowski et al., 2005; Olson et al., 2006; Russell et al., 2007) that have shown that the vascular response to hypoxia is identical to that of H₂S irrespective of whether this response is contraction, relaxation, multi-phasic, or, as in the case of hagfish ventral aorta and afferent branchial arteries, no response at all. We have also observed identical hypoxic and H₂S responses in trout

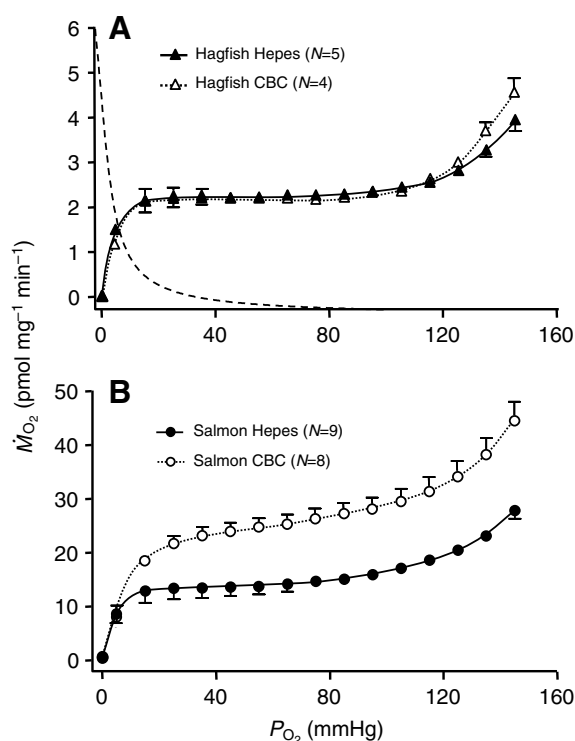


Fig. 5. Effect of P_{O_2} on oxygen consumption (\dot{M}_{O_2}) by hagfish dorsal aortas (A) and salmon vessels (B). \dot{M}_{O_2} is tightly regulated in unstimulated hagfish aortas (filled triangles) between a P_{O_2} of 15 and 115 mmHg (1 mmHg=0.133 kPa), but varies with P_{O_2} at either extreme. At a P_{O_2} of 12 mmHg \dot{M}_{O_2} falls to 90% of the regulated level and \dot{M}_{O_2} is halved at 3 mmHg (P_{50}). \dot{M}_{O_2} was not affected by pre-contracting hagfish aortas with 100 μ M l⁻¹ carbachol (CBC; open triangles). \dot{M}_{O_2} was also regulated in unstimulated salmon vessels (B; filled circles) between a P_{O_2} of 15 and 115 mmHg; however, per unit tissue mass it was five times greater than that of hagfish aortas. Pre-treatment of salmon vessels with 100 μ M l⁻¹ carbachol nearly doubled \dot{M}_{O_2} at all P_{O_2} (open circles). Mean \pm s.e.m.; N indicates the number of groups of 4–6 vessels per group in each experiment (standard error not shown when within the symbol). Broken line shows the P_{O_2} dependency of hypoxic contraction in hagfish dorsal aortas [redrawn from Olson et al. (Olson et al., 2001)].

urinary bladder (Dombkowski et al., 2006) and thus hypoxia and H₂S appear to have a common, or at least similar excitation pathway in vertebrate smooth muscle in general.

Metabolic coupling of HVC to H₂S production

Cysteine, which is presumed to be the precursor of H₂S production in animals (Julian et al., 2002) increases the magnitude of HVC at lower concentrations (Fig. 4) suggesting that it increases tissue production of H₂S. This is consistent with a cysteine-enhanced HVC in lamprey dorsal aortas and bovine pulmonary arteries and enhanced HVD observed in rat thoracic aortas (Olson et al., 2006). Further elevation of the cysteine concentration (10 mmol l⁻¹) inexplicably reduced the HVC in hagfish dorsal aorta. This may be due to a feedback-type inhibitory effect of cysteine on H₂S production, as we (R.D., S. Head, N. Whitfield and K.O., unpublished observation) have also observed elevated cysteine (10 mmol l⁻¹ or 100 mmol l⁻¹) inhibition of H₂S production in homogenized bovine heart or trout vessels, respectively, which is consistent with feedback inhibition. Alternatively, cysteine at a concentration of 10 mmol l⁻¹ may be toxic to smooth muscle cells. However, the fact that carbachol contractions on top of 10 mmol l⁻¹ cysteine were not significantly

different from the reference contractions, suggests that cytotoxicity of cysteine at 10 mmol l⁻¹ is unlikely, and the reason for this inhibition remains to be identified.

The effects of inhibitors of H₂S production provide additional evidence for H₂S signaling in hypoxic responses. As shown in Fig. 4, amino-oxyacetate (AOA), an inhibitor of cystathionine β -synthase (CBS) completely inhibited HVC in hagfish aortas, whereas the cystathionine λ -lyase (CSE) inhibitor, propargyl glycine (PPG) was ineffective (Fig. 4). This suggests that HVC in the hagfish dorsal aorta is dependent upon H₂S synthesis *via* CBS. This is in contrast to mammalian systemic vessels where CSE, but not CBS, catalyzes H₂S production (Hosoki et al., 1997; Zhao et al., 2003). We (Olson et al., 2006) have also shown that inhibition of CSE, but not CBS, blocked HVD in rat aortas, whereas inhibition of CBS, but not CSE, blocked HVC in bovine pulmonary arteries. Interestingly, in trout, H₂S produces a tri-phasic relaxation-contraction-relaxation (Dombkowski et al., 2004) and these vessels appear to possess both CBS and CSE (G. Yang, R. Wang and K.O., unpublished observation). These studies not only support the hypothesis of H₂S as a vascular O₂ sensor but they also provide additional evidence that different enzymes for H₂S production, CBS and CSE, may mediate HVC and HVD, respectively in different vessels.

Contractions produced by carbachol while hagfish dorsal aortas were exposed to AOA or PPG were not significantly different from the reference contraction produced by carbachol in the absence of inhibitors. Thus the inhibitory effect of AOA on HVC could not be due to general inhibition of the contractile apparatus. Separate H₂S and ligand-mediated responses have also been observed in other vessels (Dombkowski et al., 2004; Olson et al., 2006), indicating that the pathway for H₂S activation is not shared with some of the more common ligand-mediated mechanisms.

It is not clear why hydroxylamine potentiated HVC in hagfish aortas, although a non-specific effect seems likely. Hydroxylamine inhibits at least 100 enzymes that use pyridoxyl 5'-phosphate as a co-enzyme (Kery et al., 1999; Tang et al., 2005) including CBS and CSE. Although we expected it to act in a manner similar to AOA and inhibit vasoconstriction, it was the most potent constrictor tested, on a molar basis. Interestingly, despite turning the vasa vasorum brown, probably as a result of an action on heme groups (Canty and Driedzic, 1987; Nichols and Weber, 1989), and contracting the vessels, the vessels remained viable and the response to the final carbachol exposure was not diminished.

Effect of P_{O_2} on O₂ consumption

As shown in Fig. 5, hagfish aortas display a remarkable ability to maintain O₂ consumption (\dot{M}_{O_2}) over a wide range of ambient P_{O_2} (~15–115 mmHg). It is not clear why the vessels lose their regulatory ability when P_{O_2} exceeds ~115 mmHg, but this may be near the maximum P_{O_2} these vessels encounter in the wild, i.e. in air-saturated seawater (inspired P_{O_2} of 156 mmHg), arterial P_{O_2} was 109 mmHg (Forster et al., 1992). When P_{O_2} falls below ~15 mmHg, \dot{M}_{O_2} also falls. The P_{O_2} over which \dot{M}_{O_2} decreases is quite similar to the P_{O_2} at which HVC increases (dashed line in Fig. 5).

The P_{O_2} at which \dot{M}_{O_2} begins to decrease in hagfish dorsal aortas (15 mmHg) is somewhat less than the 20 mmHg critical P_{O_2} (P_{O_2} at which \dot{M}_{O_2} was reduced by 5%) in isolated rat aortas (Koenitzer et al., 2007). However, the \dot{M}_{O_2} for rat aortas [78 pmol mg⁻¹ min⁻¹ (Koenitzer et al., 2007)] is 32.5 times greater than the \dot{M}_{O_2} for hagfish aortas (2.4 pmol mg⁻¹ min⁻¹). Even assuming a Q_{10} of 2.4, the 25°C temperature difference between our study and that of Koenitzer et al. (Koenitzer et al., 2007) would only account for a sixfold difference in \dot{M}_{O_2} . In fact, these differences would probably be even

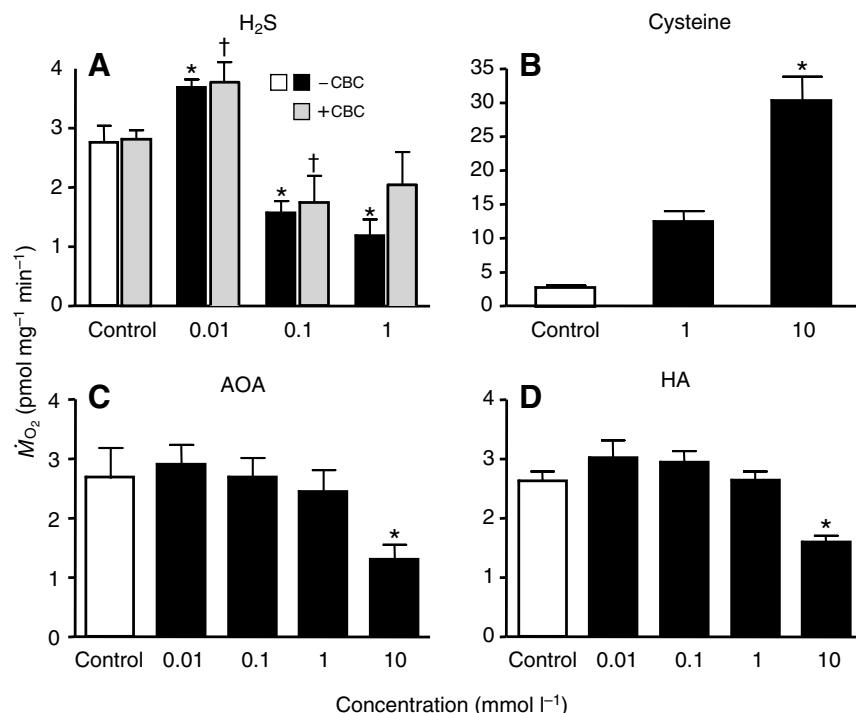


Fig. 6. Effect of (A) H₂S (as Na₂S), (B) the substrate for H₂S synthesis, L-cysteine (cysteine), and inhibitors of H₂S production, (C) amino-oxycacetate (AOA) and (D) hydroxylamine (HA), on oxygen consumption (\dot{M}_{O_2}) by hagfish dorsal aortas. \dot{M}_{O_2} was stimulated by 10 $\mu\text{mol l}^{-1}$ H₂S and 10 mmol l⁻¹ cysteine and inhibited by 100 $\mu\text{mol l}^{-1}$ and 1 mmol l⁻¹ H₂S and by 10 mmol l⁻¹ AOA and 10 mmol l⁻¹ HA. Carbachol (100 $\mu\text{mol l}^{-1}$) pre-treatment (+CBC) did not affect \dot{M}_{O_2} at any [H₂S] compared to untreated (-CBC) vessels, although \dot{M}_{O_2} was significantly different between 10 $\mu\text{mol l}^{-1}$ and 100 $\mu\text{mol l}^{-1}$ H₂S in carbachol pretreated vessels. Mean \pm s.e.m.; $N=7$ (H₂S), 5 (cysteine), 4 (AOA), 4 (HA) groups of 4–6 vessels per group; *significantly different from respective control; †significantly different from +CBC control.

greater if the O₂ solubility coefficients were accounted for; mammalian (human) plasma at 37°C is 1.26 $\mu\text{mol l}^{-1}$ mmHg⁻¹ and seawater (with the same osmolality of hagfish plasma) at 12°C is 1.72 $\mu\text{mol l}^{-1}$ mmHg⁻¹ (Boutilier et al., 1984).

Koenitzer et al. (Koenitzer et al., 2007) also showed that \dot{M}_{O_2} more than doubled when rat aortas were contracted with phenylephrine. We did not find any difference in \dot{M}_{O_2} between uncontracted and contracted hagfish aortas, perhaps because \dot{M}_{O_2} was so low to begin with, or, more likely, because once hagfish aortas are contracted they are able to maintain tension with little additional energy expenditure. The latter point may be related to the hypoxia tolerance of hagfish vessels where hypoxic contractions can be sustained for 8 h of continuous aeration with 100% N₂ (Olson et al., 2001). Many non-mammalian vertebrates, especially the more 'primitive' ones are considerably more hypoxia tolerant than mammals because of their ability to downregulate cellular metabolism and balance ATP demand with ATP supply (Boutilier, 2001). Hypoxia tolerance varies across hagfish species and interestingly, *E. cirrhatus* does not voluntarily tolerate an ambient P_{O_2} of less than 45 mmHg (82 $\mu\text{mol l}^{-1}$) at 11°C (Forster, 1992). Clearly, the lack of an increase in \dot{M}_{O_2} was not due to the technique used as carbachol nearly doubled \dot{M}_{O_2} in salmon.

Despite the elevated metabolic rate of rat aortas, the tension (in mg tension mg⁻¹ wet mass) produced by KCl contraction of rat aortas, which varies from 240 (Olson et al., 2001) to 720 (Resende et al., 2004) is only 2.5–7.5 times greater than a KCl contraction of hagfish dorsal aorta (94 \pm 12, $N=4$; data from this study). Thus it appears in rat vessels that either more oxygen is consumed for non-contractile-related activities, or that force development is energetically less efficient.

Relationship between O₂ consumption and H₂S production

In many organisms, O₂ consumption is affected by H₂S. At low [H₂S], O₂ often increases because of the use of H₂S in mitochondrial ATP synthesis or for H₂S detoxification; at elevated [H₂S], O₂ consumption often decreases because of H₂S inhibition of mitochondrial cytochrome *c* oxidase (Grieshaber and Völkel, 1998),

or perhaps even a general metabolic depression (Blackstone et al., 2005). H₂S also affects \dot{M}_{O_2} in un-contracted hagfish aortas (Fig. 6) in a manner consistent with that described by Grieshaber and Völkel (Grieshaber and Völkel, 1998). An increase in \dot{M}_{O_2} is also predicted by our (Olson et al., 2006) model of H₂S oxidation by blood vessels as a mechanism to inactivate H₂S during normoxia. Higher (100 $\mu\text{mol l}^{-1}$ and 1 mmol l⁻¹) [H₂S] inhibits \dot{M}_{O_2} (Fig. 3) but not tension development (Figs 2, 3). This likely reflects the inherently low energy cost of force development, consistent with our observation that \dot{M}_{O_2} does not change even during maximal carbachol contraction and it also provides a mechanism for sustaining HVC even when mitochondrial energy production is compromised.

The increase in \dot{M}_{O_2} produced by cysteine and the decrease in \dot{M}_{O_2} produced by AOA (Fig. 6) are also consistent with a positive and negative effect on H₂S production by hagfish dorsal aortas. It is not clear why 10 mmol l⁻¹ cysteine appeared to decrease tension, yet increase \dot{M}_{O_2} . This suggests that H₂S oxidation continues, although the mechanism that causes contraction is subject to feedback inhibition. However, other explanations are also plausible, i.e. the experimental conditions were different (anoxia in myograph studies, P_{O_2} ~40–50 mmHg in H₂S studies), this cysteine concentration is near the threshold for both processes, or there are temporal differences in responses. The effects of hydroxylamine on \dot{M}_{O_2} do not correlate with its effects on tension and may also be nonspecific as it inhibits many other enzymes (Zollner, 1989).

The authors wish to express their gratitude to R. Bishop, University of Canterbury, Christchurch (NZ) and B. Swink, US Geological Survey, Biological Resources Division, Millersburg, MI, USA for help with animal collection. This research was supported in part by National Science Foundation Grant No. IOS 0641436 (K.R.O.). K.R.O. was a recipient of an Erskine Fellowship from the University of Canterbury.

REFERENCES

- Aaronson, P. I., Robertson, T. P. and Ward, J. P. T. (2002). Endothelium-derived mediators and hypoxic pulmonary vasoconstriction. *Respir. Physiol. Neurobiol.* **132**, 107–120.

- Ali, M. Y., Ping, C. Y., Mok, Y. Y., Ling, L., Whiteman, M., Bhatia, M. and Moore, P. K. (2006). Regulation of vascular nitric oxide *in vitro* and *in vivo*; a new role for endogenous hydrogen sulphide? *Br. J. Pharmacol.* **149**, 625-634.
- Blackstone, E., Morrison, M. and Roth, M. B. (2005). H₂S induces a suspended animation-like state in mice. *Science* **308**, 518.
- Boutillier, R. G. (2001). Mechanisms of cell survival in hypoxia and hypothermia. *J. Exp. Biol.* **204**, 3171-3181.
- Boutillier, R. G., Heming, T. A. and Iwama, G. K. (1984). Physicochemical parameters for use in fish respiratory physiology. In *Fish Physiology, Vol. X, Gills, Part A* (ed. W. S. Hoar and D. J. Randall), pp. 401-430. Orlando: Academic Press.
- Canty, A. A. and Driedzic, W. R. (1987). Evidence that myoglobin does not support heart performance at maximal levels of oxygen demand. *J. Exp. Biol.* **128**, 469-473.
- Deussen, A., Brand, M., Pexa, A. and Weichsel, J. (2006). Metabolic coronary flow regulation-current concepts. *Basic Res. Cardiol.* **101**, 453-464.
- Dombkowski, R. A., Russell, M. J. and Olson, K. R. (2004). Hydrogen sulfide as an endogenous regulator of vascular smooth muscle tone in trout. *Am. J. Physiol.* **286**, R678-R685.
- Dombkowski, R. A., Russell, M. J., Schulman, A. A., Doelman, M. M. and Olson, K. R. (2005). Vertebrate phylogeny of hydrogen sulfide vasoactivity. *Am. J. Physiol.* **288**, R243-R252.
- Dombkowski, R. A., Doelman, M. M., Head, S. K. and Olson, K. R. (2006). Hydrogen sulfide mediates hypoxia-induced relaxation of trout urinary bladder smooth muscle. *J. Exp. Biol.* **209**, 3234-3240.
- Evans, D. H. and Harrie, A. C. (2001). Vasoactivity of the ventral aorta of the American eel (*Anguilla rostrata*), Atlantic hagfish (*Myxine glutinosa*), and sea lamprey (*Petromyzon marinus*). *J. Exp. Zool.* **289**, 273-284.
- Féletou, M., Girard, V. and Canet, E. (1995). Different involvement of nitric oxide in endothelium-dependent relaxation of porcine pulmonary artery and vein: Influence of hypoxia. *J. Cardiovasc. Pharmacol.* **25**, 665-673.
- Forster, M. E., Davison, W., Axelsson, M. and Farrell, A. P. (1992). Cardiovascular responses to hypoxia in the hagfish, *Eptatretus cirratus*. *Respir. Physiol.* **88**, 373-386.
- Grieshaber, M. K. and Völkel, S. (1998). Animal adaptations for tolerance and exploitation of poisonous sulfide. *Annu. Rev. Physiol.* **60**, 33-53.
- Hosoki, R., Matsuki, N. and Kimura, H. (1997). The possible role of hydrogen sulfide as an endogenous smooth muscle relaxant in synergy with nitric oxide. *Biochem. Biophys. Res. Commun.* **237**, 527-531.
- Jacobs, E. R. and Zeldin, D. C. (2001). The lung HETEs and (EETs) up. *Am. J. Physiol.* **280**, H1-H10.
- Julian, D., Statile, J. L., Wohlgemuth, S. E. and Arp, A. J. (2002). Enzymatic hydrogen sulfide production in marine invertebrate tissues. *Comp. Biochem. Physiol.* **133A**, 105-115.
- Kerkhof, C. J., Van Der Linden, P. J. and Sipkema, P. (2002). Role of myocardium and endothelium in coronary vascular smooth muscle responses to hypoxia. *Am. J. Physiol.* **282**, H1296-H1303.
- Kery, V., Poneleit, L., Meyer, J. D., Manning, M. C. and Kraus, J. P. (1999). Binding of pyridoxal 5'-phosphate to the heme protein human cystathionine β -synthase. *Biochemistry* **38**, 2716-2724.
- Koenitzer, J. R., Isbell, T. S., Patel, H. D., Benavides, G. A., Dickinson, D. A., Patel, R. P., Darley-Usmar, V. M., Lancaster, J. R., Jr, Doeller, J. E. and Kraus, D. W. (2007). Hydrogen sulfide mediates vasoactivity in an O₂-dependent manner. *Am. J. Physiol.* **292**, H1953-H1960.
- Kubo, S., Doe, I., Kurokawa, Y., Nishikawa, H. and Kawabata, A. (2007). Direct inhibition of endothelial nitric oxide synthase by hydrogen sulfide: contribution to dual modulation of vascular tension. *Toxicology* **232**, 138-146.
- Liu, Q., Sham, J. S., Shimoda, L. A. and Sylvester, J. T. (2001). Hypoxic constriction of distal porcine pulmonary arteries: endothelium and endothelin dependence. *Am. J. Physiol.* **280**, L856-L865.
- Madden, J. A., Vadula, M. S. and Kurup, V. P. (1992). Effects of hypoxia and other vasoactive agents on pulmonary and cerebral artery smooth muscle cells. *Am. J. Physiol.* **263**, L384-L393.
- Nichols, J. W. and Weber, L. J. (1989). Comparative oxygen affinity of fish and mammalian myoglobins. *J. Comp. Physiol. B* **159**, 205-209.
- Olson, K. R., Russell, M. J. and Forster, M. E. (2001). Hypoxic vasoconstriction of cyclostome systemic vessels: the physiological antecedent of hypoxic pulmonary vasoconstriction? *Am. J. Physiol.* **280**, R198-R206.
- Olson, K. R., Dombkowski, R. A., Russell, M. J., Doelman, M. M., Head, S. K., Whitfield, N. L. and Madden, J. A. (2006). Hydrogen sulfide as an oxygen sensor/transducer in vertebrate hypoxic vasoconstriction and hypoxic vasodilation. *J. Exp. Biol.* **209**, 4011-4023.
- Resende, A. C., Tabellion, A., Nadaud, S., Lartaud, I., Bagrel, D., Faure, S., Atkinson, J. and Capdeville-Atkinson, C. (2004). Incubation of rat aortic rings produces a specific reduction in agonist-evoked contraction: effect of age of donor. *Life Sci.* **76**, 9-20.
- Rudin, A., Healy, A., Phillips, C. A., Gump, D. W. and Forsyth, B. R. (1970). Antibacterial activity of gentamicin sulphate in tissue culture. *Appl. Microbiol.* **20**, 989-990.
- Russell, M. J., Pelaez, N. J., Packer, C. S., Forster, M. E. and Olson, K. R. (2001). Intracellular and extracellular calcium utilization during hypoxic vasoconstriction of cyclostome aortas. *Am. J. Physiol.* **281**, R1506-R1513.
- Russell, M. J., Dombkowski, R. A. and Olson, K. R. (2007). Effects of hypoxia on vertebrate blood vessels. *J. Exp. Zool. A* **309**, 55-63.
- Smith, M. P., Russell, M. J., Wincko, J. T. and Olson, K. R. (2001). Effects of hypoxia on isolated vessels and perfused gills of rainbow trout. *Comp. Biochem. Physiol.* **130A**, 171-181.
- Smith, M. P., Dombkowski, R. A., Wincko, J. T. and Olson, K. R. (2006). Effect of pH on rainbow trout blood vessels and gill vascular resistance. *J. Exp. Biol.* **209**, 2586-2594.
- Tang, G., Wu, L. and Wang, R. (2005). The effect of hydroxylamine on KATP channels in vascular smooth muscle and underlying mechanisms. *Mol. Pharmacol.* **67**, 1723-1731.
- von Euler, U. S. and Liljestrand, G. (1946). Observations on the pulmonary arterial blood pressure in the cat. *Acta Physiol. Scand.* **12**, 301-320.
- Wang, R., Cheng, Y. and Wu, L. (2004). The role of hydrogen sulfide as an endogenous vasorelaxant factor. In *Signal Transduction and the Gasotransmitters* (ed. R. Wang), pp. 323-332. Totowa, NJ: Humana Press.
- Weir, E. K. and Archer, S. L. (1995). The mechanism of acute hypoxic pulmonary vasoconstriction: the tale of two channels. *FASEB J.* **9**, 183-189.
- Zhao, W. and Wang, R. (2002). H₂S-induced vasorelaxation and underlying cellular and molecular mechanisms. *Am. J. Physiol.* **283**, H474-H480.
- Zhao, W., Zhang, J., Lu, Y. and Wang, R. (2001). The vasorelaxant effect of H₂S as a novel endogenous KATP channel opener. *EMBO J.* **20**, 6008-6016.
- Zhao, W., Ndisang, J. F. and Wang, R. (2003). Modulation of endogenous production of H₂S in rat tissues. *Can. J. Physiol. Pharmacol.* **81**, 848-853.
- Zollner, H. (1989). *Handbook of Enzyme Inhibitors*. Weinheim: VCH Verlagsgesellschaft.